POSSIBLE WAYS TO IMPROVE THE COMFORT, FIT AND VISUAL PERFORMANCE OF SWIMMING GOGGLES

By

Daniel Coe

A thesis submitted in partial fulfilment of the requirements for the degree of

Doctor of Philosophy

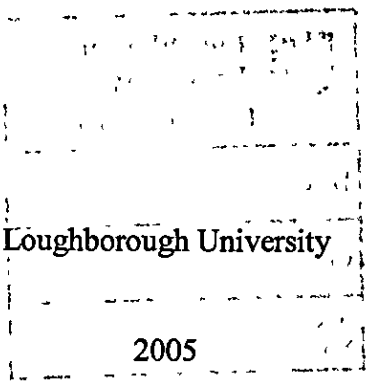

ABSTRACT

The primary aim of this thesis was to provide a comprehensive evaluation of the human face so that it can be used to improve the design of swimming goggles with regards to comfort and fit. The secondary aim was concerned with vision and was to identify whether a curved lens could be plausible for use in a performance racing goggle.

In order for these aims to be achieved, 5 main objectives were addressed. These are listed below with a brief indication of their outcome.

- A technique (based on the Y-Grid Skin Sensitivity Measurement Technique) capable of accurately measuring skin sensitivity within the facial region, was developed in order to generate data that was then used to identify the most comfortable path for the seal gasket. The resulting data indicates the seal should sit lower on the face.
- A technique capable of accurately measuring facial tissue compression was developed in order to generate data that can be used to help determine the compression values of the seal gasket throughout its circumference (to also help improve comfort).
- A technique capable of averaging facial surfaces to represent specific target populations was developed to provide moulds for designing swimming goggles with improved fit.
- Numerous techniques were developed to accurately evaluate a new prototype curved lens design, to assess the potential of using curved lenses in elite performance swimming goggles. Although the optical performance of the prototype was superior to all its competitors in the majority of aspects, there were problems with its size as well as it dual role of being used in both water and air. Therefore, although a curved lens for use in an elite goggle is plausible, further work needs to be conducted for a complete evaluation.
- A technique for incorporating the aforementioned generated data in a data led designed pair of conceptual goggles was developed. This will help designers with the task of understanding how data driven design can be used to achieve a 'better goggle'.

The thesis provides a number of techniques and protocols which have been used to generate a substantial amount of data relating to both comfort and fit as well as visual performance. The facial data has not only been shown to help improve many aspects of swimming goggles through data driven design, but may also be useful within the medical industry, more specifically reconstructive surgery. Although no definitive answer to whether a curved lens could be used in a competitive goggle, significant progress has been made in this area of research, with the development of numerous techniques for lens evaluation. This will allow future work in this area to be comparatively assessed in relation to the prototype that has already be produced, and therefore help advance research at a much faster rate.

ACKNOWLEDGEMENTS

Firstly, I would like to thank my supervisor, Dr. Michael Caine, not only for his practical support throughout the research, but also for his abilities at managing to maintain my sometimes waning motivation. I would also like to thank Prof. Roy Jones for initially recommending me as a PhD candidate, as originally it would never have been a conceivable chosen path.

From a technical point of view, the help received from Chris Wright in relation to evaluation of the curved lens test technologies was invaluable. Chris was involved in helping devise and implement the many user trials. Thanks must also go to Dr. Jeremy Coupland for initially designing the new curved lens, along with the participants who volunteered for the various studies, especially Gareth Davies, Mike Needham and Lee Gunton who endured many hours of facial probes at the early stages of test developments.

Thanks must also go to those at Speedo International who gave their time as well as recommending funding for the project, especially Zoe Dodge, Mel Jones and David Robinson.

On a personal note, I would like to give many thanks to my parents and my sister, Edward, Susan and Allison for their support and encouragement which enabled this to be possible.

PUBLICATIONS ARISING FROM THIS WORK

Due to the confidentiality agreements with Speedo International surrounding this thesis, it was only possible to publish one paper, however, further publications are planned.

Coe DA and Caine MP (2003). The feasibility of using a co-ordinate measurement machine to assess tissue compression and skin sensitivity pp321-327. *Sports Dynamics, Discovery and Application: conference proceedings.* Edited by A. Subic, P Trivalo and F. Alam.
Melbourne, Australia: RMIT University.

TABLE OF CONTENTS

Error! No table of contents entries found.

TABLE OF FIGURES

Chapter 3

Chapter 6

Chapter 7

Chapter 8

1.0 INTRODUCTION

1.1 Background

Swimming, whether for leisure, exercise or competition, is one of the most participated activities in the sporting domain. This equates to the fact that a large percentage of the population will own the paraphernalia commonly used in such an activity. Being a relatively simple sport, all that is actually required to go swimming, is a place to swim (a pool) and a swimming costume. However, the vast majority of those who swim (and can afford to do so), chose to wear swimming goggles, as they help with vision while under the water, and protect the eyes from various chemicals found in the water.

Unfortunately, considering the huge market potential and the money which people are prepared to pay for an "ideal" pair of swimming goggles, there has been little research into the data required to help properly fulfil this requirement. Although a certain percentage of the population can comfortably wear a pair of goggles that provide little or no irritation and never leak, there is still a large percentage who are constantly in search of this "ideal" goggle.

It is not only the aspects of comfort and fit that are an issue, but there are also potential problems with goggle hydrodynamics and the visual performance of the lens used. These two characteristics are often linked, as it is thought that by curving the surface of the lens, a more preferable goggle contour might be achieved to reduce the drag profile. However, in all swimming goggles that have been launched with a curved lens, the visual performance has been dramatically reduced, and has therefore never been considered as a viable competitive product.

This thesis provides techniques and data that can be used to help design swimming goggles with improved comfort and fit, as well as furthering the work in curved lens technologies, to help ensure that Speedo International (the sponsoring company) remain the leading company in this particular market.

1.2 Sponsorship Company's Initial Requirements

The PhD was sponsored by Speedo International (a brief history of Speedo can be found in the Appendix – Speedo the Company), and so it was they who initially directed where energies should be spent with regards to the research. Preliminary meetings with Zoe Dodge (primary contact and Design Manager from Speedo), led to an opening aim that was to be developed as work progressed. In effect, the idea was to design an 'Olympic swimming goggle' that would be superior to that of any competitive product. This was to be achieved by completing a number of purposefully vague objectives;

- To design and utilise specific tests for evaluating facial parameters (of explicit user groups, i.e. Competitive swimmers, age 20 to 25 years), in order to propose a more comfortable goggle, with superior fit to that of any competitor.
- To design and achieve optical clarity within a patentable curved lens that can be used practically within a racing pair of goggles.
- To consider and improve hydrodynamics of the swimming goggles, with a suggested concept incorporating the new curved lens and improved comfort and fit for an 'Olympic goggle'.

Significant changes within the structure of Speedo International (7 months into the research), resulted in certain aspects of the aims and objectives rendered obsolete. The aim was no longer to produce an 'Olympic Swimming Goggle', with all the desired features as mentioned, but was instead to provide data to help with the design process.

1.3 Aims & Objectives of Thesis

The current process of swimming goggle design, in relation to comfort and fit, highlights that the main reason the product is not as good as it should be, is due to lack of certain fundamental information for the designer. This topic was raised at discussions with Speedo International approximately 7 months into the PhD, and resulting from this meeting, the overall aims were significantly modified. Although the comfort and fit can be evaluated from a psychological aspect, it was decided to only research into the physiological aspect. This was simply chosen as there would not be enough time to research into both, and Speedo International was already well acquainted with the psychological viewpoint.

Primary Aim – To provide a comprehensive evaluation of the human face to be used to improve design of swimming goggles with regards to comfort and fit.

Secondary Aim – To identify whether a curved lens could be plausible for use in a performance racing goggle.

The primary and secondary aims were to be achieved by completing 5 main objectives with numerous sub-objectives;

Objective 1) To generate data that could be used to identify the most comfortable path for the seal gasket.

- To evaluate all current skin sensitivity measurement techniques.
- To either develop an existing measurement technique, or generate an entirely new method of measuring skin sensitivity with the required measurement resolution.
- To measure the facial skin sensitivity of a given number of participants and then calculate the averages for each measurement location.

Objective 2) To generate data that could be used to help determine the compression values of the seal gasket throughout its circumference to also help improve comfort.

- To research all seal technologies, and assess whether there are any that might already partially prevent variable pressures throughout its contact with the skin.
- To evaluate possible methods of measuring compression of facial tissue under constant load.
- To develop a repeatable and accurate technique of measuring facial tissue compression under constant load, and to then conduct a trial with a target population to calculate the average compressions for each point location.

Objective 3) To generate an average facial surface, representative of a target population that could be used as a mould for designing a swimming goggle with improved fit.

- To evaluate all current methods of capturing three dimensional data.
- To capture accurate three dimensional data for a target population.
- To develop a technique that can accurately average the three dimensional data into categories of large, medium and small for both the male and female population.

Objective 4) To prototype an 'ideal' curved lens and evaluate its optical performance against a range of goggle lenses available on the commercial market today.

- To provide the specifications for a prototype curved lens in order for it to be designed by a third party.
- To manufacture a goggle housing (that incorporates the prototype lens) that can be used by participants in a swimming pool environment.
- To generate techniques that can be used to assess the performance of the curved lens (and any other lens) in the areas of visual acuity, stereoscopic vision, magnification and visual distortion.
- To implement the developed measuring techniques, and directly compare the prototype lens with other goggle lenses on the commercial market today.
- To assess whether or not there is potential for the use of a curved lens in an elite racing swimming goggle.

Objective 5) To demonstrate how data generated from completion of the previous objectives can be used to help improve swimming goggle design.

- To create a step-by-step technique on how to generate a data led designed pair of swimming goggles.
- To generate novel design features that have been generated as a result of data led design.
- To adhere to a simple specification and generate an example data led conceptual design of a pair of swimming goggles.

1.4 Report Structure

This thesis is structured so that each objective that was stated in Section 1.3 has been researched in its own discrete chapter. A literature review precedes these chapters, with the evaluations and future work at the end.

Chapter 1) Introduction
Chapter 2) Literature review
Chapter 3) Objective 1 – Identifying most comfortable seal path
Chapter 4) Objective 2 – Determining compression values of the seal gasket
Chapter 5) Objective 3 – Generation of average facial surfaces
Chapter 6) Objective 4 – Potential of curved lens design
Chapter 7) Objective 5 – Demonstration of data led design
Chapter 8) Conclusions
Chapter 9) Further Work
Chapter 10) References

2.0 LITERATURE REVIEW

In order to gain all of the information necessary to research into the chosen fields relating to swimming goggle comfort and fit, as well as curved lens design, a critical review of relevant literature was completed.

2.1 Current design process for swimming goggles

Swimming goggles have been in use, in one form or another, for hundreds of years, and a brief history of their evolution can be found in the Appendix – A Brief History of Swimming goggles. Considering this large time period for development, it is quite surprising the manner in which modern goggles are designed today.

Swimming goggles are currently designed using a trial and error process, due to the fact that very little scientific information is available to maximise fit and function. In the majority of companies, a designer will take an existing 'successful' goggle shape, and simply create hand drawings to represent its new aesthetic form. The manufacturing company will then generate clay moulds that represent these drawings. The clay moulds are then reverse engineered onto a CAD package so that tooling can be designed and built.

This process obviously prevents any significant improvements in comfort and fit, as the areas that actually interact with the face, largely remain unchanged. Therefore any changes that a designer might include for the purpose of improving fit and function are based on guess work.

The most significant improvements have been seen in the manufacturing and assembly processes and material selection, with no noteworthy developments being made in the actual goggle itself. The majority of current day swimming goggles are simply aesthetic evolutions of previous editions that have performed well in the past. This effectively means that the underlying performance of the goggles, never make any substantial steps in improvement.

Only recently, have top line models been designed using scientific data, but this data is still very limited, so trial and error is still utilized for a large percentage of the process. Data relating to facial structure is the key to moving goggles into the next stage of progression.

2.2 Problems with current swimming goggle design

2.2.1 Comfort and fit

There are significant problems with the comfort and fit of a large percentage of goggles currently sold on the high street. The 'one size fit all' phenomena is largely quite untrue, with the percentage of the target user population who are completely satisfied with these products being negligible.

The design process is largely at fault, and the lack of innovation that follows has prevented novel technologies being introduced, resulting in unnecessarily inferior products. The most significant arises from the lack of understanding of facial structure, ergonomics and categorisation of the target population.

The poor fit that many swimmers become accustom to can result in not just discomfort and the occasional leak, but might even lead to severe medical issues. The most serious of the medical problems are due to the pressure exerted on the eyes from the relentless tightening of the strap. A resulting ocular purpura can occur (known as 'Purpura gogglurum' when generated specifically by over tight goggles, and is in effect bleeding of the eye), and can result in permanent damage to the eye and in severe cases, possible loss of sight. These health incidents generally are reported as being found in younger children, but it is not unheard of in the adult population.

Another (but less severe) medical issue resulting from the strap being too tight is when the user begins to get headaches. The first recorded evidence of this was when a neurologist developed bitemporal headaches after 1 to 2 hours of swimming. The father of the neurologist, who was a sporting goods retailer, noted that some of his customers were experiencing the same headaches associated with the use of ill-fitting

goggles. It was found that by using goggles made from a softer compound, with a looser fitting strap, the headaches stopped (Pestronk A,1983).

A very similar phenomena also causes headaches but is not present in everyone (even if they all wear over-tight straps) as part of the problem is due to nerve position. Swimmers with a supraorbital notch (<100% bony encasement of the nerve) rather than a supraorbital foramen have a greater risk of developing the problem due to the exposed portion of the nerve (Knize DM, 1995). The affected nerves both in these cases of swimmer's headache are illustrated in Figure 2.1.

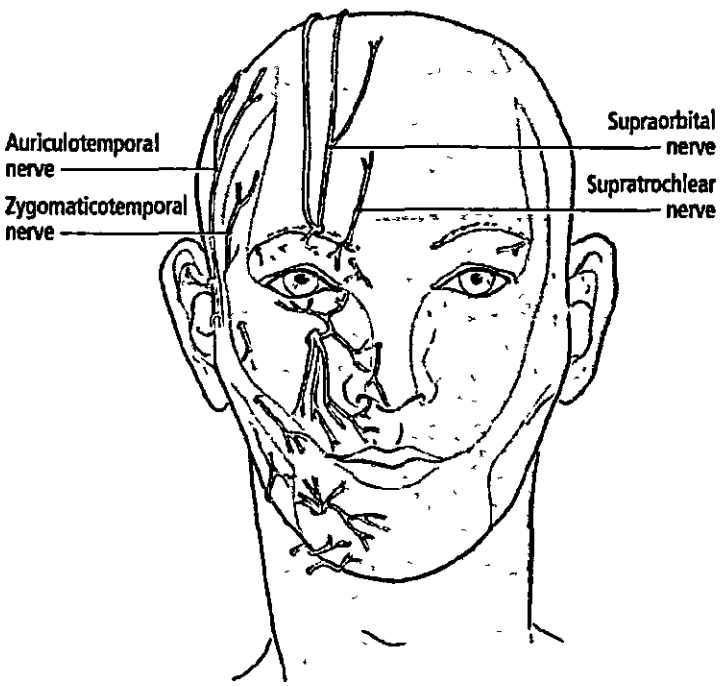

Figure 2.1, Nerves involved in generating headaches, *(Proc (Bayl Univ Med Cent) 2004 October, 17(4): 418)*

The final condition relating to goggles being worn too tight (besides general discomfort) is eyelid neuromas, caused by the edge of the goggles (Wirta DL, 1998) (Jordan DR, 2001).

The less severe but more common issue of bad fit is when the goggles leak, and apart from the obvious problem of not being able to see, the user might be allergic to the chlorine found in the swimming pool. The most likely resulting condition is conjunctivitis (Hammer RW, 1997), which is an inflammation of the conjunctiva. This is a thin, transparent membrane that covers the surface of the inner eyelid and the

front of the eye. This membrane reacts to a wide range of bacteria, viruses, allergy-provoking agents, irritants and toxic agents, as well as to underlying diseases within the body. The conjunctiva is usually clear, but if irritation or infection occurs, the lining becomes red and swollen.

2.2.1.1 Recent attempts to improve goggle comfort

Besides the use of new materials and seal composites, there has only been one company that has taken a significant step in improving goggle comfort to the user while still maintaining a racing profile. The Speedo Speedlite Racing goggle was marketed towards the elite swimmer, and was the first goggle of its type to use a purposefully designed variable thickness gasket.

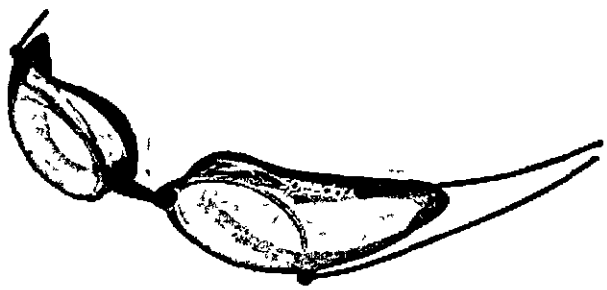

Figure 2.2, Speedo Speedlite Racing goggle

The design intention was to have the thicker gasket padding (and therefore more flexibility) only where it was required. This was supposed to then minimise the protrusion of the goggle (to help improve hydrodynamics) while enhancing the comfort to the user. Unfortunately, the goggle was designed without the use of any detailed scientific data, and therefore suffered two major flaws. Firstly, the gasket thickness was distributed to the wrong areas, and secondly the contours of the seal meant that the goggle only fitted a small percentage of the population. Due to both these reasons, the goggle was only temporarily in production.

2.2.2 Hydrodynamics

Although not a target area for research, the impact of hydrodynamics still needs to be completely understood. In relation to the hydrodynamics of swimming goggles, there

are three forms of drag being exerted, wave drag, surface drag and form drag (also known as profile or pressure drag).

- Wave drag is where waves are formed at the surrounding interface between the air, water and the swimmer. The energy used to create these waves comes from the swimmer, and resulting this, the swimmer needs to exert more energy to maintain speed.

- Surface drag is caused by the friction between the water and the swimmer's surface (skin, swimsuit, swim cap and goggles). Physics laws suggest there is no slippage of water immediately adjacent to the skin from the moment the swimmer dives into the water to the end of an entire length of an Olympic size swimming pool (50m).

- Form drag is created by the resistance produced by the displacement of still water around the moving swimmer. The drag coefficient is increased in proportion to the square velocity of the swimmer.

By improving the hydrodynamics and material selection, more energy can go to the swimmers stroke, rather than being wasted on drag. It would be unwise to think that this improvement could reduce race times by a significant amount, but considering races are won in fractions of a second, any improvement would be an advantage. Swim suits, such as Speedo's 'Sharkskin' are widely used in competitive events, and although the difference they make on times are more significant than any 'ideal' goggle, swim competitors would most likely relish the opportunity.

2.2.3 Vision

Although not being the most obvious of problems, during general interviews with a significant number of swimmers at a Masters Championship, it was found that visibility was of concern. During racing it is clear that many swimmers need to be able to precisely see when to turn, and if inferior vision due to clarity, distortion, magnification, misting or reduced peripheral vision is evident, then time might be lost.

2.2.4 Reliability

The last significant problem is with swimming goggle reliability. Swimmers complain that within a reasonable period of use, various issues become apparent. When diving, the goggles become miss-lodged allowing entry of water, unless they are repeatedly tightened to an unbearable level of discomfort. The seals distort and create the same problem, while the fasteners lose their grip and require the need for re-tightening. If the goggles were to fit better in the first place, and were to have a lower profile protruding from the face, this problem would be less significant.

2.2.5 Eyeball oxygen uptake

Although not specifically relevant to poor fit, another medical issue is with oxygen uptake of the eye. Studies have shown, that the amount of oxygen contained within a typical pair of goggles, is insufficient for the amount of time some people spend swimming. This results in the eye becoming dry and uncomfortable, and although all that is necessary for oxygen replacement is to quickly remove the goggles, the situation is not ideal.

2.3 Facial structure and characteristics

2.3.1 The skin

Primarily acting as a barrier between the external environment and the internal, the skin is the largest body organ in both weight and surface area. Within a typical adult, the skin accounts for approximately 16% of the total body weight and has many essential functions.

Purposes of the skin include,

- serving as a barrier to the environment
- ***acting as a channel for communication to the outside world*** (most relevant).
- protecting us from water loss, friction wounds, and impact wounds.
- using specialized pigment cells to protect us from ultraviolet rays of the sun.

- producing vitamin D in the epidermal layer, when it is exposed to the sun's rays.
- helping regulate body temperature through sweat glands.
- helping regulate metabolism.
- having aesthetic and beauty qualities.

Most of the above functions are irrelevant in the consideration to designing swimming goggles. However, communicating information about physical state is what leads to discomfort and so it is this area that needs to be understood.

2.3.1.1 Structure of the skin

The skin is generally described as having three layers. The outer layer is called the epidermis. Below that is the dermis, and underlying these is a layer of fat-producing cells called subcutaneous tissue (Figure 2.3).

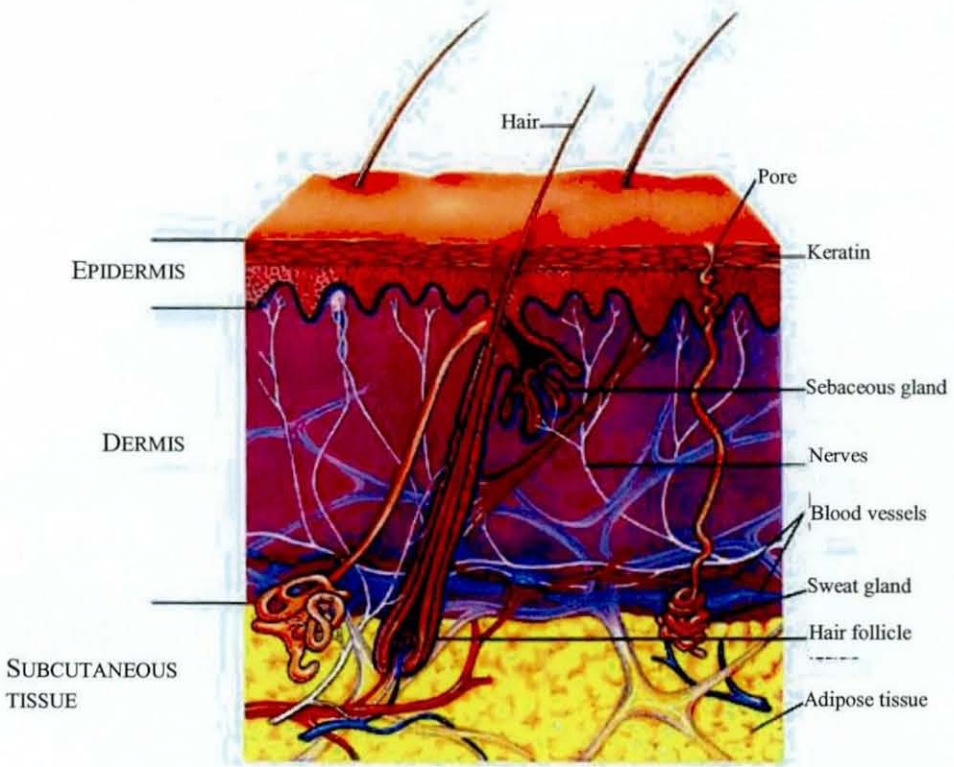

Figure 2.3, Structure of the skin, *(www.nurse-prescriber.co.uk/education/visual_lib)*

2.3.1.1.1 The Epidermis

The outer epidermis is cellular and avascular, and within humans is generally between 0.06 and 0.1mm thick in most regions. However, this is greatly increased where there is likely to be more friction (or wear) from the external environment, such as the soles of the feet or other callus areas. The epidermis consists of keratinized stratified squamous epithelium and contains four distinct layers. Starting from the very deepest to the most superficial (Wood, 1985);

Layer	Brief description
Stratum basale	Composed of a single row of cuboidal or columnar-shaped keratinocytes that are capable of continuous cell division. The cells of the stratum basale also contain cyto-skeletal intermediate filaments composed of the protein keratin (this helps to protect lower layers from injury). These filaments attach to desmosomes, which bind stratum basale cells to each other and to the cells of the next stratum, and to hemidesmosomes, which bind the keratinocytes to the basement membrane. More relevant however, is the fact that within this layer are tactile (Merkel) discs that are sensitive to touch and free nerve endings.
Stratum spinosum	This layer of the epidermis contains 8-10 rows of polyhedral keratinocytes that fit closely together, and the cells in the more superficial layers are to a certain extent flattened.
Stratum granulosum	Consisting of three to five rows of flattened keratinocytes, their nuclei and other organelles begin to degenerate, with the intermediate filaments becoming more apparent. Membrane-enclosed lamellar granules are also present in the keratinocytes, and these produce a lipid-rich secretion. This secretion functions as a waterproof sealant, preventing water loss and the entrance of foreign materials.
Stratum lucidum	More apparent where the skin is quite thick (soles of feet etc.), this layer consists of three to five layers of clear, flat, dead keratinocytes that contain densely packed intermediate filaments and thickened plasma membranes.
Stratum corneum	This layer serves as an effective waterproofing barrier and also protects against light, heat, bacteria and many chemicals. To all intents and purposes, it is approximately thirty layers of dead keratinocytes that are constantly shed and then replaced from the lower layers.

Figure 2.4, Layers of the Epidermis

From these descriptions, it is apparent that the epidermis has very few sensory receptors, or holds any other suitable information that might be used in better understanding comfort from a biological point of view. The Stratum basale is the only layer which contains any type of receptor, being tactile (Merkel) discs. Known as

Merkel's corpuscles, they are disc shaped axon terminals applied to certain spherical 'clear' cells, and send a steady signal that allows the perception of continuous touch of objects against the skin. Receptors that continue to respond as long as the stimulus is applied are known as slowly adapting receptors. Merkel discs also have small receptive fields, which is the region of skin capable of activating the receptor. Therefore, although not directly related with touch-pressure, this type of receptor still has a small part to play when detecting goggles on the face, and the continuous awareness of their presence. Distinguishing the types of touch, sensory receptors in the skin detect stimuli that the brain interprets as two forms of touch, light touch and touch-pressure. Light touch is perceived when the skin is touched but not deformed, while touch-pressure results from a deformation of the skin, no matter how slight. Regarding goggle comfort, touch-pressure is of most significance; while light touch is almost irrelevant (goggles will almost definitely deform the skin wherever in contact). Another sense that might be caused by particularly uncomfortable goggles is pain, and this sense is received by free nerve endings. Free nerve endings originate from fine myelinated or unmyelinated fibres that branch extensively in the dermis and penetrate into the epidermis. These endings respond to strong mechanical and thermal stimuli, as well as being predominantly activated by painful stimuli.

2.3.1.1.2 The Dermis

The lower connective tissue layer or dermis, is much thicker than the epidermis and varies from 2 to 4mm. Similar to the epidermis, the dermis is at its thickest in areas such as the soles of the feet and the palms of the hands, while being very thin in areas such as the eyelids. The dermis is composed of connective tissue containing collagen and elastic fibres, with the very few cells being made up of fibroblasts, macrophages and adipocytes. Blood vessels, glands, hair follicles and most importantly nerves are all embedded within the dermis. The dermis can be categorised into two main regions, the Papillary region and the Reticular region.

The superficial portion of the dermis, which is approximately one fifth of the thickness of the total layer, is the Papillary region. This layer consists of areolar connective tissue containing fine elastic fibres, and its surface is greatly increased by small finger-like projections called dermal papillae. These indented structures contain

loops of capillaries, with some containing certain tactile receptors called Meissner's corpuscles (Tortura GT, 1996). These Meissner's corpuscles are associated with the tactile sense called fluttering (felt as gentle trembling of the skin). Each has a small receptive field and is a rapidly adapting receptor. This type of receptor provides information primarily when the stimulus changes, and so when for example clothes touches a persons skin, this sensation is soon lost. Therefore the person will not be continually aware of where the clothes are continually in contact.

The deeper portion of the dermis consists of dense, irregular connective tissue that contains interlacing bundles of collagen and some coarse elastic fibres and is known as the Reticular region. Within the reticular region, bundles of collagen fibres interlace in a netlike construction, with the spaces between being occupied by a small quantity of adipose tissue, hair follicles, oil glands, ducts of sweat glands and nerves. Varying thicknesses of the reticular region contribute to the differences in the thickness of the skin. The combination of collaen and elastic fibres in the reticular region provides the skin with strength, ability to stretch and elasticity.

2.3.1.1.3 The Subcutaneous layer

The layer which attaches the epidermis and dermis to the underlying organs, such as bone and muscle is known as the subcutaneous layer (also called the hypodermis and the superficial fascia). In addition to areolar connective tissue and adipose tissue, the subcutaneous layer also contains nerve endings called lamellated or Pacinian corpuscles. Pacinian corpuscles are not only abundant within the subcutaneous layer, but also occur in deep structures including nervous membranes, joints, tendons and various other areas. They are involved in sensing vibration (felt as a diffuse humming sensation) and slightly in the perception of touch-pressure. Vibratory sense is poorly localised because pacinian corpuscles have large receptive fields. In addition, they are rapid adapting receptors.

The receptor type which has the most significance in detecting touch-pressure (as well as being associated with vibratory sense), are the Ruffini corpuscles. These receptors have quite large receptive fields and are also slow adapting (therefore respond as long as the stimulus is applied). Therefore it is the subcutaneous layer that is of most

importance, and so if any sensitivity tests are to be conducted, then the skin must be deformed to at least this layer (minimum of 2.1mm).

2.3.1.1.4 The hair

The body has two types of skin, depending on function, thin hairy (hirsute) and thick hairless (glabrous). The latter is found where regular friction is incurred, such as the soles of the feet and the palms of the hand, while the face is as the majority of the body and is covered with thin hairy skin.

Hairs are growths of the epidermis variously distributed through the entire body, and serve a range of functions. Although in a very limited manner (compared to humans lower down the evolutionary ladder), hairs are there to provide protection and warmth, but more relevant is there function as an aid to sensitivity. Touch receptors associated with hair follicles are hair root plexuses, and these are activated whenever a hair is slightly moved, and therefore responds to light touch.

2.3.1.2 Summary of Receptor function and location

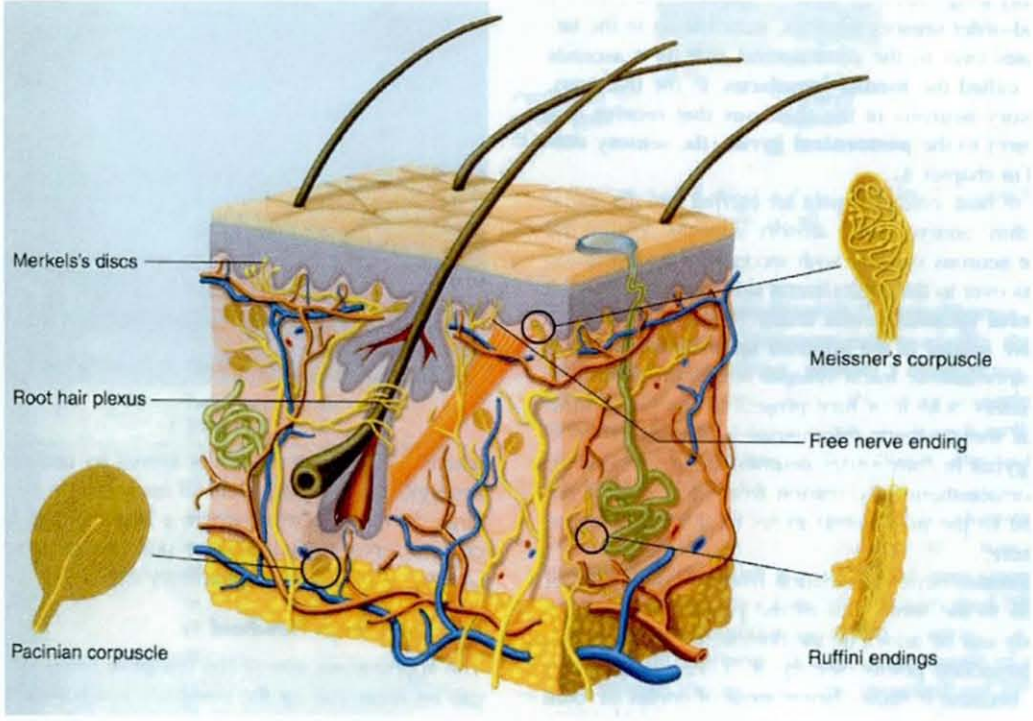

Figure 2.5, Section through skin showing various nerve receptor types,
(http://faculty.concord.edu/rockc/intro/)

Receptor	Sensation	Location
Free nerve endings	Light touch, hot, cold, pain	Around hair follicles, throughout skin
Merkel's discs	Sustained touch and pressure	Base of epidermis (stratum basale)
Ruffini corpuscles	Sustained pressure	Deep in dermis and subcutaneous layer
Meissner's corpuscles	Changes in texture, slow vibrations	Upper dermis (papillary layer)
Pacinian corpuscles	Deep pressure, fast vibrations	Deep in dermis
Root hair plexus	Light touch	Lower dermis (reticular region)

Figure 2.6, Receptors in the skin

2.3.1.3 Understanding sensory reception

The structures that are capable of perceiving and reacting to applied stimuli, as mentioned before, are known as receptors. These receptors are the bodies' link between the swimming goggles that are worn and the sensations which are endured.

2.3.1.3.1 Basic Characteristics of all Sensory Receptors

Sensory receptors may either be a nerve ending of a neuron or a specialised receptor cell. Although there are several types of sensory receptors and many ways to classify them, certain features are basic to all sensory receptors.

- They contain sensitive receptor cells that respond to certain minimum (threshold) levels of stimulus intensity. That is, the stimulus must be strong enough to generate a receptor potential and then an action potential.
- Their structure is designed to receive a specific kind of stimulus.
- Their primary receptor cells interact with afferent nerve fibres that convey impulses to the central nervous system along spinal or cranial nerves (Noback C, 1996)).

2.3.1.3.2 The process

In terms of the nervous system, a receptor is the peripheral end of the nerve fibres of afferent neurons. All sensory receptors are structures that are capable of converting environmental information into nerve impulses, and can be considered as transducers (converting one energy form into another).

The mechanical transduction from the application of stimuli to the receptors through to the generation of action potentials in the sensory neurons, is conventionally viewed as a three stage process.

1) The stimulus (touch or movement) is mechanically applied to the cells encapsulating the receptor nerve ending.
2) The deformation is transduced into an electrical signal – the receptor (generator) potential.
3) The receptor potential is encoded into an action potential for transmission by the sensory neuron to the central nervous system

At this stage, each receptor may be characterised by quality of modality perceived, size of its receptive field, its stimulus threshold, its speed of adaptation, and its first order fibre type projecting to the central nervous system (Carola R and Fox SI, 1995).

2.3.1.3.3 Touch Pressure receptor specific characteristics

Fortunately, humans are able to 'pin-point' feelings such as touch-pressure with a reasonable level of accuracy, even though varying quite considerably throughout the body and from person to person. The skin surface sensations are more precise to that of any sensation located lower in the tissue and internally. Pain being a similar feeling type, shows a good example of how people are able to localise cutaneous pain remarkably precisely, compared to the much lower spatial resolution of deep (somatic and visceral) pain (Arendt-Nielson L., 1997).

As stated previously, the specific receptors involved with touch pressure are Merkel's discs, Ruffini corpuscles and Pacinian corpuscles. In relation to point discrimination, touch-pressure is perceived largely by the slowly adapting fibre/receptor system. It is

commonly known that the innervation density of these receptors is primarily correlated to the discrimination threshold (Wheat HE., Goodwin AW, 2000). However, pressure has been also found to be a significant factor, and in his earlier work, Mountcastle related the intensity of a stimulus (pressure) to an increase of impulse response (frequency discharge). Therefore spatial sensitivity is reduced at sites where innervation is less dense, but it is not possible to predict the threshold based on the density of innervation estimates alone. Other factors such as skin mechanics need to be taken into consideration, even when small distances are involved.

The way in which the receptors are innervated also has a significant effect on the perceived feelings involved. It has been demonstrated that many mechanoreceptors, particularly the slowly adapting units, discharge in a surprisingly consistent manner upon replication of the same stimulus to the receptive field. From the same study, it was also found that highly reliable differences are evoked in the discharge by varying the velocity at which the stimulus moves across the receptive field. Furthermore, different directions of movement induce differences in the discharge that are consistently observed upon replication of the same stimuli. This was also reported for the mechanoreceptors innervating the hairy skin of the monkey hind limb (Whitsel et al., 1972).

Most low-threshold mechanoreceptors exhibit distinct differences in response to brush stimuli moving in different directions even at the same stimulus velocity. These differences are most pronounced in the spatial discharge patterns. Directional differences in the discharge maybe explained by asymmetrical sensitivity to stretch or compression with respect to the orientation of the stimulation. Indeed, many human SAII units in the glabrous skin exhibit differential sensitivity to stretch in opposite directions (Johansson RS., 1978). Receptor fields are often thought of as being circular, but in actual fact, the receptor fields relevant to touch pressure are elliptical (Schlereth T. et al., 2000). This is thought to be another reason for different sensitivity readings being recorded in the same location, when only direction of application is varied.

2.3.1.4 Global sensitivity within the face

The trigeminal nerve (fifth cranial pair) is the chief sensory nerve of the face and is composed of two roots, sensory and motor. As the name indicates the trigeminal nerve is composed of three large branches. They are the ophthalmic (V1, sensory), maxillary (V2, sensory) and mandibular (V3, motor and sensory) branches. Figure 2.7 shows which segments of the face each branch relates to.

The ophthalmic branch travels through the superior orbital fissure and passes through the orbit to reach the skin of the forehead and top of the head. The maxillary nerve enters the cranium through the foramen rotundum via the pterygopalatine fossa. Its sensory branches reach the pterygopalatine fossa via the inferior orbital fissure (face, cheek and upper teeth) and pterygopalatine canal (soft and hard palate, nasal cavity and pharynx). The sensory part of the mandibular nerve is composed of branches that carry general sensory information from the mucous membranes of the mouth and cheek, anterior two-thirds of the tongue, lower teeth, skin of the lower jaw, side of the head and scalp and meninges of the anterior and middle cranial fossae.

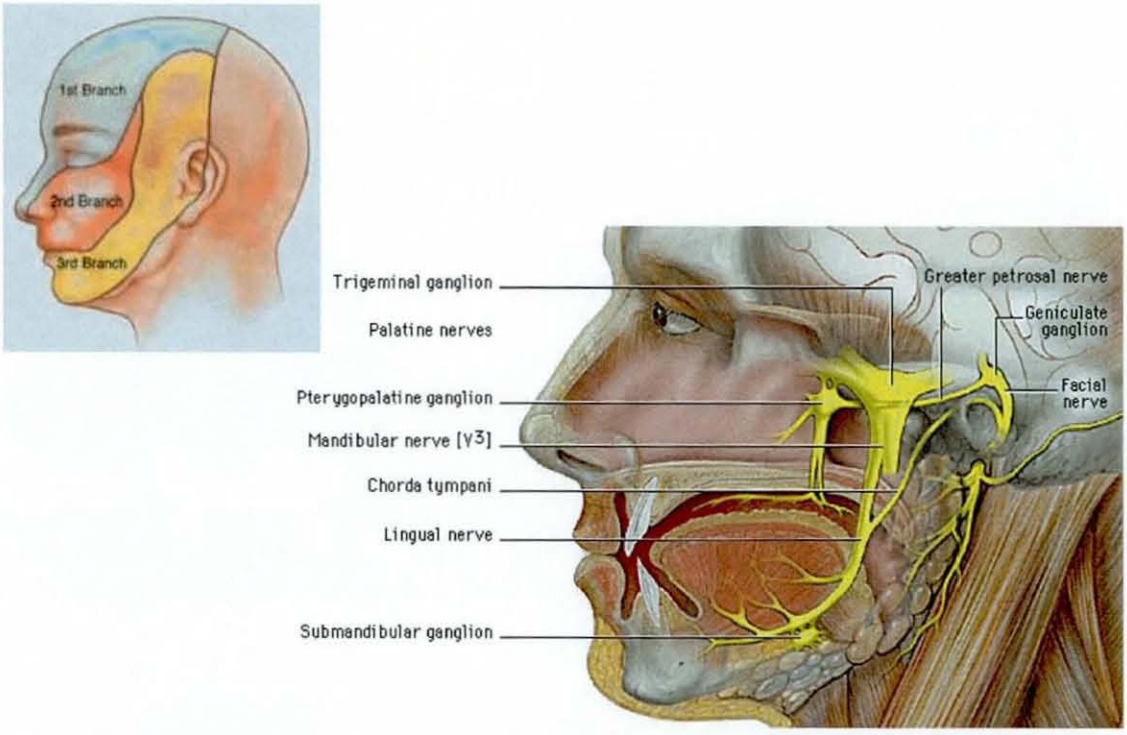

Figure 2.7, Showing the three nerve regions within the face, (http://www.neuro.times.lv/images/trig)

2.3.1.5 Localised sensitivity within the face

Although providing a global overview of which nerves go where within the face, a greater understanding of more localised sensitivity was required. No current research has clearly mapped out the face in detail in terms of point sensitivity, and so a test method was needed to obtain this information.

There are a number of test methods used in obtaining skin sensitivity, but they were generally originally designed for use in the field of rehabilitation, or for patients with neurological impairment, diabetes, thyroid disorders, collagen vascular disease and alcoholism.

2.3.2 Current skin sensitivity test methods

There are a number of methods currently available that measure the localised sensitivity of skin, including:

- Two-point touch threshold test
- Depth sense aesthesiometry test
- Point localisation Y-grid test
- Pressure sensitivity Von Frey filament test
- Suction perception test
- Neurophysiological recording technique of tactile stimulation

The choice of which test to use, depends entirely on the circumstances and the type of information required. Unfortunately, there are inherent floors in all of those mentioned, either relating to their accuracy and repeatability, or the time and resources required to perform the test.

2.3.3 Variations in skin

Although the skin has been discussed in general terms, with no differentiation between individuals, it is quite apparent that skin varies enormously throughout an individual as well as from person to person. Variations in the biomechanical

properties of skin have also been shown to vary with health conditions, sex, age and female menstruation and the environmental conditions of temperature, moisture, etc.

2.3.3.1 Differences in skin sensitivity due to sex

The skin of a male is generally thicker, with strengthened tissues of the dermis due to chemicals from the male glands, while the female sex glands on the other hand make their skin softer. This in itself does not mean that harder, thicker skin is less sensitive. One particular study showed no relationship between decreased sensory perception and increased skin hardness (Dellon et al., 1995), and another showed no relationship between decreased sensory perception and sex (Samje, 1981). A possible reason is that the slowly adapting fibre/receptor system that transmits the perception of pressure, functions independently of skin compliance due the force being directly applied to the nerve fibre/receptor itself. Although there were limited participants (all of which had either carpal tunnel syndrome, cubital tunnel syndrome or both), this theory was also shown by a previous study proving a surgeons ability to discriminate pairs of satures while double gloving. It was found that while covering the fingertip with one and then two pairs of gloves caused a significant increase in skin hardness, and in the pressure required to discriminate one from two points set 3mm apart, double gloving did not affect identification of pairs of sutures (Watts et al., 1994).

Another significant difference in sex is the number and type of hairs located over the body. While women have fewer and shorter hairs, men are somewhat hairier and the hairs themselves are longer and coarser. This can be more related to light touch, whereas the more relevant touch pressure is unaffected by hair and their associated follicles.

The most noteworthy factor directly relating to sensitivity is with women's menstruation cycle. Depending on time of cycle, the skins sensitivity can vary considerably. More information is required before any further statements can be made.

2.3.3.2 Differences in skin sensitivity between left and right sides of the body

Each side of the body is controlled by different opposite sides of the brain, and so it would be feasible to assume that there would be variations in skin sensitivity from one side to the other. However, certain studies have shown contrary to this with a recent study testing for both touch and pain on the left and right hand, concluding no difference (Schlereth et al., 2000). This had also been previously demonstrated when evaluating the depth sense aesthesiometer as a reliable device for measuring sensitivity in bedside conditions (Smaje, 1981). The test was again completed on the hand, and so there is little proof however that this is true for the entire body.

2.3.3.3 Differences in skin sensitivity due to age

With age, the elasticity of the skin decreases from 5 to 75 years and the tension of skin also decreases (Escoffier, 1989). As age progresses, there is a tendency toward dryness and cracking of the horny layer of the skin. The colour may be yellowish with a sallow greyish hue. Often these are areas of discoloration and scaling. The fine wrinkles which appear are the result of atrophy of the dermal papillae and the flattening of the epithelium. Linked with the differences in sensitivity due to sex (where the male has harder, dryer and thicker skin), the results of age have a similar effect and so it would seem that age has little to do with levels of sensitivity. Age is however likely to be responsible for more skin conditions which will definitely cause a reduction in receptor sensitivity.

2.3.3.4 Differences in skin due to climate

Weather conditions affect the skin in so far as the reaction of the skin's surface can vary from season to season due to variations in temperature and humidity. Dry hot summer days tend to dry out the surface of the skin. In a similar manner, the dry heated air of a cold home in winter will produce the same effect. However, as none of these factors effect the skin sensitivity, then climate is of little concern.

2.3.4 Facial Anthropometrics

The word anthropometrics refers to the measurement of humans. In order for swimming goggles to be designed to the correct shape and size for a specific target population, detailed anthropometric data regarding the face is required.

Although published anthropometric data for the human head is already available, the level of detail is not sufficient to enable improvement in goggle fit and comfort. Example measurements that are currently available for the 5th and 95th percentile 'normal' person can be seen in figures 2.8-2.13.

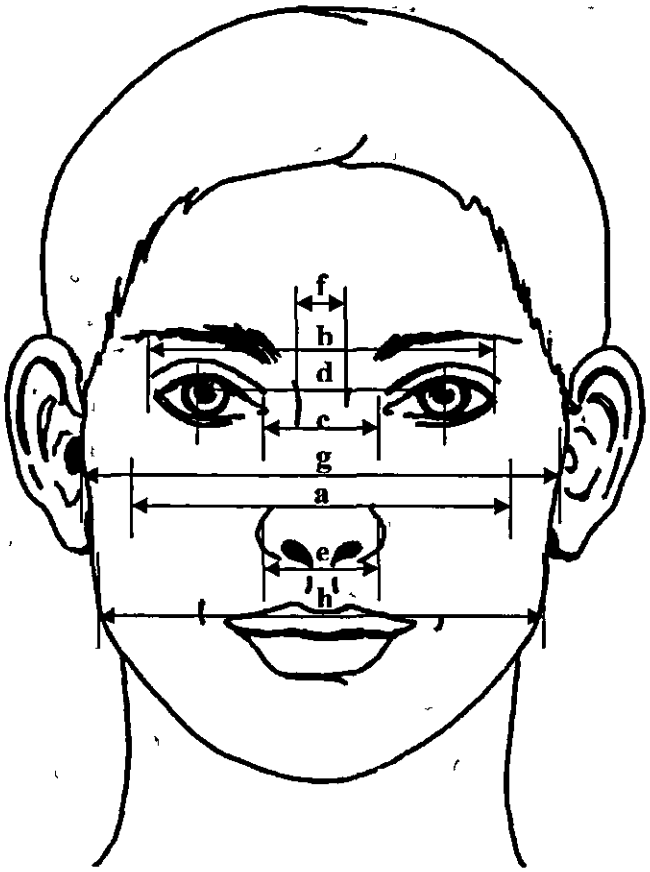

Figure 2.8, Varying anthropometric data for a front profile of the face

	Measurement	Maximum Value (mm)	Minimum Value (mm)
a	Face Breadth (across cheekbones)	156	85
b	Distance between outer corners of the eyes	103.4	84.8
c	Distance between inner corners of the eyes	42.5	24
d	Distance between the centres of the pupils	75.7	50
e	Nose Breadth (maximum at bottom)	45.3	29
f	Nose Breadth (minimum at top)	17.3	12.5
g	Head Breadth (in front of ears)	163.6	110
h	Jaw Width	126.5	74

Fig 2.9, Maximum and minimum measurements for facial measurements

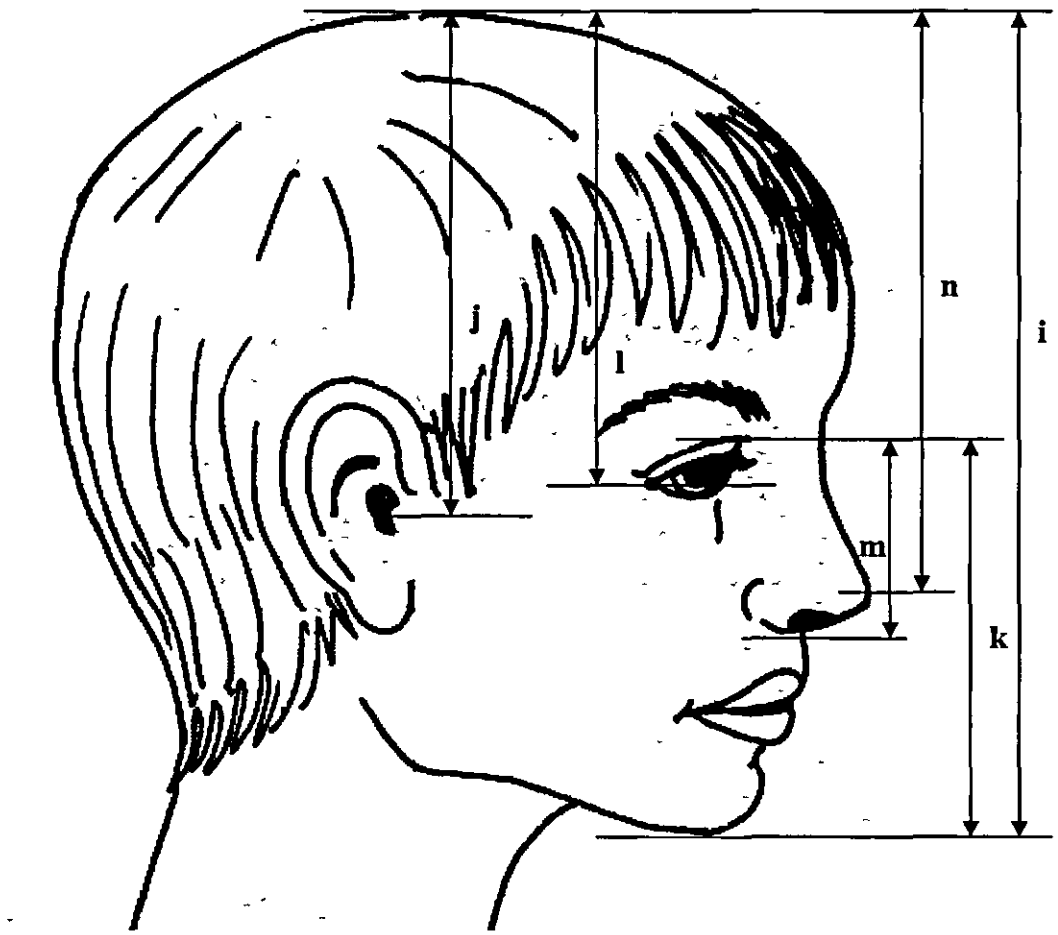

Figure 2 10, Varying anthropometric data for a side profile of the face

	Measurement	Maximum Value (mm)	Minimum Value (mm)
l	Head Height	248.1	176.8
j	Ear to the Top of the Head	153	106
k	Face Length	144	89
l	Corner of the Eye to the Top of the Head	133.9	96
m	Nose Length	58.8	38.3
n	Tip of the Nose to the Top of the Head	167.6	125.6

Figure 2.11 Varying side profile dimensions of the face

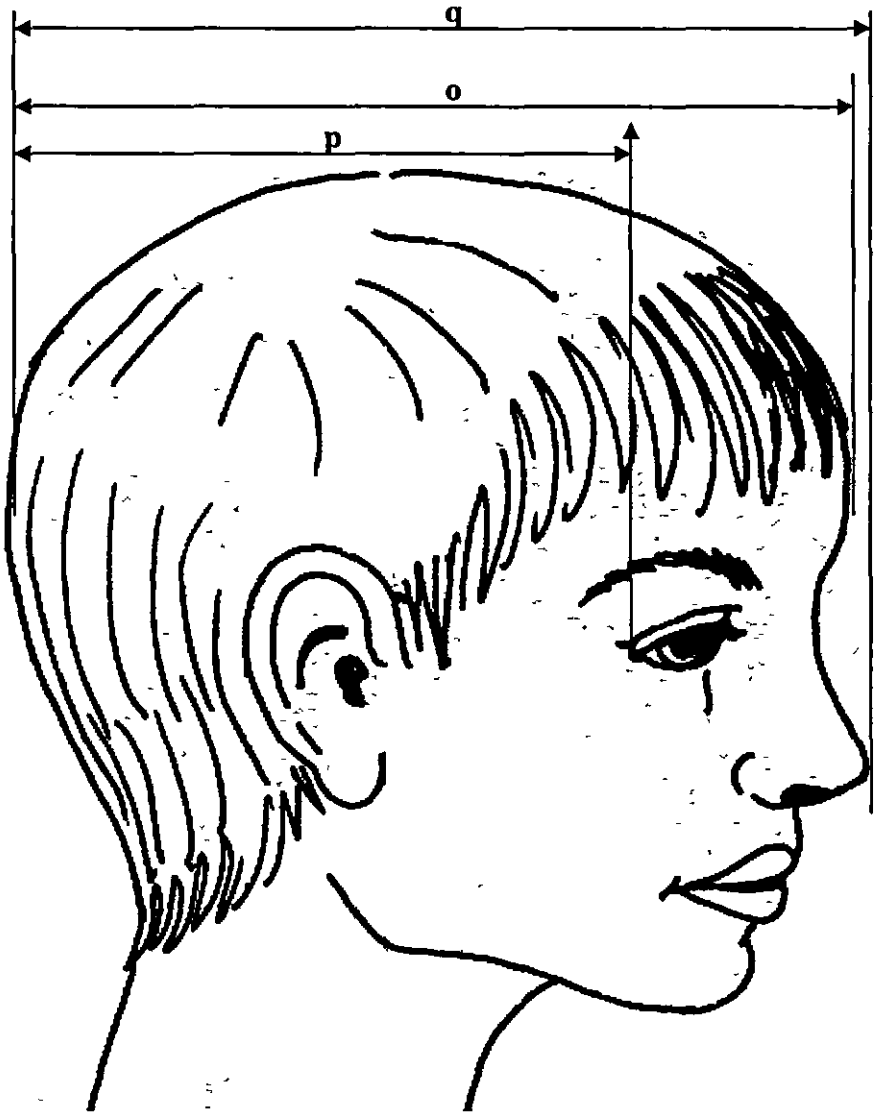

Figure 2.12, Varying anthropometric data for a side profile of the face

	Measurement	Maximum Value	Minimum Value
o	Head Length	213.6	149
p	Corner of Eye to Back of Head	185.3	143.0
q	Tip of Nose to Back of Head	235.6	179.6

Figure 2 13, Varying side profile dimensions of the face

Although the level of detail is quite high, important information relating to the facial surface is unavailable. Before the comfort and fit of swimming goggles can be improved, 'average' facial surfaces (such as the face shown in Figure 2.14) for both the male and female population are required.

Figure 2.14, 3D scan of a facial surface, *(www anilalexander org/gal/albums/album11/)*

Facial measurement of this level has been mostly utilised in the medical sector to improve the harmonious facial form as well as facilitating functional improvements in areas such as speech and feeding. In particular this process of measurement needs to be as precise as possible when dealing with children who have problems such as cleft lip, as primary cleft lip and nose repair has an enormous influence on facial form and growth (Yamada et al., 1998).

Traditionally, the analysis of facial form was performed subjectively or by two-dimensional evaluation of photographs. These methods were obviously less than ideal as they were left to personal interpretation. Other methods were soon developed, with the least sophisticated including direct anthropometry (Farkas et al., 1993) and direct or non-contact measurements of facial plaster models (Mishima et al., 1996). More advanced systems were developed capable of automating the process, such as stereophotogrammetry (Deacon, 1991), moiré stripes (Kawai, 1990) and laser scanning (Moss, 1989), however these processes are time consuming, and where children are concerned, highly impractical (it is more than difficult to keep a child's head stationary for 30 seconds).

A rapid three dimensional measuring system for facial surface structure was developed to measure more than 30,000 data points in one second. This liquid crystal range finder was developed by Inokuchi et al. in1984 and used a process of grey-coded pattern projection. Within this device, a crystal optical shutter is used to project patterns of light, and a charge-coupled device video camera then captures the scene. The three dimensional co-ordinates are calculated using a space-encoding method based on the triangulation principle.

Unfortunately, all of the automated systems mentioned are very complicated and expensive and still have certain inherent problems. Even with the ability of being able to obtain 3 dimensional scans, a process of morphing the faces together to get the required average surfaces is needed.

2.4 Curved lens design and vision

The use of curved lenses within swimming goggle design is relatively new, but not particularly ground breaking. Only a few goggles within the market use the technology, even with their potential for improved hydrodynamics and aesthetic appeal. Unfortunately, there are various inherent optical problems with all of the curved lens products currently on the market, and so rather than being targeted at the performance athlete, they are sold as 'fun' goggles.

It is important to understand how lenses work at the fundamental level to be able to appreciate why there are such technical issues with curved lens design.

2.4.1 Basic properties of Light

Light is often considered to consist of rays, but for most calculation purposes, light is thought of as a sequence of waves. In this respect, they directly relate to waves in general, using similar terms of amplitude (a, wave height), wave length (λ, distance from one crest to the next) and frequency (v, number of oscillations per second).

The distance between two points which light may travel, would be referred to as distance '*L*', however the time it takes for light to travel this distance entirely depends on the medium that it travels through. For instance, light travelling through water would be slower than if it were travelling through air as it interacts with, and is hindered by the molecules of the water. Therefore, another length, '*S*', is needed to take into account the delay, and is known as the optical path length, and is a product of the distance length and the refractive index, '*n*'.

The refractive index of a particular matter, is the ratio of the velocity of light in free space '*c*' to the velocity of light in matter '*v*'. Due to the higher refractive index of matter, light appears to go through a longer optical path, as can be seen in Figure 2.15.

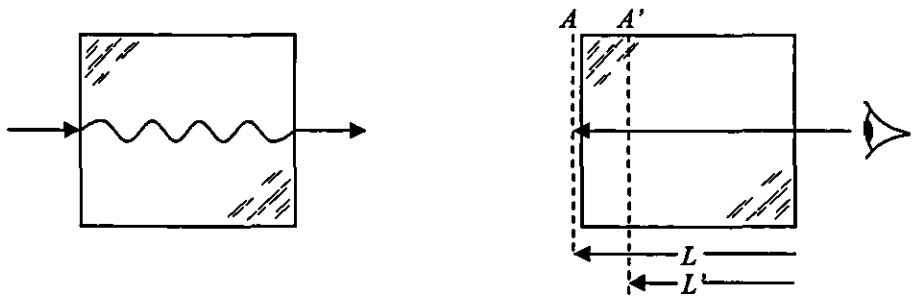

Figure 2 15, To the observer a longer optical path makes the distance appear less

The situation from the other point of view, where an observer views an object A through a medium of index 'n' almost seems to do the opposite. In reality the object is in plane *A*, but to the observer appears to be in plane *A'*. These two distances, the optical path length in air, Ln_0, and the optical path length in matter, *L'n*, has to be the same. Therefore, since the index of air $n_0 \approx 1$, the reduced distance *L'* is equal to the actual distance *L* divided by the refractive index.

Due to the fact that the refractive index is a dimensionless quantity, it has no units, and consequently the optical path length, the reduced distance and the actual distance are all measured in the same units as length in general (preferably mm).

2.4.2 Reflection & Refraction

The next area to be considered is the direction in which the light interacts with the medium that it comes into contact with.

2.4.2.1 Law of reflection

The law of reflection describes what happens to light as it is reflected at an interface dividing two uniform media. It states that the reflected ray remains in the plain of incidence and the angle of reflection equals the angle of incidence. Figure 2.16 clearly shows the beam of light within the plane of incidence and the incident and reflected angles θ_i and θ_r respectively.

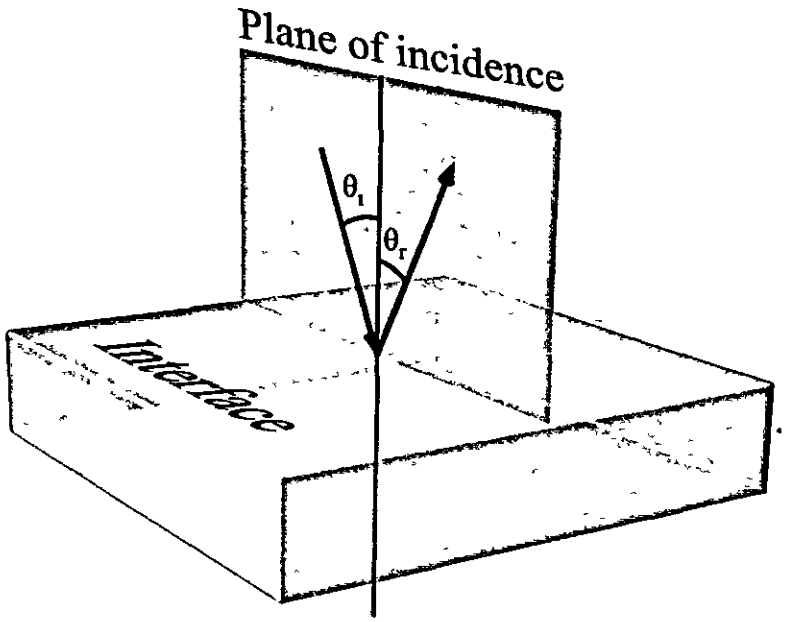

Figure 2 16, Definition of Plane of incidence

The plane of incidence can be further defined as the incident ray and the normal to the point of incidence. Surface geometry is also very important, as a beam of light reflecting off a smooth surface (where irregularities are small compared to the wavelength) is called specular reflection, where the reflected atoms form a well defined beam. In contrary, a rough or uneven surface will scatter the light in a diffuse pattern (Figure 2.17).

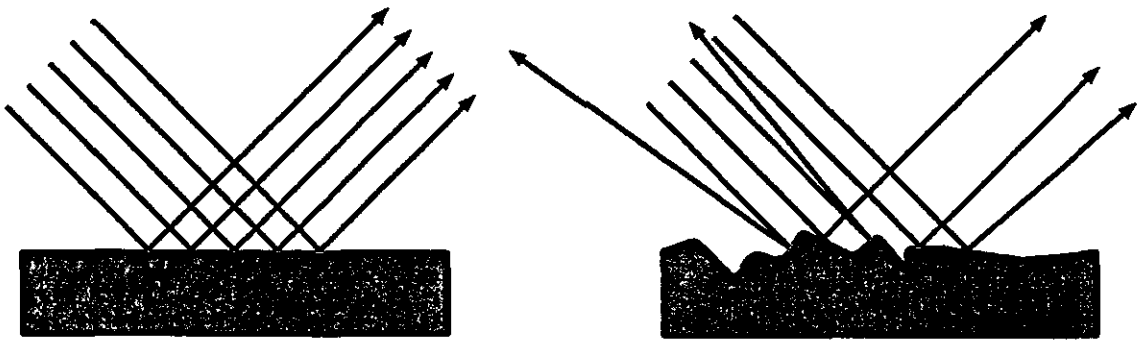

Figure 2 17, Specular reflection (left) & Diffuse reflection (right)

2.4.2.2 Law of refraction

Refraction is effectively the bending of waves and occurs where there is a difference in medium through which they travel. The law of refraction is also affected by the surface qualities at the interface. Assuming the interface is smooth the law of refraction, also known as Snell's Law, describes how the sine of the angle of refraction is directly proportional to the sine of the angle of incidence. As with the law of reflection, the incident and refracted rays are within the plane of incidence.

The equation of Snell's Law,

$n_i \sin \theta_i = n_t \sin \theta_t$

By rearranging the equation, Snell's Law can be written,

$\sin \theta_i / \sin \theta_t = n_{it}$

where $n_{it} \equiv n_t / n_i$ is the relative index of refraction of the two media.

The behaviour of the light ray can then be understood by comparing the refractive indexes of each medium, and can be described as follows:

- A ray entering a higher-index medium bends towards the normal.
- A ray entering a lower-index medium bends away from the normal.

Both of these laws are summarised in Figure 2.18. In the particular example shown, the incident ray is partially reflected and partially transmitted at the point of contact with a transparent media of a higher index.

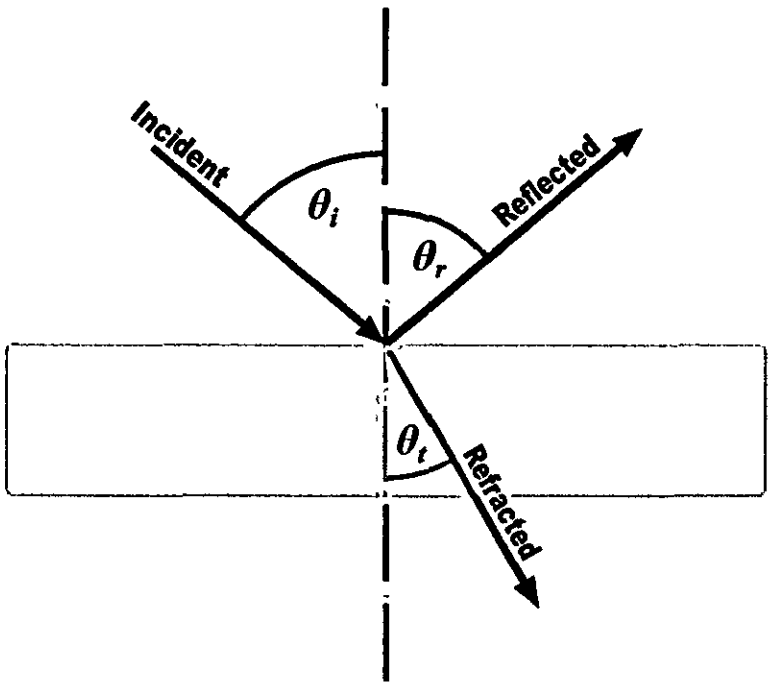

Figure 2.18, Illustration of Snell's Law

The refractive indices of different mediums necessary for swimming goggle lens design as used in the Snell's law equation, are highlighted in Figure 1.19.

MEDIUM	REFREACTIVE INDEX
Air	1.000
Water	1.333
Glass	1.520
Acrylic	1.490
Polycarbonate	1.585

Figure 2 19, Indices of refraction for different mediums

2.4.2.3 Critical Angle

There are two limiting cases that follow from the mentioned laws. If for example, light passes from a medium of lower index to a medium of higher index, and at first assume that the light is incident normal, with the angle of incidence zero ($\theta = 0$), the light is passing through without deviation. As the angle of incidence is gradually

made larger, the angle of refraction becomes larger too, although not as fast as θ. The light, therefore, is bent toward the surface normal. As θ reaches 90° and the ray is tangeant to the surface, sin θ becomes unity and Snell's law reduces to,

$n = n' \sin \theta'$

where θ' is the limiting angle of refraction.

From the other perspective, the light originates from the side of the higher index. As the angle θ is now gradually made larger, the light is bent away from the normal, at a rate faster than the increase of θ. The angle of refraction increases until a critical angle of incidence is reached for which the angle of refraction is $\theta' = 90°$ and $\sin \theta' = 1$. Snell law then becomes

$n \sin \theta = n'$

where θ is now the critical minimum angle of total internal reflection. At angles larger than that, the light is returned to the first medium. The limiting angle (of refraction) and the minimum angle (of total internal reflection) are numerically equal; they both lie in the higher index medium.

2.4.2 Lens Design

In general terms, a standard lens itself has two or more surfaces that enclose a medium of a refractive index different to that of the index outside of the lens. Any lens is completely identified by what is called its 'lens description'. This description consists of,

- The number of glasses within the system
- The glass type
- The radius of every curve
- The thickness of the lens
- The distance between the several elements
- The diameter of every lens

When a light ray, originating from an object, passes through the lens surface, it will be refracted (as mentioned before) to a certain extent depending on the refractive index. If the lens designer knows the location on the front element where a certain light ray will enter and the angle of incidence of this ray, then the path of the ray can be followed through the optical system with a high level of accuracy. The angles and distances can be determined through using sine and cosines, and therefore will relatively simple geometry, the exact path of a ray can be traced through the optical system.

A designer would begin with a small point (in fact simply a co-ordinate) located on the optical axis and trace a few rays. The object point will always be represented on the image plane as a point. All rays emanating from the object point will converge on the same image point, which has the same relative location as the object point. This is what is known as Gaussian fiction, and for object points close to the optical axis, the designer can assume that this theory holds true.

Although in relative terms, the formulae are quite simple (for a lens designer), the figures need to be calculated with an accuracy of 5 to 8 decimal places.

2.4.3 Computer Aided Lens Design – CALD

The vast number of equations involved in designing even a relatively simple lens system is completely impractical if high accuracy is to be maintained. It takes several minutes for a skilled person to trace a single ray through an optical system, and with the high number-of rays requiring tracing, not only is time an issue, but also the likelihood of human error.

With the development of the computer, it is now possible for what seemed an almost impossible task to be completed in a manner of seconds (depending on the RAM of the computer in question). The computer accounts for the rays as they propagate through the system, and mathematically, a line is completely specified if at any point both its height and slope are known. In ray tracing, the height is given by y and the slope by u, hence the expression y-u tracing.

Once a designer has entered all of the parameters into a CALD program, a graphical layout of the system can be generated. Along with this, a series of rays, including skew rays (rays that proceed in three dimensional space) can also be produced. If the results look relatively promising, some of the data within the spreadsheet can then be used as variables.

If the radius of curvature of the first surface is slightly altered, then the radius of curvature of one of the other surfaces must also be changed accordingly. If the other surface was not corrected, then the focal point would be different, and usually this other surface would be the last in the system. If this overall change has lead to an improvement of the optical system, then the change would be amplified slightly in the same direction until the trend reverses. If the variables are changed within preset limits, the computer is in effect responding to the results of its own computations and is therefore called optimisation.

However, even with the computer severely reducing the time it might take to design a lens system, the computer is still only an aid and there to remove the repetitiveness. Optimisation is still far from an ideal methodology, as on more than the odd occasion, a system will have more than one solution. Even more importantly, in certain cases where by making some changes to the overall layout, a temporary deterioration to the system will occur, but new avenues may lead to a superior final design.

Even with the knowledge of simple lens design, the development of a lens system can be extremely difficult and often considered to be an art. Therefore to design a lens system for use under water, with complete optical optimisation and with specific dimensional limitations, it would be completely unfeasible for a person with only a few months learning to undertake.

2.4.4 Mediums involved in the new lens system

In order for an underwater lens to be designed, there are at least four different types of medium that are involved and therefore must be understood; the water, the eye, the lens (may use more than one material) and the air.

2.4.4.1 Water and its effects on light

The optical properties of water are extremely variable and determined by pure water itself and the types and amounts of materials dissolved and suspended within it (such as chlorine). Water is a substance which is approximately 800 times denser than air and has a relative index refraction of 1.33. As soon as light enters the water, it interacts with the molecules and suspended particles to cause two main side affects, light attenuation and colour changes.

2.4.4.1.1 Light attenuation

Light attenuation is effectively the reduction of the amount of light energy underwater with increasing depth, and is caused by Absorption and Scattering.
When measuring the light intensity in water, the reduction in light energy with depth is mostly the result of absorption. The molecules that make up water, particulate matter and dissolved substances within the water can convert the photons, which make-up the light energy within a light beam, into a non-radiant form when the photons come into contact with the substance. This non-radiant form is usually given off as heat. As a result of absorption, fewer photons, therefore less light, are penetrating further downward into the water column.

Scattering also contributes to the attenuation of light whenever there are particles in the water. The effect of scattering, is that when looking underwater, the image appears blurry and less in focus. This is happening due to the fact that the light illuminating the object is being scattered away from its edges, causing the distinct outlines of the object to fade. Particles scatter the light in all directions via the already mentioned reflection and refraction. However, there is additional source of light manipulation known as diffraction.

Diffraction is a change in the direction of the light (Figure 2.20), due to the proximity of the particle. As a beam of light approaches a particle, the effect of the particle on water causes the light to change directions. Diffraction affects as much light as a large particle itself absorbs and scatters, doubling the amount of attenuated light by one particle (Davies-Colley et al., 1993).

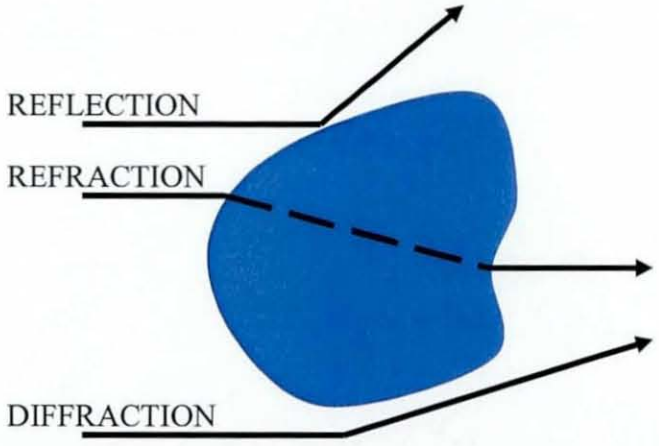

Figure 2.20, Interaction of light with particles

Scatter also leads to further absorption, as the changing directions increase the pathlength of the light, therefore increasing the probability of being absorbed.

2.4.4.1.2 Colour changes

The intensity with which a substance absorbs light depends on the wavelength of the light. It is the wavelengths that penetrate deepest that determine the colour of the water. For example, water molecules selectively absorb energy from lower energy wavebands in the reds, yellows and greens, leaving only blue light. Certain calculations can be made to predict approximately when each colour disappears (Figure 2.21), although this is quite dependent on the specific water in question.

Light colour	**Depth light disappears at (m)**
Red	30
Green	250
Blue	700

Figure 2.21, Depth colour of light disappears at in water

2.4.4.2 The Human Eye

2.4.4.2.1 Physiology of the human eye

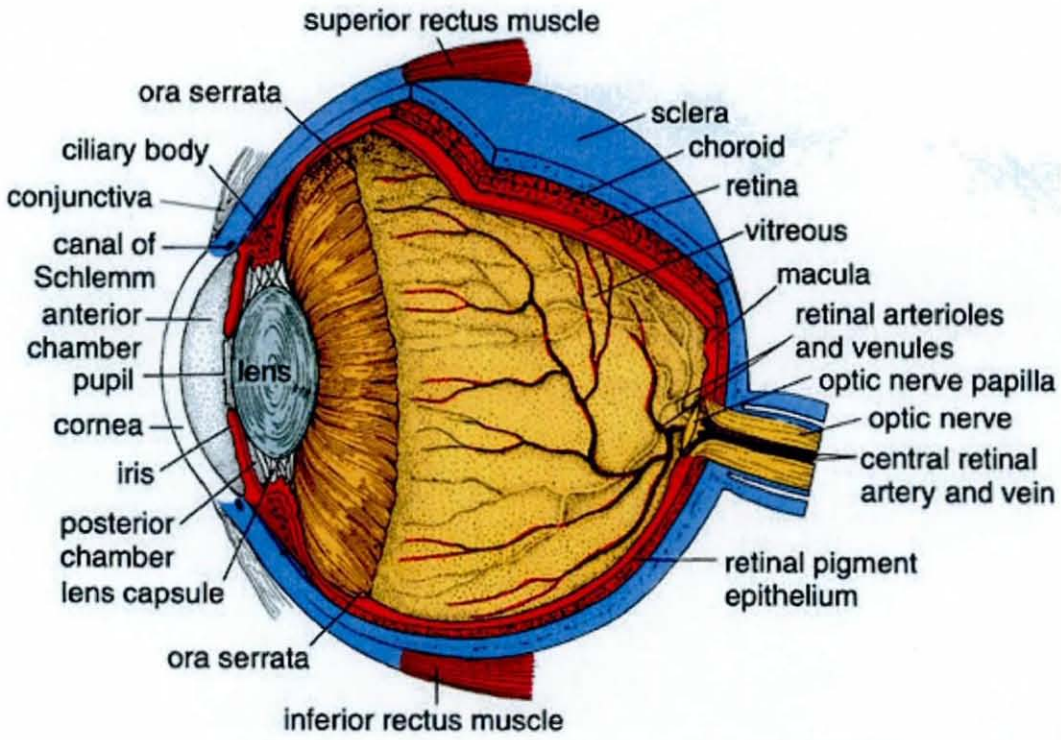

Figure 2.22, Cross-section through the human eye, (www.brother.com/europe/printer/advanced/lcv)

PART OF THE EYE	DESCRIPTION	FUNCTION
Ciliary muscle	Ring of muscle fibres around lens	Controls lens thickness and curvature
Conjunctiva	The membrane covering the exposed front part of the eye, and lining the eyelids. It is kept moist by antiseptic secretions from the tear glands.	Protects the cornea
Cornea	Front part of the tough outer coat, the sclera. It is convex and transparent.	Protects front of eye and bends light to form an image on the retina.
Iris	Pigmented (decides the colour of your eyes) so light cannot pass through. Its muscles contract and relax to alter the size of its central hole or pupil	Protects the photoreceptors in the retina from being damaged by too much light
Lens	Transparent, bi-convex, flexible disc behind the iris attached by the suspensory ligaments to the ciliary muscles	Brings the light entering through the pupil to a focus on the retina. The ciliary muscles control the lens' thickness and curvature

Optic nerve	Bundle of sensory neurones at back of eye.	Carries signals from the photoreceptors of the retina to the brain. At the point where the sensory neurones leave the retina to form the optic nerve - the so-called 'blind spot' - there are no rods and cones, and no image can therefore be seen
Pupil	A black hole in the centre of the iris. It is the dark pigmented layer inside the eye - the choroid - which makes the pupil appear black.	Allows light to enter eye
Retina	The lining of the back of eye containing two types of photoreceptor cells - rods (sensitive to dim light and black and white) and cones (sensitive to colour) A small area called the fovea in the middle of the retina has many more cones than rods.	Screen on which images are formed as a result of light being focused onto it by the cornea and lens. The fovea is the point of maximum visual sharpness.
Suspensory ligaments	Ligament between lens and ciliary muscle	Supports lens and connects it to the ciliary muscle

Figure 2 23, Features of the eye and their function.

In very simple terms, the eye effectively acts like a pin-hole camera, with a lens that forms an upside down image on a light sensitive screen. However, due to the fact that the eye has to focus on objects near and far, the system becomes far more complicated.

On entering the eye, the light passes through the cornea (the 1st surface of the system) and then the anterior chamber, which is filled with the aqueous humor. This chamber is bounded by the iris with a central hole that's diameter adjusts according to the wavelength of light passing through. This is known as Adaption, and is the eye's ability to respond to varying signals of brightness from very dim to very bright. This range of light intensity can vary by as much as 10^5. The amount of light entering the eye is obviously first regulated by the iris. The pupil can range from 2mm in very bright light to 8mm in dim conditions to allow as much light as possible. The pupil's adjustment is only one part of the eye's ability to adapt.

Following this, is the Crystalline lens which is particularly rich in proteins which help maintain the high transparency and refractive index of 1.41 at the centre and 1.37 at the equator. The curvatures of the surfaces of the lens are controlled by the circumferential ciliary muscle. After passing through the large central area, known as the Vitreous, the light reaches the retina which also has the ability to adapt. Photoreceptors in the retina (rods and cones, Figure 2.24) contain a pigment called visual pigment which changes chemically depending upon the intensity of light received. The rods are most stimulated by low level light (scotopic vision) and the cones more sensitive to higher intensity light and of variable colour composition. These photoreceptors then send the chemical signals to the brain where they can be translated into a visual image.

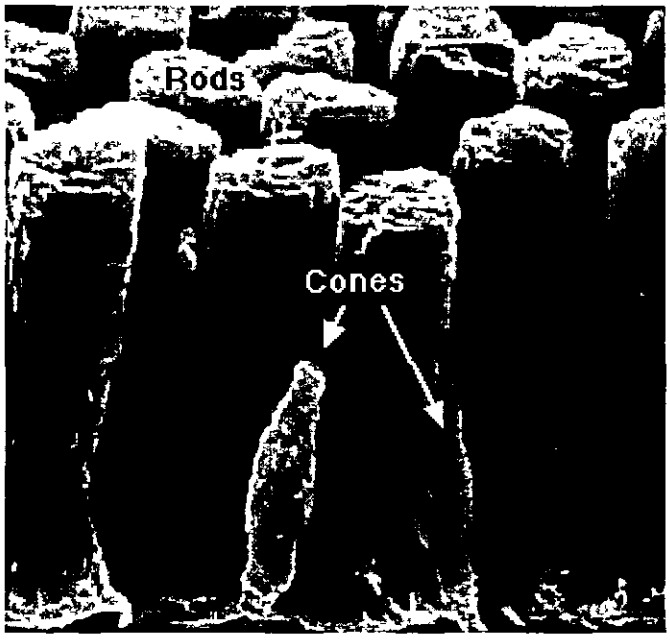

Figure 2.24, Photoreceptors in the retina,
(www lis inpg fr/pages_perso/herault/Documents_files/Lectures/pres_HTML/3_Retina/)

For purposes of lens design, a 'reduced eye' can be used which is generally considered to have a radius of curvature R = +5.7mm. The two focal lengths are f_1 = -16.8mm and f_2 = +22.5mm, and the power is +60 diopters (a unit of measurement of the refractive power of a lens which is equal to the recipricol of the focal length measured in meters).

When a more complicated system is required, Gullstrand's schematic eye is used as it has 3 represented surfaces (Meyer-Arendt J, 1995). The three surfaces are the front surface of the cornea and the front and rear surfaces of the lens

Focusing of the eye is brought about by accommodation. Accommodation of the eye refers to the act of physiologically adjusting crystalline lens elements to alter the refractive power and bring objects that are closer to the eye into sharp focus. Contraction of the ciliary muscles relaxes the tension on the lens that rounds its shape by virtue of its elasticity while also moving forward slightly. The net effect of the lens changes is to adjust the focal length of the eye to bring the image exactly into focus onto the photosensitive layer of cells residing in the retina. Accommodation relaxes the tension applied through zonule fibers to the crystalline lens, and allows the anterior surface of the lens to increase its curvature. The increased degree of refraction, coupled with a slight forward shift in the position of the lens, brings objects that are closer to the eye into focus.

Focus in the eye is controlled by a combination of elements including the iris, lens, cornea, and muscle tissue, which can alter the shape of the lens so the eye can focus on both nearby and distant objects (Figure 2.25).

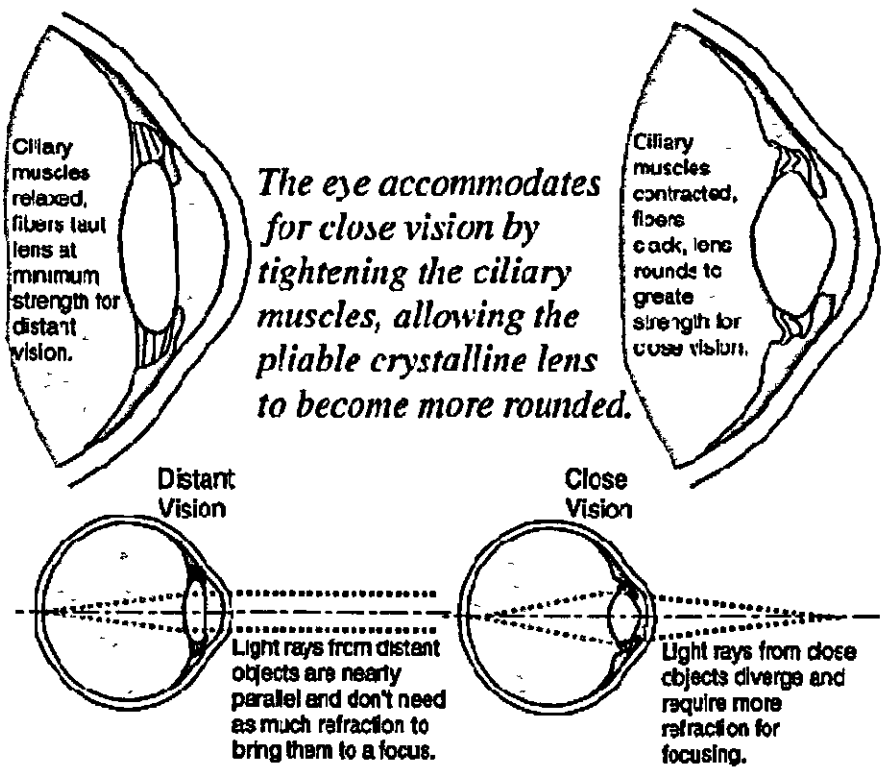

Figure 2 25, Accomodation of the eye, (www.crescentlighting com/onlinetrain/images/)

The human eye can function from very dark to very bright levels of light - its sensing capabilities reach across many decades. This means that the brightest and the darkest light signal that the eye can sense are a factor of roughly one billion apart. However, in any given moment of time, the eye can only sense a contrast ratio of one thousand. What enables the wider reach is that the eye adapts its definition of what is black. The light level that is interpreted as "black" can be shifted across six decades - a factor of one million. If you move from bright sunlight to a completely dark room, it will take your eye about half an hour to adapt to maximum sensibility - one million times more sensible than at full daylight. In this process, the eye's perception of color changes as well.

2.4.4.2.2 Stereoscopic Vision

The majority of sporting activities require the judgment of an object moving or stationary in their field of vision. Stereoscopic vision is the ability to judge an object's depth or position within a three dimensional field. Stereoscopic vision requires the use of both eyes, as their distance apart provides two different images that can be interpreted by the brain into one image based in three dimensions (known as binocular vision. However, this is not to say that humans are incapable of depth perception through one eye, as other visual clues such as familiar objects, perspective, parallax or shadowing from the surrounding field allow whats known as monocular vision. Although to maintain a reasonable level of accuracy of depth awareness, binocular vision is most important.

When the axis of the eye or optical system is not correctly aligned, then double vision will occur as the object images do not fall on the correct path for the retina. This effect can be seen when an optical device such as a pair of binoculars are not correctly aligned to the viewers face. The image seen will be two circular images that do not overlap. This can be translated to when a pair of swimming goggles are not fitted evenly over each eye, and the resultant image viewed is blurred due to the off axis alignment of the lenses. As shown in Figure 2.26, the total field of view is approximately 210° of which the central 120° are binocular overlap.

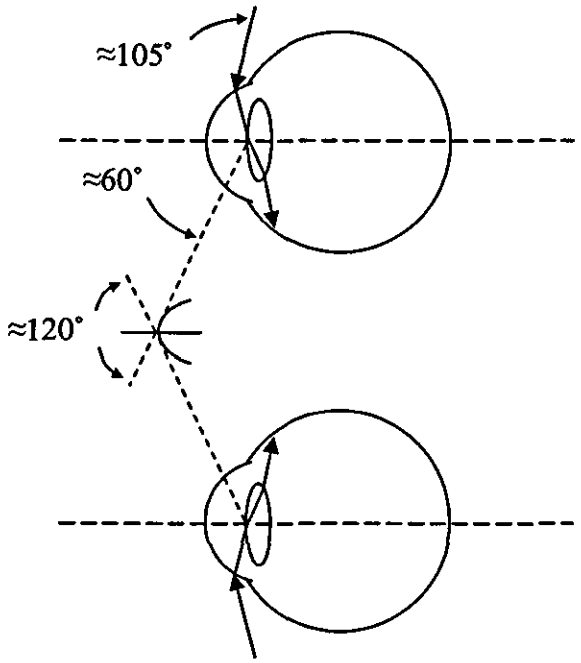

Figure 2 26, Horizontal field of view in monocular and binocular vision

2.4.4.2.3 Visual Acuity

Visual acuity (often referred to as "Snellen acuity") is concerned with the clearness of vision from which details and shapes of objects can be distinguished. The word 'acuity' comes from the Latin word 'acuitas', which means sharpness. For the eye to be able to resolve the image correctly, the optical system, such as a pair of goggles must not impact on the maximum resolving power of the human eye.

There are four major factors that affect visual acuity including, size, luminance, contrast and time (Figure 2.27).

SIZE	Size is the most generally recognised and accepted factor in seeing. Visual acuity is dependent upon the size of an object, which affects the size of the image on the retina. When the object is brought closer to the eye, the visual angle is being increased, and it is this visual angle that the object subtends at the eye that is most important.
LUMINANCE	Luminance is dependent on the amount of light striking a surface and the amount of light being reflected back to the eye. It should not be confused with brightness, which is simply a subjective

	evaluation of the amount of light reaching the visual system. Surfaces with low reflective values require more light than those with high reflective qualities if the luminance is to be equal. Comfort and visibility are dependent upon the luminance patterns within the visual field. Comfort is dependent on the variation in luminances in the visual field (luminance ratios). Visibility is affected by the adaptation state, quality of luminance patterns, and clutter within the visual field. Clutter can create an overload of the visual system due to excessive luminance ratios.
CONTRAST	Contrast is the basic seeing mechanism in vision. Contrast is a measure of the ability of an observer to distinguish a minimum difference in luminance between two areas a given percentage of the time. The contrast threshold is expressed as a fraction. The surrounding luminance is much greater than the target luminance, the task contrast will be lost and the target will go into silhouette. If surrounding luminance is much less than target luminance, the task contrast may not be affected by excessive luminance but may create discomfort, and hence a reduction in visibility. To see surface detail, that is to have good surface discrimination, the luminance ratios in the visual field must be controlled. Maximum visual efficiency occurs when the surrounding luminance, has a ratio to target luminance that ranges from 1/10 to 1.0. The highest visibility occurs when the object is brighter than the background (white print on black paper).
TIME	Time is the fourth factor that affects visual acuity. Seeing is not instantaneous. A time lag exists in the electrochemical processing of the retinal signal that reaches the brain. As the level of background luminance increases, the time required to interpret details will decrease. Just as the camera requires a longer exposure time in dim light than in bright light, so does the eye. The eye can distinguish and discriminate details at low luminance levels if given enough time

Figure 2.27, Factors affecting visual acuity

2.4.4.3 Eye defects (Refractive Anomalies)

Although it would be unlikely that a pair of goggles would be designed and manufactured specifically for a person with an eye defect, an understanding of the reasoning behind the resolving of such a problem may be of some benefit. The two most common refractive errors of the eye are myopia (nearsightedness) and hyperopia (hypermetropia, farsightedness).

In myopia, the image of the distant object is seen out of focus as it is formed in front of the retina. If an object is nearer than a specific 'far point', only then will it appear on the retina and therefore in focus. The use of a minus lens corrects this problem, as it makes the object appear as if it were coming from the 'far point'

At the other end of the spectrum, hyperopia makes the object appear behind the retina. If a correction lens is used to make the second focal point coincide with the 'far point', then the image once again appears on the retina where it should be. Cataracts are also quite common on the crystalline lens of the eye rendering them useless. A slightly invasive surgey technique allows Intraocular lenses (IOL) to be implanted in the eye to replace the natural crystalline lens of the eye that would need to be removed. A typical IOL is made from polymethyl methacrylate, has a diameter of 5 to 7mm and is supported by haptics (flexible loops). Bifocal and even multifocal lenses can now be achieved, but most are still monofocal.

2.4.5 Performance measurement of the eye

The purpose of this chapter is to evaluate a new lens technology, and as the new lens should practically mimic vision in air while in the water, the performance of the eye in air should be no worse than the performance of the eye looking through the lens in water. It is therefore quite apparent that current testing techniques for measuring all performance characteristics of the eye would be useful in measuring performance of the lens.

There are seven main tests that a doctor would initially perform to define a patients visual abilities:

- Eye alignment
- Near convergence – point at which both eyes together can see a single image
- Near point of accommodation – closest point at which an image is clearly seen
- Stereopsis – ability to see three dimensionally
- Colour vision
- Peripheral (side) vision
- Visual Acuity

2.4.5.1 Eye Alignment

To ascertain as to whether there is a deviation of the eyes is generally quite straight forward. Measuring the extent of this deviation on the other hand, can be considerably more complex, and requires a greater understanding of optics. There are several different methods used, some of which are considered better than others.

2.4.5.1.1 Cover testing

During cover testing, the patient is asked to focus on a particular target, and then the examiner covers one of the eyes. Immediately afterwards, the opposite eye is examined for any movement to pick up fixation on the target. If there is such movement, the eye is deemed to be misaligned in the direction that it moves towards.

2.4.5.1.2 Alternate Cover Testing

During Alternative Cover Testing, the eyes are alternatively covered numerous times to dissociate the eyes into maximal deviation. Once completely dissociated, the deviation is then neutralized by placing prisms in front of either eye. When the prism power in front of one eye prevents movement of the eyes as the cover is alternatively switched from one eye to the other, then neutralization has occurred. The prism power is recorded, which signifies the degree of misalignment.

2.4.5.1.3 Hirschberg Test

During the Hirschberg test the examiner shines a light at the patient and observes the reflection of light from the cornea (known as the corneal light reflex). This corneal light reflex is usually slightly nasal to the centre of each cornea, and therefore if positioned elsewhere, there is misalignment. The eye is deviated nasally (estropia), if the reflex is positioned lateral to the centre, whereas if positioned nasal to the centre, then the eye is deviated laterally (extropia). Simple nomograms can be used to approximate the angle of deviation.

2.4.5.2 Near Convergence

The Near Convergence test is used to ascertain whether or not the patient has the ability to maintain binocular function while working at a near distance. It is effectively making sure that the two eyes are working together. The examiner will ask the patient to focus on a near target, and as it is brought closer, the patient has to state when the target becomes two images. There is a normal range at which a person should be able to see a single target. In certain cases, one eye will turn outward, and this is known as intermittent exotropia.

2.4.5.3 Near point of accommodation

Accommodation of the eye is usually tested by a very simple technique. The doctor will move an object gradually closer to the eye until the participant can no longer focus on that object.

2.4.5.4 Stereoscopic Vision

The purpose of Stereopsis testing is to ascertain as to whether or not the eyes are working together. When the brain is able to blend the separate images from each eye into one complete image, then the person can perceive three-dimensional space and is said to have binocular vision, or stereopsis.

Although there is more than one test available, they all work along a very similar theme and the Howell Phoria card is most commonly used to assess binocularity of vision. The card is placed at a set distance from the patient and has a horizontal line with numbers at regular distances along the line. An arrow points to the centre of this line and a prism is held in front of the patient's eye which frees the eyes ability to roam. As one eye is focused on the card and the other viewing through the prism, the arrow will appear to hover at a point on the scale. This number corresponds to a person's binocular vision.

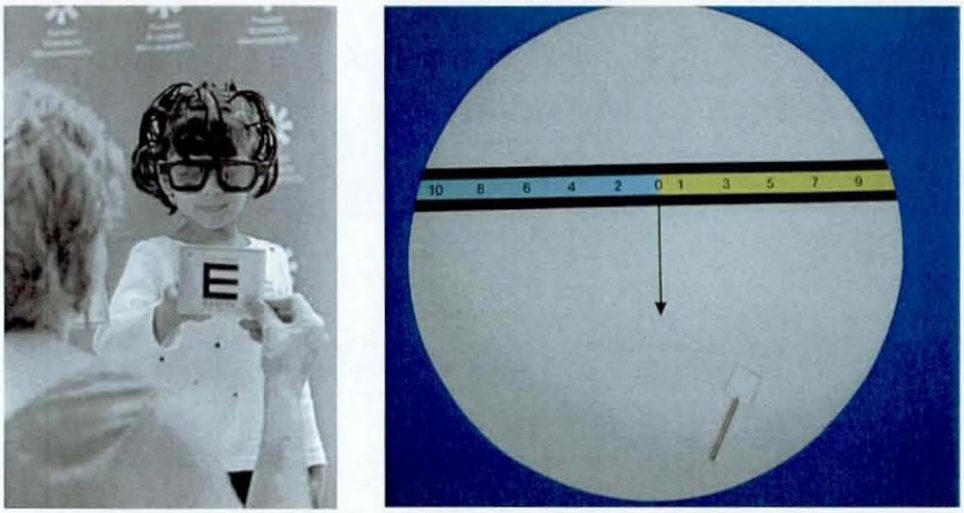

Figure 2.28, Random Dot E technique (left) and the Howell Phoria card (right) used for testing Stereopsis

The second most commonly used technique is the 'Random Dot E' test, and is where a raised 'E' figure on a demonstration card is employed (Figure 2.28). The participant is shown the card and told that the 'E' is 'popping off the card', and then asked to point at it. A pair of polarized glasses are to be then worn by the participant, and mixture of blank cards with one 'E' card is shown randomly at a distance of 5 feet. If the person identifies the 'E' card four out of five trials, the participant has passed (Am J, 1994).

More recently techniques (in the form of the Titmus Stereo, the Stereo Reindeer , the Random Dot Butterfly, the Random Dot Figures, circle, square and the Random 'E' tests) have been developed that no longer require the use of a prism or polarized glasses. These polarized-free tests employ a special prismatic printing process

creating a panagraphic presentation. This is where a separate image is presented to each eye without the need for polarization.

Through certain studies, it was concluded that these five polarized-free tests were just as valid in measuring the subjects' stereopsis as their traditional polarized version. The use of goggle-free testing has potential clinical advantages, e.g., testing of young children who will not wear the glasses or the improved observation of the ocular alignment during stereopsis testing (Hatch SW & Richman JE, 1994).

2.4.5.5 Colour Vision

Eye conditions that cause defects in colour vision are in actual fact more common in the male population. In the most part, the colours that cause most confusion are the reds and greens, however, some individuals have problems with colours in the blue-yellow range. The standard test for assessing colour vision defects is the Pseudoisochromatic plates and an example of these are shown in Figure 2.29.

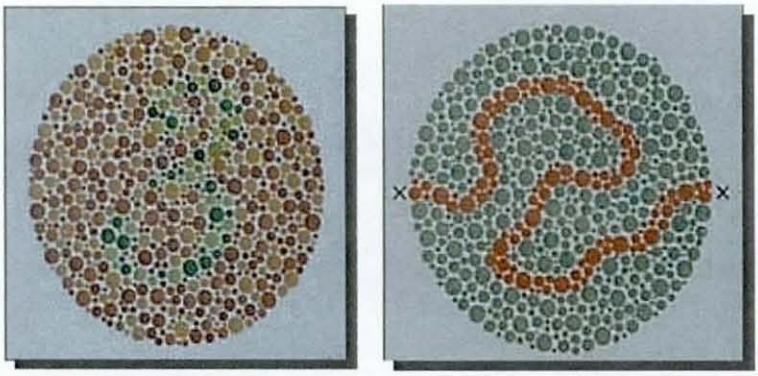

Figure 2.29, Pseudoisochromatic plates used for colour vision testing

There are many different plates available, that have distinct patterns such as numbers, letters, figures, or a winding path within a series of dots that vary in hue and brightness from the background. For example, one plate may have a background of orange dots and the number '4' will be displayed using olive dots. A person with 'normal' colour vision will be able to readily distinguish this, but to someone who is dichromatic (to colours appear to be the same), the number '4' will not be visible.

2.4.5.6 Peripheral (Side) Vision

The Aimark is a piece of test equipment that has been around for many years, but it still useful in relatively accurately assessing peripheral vision. The device accommodates the participant with a chin rest located at the centre of rotation. The participant is required to look straight ahead at a fixation point or crosshair on the device. The optician then moves a small white ball until the patient indicates that they have seen this ball. The subsequent angle from the fixation point and the centre of rotation describes the maximum extent of peripheral vision.

Field screen testing is very similar to the Aimark except it is a modern day equivalent, whereby the participant places there head into a spherical chamber and lights are illuminated and extinguished by pressing a button.

A very quick and simple test can also be achieved without the use of any additional equipment. However, the confrontation visual field test is a method that only allows detection of large field defects. A participant sits facing the tester approximately 1 meter away and instructed to look at the testers nose and cover their own left eye. The tester then covers their own right eye so that the visual fields correspond, and holds up fingers in each of the visual quadrants for the participant to count. If the participant cannot see one or more fingers in any quadrant, then the defect can be explored by placing a small object, such as a cotton tipped applicator, in the non-seeing area and moving it until the object can be seen by the patient. The same procedure is repeated for the left eye.

2.4.5.7 Visual Acuity

There are a number of tests used to measure the maximum eye resolution, for example, Logmar and Peli Robson, but the most commonly used is the Snellen eye chart and this it is why it is often called the 'Snellen Acuity'

The tests generally come in either 3m or 6m test distances for use in air and have a high contrasting black on white format. More advanced charts are automated with a revolving screen or can be displayed on a digital screen.

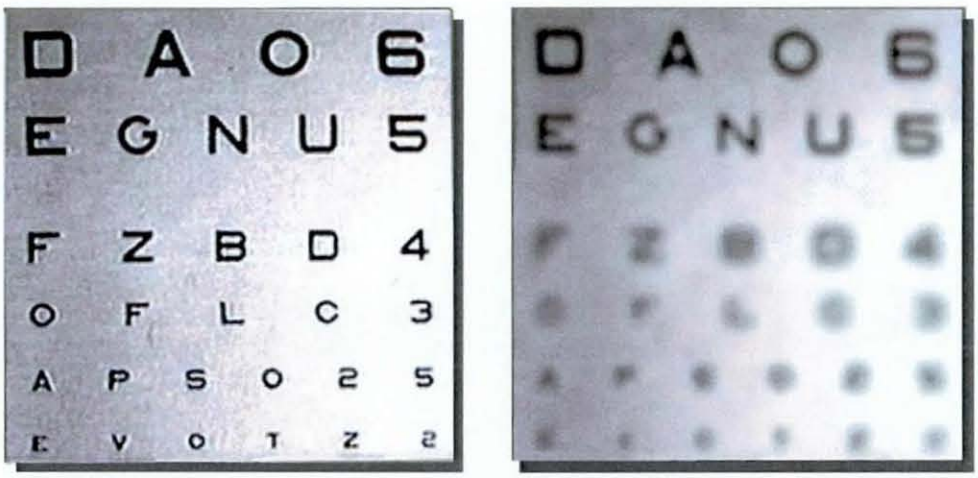

Figure 2.30, Example of the Snellen Chart (left), viewed from the perspective of a person with less than 20/20 vision (right)

When talking in relation to visual acuity, people associate 20/20 to having perfect eyesight, however in Britain opticians more commonly use 6/6. The reason the number '20' is used in visual acuity measurements is because, in the United States, the standard length of an eye exam room (patient to chart) is 20 feet (which is approximately 6m, and considered close to optical infinity).

A person with 6/6 vision (visual acuity) is just able to decipher a letter that subtends a visual angle of 5 minutes of arc (written 5') at the eye. (5' of arc is 5/60 of a degree, because there are 60' of arc in 1 degree.) This means that if you draw a line from the top of a 6/6 letter to the eye and another line from the bottom of the letter to the eye, the size of the angle at the intersection of these two lines at the eye is 5' of arc. (Also, the individual parts of the letter subtend a visual angle of 1' of arc at the eye.) It does not matter how far away something is from the eye; if it subtends an angle of 5' of arc at the eye, then a person with 6/6 visual acuity will just be able to determine what it is.

A mentioned previously, the statement about a person who has 20/20 vision having perfect eyesight is not entirely correct, it is simply considered to be normal eyesight. The number itself is a ratio, and the less the bottom number is, the better the eyesight (a person with truly excellent eyesight may have a ratio of even 20/10).

The distances involved when setting up the test area for measuring visual acuity should be accurate in relation to the sizes of letters. However, in general, the size of a 20/20 letter (in millimeters) is .4433 × d (where d is the viewing distance in feet).

2.4.6 Vision defects as a direct result of using a lens

All of the areas of vision that have been researched up to this point are directly linked to the performance of the eye. However, the lens itself can cause additional problems relating to viewing an object.

One of the defects seen in images when viewed through a lens is called chromatic aberration. Chromatic aberration is caused by the dispersion of the lens material, the variation of its refractive index with the wavelength of light.

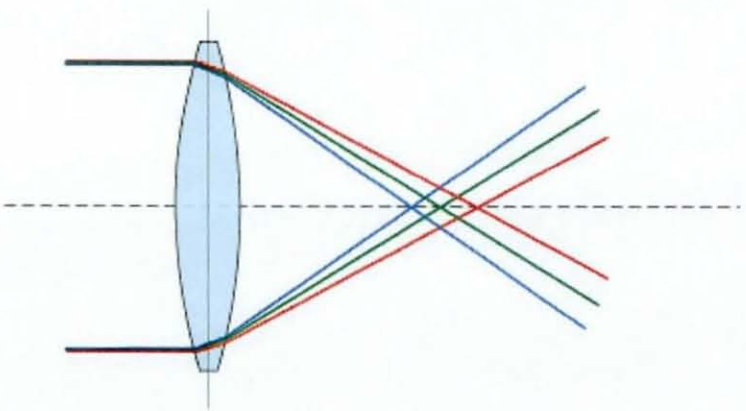

Figure 2.31, Chromatic Aberration

Since the focal length of a lens is dependent on the wavelength, different wavelengths of light will be focused on different positions. Chromatic aberration of a lens is seen as "fringes" of colour around the image. This is due to the fact that each colour in the optical spectrum can not be focused at a single common point on the optical axis. However, there is a point that exists called the circle of least confusion, where this effect can be minimized.

The use of a strong positive lens made from a low dispersion glass (such as crown glass), coupled with a weaker high dispersion glass (such as flint glass), can further reduce the effect of chromatic aberration for pairs of colours, e.g., red and blue. This pair of lenses are often cemented together and known as an achromatic doublet (Figure 2.32).

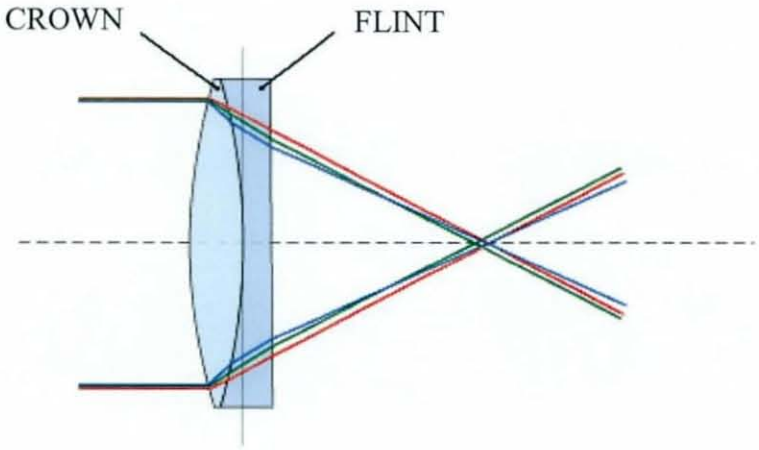

Figure 2.32, Example of an Achromatic Doublet.

2.4.7 Overview of the interaction of the complete underwater system

The human eye is set up to be at its optimum in air. The relative index of refraction between the cornea and the air, provides the necessary power of refraction so that light travels directly through the eye and is focused correctly on the retina. If however, the medium at which the incident ray is interfacing with the cornea is different, then this refractive power is altered and the eye can no longer operate efficiently. By wearing a pair of swimming goggles, the air/cornea interface will be restored due to the relative index of refraction between the cornea and the air trapped inside the swimming goggle.

This application solves one problem, but also brings with it another set of issues. The goggle is now providing a barrier between the water and the eye. It is at this barrier interface between the water and the goggle lens that causes the first problem. Refraction occurs at the interface and drastically affects what the eye sees through the goggle. An object viewed when fully submerged appears to have a magnify effect. Due to the fact that the relative index of refraction of water and air is 1.33 and 1.0 respectively, the object appears one third larger and therefore 25% closer to the viewer than is in fact the case.

When using a curved lens (depending on the specific radii involved), the magnification is in part amplified and distortion of the image is also increased.

2.4.8 Current Swimming Goggle Lens Technologies

There are currently three general types of lenses found in modern swimming goggle products, including the flat (plano) lens, the arc shaped lens (curved in a single plane) and the spherical lens (curved in three dimensions).

2.4.8.1 Flat (Plano) Lens

The front face of the goggle lens is completely flat with a pronounced shoulder where the lens and the contoured walls of the goggle join to fit securely around the eye socket. A good example is the minimalist design of the Swedish type of goggle as seen in Figure 2.33.

Figure 2.33 Example of a swimming goggle using a flat (plano) lens.

This type of lens is the simplest and cheapest to manufacture and least affect overall magnification and visual distortion.

2.4.8.2 Arc Shaped Lens

Arc shaped lens goggles have a curved surface in one plane which is usually wrapping around the face from nose to ear. This type of lens is more costly to design and manufacture, and the optical properties are always quite poor. The reason for their existence, is their potential for improved hydrodynamics and aesthetic appeal.

2.4.8.3 Spherical Shaped Lens

This type of lens is similar to the Arc shaped lens, but instead is curved on both planes of the viewing surface. Their potential for improved hydrodynamics is even greater, but with it comes even worse optical properties.

2.4.9 Current Lens Technologies from other Fields

2.4.9.1 Fluid Goggles

Along a very similar path to the standard swimming goggle, a recent product has been developed that replaces the air void (surrounding the eye) with a saline solution. Originally developed by freedivers, 'fluid goggles' relieve the discomfort caused by ordinary air-filled masks in deep dives, as being fluid, they equalize with the surrounding water pressure. They are engineered with corrective lenses to optically compensate for lack of air on the eyeball.

Unfortunately, due to the very nature of the fluid goggle, saline solution has to be carried around with the user at all times in case of leakage. They also cause considerable magnification out of the water, and there is little possibility of being able to incorporate bi-focal abilities.

Figure 2.34, Saline being used to fill a pair of 'fluid goggles'.

2.4.9.2 Underwater cameras

The design of the swimming goggle lens draws many similarities to the underwater camera lens, as they have the same optical system of air / transparent material / water interface and inherently have the same problems.

The effects of viewing through a lens underwater can cause images to be distorted or have blurriness around the perimeter of the object due to chromatic aberration. This distortion can be described as Pincushion where the magnification of the outer portions is greater than the magnification of the centre portion, or Barrel distortion which is the opposite and results when the magnification of the outer portions is less than the magnification of the centre portions of the image. Also, the chromatic aberration caused by the dispersive nature of the transparent material blurs the edges of the object because of its inability to focus light of all wavelengths onto a single point.

Figure 2.35, 'Fisheye' spherical port used on certain under water cameras, *(www.photo.net/learn/underwater/uw2/housings.html)*

There are currently devices in the photographic world that address the previously mentioned problems, but have their own specific faults, mainly being quite large in volume. A spherical port (often known as 'fisheye') can be used to form a window around the lens and its centre point (Figure 2.35). This method practically eliminates image deterioration, however, it does not prevent the considerable magnification effect.

A lens using this technique in conjunction with swimming goggle design would be far too large (as well as magnify), and therefore another solution is required. The Ivanoff-Rebikoff correcting lens has been developed to solve all the mentioned problems and effectively consists of a negative lens followed by a positive lens.

2.4.9.3 Fresnel Lens

Two areas of investigation which generally would not be considered to help with swimming goggle lens technology are Spacecraft and Lighthouses. One of the main problems with the previously mentioned 'fish eye' is the volume that it takes up. A lens that could maintain all of its benefits while being reduced drastically in size could be of considerable benefit, and this is where the Fresnel lens comes in.

Augustin Fresnel worked out a number of formulas to calculate the way light changes direction, or refracts, while passing through glass prisms. Working with some of the most advanced glassmakers of the day, he produced a combination of prism shapes

that together made up a lens. The Fresnel lighthouse lens used a large lamp at the focal plane as its light source. It also contained a central panel of magnifying glasses surrounded above and below by concentric rings of prisms and mirrors, all angled to gather light, intensify it and project it outward.

Figure 2.36, Fresnel lens used on lighthouses

The technology, although barely changed in theory, has been developed significantly to the stage where it is an essential part of certain space travel. In the middle of the 1990's, a new line-focus Fresnel lens concentrator was developed and formed the basis of the Scarlet solar array. This system used an 8.5cm wide aperture glass/silicone laminated Fresnel lens to focus sunlight at 8x concentration onto radiatively cooled triple-junction cells. In simple terms, it effectively powered the spacecraft.

In order to use this technology for a swimming goggle lens, the process would have to be slightly altered. Instead of trying to make a flat lens perform the function of a curved lens, a 'lesser' curved lens would be performing the function of a large curved lens.

3.0 MEASUREMEENT OF FACIAL SKIN SENSITIVITY – An aid to assess seal location

3.1 Introduction

In order for swimming goggles to be designed so that their comfort and fit potential is exploited to the maximum, an in depth knowledge needs to be gained about all relevant facial parameters. One of the more significant of these being localised skin sensitivity. The availability of this data would aid designers to scientifically evaluate where the seal should be positioned when exclusively concerned with comfort. Other factors such as hydrodynamics and facial movement would also need to be considered and so a compromise will eventually have to be made.

3.2 Chapter Aims

It is quite apparent from the literature review, that the perceived comfort of an object pressed against a persons skin, is directly linked to the type and density of sensitivity receptors in that region. The variation in these types of skin receptors and their density between different parts of the body is quite considerable. The variation within a single part of the body, such as the face, can also be quite substantial. It would therefore be logical, that if the seal path could be positioned on an area where the skin sensitivity is low, then the perceived comfort should be relatively high.

The aim of this chapter is to therefore map the sensitivity of the facial region where the path of a goggle seal could be positioned.

3.3 Chapter Objectives

The objectives of the chapter are;

- To evaluate all current skin sensitivity measurement techniques.
- To either develop an existing measurement technique, or generate an entirely new method of measuring skin sensitivity with the required measurement resolution.
- To measure the facial skin sensitivity of a given number of participants and then calculate the averages for each measurement location.

3.4 Background

3.4.1 Current seal positions with relation to the eye

The vast majority of all standard swimming goggles (those using a conventional nose bridge and strap system) use an almost identical seal footprint around the socket of the eye. The small differences that do occur are generally made to either try and reduce the size of the overall profile of the goggle for performance enhancement, or to increase the size of the seal for improved comfort. Good examples of these are the Speedo Aquablade racing goggle and the Speedo Airframe training goggle. The Aquablade is made from one material and has no flexible sealing system, relying on the compression of the facial tissue around the eye socket to ensure no leakage. The Airframe is at the other end of the spectrum and rather than using the more common style of seal, it uses an air filled pocket to provide added cushioning and therefore higher comfort.

Figure 3.1, Pictures of the Speedo Aquablade (left) and Airframe (right) showing variances in profile

It can easily seen from Figure 3.1 that the footprint of the seal has been only slightly increased in the Airframe, with the most notable difference being the amount the goggle protrudes from the face. Once again, this illustrates that even at the extreme ends of goggle design, the seal footprint varies only a relatively small amount.

3.4.2 Why is there little variation between modern seal positions?

Looking at the history of swimming goggles, it would be easy to assume that the best position for the seal footprint of a racing goggle would be like that of the Speedo Aquablade or the conventional Swedish type goggle. In circumstances where goggles have been designed with more contemporary and larger footprint styles, it has usually resulted in a more bulky goggle aimed at either children or the 'fun' swimmer.

Situations where the footprint is seen at its largest is only ever seen in either diving masks or the more recent swimming/watersport mask category (Figure 3.2), again aimed at the 'fun' swimmer, but becoming more and more popular. The only apparent reason for this increased footprint, is so that the lens dimensions can be increased to improve the viewable area.

Figure 3.2, Speedo Watersports mask

As mentioned before, the problem with past swimming goggle design, has been the lack of any real scientific data. New goggles are generally based on the success of old goggles, and with this approach new radical technologies will never be developed. Wiping the slate clean, and building the design from scientific data and modern research will hopefully prevent mistakes of the past. Rather than asking swimmers what they want, a development process of assuming they don't know what they want and instead giving them what they need, should be more productive.

3.4.3 Limitations of positioning the seal footprint

The human face is a very irregular structure, varying from person to person. The problem is further compounded with interior details such as muscles, bones, tissues, and motion which involves complex interactions and deformations of different facial features. Expressions and movements of one part of the face can therefore effect positions of facial features elsewhere. The face has many muscle groups (Figure 3.3), however, only a small proportion might have an effect on the movement of the skin in areas where a seal could be positioned.

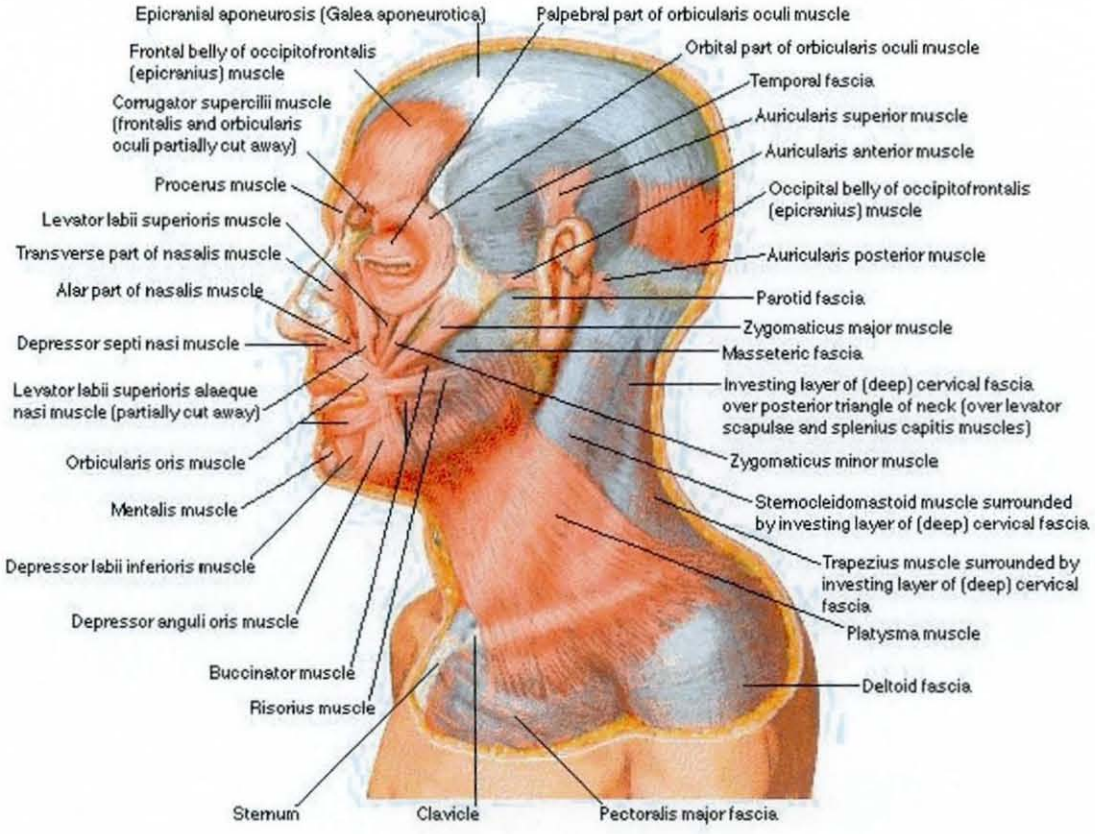

Figure 3.3, Muscle groups of the face

Ideally, the top of the seal should be positioned below the brow, while the bottom of the seal should be positioned as close to the bottom of the eye as possible. This would give the minimum amount of movement between the skin and the seal through all motions of the face. However, this does not mean that the seal footprint can not lie outside of these boundaries. In products such as diving masks, the top and the bottom of the seal footprint both extend beyond these boundaries, and yet the seal is still water tight and comfortable. With the correct seal design, there is no reason that the footprint should not extend to as far down as just above the mouth line. Conversely, if the footprint were to go below this boundary, the movements involved in opening the mouth (for breathing etc) would most likely be too great and therefore the contact between the seal and face would be broken.

Fortunately, there are no muscle groups which would effect movement in the horizontal axis. This results in the seal footprint having no movement related boundaries in this axis, and can therefore be as wide as required. There are however non-movement related boundaries such as the hair line.

3.5 Developing an improved method of measuring skin sensitivity

Measurement of skin sensitivity has been researched to a relatively advanced level within the medical community, with numerous test methods having been developed. These include the two point touch-threshold (Dellon E.S. et al., 1995); depth sense aesthesiometry (Smale J.C. et al., 1981), point localisation Y-Grid (Wood E.J. et al., 1985) and pressure sensitivity Von Frey filament (Fruhstorfer H. et al., 2001) tests. Unfortunately, all of the aforementioned techniques (as well as those that are not mentioned) are highly susceptible to human error and although they give an approximate guide to the level of sensitivity, do not offer a solution for measuring sensitivity with a high resolution in localised areas. This is due to the medical communities difference in requirements. Although measurement of skin sensitivity is essential, it is generally only required to give an indication of illness and healing progress.

The high resolution is required for this particular experimentation, as in reality the possibilities of seal paths lie within a very narrow band (maximum of approximately 30mm, Figure 3.4), and if the resolution isn't at a suitable level, the study would be practically pointless.

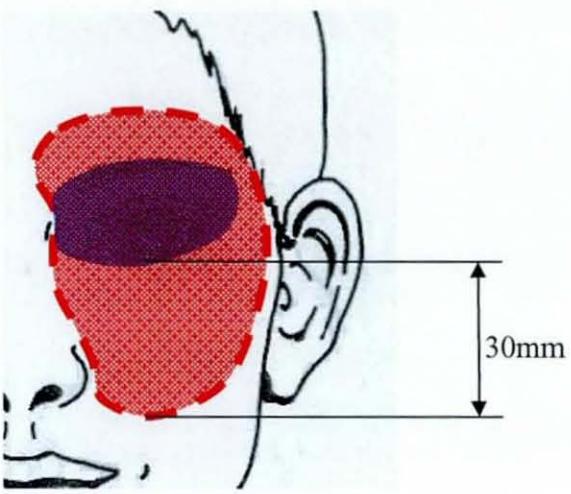

Fig 3.4, Representation showing approximate area of required sensitivity measurement.

Figure 3.4 demonstrates an approximate area of where the skin will be measured for sensitivity. Although the region above the eyebrow will be taken into account, the area below is of a far higher priority. Ideally the results from the sensitivity test would

be able to highlight and distinguish between a minimum of three separate paths for the seal footprint to take.

3.5.1 Available skin sensitivity measurement techniques

Although there are a vast array of skin sensitivity measurement techniques, with numerous variations within each (depending on their intended purpose), six main categories can be clearly identified. There is no obvious consensus as to which is the better for any specific task (especially for that of measuring high resolution sensitivity variations), and so each technique needs to be understood before selecting a preference to use or develop. The techniques are the:

- Two-point touch threshold test
- Depth sense aesthesiometry test
- Point localisation Y-grid test
- Pressure sensitivity Von Frey filament test
- Suction test
- Neurophysiological recording technique of tactile stimulation

3.5.1.1 Two-point touch threshold test

One of the more predominant sensitivity discrimination tests is the two-point touch threshold test. For this procedure, two points of a pair of callipers are lightly touched to the skin at the same time. When the distance between the two points is sufficiently large, each of the points will be stimulating separate receptive fields and different sensory neurons. This results in the subject being able to feel the two separate points. However, if the distance between the two points is sufficiently small, they will both touch the same receptive field of the same sensory neuron, resulting in only one point being felt.

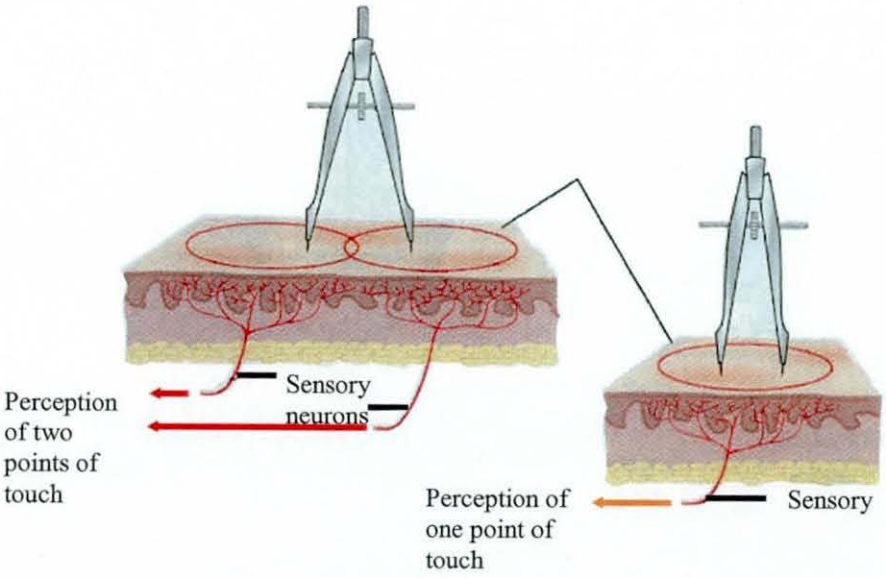

Figure 3.5, Two point discrimination test

The distance at which two points can be just perceived as being separate is known as the two point touch threshold, and is a measure of the distance between two receptive fields. The two-point touch threshold is thus an indication of tactile acuity, or sharpness of touch perception.

Although this test is quite simple, there are certain problems associated with it, preventing high accuracy and repeatability. Until recently, application of the test was the most significant, due to there being no controlled method of touching the two points onto the skin with equal force, preventing unwanted movement and high repeatability. The development of the Pressure-specified Sensory Device (Sensory Management Services, Lutherville, MD) has almost eliminated the problem, as it permits the recording of the pressure at which two-point discrimination occurs (Aszmann, 1998). However, this still does not prevent unwanted hand movement, or allow a method of applying a constant pressure, just measuring it. This in turn results in less than ideal data, when trying to distinguish different sensitivity ratings in such a small localised area (the face).

Examples of two-point threshold measurement devices include the disc discriminator, the 2 point aesthesiometer and the 3 point aesthesiometer. The disc discriminator uses the theory of two-point threshold discrimination, although has incremental set distances between blunt metal pins for simple and quick application. The 2 point aesthesiometer is very similar to this with the exception of total adjustability between

the two points. The 3 point aesthesiometer is an extension of this technique, using the 3rd point as a guide for the subject being measured. The extra point is initiated before hand, and its surface area exactly matches the combined surface area of the other two.



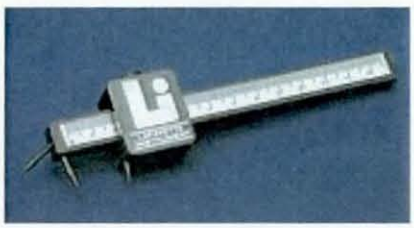

Figure 3.6, Variations of the two-point touch threshold test

3.5.1.2 Depth Sense Aesthesiometry

Invented by Renfrew (Renfrew, 1960), the 'Depth Sense Aesthesiometer' is one of the quickest and simplest of the sensitivity measurement devices. Usually being a single piece of transparent acrylic (approx. 2cm x 10cm x 3mm) bearing on one surface a narrow (2mm) ridge rising progressively from zero to 1mm in height over a length of 70mm. The device is used by drawing the ridged surface of the device lengthwise over the designated area of skin (normally the finger), starting at the flat end. The point at which the subject feels deformation of skin, the height of the ridge is measured and then recorded. It is important while completing this test, as well as most of the others, that the subject is asked to close their eyes throughout.

Although still measuring a form of skin sensitivity, is must be noted that there is a certain distinction between 'Depth Space Feeling' and 'Touch Feeling Discrimination'. Using both together, may provide less or more information, depending on the application of data recorded.

Renfrew observed that, among 100 hands with sensory disturbance, 36 possessed an abnormal depth sense threshold when two point discrimination was normal, but the reverse never occurred. From this, it was concluded that two point discrimination was the less sensitive of the two (Renfrew, 1969) and these findings were again supported 12 years later (Samje, 1981).

3.5.1.3 Point localisation Y-Grid test

One of the most significant point localisation tests is the Y-stamp discrimination test. This involves using a "Y" shaped grid pattern (Figure 3.7) with incremental points along each axis. The Y-shaped grid pattern would be stamped onto the skin with a "skin friendly" ink. The incremental distances between points is not set, as long as they are the same for each (1mm is generally accepted as the standard). A probe is touched in the centre of the "Y" grid, and then working along one axis at a time, the probe is then touched at incremental distances from this centre reference point. A distance value is recorded when the subject can just distinguish that the probe was placed in two separate positions. This is then repeated along each axis, and the average of the three axis is recorded as the sensitivity for that specific reference point.

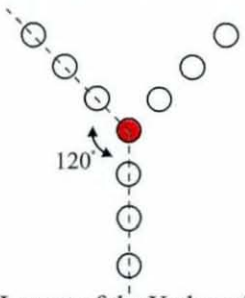

Figure 3.7, Layout of the Y-shaped grid pattern

This test has a similar problem to that of the two point touch threshold test, and is that it is difficult to maintain a repeatable pressure when the probe is applied for every point, and that there is no vibration or any other unwanted movement. However, unlike the two point touch threshold method, only one probe is applied at any one time, consequently the process could be more easily automated. It has also been shown that sequential spatial discrimination is known to be more precise than simultaneous spatial discrimination (Weinstein, 1968). It was found that the spatial discrimination threshold on the back of the hand was significantly wider when estimated by grating orientation (a simultaneous spatial discrimination task), than when estimated by point localisation (a sequential spatial discrimination task). Although this was the case, the results did show that the thresholds (although wider for the grating orientation) were relevant to the various positions that were measured (Schlereth et al., 2000).

3.5.1.4 Pressure sensitivity Von Frey filament test

An advanced version of the Semmes-Weinstein test (Figure 2.8) where calibrated nylon monofilaments are used to exert specific forces at the point where the filament begins to bend. The size of filament is increased until the specific filament force can be felt by the subject. Unfortunately the filaments are considered to be mechanically unstable, and so accuracy and repeatability are difficult to obtain.

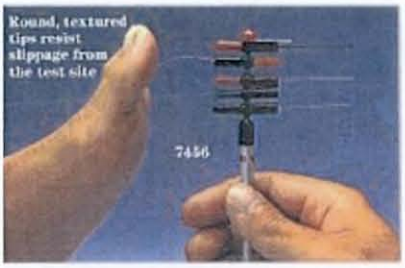

Figure 3.8, WEST Hand / Foot nerve tester

3.5.1.5 Suction Perception test

A more recent test involving the method of suction to attain the sensitivity of skin under stretching. Using a device such as a Cutometer SEM 474, different probe sizes can be attached which can then exert progressive or steep suction on the skin. The intensities of both the suction and the skin deformation observed at the earliest moment the traction can be observed by the subject, is recorded. Due to the method being quite recent and therefore having had little use, accuracy and repeatability are of concern. One of the more significant problems is measuring the deformation of the skin to a high level of precision.

The method has already be used in measuring sensitivity in the facial area, and it was found that skin deformation corresponding to the liminar sensorial perception was almost constant for each subject under test (Martalo, 2001).

3.5.1.6 Neurophysiological recording technique of tactile stimulation

This technique is the most complex and time consuming of all the sensitivity tests (although not directly measuring sensation). Recently, the test was used by Benoni

Edin et al (Edin et al., 1995) for receptor encoding of moving tactile stimuli in humans, where stimulus consisted of a brush movement over a thin Teflon plate taped to the skin. Single-unit recordings from mechanoreceptors originating in the glabrous and nonglabrous skin of the hand, were obtained from a tungsten microelectrode percuaneously inserted into the median and radial nerve. The neural signals were then amplified by a probe positioned near the recording site and information about signals from the receptors was monitored and understood.

3.5.2 Assessing current measurement techniques

From the descriptions alone, it can be clearly seen that the Suction test and the Neurophysiological recording technique of tactile stimulation are impractical for the intended use of high resolution sensitivity variations. As mentioned, the four remaining techniques all have their own specific problems, most of which being the result of human error. In order to decide upon a suitable technique to either use or develop, each technique needs to be graded on cost, ease of use, time of use, macro constraints, micro constraints, potential for development, repeatability / accuracy and comfort to user.

As each of the mentioned factors vary on importance, a grading factor will also be given to each, varying from 1 to 3. The actual grading will also be on a scale from 1 to 3 with intervals of 0.5. Only five interval options are therefore possible, and this was done as the figures given are an approximate guide with no real scientific data to back them up. The answers were based on general research, including comments made in papers, simple interviews with people who have used the techniques as well as common sense.

3.5.2.1 Cost

Cost could be an issue if any major equipment or software needs to be purchased rather than being borrowed or hired. However, none of the techniques use disposable components, and so there will be no or very little running costs (unless equipment is hired). The scale factor will be set to 1.5.

3.5.2.2 Ease of use

Ease of use is unlikely to be a problem, as all of the techniques can be learned within a short period of time. The only situation where this could cause significant problems, is repeatability between users. If a technique's performance relied heavily on the skill of the user, then the same user would have to conduct the entire study. The scale factor will be set to 1.

3.5.2.3 Time of use

Due to the nature of the tests, it is important that a good sample of participants are taken. Although there is no way of predicting the number of participants that would statistically validate the test accurately, there would need to be at least approximately 50 people's skin sensitivity measured. Therefore, although not critical, time could be an issue if it takes more than an hour or so per participant. The scale factor will be set to 2.

3.5.2.4 Potential for useful development

As all of the tests discussed so far have either significant issues with repeatability due to human error or other major problems, the techniques must be able to have room for development and improvement. The most likely area of improvement would be to remove the human element and automate the process. The scale factor will be set to 3.

3.5.2.5 Macro constraints

The Macro constraints are concerned with how near each sensitivity reading can be taken to any others. This particular problem is more likely to be associated with a technique that requires grids to be marked onto the skin. This situation could be resolved by wiping previous grids when a new one is required, but this will take extra time. The scale factor will be set to 1.5.

3.5.2.6 Micro constraints

The micro constraints are concerned with the resolution of each sensitivity reading. If the resolution is very low, then all of the readings will show the same sensitivity and therefore be pointless. The higher the resolution, the better the technique will be able to distinguish between slight variations of sensitivity and the more worthwhile the study. The scale factor will be set to 3.

3.5.2.7 Accuracy / Repeatability

Although accuracy and repeatability have two different meanings, they are named under the same classification for this particular graph. The true accuracy of the technique is quite self explanatory, and if the accuracy is high then the repeatability will be high. However, if the repeatability is high, then accuracy is not necessarily so. The test could show systematically incorrect results, which is more likely with a technique that has low resolution. The scale factor will be set to 3.

3.5.2.8 Comfort to user

As all of the tests discussed are conducted *in vivo*, there is a chance that some may be more unpleasant than others. However, as none of the techniques require any piercing of the skin with needles etc., this unlikely to cause a significant problem. The only issue with discomfort is most likely to be with the participant having to be still for extended periods of time. The scale factor will be set to 1.5.

Technique	Cost (1.5)	Ease of use (1)	Time of use (2)	Potential (3)	Macro constraints (1.5)	Micro constraints (3)	Accuracy/Repeatability (3)	Comfort to user (1.5)	TOTAL / 49.5
Two-point touch threshold	3	2	2	2	2	2	2	2	**34.5**
Depth sense aesthesiometry	3	3	3	1	2	2	2	2	**34.5**
Point localisation Y-Grid	*3*	*1*	*1*	*3*	*2*	*3*	*3*	*2*	***40.5***
Pressure sensitivity Von Frey Filament	2	3	2	1	3	1	2	2	**29.5**
Suction perception test	1	1	1	1	3	2	2	2	**26.5**

Figure 3.9, Table showing point scores for each characteristic of each technique

Although Figure 3.9 clearly shows that the Point localisation Y-Grid technique is the most suitable to develop, the chosen test should also closely represent what is actually happening at the interaction point between swimmer and goggle seal. When wearing a pair of goggles, the seal is applying a low intensity constant pressure (although the pressure does vary from one point of the seal to another). There are only two tests that behave in a similar fashion and these are the 'Two-point touch threshold test' and the 'Point localisation Y-Grid test'. Therefore, as 'Point Localisation Y-Grid test' adheres to both, it would be prudent that this was the technique to be developed and possibly automated.

3.5.3 Initial development of the 'Point localisation Y-Grid' technique

An excellent quality about the 'Point localisation Y-Grid' technique is that it is relatively simple to increase or decrease the micro spatial resolution (Figure 3.10) to an appropriate amount depending on the application. Although for this particular application, it would be thought that the higher the resolution the better, if it is too high then certain problems may occur. The problem being that the more points within each Y-Grid being measured, the longer the test will take, and as this is one of the lengthier skin sensitivity tests, the participants (as well as the tester) would get uncomfortable.

Rather than using the suggested 2mm spacing between markers within the Y-Grid, a 1mm spacing would be more suitable for the higher resolution while not being impractical in terms of time or being too awkward to operate.

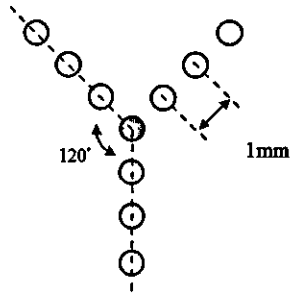

Figure 3.10, Diagram representing Y-Grid pattern with a micro special resolution of 1mm.

However, there is still a significant problem with the technique and this is that there is too much reliance upon human skill of operation. The technique assumes that every tester can apply the same pressure at each point with no unwanted hand movement of any kind. As mentioned before, the way to prevent this would be to automate the process and remove the human element. As this particular technique only requires one point to touch the skin at any one time, the task of automation is made significantly easier.

Automation could be achieved with a 'robot arm' controlled via a manual joystick or a pre-programmed path. The latter would be particularly difficult to achieve due to the complex and varying curves of the face, that are greatly different from person to person. However, using a manual joystick would provide more options for the type of control system required. It was therefore decided to conduct a pilot study assessing such a system such as a co-ordinate measurement machine (CMM).

3.6 Assessment of using CMM for measuring skin sensitivity – Pilot study

3.6.1 Objectives

The purpose of this study was to identify whether CMM can be used to assist in data collection for skin sensitivity. Using the CMM significantly reduces the human input and therefore theoretically increases the repeatability, accuracy and resolution of the technique. This pilot study will show the feasibility of automation and its repeatability, as well as high-lighting potential problems within the modified technique.

3.6.2 Subjects

Although in an ideal world, it would have been preferable to use participants of all nationalities, sizes and ages, doing this would have required thousands of participants and spending years completing the research. The original objectives of Speedo were to design a racing goggle suitable for an Olympic athlete, and although this was no longer the case, it provided a small enough and suitable target population, and so the target population were those with similar attributes to that of the typical Caucasian British elite swimmer.

	Height (cm)	Weight (kg)	Body fat %
Male	175-195	72-88	9-15
Female	164-180	58-73	17-23

Figure 3 11, Typical statistics for a Caucasian British elite swimmer

Following Ethical Advisory Committee approval and informed written consent, 7 participants (4 male) completed the testing procedure. For the male population, the average age was 23.1years (S.D.= ± 1.6years), height was 1.83m (S.D.= ± 0.08m) and weight was 81.2kg (S.D.= ± 4.6kg). For the female population, the average age was 22.8years (S.D.= ± 1.3years), height was 1.70m (S.D.= ± 0.05m) and weight was

66.3kg (S.D.= ± 5.1kg). The limited participation was due to the purpose of this study being to assess the modified technique using CMM, and not use any of the results.

3.6.3 Apparatus

3.6.3.1 Co-ordinate measurement machine choice and setup

Although the technique could have been achieved with many types of CMM, there were key features that that the machine had to offer for best chances of success. A variable preset pressure trigger was critical for this pilot study. This is where the probe can be set at different pressures before it activates and gives a three dimensional co-ordinate position. The technique does not work if the probe is too light so that it cannot be felt by the participant, or even worse if the probe is too heavy and injures the participant. A good range was required in order to find a pressure that closely mimicked the pressure from wearing a pair of swimming goggles as well as optimising the technique for highest reliability.

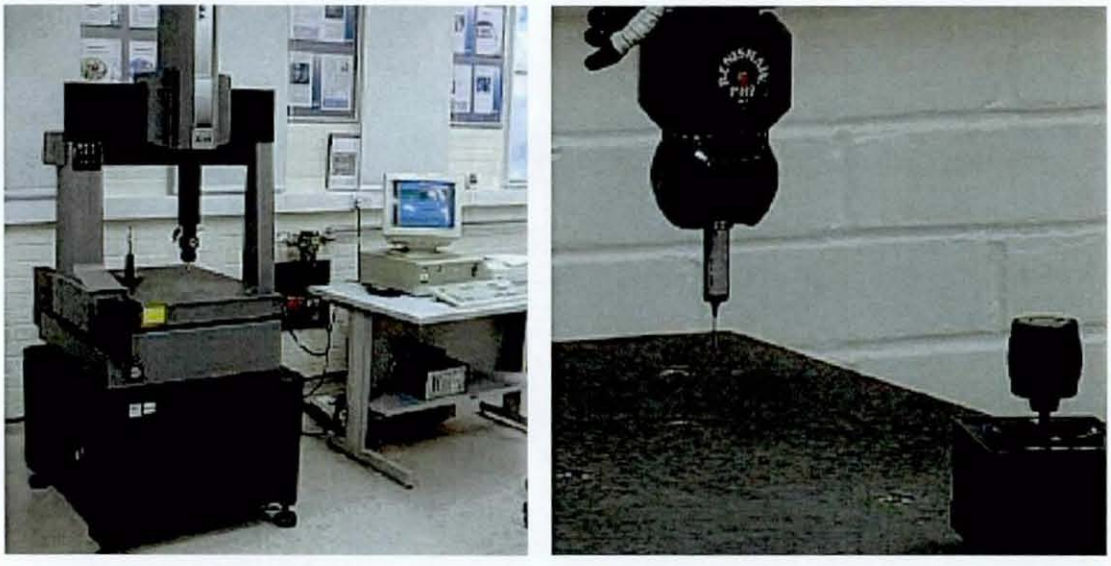

Figure 3.12, Example picture of the Browne & Sharpe co-ordinate measurement machine

A Browne & Sharpe Co-ordinate Measurement Machine was used to control a 1mm ball-tipped probe. The probe was moved using a 3-axis joystick, with variable speed and emergency cut-off controls. The graphical user interface was a standard PC displaying the 3 dimensional co-ordinates to an accuracy of 0.001mm. The probe gave

a reading once it reached a preset threshold pressure (i.e. as a result of the resistance provided by the tissue upon compression).

The CMM arm motion is powered by compressed air, and so there was a small chance that the gas supply could have either run out or blocked. The machine itself monitors for such events, and in the case that one might happen, the probe arm locks into position, preventing it from falling. Due to the probe being operated manually, there is a specific button that needs to be held down while the probe is in motion. There is also an option for two speeds, with the slower allowing for controlled and accurate movements. As mentioned before, the probe cannot proceed vertically downwards once the specified force has been reached, or the object being measured has been removed.

As there is an option for the probe to be controlled in two speeds, the faster was not required during testing and so a plate was permanently fixed onto the control panel preventing accidental buttons being pressed.

Another area where accidental button pressing can cause severe consequences are the X, Y, Z control switches. If these are flicked into the 2nd mode, then that particular axis is locked. The 3rd mode moves the probe into a default position away from the face. However, if gas fails and the z-axis switch is in mode 3, the probe would fall. This was prevented by fixing a plate over all three switches

3.6.3.2 Eye protection

The facial surface area required for measurement of skin sensitivity is surrounding and very close to the eyes, and so the eye protection needed to take up as little space as possible (Figure 3.13). Sun-bed goggles used in tanning salons seemed an ideal product, as they were not only very small, but were also dark tinted to reduce the likelihood of the participant seeing the movements of the probe. This was important, as it ensured the participant was relying on the sense of touch and not his or her eyesight to identify probe location.

Figure 3.13, Protective sun-bed goggles.

3.6.3.3 Head location

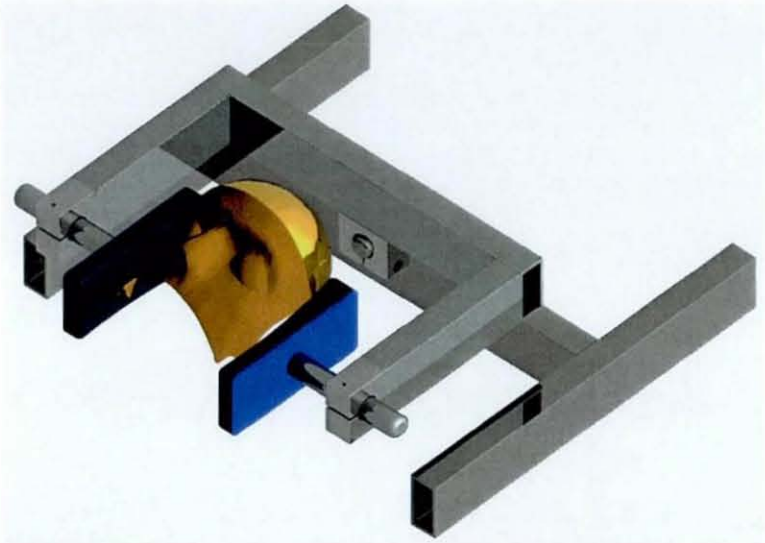

Figure 3.14, 2 axis clamping device for securing participants head during testing.

Due to the nature of the experiment, a head clamp (such as illustrated in Figure 3.14) was used for both safety as well as for ensuring reliable results. As shown in Figure 3.12, the relatively small probe is moving in very close proximity to the eye. Although eye protection is worn, if the participant were to move erratically, the probe could quite easily knock the eye protection to the side and injure the eye. However, although a head clamp could prevent this, the participant must still be able to rotate his or her head from side to side to allow the probe reach the sides of the face.

From the point of view of ensuring that the results are reliable, preventing unwanted facial movement is essential. If the participant is moving while the probe is in contact with their skin, the depth and the position might be altered therefore activating different sensory receptors. Not only will other receptors of the same type be affected, but receptors that detect other senses than sustained touch pressure.

3.6.3.4 Y-Grid stamp

It was found that the best method for imprinting a to scale and accurate image of the 1mm spaced Y-Grid onto the skin, was to use a rapid prototyped stamp as shown in Figure 2.15.

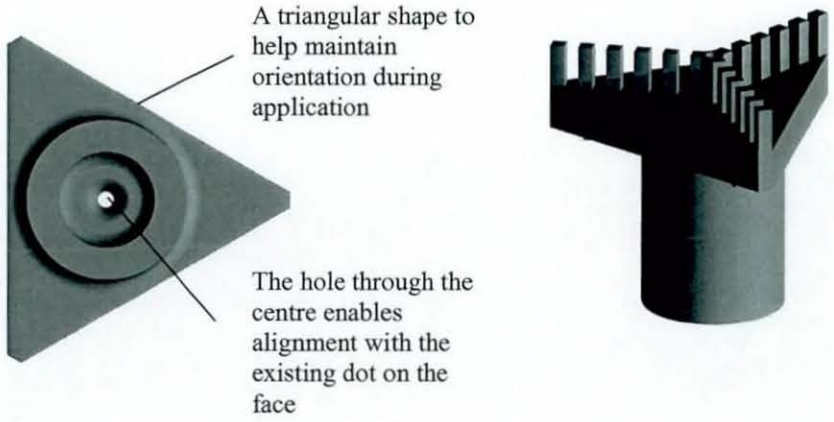

Figure 3.15, Illustration of the Y-Grid stamp

Due to the fine detail that was required for the 1mm prongs, the stamp was made using a thermojet printer. The resulting wax part had the additional quality of being able to absorb a small portion of the ink, ensuring a quality print every time. Numerous other pieces of less substantial equipment was also used, including a projector, wax Y-Grid stamps (with ink), bench with head support

3.6.4 Study protocol

After obtaining the participants statistics (to ascertain whether they were within the accepted boundary), they were shown a video of the experiments (to comply with ethical standards set by Loughborough University), and were made aware of the potential risks that might be involved. A projector was then used to map a grid pattern of 16 points onto the participants face (Figure 3.16). This specific number of points was chosen, as measurement time would approximately fit within a 1 hour session (including set-up etc.). If measurement time were to exceed 1 hour, the participant would lose interest and fail to concentrate to the required amount.

Figure 3.16, Points being projected onto participants face

The position of the grid pattern was standardised using two sets of reference points, with the pattern being stretched in both the vertical and horizontal plane to match the shape of the participants head. As the structure of human faces varies quite considerably, the reference points were positioned on prominent features relevant to the area being measured. For those points on the front of the face, the height of the nose and the eye spacing was used, while the height of the nose and the corner of the eye to the ear were used for the side of the face (Figure 3.17).

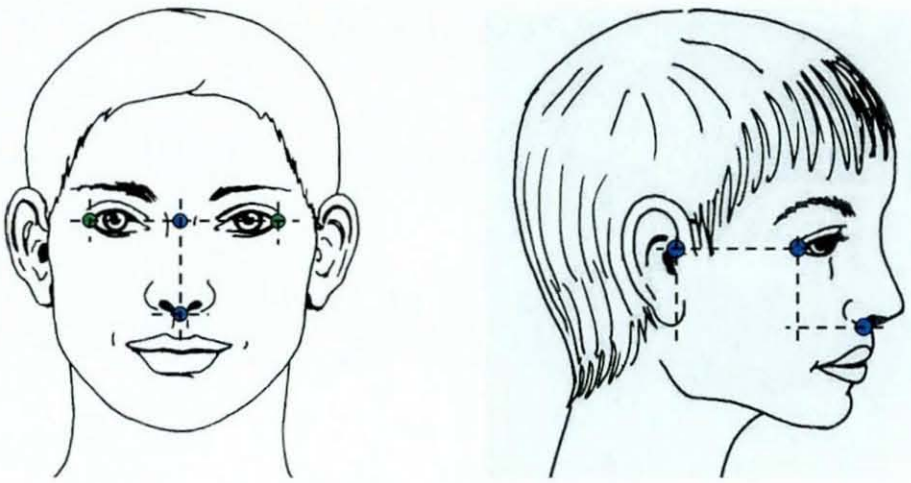

Figure 3.17, Reference points used for positioning grid patterns

Using the reference lines, a grid pattern was over-layed, with points evenly distributed in the more significant areas where the goggles might be positioned (Figure 3.18).

Due to the two outer sets of three points being out of position (due to curvature of the face), these were incorporated in the projection onto the side of the face.

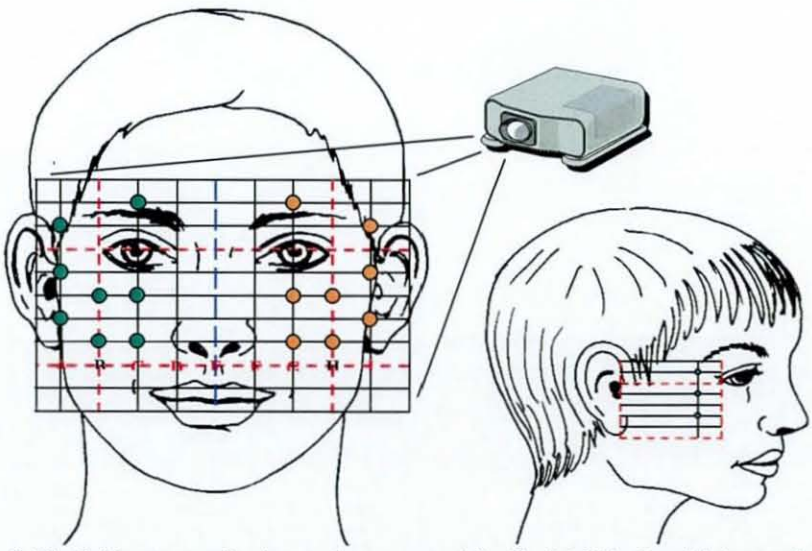

Figure 3.18, Grid pattern of points to be measured for Facial Skin Sensitivity testing.

The points were marked onto the skin using a fine 'make-up' pen and then the Y-Grid stamp was printed over the top ensuring the same orientation every time. Before the participants head was clamped into position, the probe pressure was set to 15 grams and then tested on the participants arm to give an indication of discomfort.

Figure 3.19, Example setup of procedure testing sensitivity.

Concentrating on one Y-Grid at a time, the probe was moved so as to just touch the surface of the skin in the centre of the Y-Grid, and then immediately moved downwards (Z direction) until the CMM stopped under the specified pressure.

Figure 3.20, Probe positioning on Y-grid.

The probe was maintained in this position for 3 seconds and then removed. Working on the first Y-stem, this process of 'point contact' was repeated, except being at the 1st interval of 1mm out. The participant was then asked as to whether the probe felt as if it was in a different position from the centre reference point. If the answer was 'no', then point contact was made again in the centre and then 2mm out. The interval steps increased until point differentiation was made, and this was repeated for each stem of the Y-Grid. The average of the three distances recorded was noted, and then the process was repeated for each Y-Grid.

3.6.5 Results

The raw data retrieved from the experiment is shown in the Appendix – Skin Sensitivity Pilot Study Data, and shows the sensitivity for each stem of each Y-grid for both the male and female population. Rather than display the actual sensitivity results which were recorded, Figure 3.21 is probably of more importance. It is a table showing the variance in sensitivity from the left side of the face to the right side. The highlighted green italic numbers are those points where the right side of the face was more sensitive, while the standard black numbers are those where the left side of the

face was more sensitive. They are categorised into specific mirror points, for example, 'A1-I1' are two points located in the same position on each side of the face. The split is approximately even, with no indication of either side being more or less sensitive in either the male or female participants.

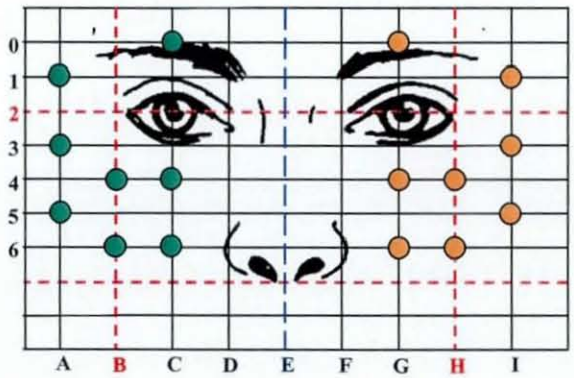

Participant no.	Sensitivity of left - sensitivity of right points							
	A1-I1	A3-I3	A5-I5	B4-H4	B6-H6	C0-G0	C4-G4	C6-G6
1	0.33	-0.67	1	0	1	-0.67	1.33	-0.33
2	-1	-1.33	-1	0	-1.33	0	-1.67	-4
3	-1	-1	-2.67	-1.33	-3	0.67	1	0
4	0.33	0.67	0	0.33	0.33	0.33	-0.67	1.33
5	2.33	1.33	1.33	0	-1	-0.67	0	1.33
6	3	2	4	0	-1.67	1.67	0.33	0.67
7	-1.67	-2.33	-2	-1	-0.67	1	-2	-0.33

Figure 3.21, Variations in sensitivity from left to right side of face in all participants. The numbers are the difference between the left and right side of the face for the equivalent mirrored point.

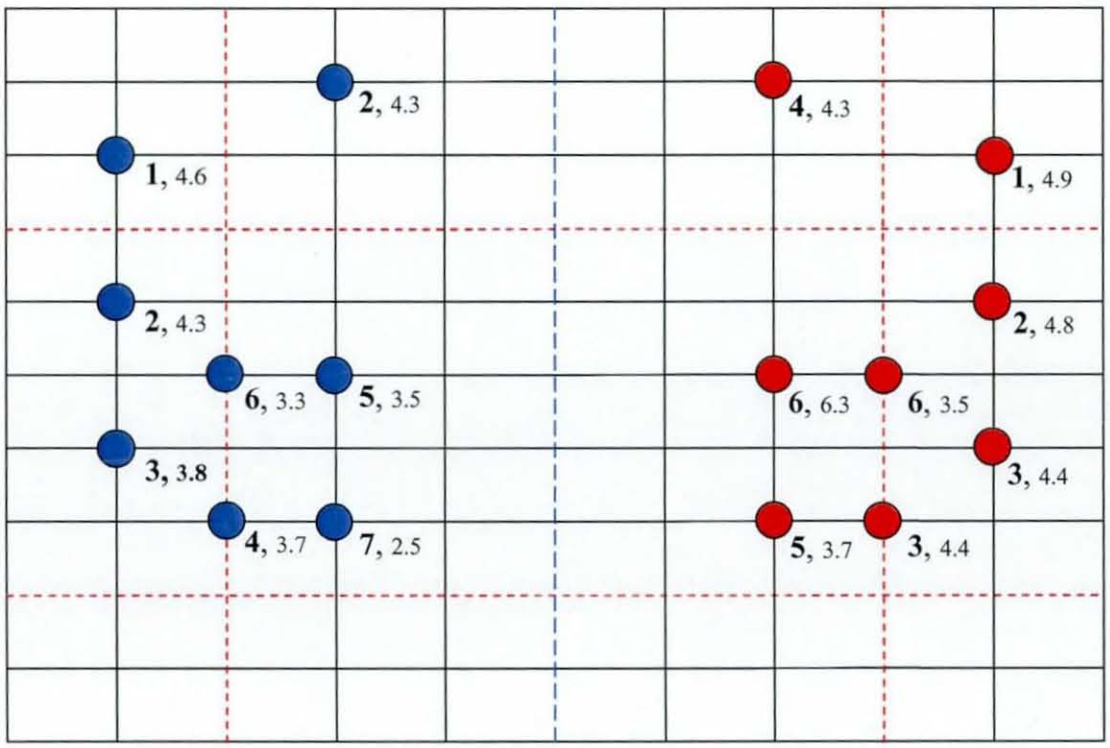

Figure 3.22, Average skin sensitivity and order in relation to grid location for the female participants. Larger no. showing order of sensitivity, while smaller no. showing actual sensitivity reading.

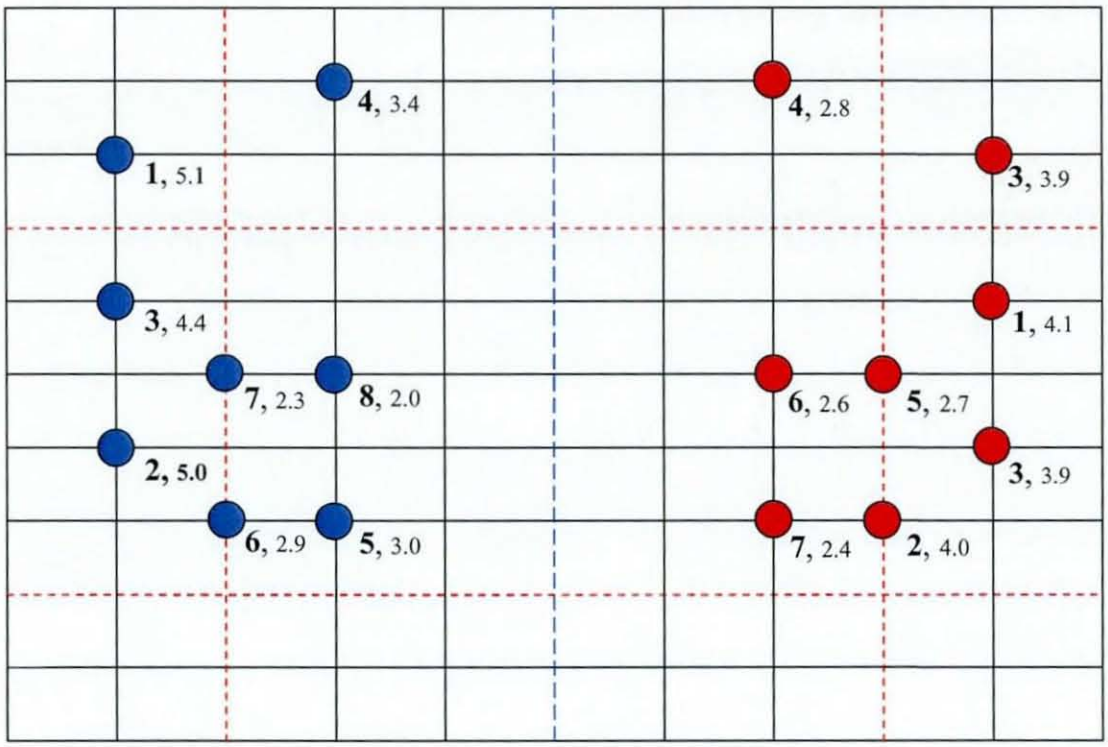

Figure 3.23, Average skin sensitivity and order in relation to grid location for the male participants. Larger no. showing order of sensitivity, while smaller no. showing actual sensitivity reading.

Concerning more specific patterns within the face, figures 3.22 & 3.23 show the average skin sensitivity for both the male and female pilot groups. The bold black numbers show the order of sensitivity for that specific side of the face, with the number 1 being the least sensitive. Unfortunately the most important area, which is below the eyes, is the least clear as to suggest a pattern. However, there is an indication that the skin is less sensitive, further away from the eyes (vertically downwards).

3.6.6 Discussions

The main purpose for conducting this study was to evaluate the use of CMM in measuring facial tissue compression and skin sensitivity. However, the general techniques involved in the other areas of the experiment, were just as unfamiliar and so these areas needed to be assessed as well.

3.6.6.1 Point location

Two of the most important aspects of this study (besides data collection), was in deciding how many points should be measured, and where they should be positioned. The number of points was slightly simpler, as it was a matter of time being the main restriction. In order to maintain a reasonable level of concentration and a certain amount of 'willingness' within the participants, duration of sessions was kept to approximately one hour.

Regarding the location of the points, it has already been mentioned that reference lines were used relating to key features on the face, and then a grid was stretched into position. The points were then evenly distributed at suitable positions on the grid. However, after completing the sensitivity test, it was clear that there would be insufficient points to map a suitable path for the goggle seal to go. From Figure 3.24, it can be seen that there is only two options (shown by the green lines) for seal path, with certain points providing no real purpose at all.

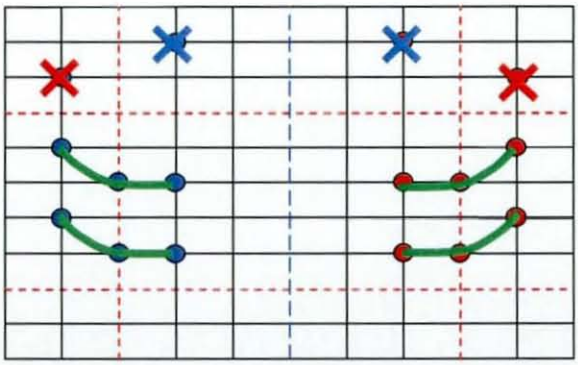

Figure 3.24, Point location for sensitivity test during pilot study

For development in this area, a compromise was needed, as adding more points would significantly increase duration of the test. In conclusion to this, it was decided that the points with red crosses would not be measured. However, the points with blue crosses would remain, as although they did not directly offer any other local route, they did give a sample sensitivity comparison to global areas of the face. This allowed additional points to be measured where they would be of more use in the design process (figure 3.25).

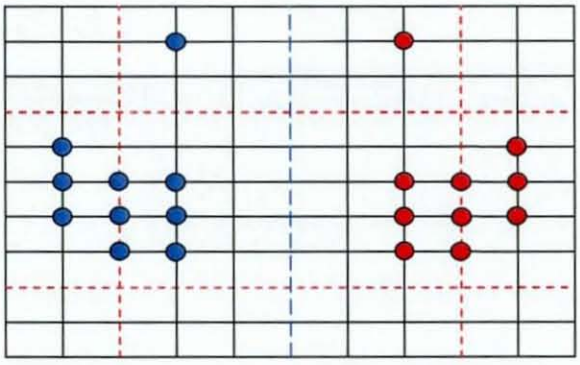

Figure 3.25, Development of Sensitivity point location

3.6.6.2 Participant concentration

In regards to more general problems, loss of concentration seemed to be quite an issue, caused by the participant partially falling asleep during testing. Apparently the fact that the experiment set-up was actually a little too comfortable, combined with having their eyes closed for a significant period of time, proved to be ideal sleep conditions (even for those who felt exceptionally alert before the test began). The lack

of concentration was more evident in the last third of the testing period, and sensitivity readings were having to be repeated to achieve an informative result. The time of day might have been a partial factor, and for the following study all testing was restricted to the mornings. The most simple remedy was to force the participants to have at least one break during the test, or maybe more, depending on the individual.

3.6.6.3 Experiment variability

The tests were conducted in an environmentally controlled room, with the temperature and humidity remaining the same for each participant. However, there were numerous factors affecting the participant prior to testing, such as length and condition of sleep, the clothing they were wearing (warmth) and hydration of the body. Although these were all uncontrolled, it was considered that these were not a significant factor in test repeatability, as although skin stiffness and elasticity would have been considerably variable (Lindahl et al., 1998), this would have not affected skin sensitivity itself (Dellon et al., 1995 and Watts et al., 1994). Unfortunately, the number of parameters affecting the condition of the participant and their skin would be too high to record for the small variation in results, but one cause of sensitivity variation is deemed too significant not to be recorded. For female participants, their position in the menstruation cycle was noted (Berardesca et al., 1989) in the following tests.

3.6.6.4 Probe motion control

The Browne & Sharpe co-ordinate measurement machine had a manually controlled probe (via joystick), and consequently there was always going to be human error:

- The probe being miss-aligned with a specific position on the y-grid
- The probe going into the skin too quickly or too slowly
- The probe staying in contact with the skin for too long or too short a period of time
- The time period between contacts of points being too long

Each of the above errors may have caused the participant to be confused, and possibly initiate playing "mind games" with themselves, resulting in an unreliable answer.

Resulting from this, during later tests, if any noticeable probe errors did occur, then the participant were asked to ignore that point-set, and then have the point set repeated.

The most notable of the mentioned problems was the rate at which the probe impacted the skin, especially when there was no measurable way of keeping it constant. The speed of the probe was related to the amount the control joystick was rotated, and so it was impossible to maintain exactly the same amount of rotation for each point measured. As it has been shown that differences in the discharge (sensation), vary considerably depending on the velocity at which the stimulus moves across the receptive field, then to improve data repeatability, a test for evaluating probe velocity repeatability needed to be completed.

Error from the pressure reading of the probe seemed to be also enhanced when the probe was positioned directly parallel to direction of movement. Therefore to gain greater repeatability, the probe was to be tested at different orientations (such as 45 degrees normal to that of the participants face, as shown in Figure 3.26.

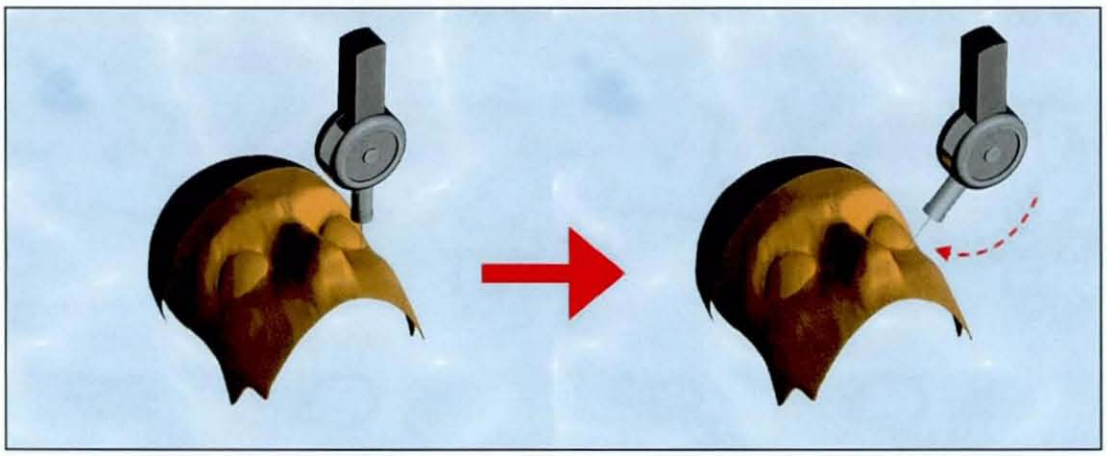

Figure 3.26, Re-orientation of probe to gain greater repeatability in force measurement

3.6.7 Conclusions and required modifications

From the results alone, it is difficult to prove whether or not the test method is accurate and repeatable. The lack of participants prevents any theories about sensitivity within the face to be made, and any discrepancies that might be apparent

maybe a natural phenomena and not a problem with the test method itself. It was noted that there was a strong indication that for certain Y-Grid measurements, there was a large variability between each stem, and yet when re-measured there was high repeatability. During a previous study researching into spatial discrimination thresholds for pain and touch in human hairy skin, it was observed that orientation was a significant factor for two-point discrimination (Schlereth et al., 2000). For the study, it was showed that it was easier to discriminate stimulus location in the radial-ulnar direction than in the proximal-distal direction on the back of the hand (threshold ratio approx. 2/3). It was suggested that this variation was due to oval shaped receptive fields that were oriented in the longitudinal direction. Receptive fields of nociceptors innervating the hairy skin (such as the face) often have an oval shape for mechanical stimuli (Treede et al., 2000). When specifically related to the hand, the Merkel and Meissner receptors (involved in spatial discrimination of touch), have been found to be preferentially oriented in the longitudinal direction of the hand, however there is little information of orientation regarding the facial areas concerned.

There were however specifics of the test method which were noted to be less than ideal. When the participant was first subjected to the probe, they were often unsure of the sensations they were feeling. This lead to quite random results, with no conclusive repeatability. During the early stages of the pilot study, it was decided that the first Y-Grid pattern would be repeated twice before the test would begin. This gave the participant a suitable time period in which to learn the process before any data was collected.

Although dark-tinted protective goggles were used during the pilot study, it was still noted that a couple of the participants could occasionally see the probe move (even though they had been asked to keep their eyes closed). This could have considerably affected results, as they would have been able to distinguish visually whether the probe was in a different place. To remedy this problem, the goggles should be completely opaque to prevent the participant from glancing through. The participant should also be reminded on numerous occasions to keep their eyes closed, as this also ensures a more constant facial composition. The goggle straps were also occasionally interfering with the areas where the sensitivity was being measured. This caused unnecessary problems and therefore strapless goggles needed to be used.

As custom protective goggles were required, it was decided to design them to be as small as possible, as the measured facial surface area is surrounding and very close to the eyes. The pads were made completely opaque and were held in place by aharmless, semi- tacky glue.

Figure 3.27, Protective eye pads

In order to obtain reliable data, certain aspects of modifications to the experiment need to remain withheld from the participant. This is to prevent particular issues arising with regard to the participant learning or in fact cheating (consciously or subconsciously) throughout the duration of the test. During this study, there were many key areas where possible significant errors could have mostly been avoided.

To achieve greater reliability of the sensitivity of each axis of the y-grid, the first point identified by the participant as not being in the same position as the reference position, should be repeated. If the participant once again recognised the points as being different, then that would be recorded as the sensitivity. However, if the points were considered to feel as if they were in the same position, then the next point would be tested. This procedure would of course be applied to the next point that was identified as being in different positions, and so on.

Another significant cause of error happened when there was an insensitive area at a particular Y-Grid. The participant was more inclined to say that they could feel the points were in different positions, even when they probably couldn't notice. This was due to them feeling that too many points had been tested and that they should have already felt the difference (participant impatience). The best way to prevent this is to increase the number of "fake" separate points to that of the reference point, therefore making the procedure quite random. The number of "fake" points should be recorded, as well as the number of times the participant incorrectly identifies a different position.

Once a participant had made a mistake, by reporting that the second point was in a different position to the reference point (when in fact it wasn't), a certain characteristic arose for all those that took part. For the next couple of points being tested, the subject became overly cautious, and therefore seemed particularly insensitive. The reason for this was that they weren't willing to risk being incorrect again. However, this only lasted for a couple of touches from the probe, and therefore the following modifications to the procedure were made;

- When the participant incorrectly identifies the points being different, the following three point sets should be repeated (One point set consisting of the probe touching the reference position and then a position elsewhere on the y-grid).

- Hesitation from the participant when trying to identify whether the probe was in the same position as the reference point, was a good sign that they were unsure. If this indecision period was significant, then the likelihood of a reliable answer was minimal. Another modification implemented as a result of the pilot study was that, if the hesitation is longer than three seconds, the answer should be ignored and that point will be re-tested.

The pilot study was therefore a success, and so the Point localisation technique when applied with a CMM and adapted with all the mentioned modifications should be a viable means of accurately recording skin sensitivity with a high resolution.

3.7 Repeatability of force measurement from probe

The Browne & Sharpe Co-ordinate measurement machine was originally intended for simply measuring rigid objects. The process involved in the facial tissue compression and skin sensitivity experiments takes advantage of the machines ability to register a measurement under a certain force. It was noted however, that during the pilot studies, there seemed to be variations in the depth at which the probe registered, depending on the speed at which the probe was moving and the angle at which it was positioned. Before the experiments could finally be approved, there was the need to develop a test method to determine the optimum setting for repeatability varying the three parameters of probe speed, probe angle and force at which probe registers.

3.7.1 Methodology

The speed of the probe was tested at the four settings, ranging from the slowest to the fastest achievable using the standard joystick setup. Due to there being no easy way of consistently maintaining accurate speeds (during normal experimental conditions), the joystick was marked at specific rotation angles which gave sufficient approximations. At each of the 4 speeds, the force at which the probe registered was set at three different positions with a low, medium and high configuration. At each of the mentioned settings, the force was also measured with the probe being moved normal to the surface as well as at a 45° angle to the surface. For all of the mentioned settings, 10 trials were completed for each, to give a fair representation.

The device used for measuring the force at which the probe was registered was a analogue peak force gauge that measured from 0 to 20 grams. To ensure there was no slippage between the probe 'point-ball' and the calibration device, the 2 mm probe ball was selected, as this was comfortably secured on the tip of the calibration device arm (the 1mm ball tip was very difficult to keep situated correctly).

3.7.2 Results

The complete results for this calibration study can be seen with the variance for each setting in Figure 3.28. The highest repeatability was found using two separate set-ups and are highlighted in green. The setup using the highest force setting produced an average pressure of approximately 11 grams, which was deemed to be too high for testing skin sensitivity. The probe would have interacted with bone and the wrong sensitivity receptors. The best combination was therefore found when the probe speed was set at 0.005m/s (2nd slowest setting), the probe angle was set at 45° and the threshold pressure setting was at force 1. The variance of the ten results at this setting was 0.044.

Force setting	Speed	Angle	Force										Variance
1	Slow	0	4	5	5	5	4	4.5	4.5	5	5	5	0.177778
		45	3	3	2.5	3	3	2.5	3	3.5	3	2.5	0.1
	Med	0	7	7	6	6	6.5	6	7	7	6.5	6	0.222222
		45	3	3	3	3	3	3.5	3	3.5	3	3	0.044444
	Med 2	0	8	8	8	8	8.5	8	8	8.5	8	7.5	0.080556
		45	3.5	3	3	3	3	3	3.5	3	3	3.5	0.058333
	Fast	0	11.5	12	12	12	11.5	12	11	12	12	11.5	0.125
		45	4	4	3.5	4	3.5	4	4	3.5	3	3.5	0.122222
2	Slow	0	13	12.5	12	12	11.5	11.5	12	11.5	11.5	12	0.247222
		45	6	5.5	5.5	6	5.5	5.5	6	6.5	5	5.5	0.177778
	Med	0	13	14	13	13	13	13	13	13	13	14	0.177778
		45	6.5	7	7	7	6.5	6.5	6.5	7	6	6.5	0.113889
	Med 2	0	15	15	15	16	15	15	15	15.5	15	15	0.113889
		45	7.5	8.5	8.5	7.5	8	8.5	8	8	9	9	0.291667
	Fast	0	17.5	19	19	19.5	18.5	19	18	18.5	18	18	0.388889
		45	13	7	14	8	7.5	7	8	13	13	7	9.291667
3	Slow	0	23	22.5	21.5	22	22	21.5	21.5	22	22	22	0.222222
		45	11	11	11	11	10.5	11	10.5	11	11	11	0.044444
	Med	0	23	23	23	23.5	22.5	23.5	23	23	23.5	23	0.1
		45	12	12.5	12	12	12	13	12	13	12.5	13	0.211111
	Med 2	0	25	25	25.5	26	26.5	25.5	26	25	25	25	0.302778
		45	12.5	15	15	14.5	14	14.5	14	14.5	15	14	0.566667
	Fast	0	27	28	28.5	28	27.5	28	27.5	27.5	28.5	27.5	0.233333
		45	18.5	17	18	19	19	17	18	17	18	18.5	0.611111

Figure 3.28, Results of the calibration study for optimum probe performance

3.7.3 Conclusions

After completing the optimisation experiment, it was made quite apparent how variable the machine could be, depending on its settings. When the probe was set at its fastest setting, at the medium force threshold adjustment and at an angle of 45°, the variance was 9.29. This means that there was practically no repeatability at all, and demonstrates just how important the test was.

The highest repeatability set-up which achieved a variance of 0.044 was perfectly adequate for the skin sensitivity study, and so it was these settings that were to be eventually used. The approximate force was also more suitable at 3 grams.

3.8 Skin sensitivity study

3.8.1 Subjects

Following Ethical Advisory Committee approval and informed written consent, 46 participants (23 male) completed the testing procedure. For the male population, the average age was 21.8years (S.D.= ± 1.9years), height was 1.86m (S.D.= ± 0.06m) and weight was 80.1kg (S.D.= ± 5.2kg). For the female population, the average age was 21.2years (S.D.= ± 2years), height was 1.72m (S.D.= ± 0.04m) and weight was 65kg (S.D.= ± 4.2kg).

These participants approximate the range of basic physical characteristics exhibited by a Caucasian British elite swimmer for both the male and female target population.

3.8.2 Study protocol

The modifications to the pilot study that were discussed in Section 3.3.7, have been included so that the final procedure is as follows.

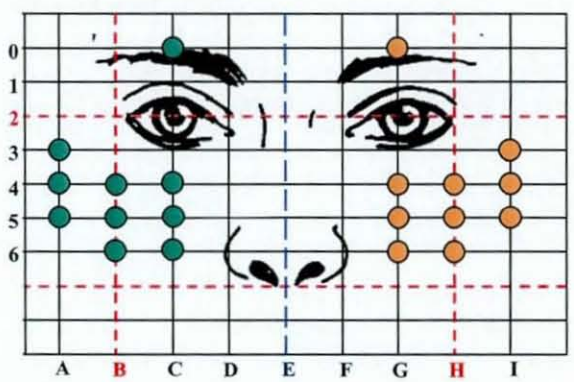

Figure 3.29, Location of points to be tested for sensitivity

The points were projected on to the site of interest (Figure 3.29), and then the Y-Grid stamp was used at each point. The probe pressure was set to register at 3 grams, with the probe angle being at 45 degrees and probe speed at 0.005m/s. Concentrating on one Y-Grid at a time, the probe was moved so as to just touch the surface of the skin

in the centre of the Y-Grid, and then immediately moved downwards (Z direction) until the CMM stopped under the specified pressure. The probe was maintained in this position for 1 second and then removed. Working on the first Y-stem, this process of 'point contact' was repeated at the 1st interval (1mm out from the centre of the Y grid). The participant was then asked whether the probe felt as if it were in a different position from the centre reference point. If the answer was 'no', then point contact was made again in the reference point and then 2mm out. The interval steps increased until point differentiation was made, and this was repeated for each stem of the Y-Grid. The average of the three distances recorded was noted, and then the process was repeated for each Y-Grid.

Occasionally participants were unsure as to whether the probe was in the same place and thus guessed. Therefore, the participants were told that if they were unsure, they should say the probe was in the same place. To minimise any learning effect, the probe was often positioned in the centre two or three times consecutively, and if the participant claimed the probe was in a different position when in fact it was in the reference position, then that specific point-set was taken again. To prevent loss of concentration, or even sleep (which was occasionally observed during the pilot study) the participants were tested in the mornings and the test procedure was punctuated with regular breaks.

3.8.3 Results

The raw data can be found in the Appendix – Skin Sensitivity Study Data. However, figures 3.30 and 3.31 show all the information required for estimating the best path for the swimming goggle seal for both the male and female target population. The lower the sensitivity reading for a specific point, the more sensitive that area is. The sensitivity readings are displayed in the centre of each circle point.

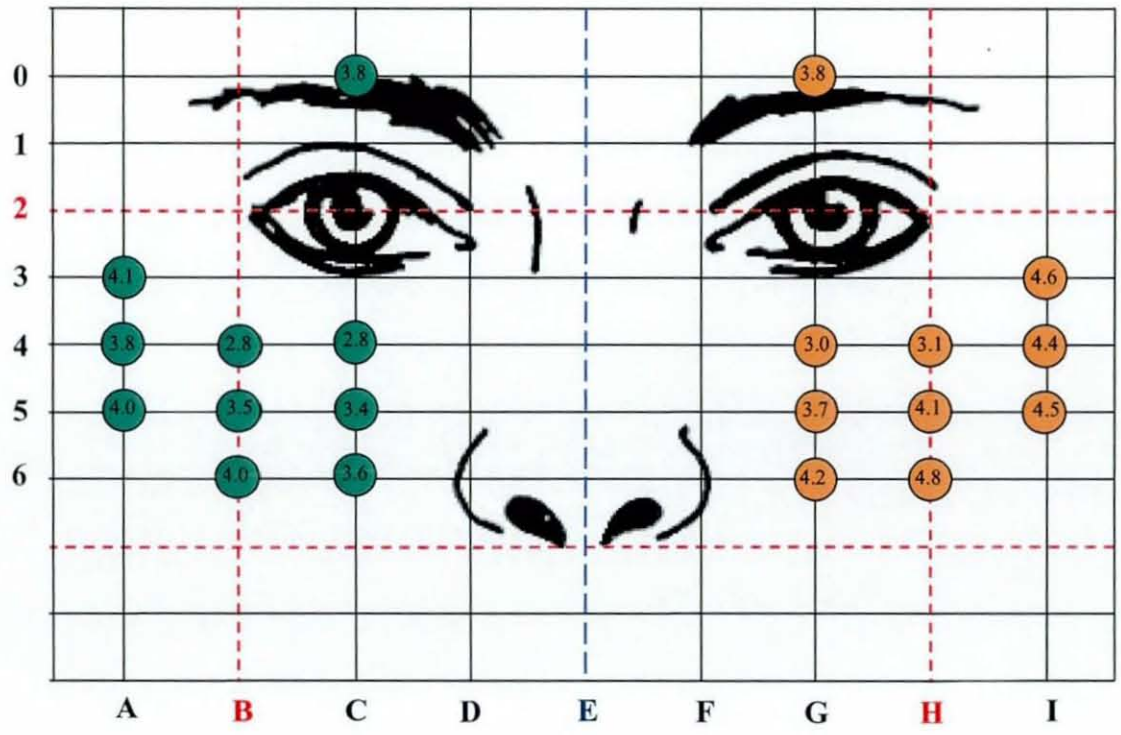

Figure 3.30, Diagram showing localised facial sensitivities for the male population. Number in each circle is sensitivity for that specific point (mm).

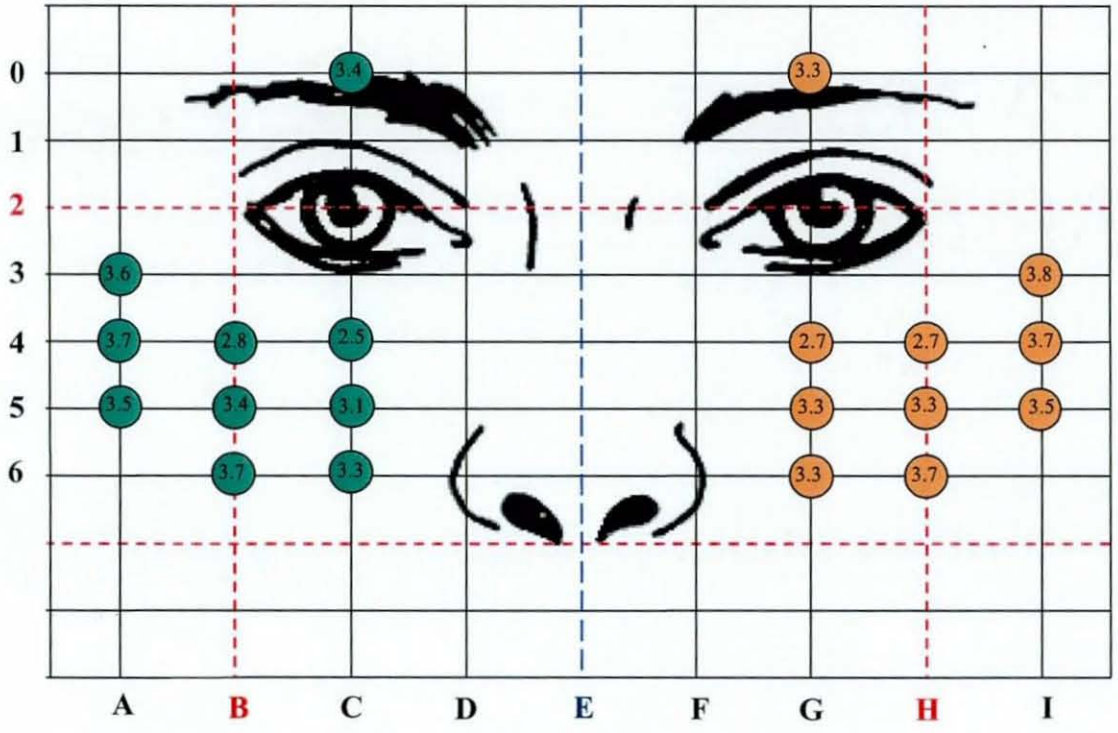

Figure 3.31, Diagram showing localised facial sensitivities for the female population. Number in each circle is sensitivity for that specific point (mm).

3.8.4 Discussion

Although the process has been already reasonably proven as an accurate and repeatable technique, Figure 3.32 gives yet another indication of its success.

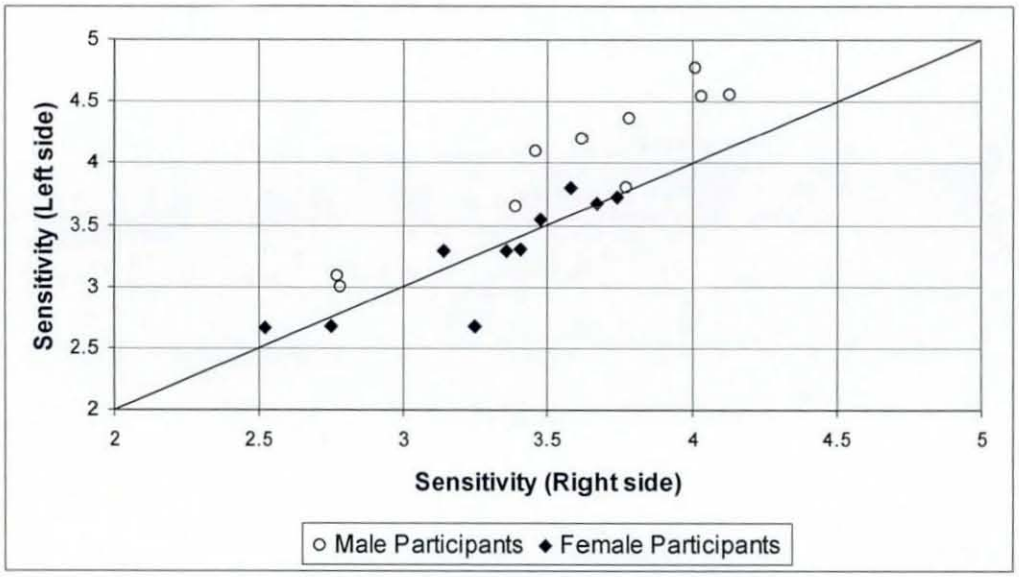

Figure 3.32 Comparison of sensitivity between left and right sides of the body. The straight lines shows where the points should lie.

The skin sensitivity results indicate that the female population was more sensitive. With regards to intra participant sensitivity, the female population showed a trend of being equal on both sides of the body, whereas for the male population the right side of the body would appear to be more sensitive, but with only an average sensitivity reading difference of 0.4mm. This difference may reflect a genuine bi-lateral disparity, it could however, be a result of participant inconsistencies or tester error. For this argument to be resolved, a far greater number of participants would need to be tested. But for the purposes of this study, an average of each point and its mirror point are used. If the results are incorrect by a small percentage, then further modifications could be made to the experiment set-up, if supplementary data was required.

When each participant was tested, the first sensitivity point to be measured was always A1 (the right side of the face), and then working through to the mirror position on the other side. This could be a possible reason for the male population supposedly having one side of the face more sensitive than the other (by way of learning). If the

experiment were to be repeated, the points could be measured in a random order, ensuring that one side of the face was not measured significantly before the other.

The speed of the probe movement is presently controlled by the degree of rotation of the joystick. Consistencies in probe speed are thus determined by the skill of the investigator, and so could be substantially improved by replacing the rotation method with a single 'low speed' button.

Another factor that may have influenced measurement was the pressure that the probe was set at before it automatically stopped. The probe preset pressure was 3 grams, which although unlikely, may interfere with the tissue underneath the subcutaneous layer, such as bone and muscle. This may mean that different types of receptors, in addition to those responding to touch, are stimulated, therefore introducing unwanted inconsistency depending on the area of testing. This could easily be resolved in future work, by simply reducing the pre-set pressure to as low as possible, without reducing repeatability of probe movement.

A fully automated process with no input from the human investigator would always be preferable, and if the funding and technology permitted, this would be the way forward.

The purpose of this study was to find where the ideal seal position would be in terms of the areas of least sensitive skin. Although it may have been preferable to have more points and more participants, some very useful information has been learned. Contrary to the current conceptions of how a swimming goggle is supposed to be, the data gives a reasonable indication that the seal should sit lower on the face. This is obviously not taking into account other factors such as tissue compression.

The exact position of the lower seal is almost impossible to speculate, but it would seem the further down the face the better. However, there is a limit which is defined where the sensitivity surrounding the mouth becomes greatly increased. It might also be that the average consumer would be put off if a new goggle design were too radical. As often seen in design, a compromise would most likely be best.

From the results, it can be seen that the greatest reduction in sensitivity (excluding the outer points) can be seen between the first and the second row of readings (Figure 3.33). This would suggest that the seal could be positioned on the middle path, and still achieve a significant percentage of the benefits relating to reduced sensitivity.

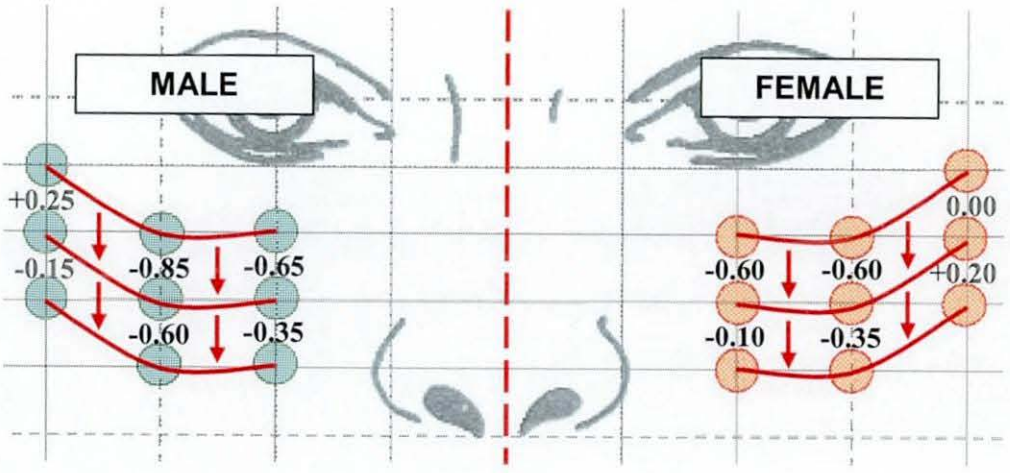

Figure 3.33, Variation between sensitivity (averaged with mirrored point)for both the male and female population.

Regarding the outer points, the opposite trend is true, where the lower down on the face the points are, the more sensitive they become. This results in a preferred seal footprint (only based on the skin sensitivity results) to be positioned within the shaded area in Figure 3.34, with the solid line being the most likely path.

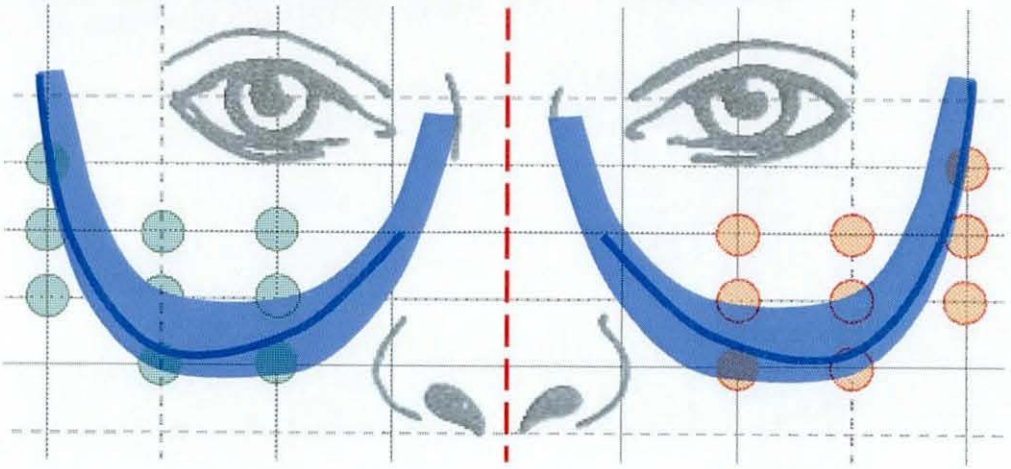

Figure 3.34, Preferred seal footprint location with regards to skin sensitivity.

When this information is combined with the results from the facial tissue compression, relevant information on the facial characteristics and past knowledge

relating to swimming goggle design, then the seal position can be more clearly defined.

4.0 SEAL FLEXIBILITY

4.1 Introduction

In very general terms, there are two main types of swimming goggles, those with flexible seals and those with rigid seals. The rigid type does not actually have a separate component for a seal, but is one piece similar to that of the Swedish type racing goggle (Figure 4.1).

.

Figure 4.1, Example of a Swedish type racing goggle

The possible development for Swedish type swimming goggles is very limited, as they are supposedly already positioned for their optimum sealing and comfort. Even with any small possible improvements that might be made on shape, they will never be as comfortable (for the majority of the population) as a flexible sealing system.

Swimming goggle flexible seal technologies have finally began to evolve in the last few years. The primitive neoprene padding that was once seen on a significant proportion of the swimming goggle product range, has practically been wiped out (except for a minority in the budget category). However, materials development has been the main driving force, with far less concentration on form and function. As with other areas of the goggle, the actual shape of the new seals are almost entirely based on that of successful previous editions. From the literature review, it is quite apparent that designers lack the science of facial structure and tissue behaviour to progress swimming goggle seal design into the next evolutionary chapter.

4.2 Chapter Aims

Human tissue compresses in different ways depending on its location and what muscle and bone structure is located beneath. This is especially the case in the facial area surrounding the eyes, where there are not only the softer cheek regions, but also the much harder nose and eyebrow regions. This means that if a rigid object is just touching the mentioned areas, and is then pressed directly into the face, the pressure on the areas will vary considerably. The pressure exerted will be significantly less where the facial tissue is more capable of flexing to accommodate the rigid object.

The aim of this chapter is to therefore determine the compressibility of the different areas of the facial region surrounding the eyes, so that a seal gasket can be designed to counter the differential pressure effect. This will hopefully result in designers being able to produce a swimming goggle, which exerts the same pressure at each point of contact when the strap has been tightened.

4.3 Chapter Objectives

- To research all seal technologies, and assess whether there are any that might already partially prevent variable pressures throughout its contact with the skin.
- To evaluate possible methods of measuring compression of facial tissue under constant load.
- To develop a repeatable and accurate method of measuring facial tissue compression under constant load, and to then conduct a trial with a target population to calculate the average compressions for each point location.

4.4 Background – The Seal

4.4.1 Purpose of the flexible seal

The most important purpose of a flexible seal is quite self explanatory, and is to maintain the air pocket surrounding the eye to allow the user to see under water. The flexibility allows the goggle to seal on a higher percentage of the population (without the need for numerous goggle sizes) as it accommodates varying facial structures.

The second purpose of a flexible seal is to provide added comfort. Generally, the more rigid the seal is, the tighter the swimming goggles will have to be secured onto the face using a strap, using the compression of the facial tissue to keep the goggles water tight. Depending on the degree to which the strap needs to be tightened, the discomfort caused can be quite unbearable. To illustrate this discomfort in real life, elite swimmers will often race in a pair of Swedish type (rigid seal) goggles, and train using a pair with flexible sealing.

4.4.2 Current seal technologies

There are numerous variations of flexible seal types on the market, but they can be classified into five categories.

4.4.2.1 Foam seals

Figure 4.2, Example pair of neoprene foam seal goggles

Foam seals are the most primitive of all the different categories. They are simply foam shapes (often neoprene) cut from a flat sheet (Figure 4.3) and then maintained in

position onto the goggle frame by use of an adhesive. This technique is very wasteful of material (only a small percentage of the sheet is actually used), and there are very limited variable factors. It would be extremely difficult to have varying flexibility within the same seal, and the seal can only be attached to a surface curved gradually in only one axis. Even with these limitations, a foam seal can still provide reasonable performance in terms of sealing and comfort relative to its moderately low cost.

Figure 4.3, Process of using sheet foam to cut seal shapes

4.4.2.2 Flexible over-moulded one-piece, soft-frame goggle

Figure 4.4, Example of a one piece, soft-frame goggle

Flexible over-moulded seals are one of the more popular current styles and are generally manufactured from either PVC or silicone. The flexibility of being able to make the seal in practically any shape, increases its potential performance considerably. The seals are injection moulded around the lens to improve durability and prevent leakage.

4.4.2.3 Double layer gasket seal

Figure 4.5, Example of a double layer gasket seal

The purpose of a double layer gasket seal is to take advantage of the better properties of different materials to provide a more comfortable, leak-resistant fit. An example of this technology can be seen in the TYR Advantage goggle (Figure 4.5), where the gasket includes a stabilising silicone ring between two thin layers of racing foam. The company claims that if you like the soft feel of foam gasketing, but don't like the way that foam gaskets stretch and "float" around your eyes, then the Advantage is the goggle for you.

4.4.2.4 Air filled seal

Figure 4.6, Example of an air filled seal goggle

Designed specifically more for comfort, the air filled polyseal technology is similar to the double layer gasket seal, in that it takes advantage of two types of matter to achieve its overall performance (one being air). The difficulty with this set-up is achieving a low profile, as the air pocket has to be of a certain size to benefit from its characteristics.

4.4.3 Future seal technologies

Due to the confidentiality of the manufacturers of swimming goggles, there is very little published information relating to future seal technologies in swimming goggles. However, there are signs that they will start to become more science driven. The most apparent development was the contoured seal Speedlite racing goggle by Speedo (Figure 4.7). The aim of the goggle was to maintain a low profile design while achieving maximum comfort. Unfortunately, the variable flexibility of the seal was not based on scientific data, but instead guess work, and therefore was quickly taken out of production, after considerable failure with fitting and comfort.

Figure 4.7, Speedlite racing goggle manufactured by Speedo

More radical forms of sealing have been suggested by Nike, with their concepts in strapless water goggles. Taking the next step in shaving off a few hundredths of a second off a race time, it is predicted that competitors shaving their legs and using low-drag swim suits will not be enough. Swimmers are expected to affix two independent goggle lenses to their eye sockets with medical grade adhesive, which effectively means superglue. Although this may seem extreme, it would not be completely impractical.

Figure 4.8, Concept strapless goggles by Nike

Slightly more conventional forms of future goggle sealing might include the following;

- Disposable wet gels that form directly to the shape of the users face with no need for added pressure.
- Fully customised silicone seals designed on 3D scans of the users face.
- Strapless goggles using suction from within a double seal profile.
- More standard sizes of goggle seals developed from scientific data of the facial form.

4.4.4 Why are seal section profiles constant throughout their circumference

It might be thought that goggle seals are constant in profile due to the limitations of the manufacturing processes used. In most circumstances this is completely untrue, it is simply the limitations of the knowledge about facial form and structure that inhibit this significant development.

Once the exact shape and location of the seal footprint has been established, the only factor that needs to be determined is the seal flexibility at each interval point. This flexibility is influenced by two main factors. The number of goggle sizes to be manufactured affects the overall flexibility, as an increased number results in the likelihood of a user obtaining a closer fit and therefore an overall reduced flexibility requirement. The factor affecting the flexibility variability within each seal is the amount of facial tissue deformation under compression.

Although certain measurable factors concerning the face are published and available to the public, there is no data concerning facial tissue deformation under compression and therefore a new study needed to be conducted.

4.5 Selecting a method of measuring tissue deformation under compression (*in vitro*)

4.5.1 Methods potentially available for measuring tissue compression

There are a number of methods that could possibly be utilised to measure human tissue deformation under compression, as all is required is a system for applying a constant and repeatable pressure, and a technique for measuring the resultant tissue deflection. There is however a significant prerequisite that the study has to be conducted *in vitro,* and the process is completely painless to the subjects being tested.

4.5.1.1 Calibrated spring compression

A spring could be used to compress against the skin, so that the skin is acting on the spring with an equal but opposite force. The spring would have to be applied with an accurate and repeatable calibrated force measurement device. The deflection of the spring could then be measured.

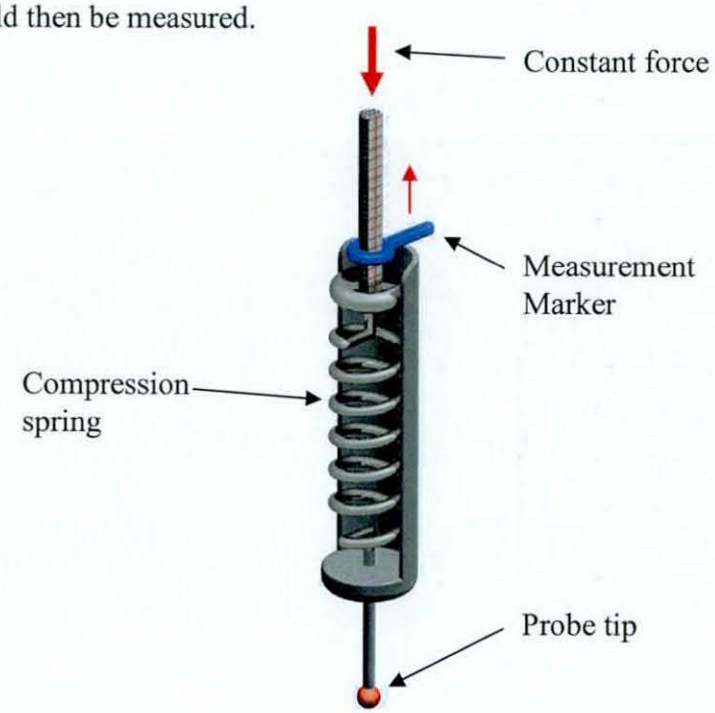

Figure 3.9, Example of a spring loaded compression measurement device

4.5.1.2 Air jet

An air jet would be an ideal method of applying a constant force onto skin. Using air to compress the tissue would also resolve many of the safety issues when working in close proximity to the eyes. The only (but quite significant) downside to using this technique would be the difficulty in finding an accurate method of measuring the resulting deformation.

4.5.1.3 Co-ordinate measurement machine (CMM)

The intended purpose of a CMM, is as its name suggests and is a machine for measuring three dimensional co-ordinates of points on solid objects. Depending on the setup, most CMM's are capable of recording the co-ordinate when a probe touches the target surface at a pre-determined pressure. If this pre-determined pressure is either already suitable for tissue deformation, or can be manually adjusted for generating suitable tissue deformation, then the technique would be ideal.

4.5.2 Method chosen to assess and develop

Choosing a technique for measuring the tissue compression was relatively straightforward. The only method that did not require substantial work in purchasing or manufacturing high tolerance custom components, was the procedure utilising the co-ordinate measurement machine. The CMM also offered semi-automatic probe location with a full range of speed and pressure recognition settings (the pressure at which the probe recorded a measurement).

The system was also already set-up and tested for measurement work on the human face due to the skin sensitivity study. This also had the significant advantage that the process of acquiring ethical approval and health and safety had already been completed, therefore saving substantial time.

4.6 Assessment of using CMM for measuring tissue compression

4.6.1 Objectives

The purpose of this study was to identify whether CMM can be used to assist in data collection for measurement of facial tissue deformation under constant pressure. Using the CMM maintains human input at a low level and therefore should insure high repeatability, accuracy and resolution of the technique. This pilot study will show the feasibility of automation and its repeatability, as well as high-lighting potential problems within the technique.

4.6.2 Subjects

The same participant population was used for that of the previous pilot study that assessed the use of a CMM for measuring skin sensitivity. This was due to their availability and their familiarity with the equipment involved. Following Ethical Advisory Committee approval and informed written consent, the 7 participants (4 male) completed the testing procedure. For the male population, the average age was 23.1years (S.D.= ± 1.6years), height was 1.83m (S.D.= ± 0.08m) and weight was 81.2kg (S.D.= ± 4.6kg). For the female population, the average age was 22.8years (S.D.= ± 1.3years), height was 1.70m (S.D.= ± 0.05m) and weight was 66.3kg (S.D.= ± 5.1kg).

As with the previous pilot study the small participant population of 7 was more than satisfactory to simply assess the technique. It may have been possible to measure the same participant several times over to assess its repeatability, but using a selection allowed the probe to interact with different facial structures, and therefore possible different problems.

4.6.3 Apparatus

4.6.3.1 Co-ordinate measurement machine choice

The same Browne & Sharpe Co-ordinate Measurement Machine was used as the one for the study that measured skin sensitivity. This was used not only because of its availability, but because it offered the important variable preset pressure trigger. The 2mm diameter probe was used as there was no need for a high resolution of positioning, and a larger contact surface area was more representative to the contact width of a seal.

4.6.3.2 Eye protection

The facial surface area required for measurement of tissue compression was similar to that of the study measuring skin sensitivity, and so the eye protection was once again required (Figure 4.10). The pads were exactly the same shape, but were made of a completely transparent material. The participants were allowed to see the movement of the probe as they were not required to provide any information, and being able to see apparently made them more relaxed. The eye pads were again held in place by a harmless, semi- tacky glue so that there would be no strap to overlap with measurement points.

Figure 4.10, Transparent protective eye pads

4.6.3.3 Head location

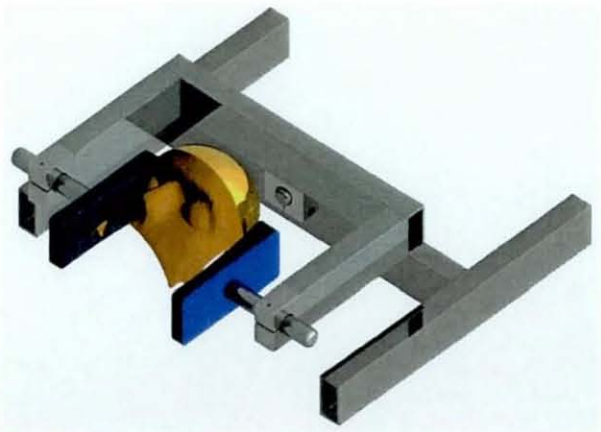

Figure 4.11, 2 axis clamping device for securing participants head during testing.

The same head clamp device was used to the one in the previous skin sensitivity measurement study. Maintaining the head in a fixed position was again instrumental to the success of the study, as any motion during a compression reading would effect the depth at which the probe would be recorded. As there were no issues with distracting the participant from making accurate judgements on probe location, the clamp device was secured slightly tighter.

4.6.4 Probe pressure calculation and system optimisation

4.6.4.1 Objectives

Although the settings of the probe had been optimised for the measuring of sensitivity, a greater force was required in order to deform the facial tissue similar to the manner in which a swimming goggle seal would. The new pressure needed to compress the tissue by a suitable amount had to be calculated and the repeatability of the system had to be measured using different settings.

4.6.4.2 Methodology

The amount a swimming goggle seal compresses the facial tissue, entirely depends on the specific goggles being worn, the person wearing them and how tight the strap is secured. Taking this into account, the compression from the probe needs to deform

the tissue enough to achieve worthwhile data, but not so much as to interact with bone structure or cause pain to the participant involved.

The results of the optimisation study for the measuring of skin sensitivity clearly indicated that force setting 3 was the only suitable force for deforming tissue similar to that of a swimming goggle seal. It was therefore decided to test the repeatability of measuring compression at this setting.

To ensure the object being tested maintained the same structural parameters throughout the investigation, a rubber compound that compressed similar to human tissue was used. The problem with using actual human tissue, is that the area being probed repeatedly might change in behaviour with increased blood flow or possibly with signs of bruising.

Similar to that of the optimisation study for measuring skin sensitivity, The speed of the probe was tested at the four settings, ranging from the slowest to the fastest achievable using the standard joystick setup. Due to there being no easy way of consistently maintaining accurate speeds (during normal experimental conditions), the joystick was marked at specific rotation angles which gave sufficient approximations. At each of the 4 speeds, the force was also measured with the probe being moved normal to the surface as well as at a 45° angle to the surface. For the mentioned settings, 4 trials were completed for each, to give a fair representation.

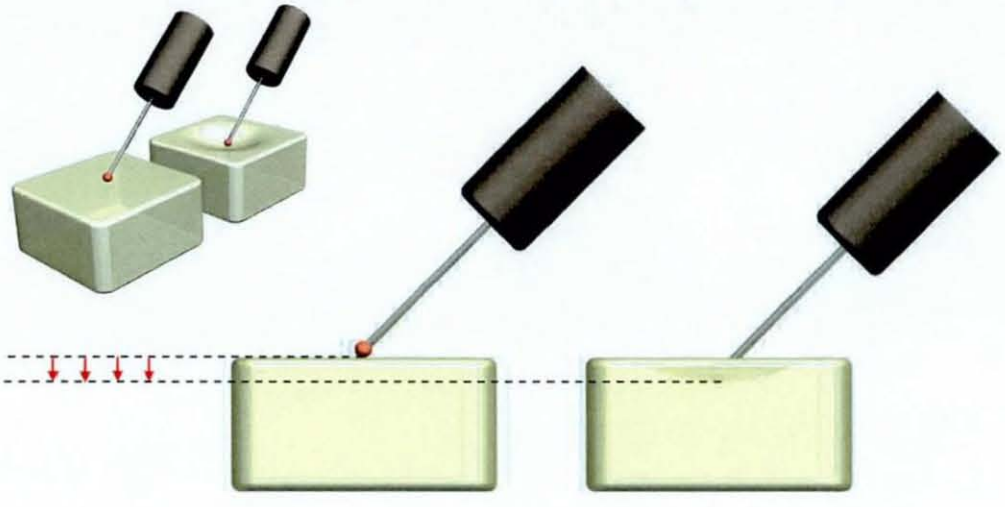

Figure 4.12, Representation of probe deforming rubber block

As Figure 4.12 shows, the probe was positioned until it was just touching the surface of the block and the 3D co-ordinate was then recorded. The probe was then lowered until the pre-set pressure trigger was activated and the co-ordinate was recorded again. The manual positioning of the probe to touch the surface but not deform it was where possible human error could occur. However, this was relatively easy to achieve with very little practice, and would not have caused errors of no more than 0.2mm at the most.

4.6.4.3 Results

Speed	Angle		Measurement 1 (mm)	Measurement 2 (mm)	Measurement 3 (mm)	Measurement 4 (mm)	Variance
Slow	0	Initial	115.583	115.583	115.583	115.583	
		Indent	118.797	118.676	119.04	119.32	
		Compression	3.214	3.093	3.457	3.737	0.081071
	45	Initial	140.876	140.876	140.876	140.876	
		Indent	143.348	143.726	143.953	143.72	
		Compression	2.472	2.85	3.077	2.844	0.062762
Med 1	0	Initial	117.004	117.004	117.004	117.004	
		Indent	120.404	120.888	120.318	120.772	
		Compression	3.4	3.884	3.314	3.768	0.076796
	45	Initial	141.439	141.439	141.439	141.439	
		Indent	143.646	143.535	143.553	143.493	
		Compression	2.207	2.096	2.114	2.054	0.004172
Med2	0	Initial	113.987	113.987	113.987	113.987	
		Indent	117.862	117.993	117.84	117.951	
		Compression	3.875	4.006	3.853	3.964	0.005255
	45	Initial	141.583	141.583	141.583	141.583	
		Indent	144.06	143.657	144.086	143.786	
		Compression	2.477	2.074	2.503	2.203	0.04407
Fast	0	Initial	113.507	113.507	113.507	113.507	
		Indent	117.9	118.585	118.62	118.671	
		Compression	4.393	5.078	5.113	5.164	0.132774
	45	Initial	141.586	141.586	141.586	141.586	
		Indent	144.683	144.118	144.344	144.155	
		Compression	3.097	2.532	2.758	2.569	0.066758

Figure 3.13, Complete results for probe optimisation for measuring compression

As Figure 4.13 clearly shows, the probe settings to achieve highest repeatability are using the medium 1 velocity, with the probe angle at 45 degrees to the normal.

4.6.5 Study Protocol

After obtaining the participants statistics (to ascertain whether they were within the accepted boundary), they were shown a video of the experiments (to comply with ethical standards set by Loughborough University), and were made aware of the potential risks that might be involved. A projector was then used to map a grid pattern of 30 points onto the participants face. This specific number of points was chosen, as measurement time (each point measured twice) would approximately fit within a 1 hour session (including set-up etc.). If measurement time were to exceed 1 hour, the participant would lose interest and fail to concentrate to the required amount

The position of the grid pattern was standardised using the same two sets of reference points as used for the skin sensitivity study (Figure 4.14), with the pattern being stretched in both the vertical and horizontal plane to match the shape of the participants head.

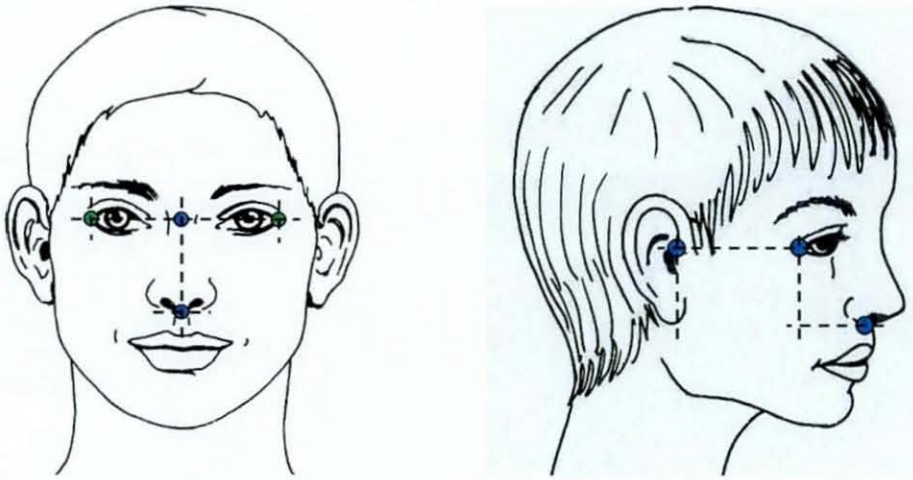

Figure 4.14, Reference points used for positioning grid patterns

Using the reference lines, a grid pattern was over-layed, with 30 points being evenly distributed in the more significant areas where the goggle seal footprint might be positioned (Figure 4.14). Due to the two outer sets of five points being out of position (due to curvature of the face), these were incorporated in the projection onto the side of the face.

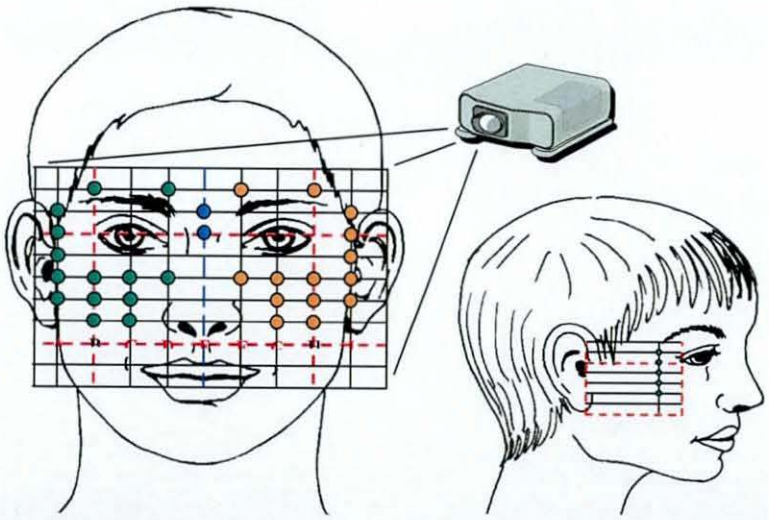

Figure 4.15, Grid pattern of points to be measured for Facial Skin Sensitivity testing.

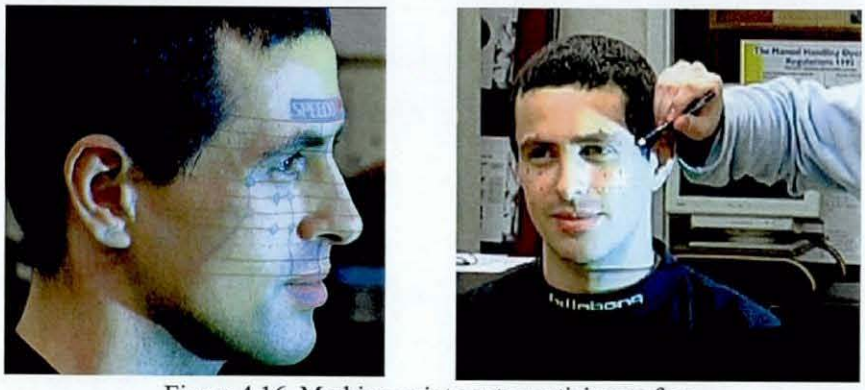

Figure 4.16, Marking points onto participants face.

The points were marked onto the skin using a fine 'make-up' pen (Figure 4.16) and before the participants head was clamped into position, the probe pressure was set to 45 degrees and setting 3 on the force trigger response. The probe was then tested on the participants arm to give an indication of discomfort, using the velocity setting medium 2.

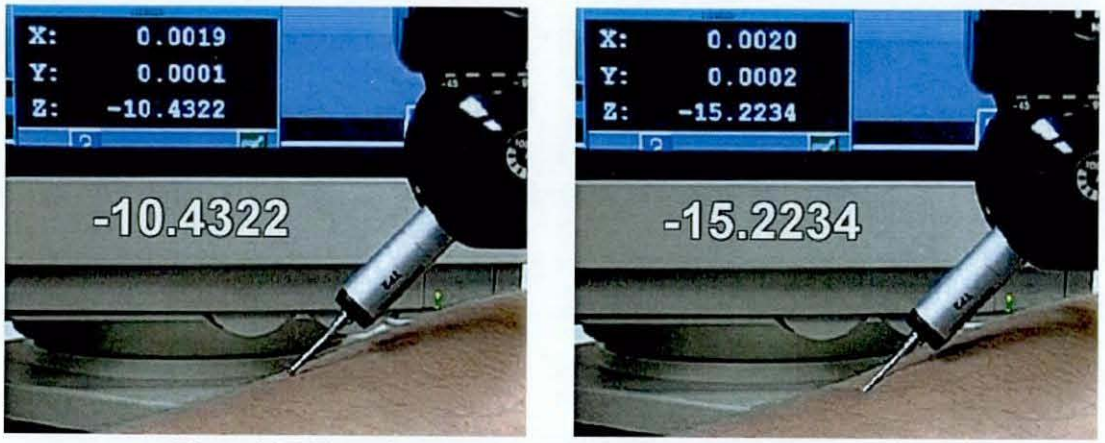

Figure 4.17, Example setup of procedure testing compression of tissue.

Concentrating on one point at time, the probe was moved so as to just touch, but not deform the surface of the skin and the vertical co-ordinate location was recorded. The probe was then immediately moved downwards (Z direction) until the CMM stopped under the specified pressure, and the vertical co-ordinate location was recorded again. The difference between the two measurements was recorded as the compression. The procedure was completed twice for each point.

4.6.6 Results

The complete results can be found in the Appendix –Tissue Compression Pilot Study Data, with the actual compression readings found in Figure 4.18.

Point	Male								Female					
	Participant 1		Participant 2		Participant 3		Participant 4		Participant 5		Participant 6		Participant 7	
	1st (mm)	2nd (mm)	1st (mm)	2nd (mm)	1st (mm)	2nd (mm)	1st (mm)	2nd (mm)	1st (mm)	2nd (mm)	1st (mm)	2nd (mm)	1st (mm)	2nd (mm)
A1	-4.2	-3.6	-7.9	-6.9	-6.6	-6.1	-6.1	-6.4	-6.4	-5.5	-5.1	-5.8	-5.3	-5.3
A2	-3.8	-3.5	-4.8	-4.8	-6.4	-6.4	-4.9	-5.4	-5.3	-5.8	-4.6	-5.8	-6.2	-6.4
A3	-4.0	-3.6	-4.9	-4.7	-5.6	-5.2	-4.7	-4.6	-5.3	-5.8	-7.0	-6.7	-6.3	-6.1
A4	-4.7	-4.8	-4.7	-4.6	-4.5	-4.7	-5.0	-4.7	-5.3	-6.3	-6.5	-7.1	-5.7	-5.9
A5	-5.6	-5.8	-6.0	-5.6	-5.5	-5.8	-6.3	-6.3	-6.0	-6.7	-6.5	-7.5	-6.5	-6.2
B1	-2.8	-3.0	-4.4	-4.5	-3.7	-3.6	-4.7	-4.9	-4.2	-3.1	-4.4	-3.9	-3.6	-3.8
B2	-3.2	-3.2	-5.0	-4.8	-4.5	-4.2	-4.5	-4.2	-6.8	-7.1	-6.3	-6.4	-3.7	-3.3
B3	-4.1	-4.4	-5.8	-5.7	-5.5	-6.0	-5.5	-5.4	-7.1	-7.4	-6.8	-6.9	-6.9	-7.0
B4	-5.2	-5.5	-7.6	-8.1	-6.2	-6.8	-7.2	-6.3	-7.5	-7.8	-7.5	-7.4	-7.8	-7.5
C1	-3.5	-3.4	-4.5	-5.3	-7.0	-9.4	-6.1	-5.0	-7.4	-7.5	-7.2	-7.3	-7.1	-12.1
C2	-6.0	-6.3	-7.9	-8.0	-7.3	-7.7	-7.2	-7.2	-10.0	-9.5	-8.2	-8.9	-8.9	-8.7
C3	-9.0	-8.2	-11.5	-11.2	-8.7	-8.8	-9.6	-8.7	-10.3	-9.1	-9.8	-9.6	-10.0	-10.5
D1	-4.5	-4.0	-3.0	-3.2	-2.7	-2.9	-4.6	-4.5	-4.2	-4.2	-3.7	-3.4	-3.1	-2.9
D2	-4.8	-5.0	-5.8	-6.8	-5.4	-5.2	-8.3	-8.4	-6.8	-6.6	-7.2	-7.1	-4.9	-5.0
E1	-4.0	-3.9	-4.3	-4.4	-2.7	-2.8	-5.2	-4.8	-3.1	-3.4	-3.0	-2.8	-2.4	-2.5
E2	-2.3	-2.2	-3.9	-4.2	-3.0	-3.2	-0.5	-1.1	-2.6	-2.7	-1.1	-0.7	-1.5	-2.0
F1	-4.7	-4.7	-3.9	-4.3	-3.4	-3.4	-4.6	-4.8	-3.9	-3.9	-4.6	-5.1	-2.8	-2.3
F2	-5.4	-5.8	-5.5	-5.6	-4.7	-5.6	-4.3	-4.7	-8.1	-8.3	-4.9	-5.0	-3.4	-3.2
G1	-3.5	-3.9	-4.6	-4.7	-6.4	-7.3	-6.7	-6.7	-8.7	-8.4	-8.9	-9.2	-8.0	-7.9
G2	-6.2	-5.9	-8.9	-8.9	-7.3	-7.6	-8.7	-8.8	-10.8	-10.5	-7.1	-7.1	-8.3	-7.8
G3	-7.5	-7.4	-12.2	-12.6	-8.2	-8.7	-11.5	-11.9	-9.6	-9.4	-8.4	-7.9	-9.6	-9.0
H1	-3.1	-3.0	-3.8	-3.4	-3.3	-3.3	-4.5	-4.1	-3.6	-4.1	-4.8	-4.8	-2.8	-2.8
H2	-3.7	-3.7	-5.1	-5.2	-5.4	-5.1	-4.5	-4.4	-7.1	-7.2	-4.4	-5.6	-3.2	-3.8
H3	-4.1	-4.0	-6.3	-5.6	-5.7	-5.5	-5.1	-6.2	-7.1	-7.0	-6.9	-6.7	-6.4	-6.1
H4	-5.1	-5.5	-9.4	-9.0	-6.0	-6.2	-8.5	-9.0	-7.8	-7.2	-7.7	-7.4	-7.1	-6.9
I1	-6.5	-6.6	-6.9	-7.6	-6.2	-6.3	-5.3	-6.1	-5.9	-5.8	-8.0	-8.3	-6.5	-6.6
I2	-5.6	-5.7	-6.0	-6.3	-5.0	-5.3	-5.7	-5.8	-5.7	-6.2	-7.1	-7.1	-6.4	-6.8
I3	-4.4	-4.2	-4.4	-4.0	-4.7	-4.5	-4.4	-4.5	-5.5	-5.3	-6.7	-7.2	-6.7	-6.6
I4	-4.1	-4.1	-3.9	-4.2	-4.6	-5.0	-5.5	-5.2	-5.1	-5.6	-6.5	-6.9	-6.3	-6.0
I5	-5.3	-6.2	-4.9	-4.5	-6.4	-6.1	-7.8	-8.0	-5.6	-5.9	-6.8	-7.0	-6.6	-6.7

Figure 4.18, Showing compression values (both sets) for the 7 participants.

4.6.7 Discussions

4.6.7.1 Experimental protocol

Two of the most important aspects of this study (besides data collection), was in deciding how many points should be measured, and where they should be positioned. The number of points was slightly simpler, as it was a matter of time being the main restriction. The time limit given for testing, so as to prevent the participants from getting too uncomfortable was set at one hour. For the seven participants tested, the longest experiment duration was one hour and five minutes, which meant that the 30 points being measured was ideal.

The positioning of the points resulted in only one minor complication, and seemed to offer a reasonable resolution for mapping tissue compression for where the seal footprint was likely to be located. The problem was caused from difficulty orientating the participants head so that the probe would be lowered in a normal direction to the surface being measured (Figure 4.19). This left the participant being slightly uncomfortable for a short period of time on specific points.

Figure 4.19, Awkward positioning of participants head.

As already mentioned previously, the only other problem with the general experimental procedure, was the positioning and movement of the probe. The most notable being the rate at which the probe impacted the skin, especially when there was no measurable way of keeping it constant. The speed of the probe was related to the amount the control joystick was rotated, and so it was impossible to maintain exactly the same amount of rotation for each point measured. However, with sufficient practise, the possible error incurred was negligible.

4.6.7.2 Environmental variability

The tests were conducted in an environmentally controlled room, with the temperature and humidity remaining the same for each participant. However, there were numerous factors affecting the participant prior to testing, such as length and condition of sleep, and levels of hydration of the body. Although these were all uncontrolled, and would have had a direct influence on the skin stiffness and elasticity (Lindahl et al., 1998), the difference would have been negligible and the relative intra participant variation would have remained constant.

4.6.7.3 Measurement accuracy

In order to obtain more useful information concerning repeatability of the test method, Bland and Altman plots were completed for each person, showing variability between 1st and 2nd readings (Figure 4.20).

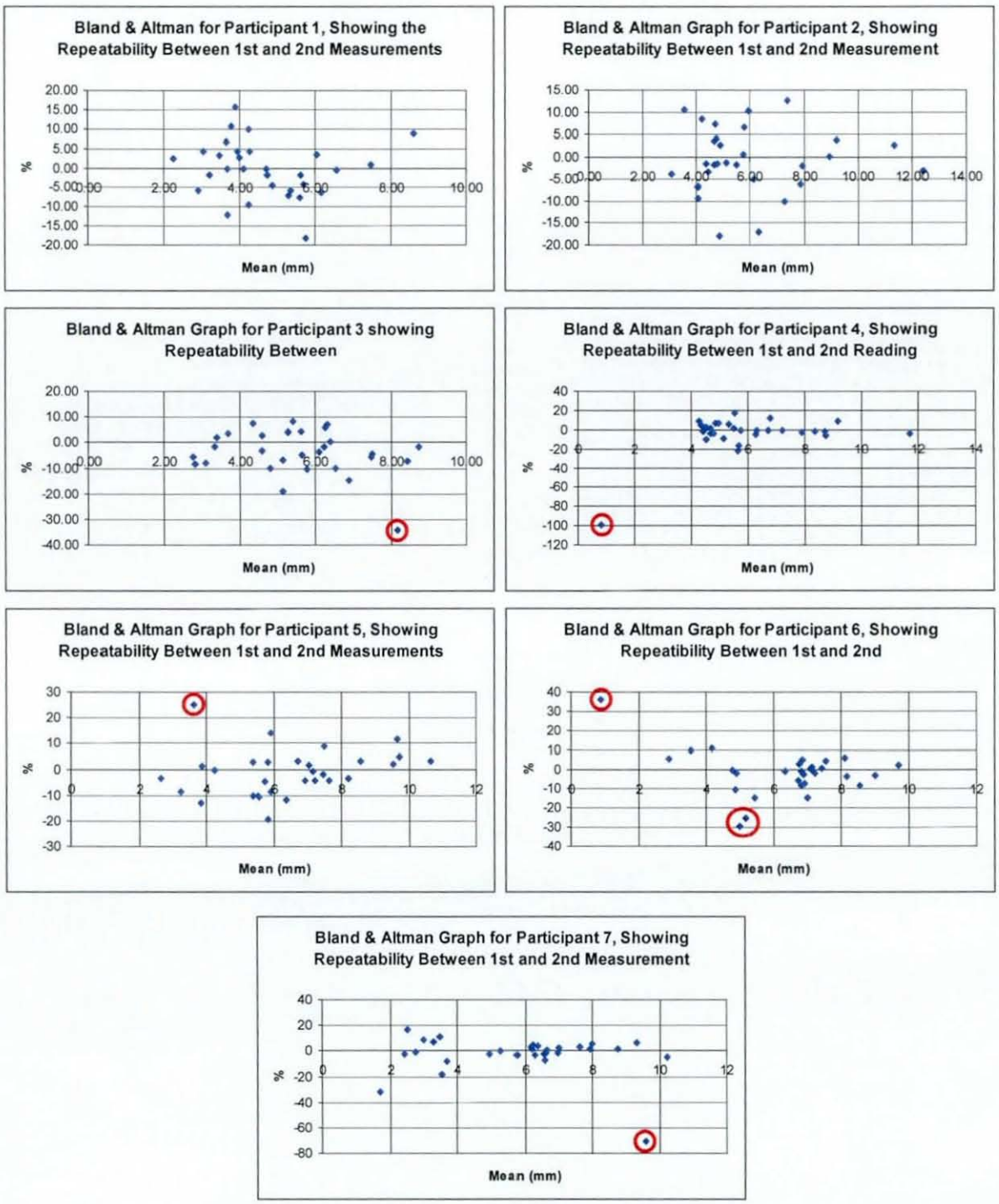

Figure 4.20, Bland & Altman Plots showing repeatability of measurements for all 7 participants. The points identified by red circles are those which exceed the 20% difference (only being 7).

Evaluating the results with regard to accuracy and repeatability, the method of using CMM for measuring facial tissue compression under fixed loads seems to be quite sound. The Bland & Altman charts show that except for 7 measurements, the 2nd set of tissue depth results were all considerably within the 20% line of agreement. The

line of agreement was positioned at 20% purely from a visual perspective, and that it seemed to exclude only the outlier points. Those which were outside of this region were generally due to very small measurements being taken, and only actually varying by 0.5mm.

Although there were certain problems with the experimental pilot study, no modifications could be made to improve on these without using a completely different process. As the results show, the measurements were accurate and repeatable enough for their intended purpose, and so no changes were required for the actual larger study.

4.7 Facial tissue deformation under constant compression

4.7.1 Subjects

Following Ethical Advisory Committee approval and informed written consent, 46 participants (23 male) completed the testing procedure. For the male population, the average age was 21.8years (S.D.= ± 1.9years), height was 1.86m (S.D.= ± 0.06m) and weight was 80.1kg (S.D.= ± 5.2kg). For the female population, the average age was 21.2years (S.D.= ± 2years), height was 1.72m (S.D.= ± 0.04m) and weight was 65kg (S.D.= ± 4.2kg).

These participants were all within the typical statistics for a Caucasian British elite swimmer for both the male and female target population.

4.7.2 Study protocol

Due to there being no modifications required after the completion of the pilot study, the study protocol is exactly the same as section 4.3.5. Again, each point was measured twice to ensure repeatability was maintained.

4.7.3 Results

Due to the large data amount, the entire results can be found for both the male and female population in the Appendix – Tissue Compression Study Data.

The average tissue compression for each point for both the male and female population can be seen in Figure 4.21.

Point position	Female average compression (mm)	Male average compression (mm)
A1	-4.26	-4.15
A2	-4.21	-3.84
A3	-4.57	-3.84
A4	-4.50	-3.85
A5	-4.74	-4.16
B0	-2.90	-2.94
B4	-4.59	-4.19
B5	-5.01	-4.36
B6	-5.52	-4.95
C4	-4.92	-4.78
C5	-5.44	-5.21
C6	-5.94	-5.99
D0	-2.64	-2.79
D4	-3.67	-3.69
E1	-2.77	-3.21
E2	-1.46	-1.49
F0	-2.63	-2.83
F4	-3.73	-4.16
G4	-5.24	-5.11
G5	-5.35	-5.20
G6	-5.66	-5.82
H0	-2.97	-2.90
H4	-4.67	-4.10
H5	-4.73	-4.14
H6	-5.16	-4.84
I1	-4.48	-4.24
I2	-4.27	-3.77
I3	-4.53	-3.79
I4	-4.49	-3.61
I5	-4.81	-4.34

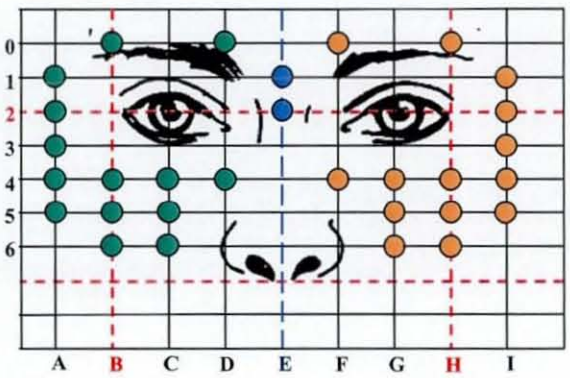

Figure 4.21, Average tissue compression for each point for both the male and female population

4.7.4 Discussions

Although the pilot study gave a strong indication that measurement accuracy was quite high (for its intended purpose), it was important to ensure this was maintained throughout. The influence of human error was still present, and therefore accuracy was variable, even if only by a small amount. The results show each measurement being repeated, and therefore measurement error was again quantifiable (to a certain extent.

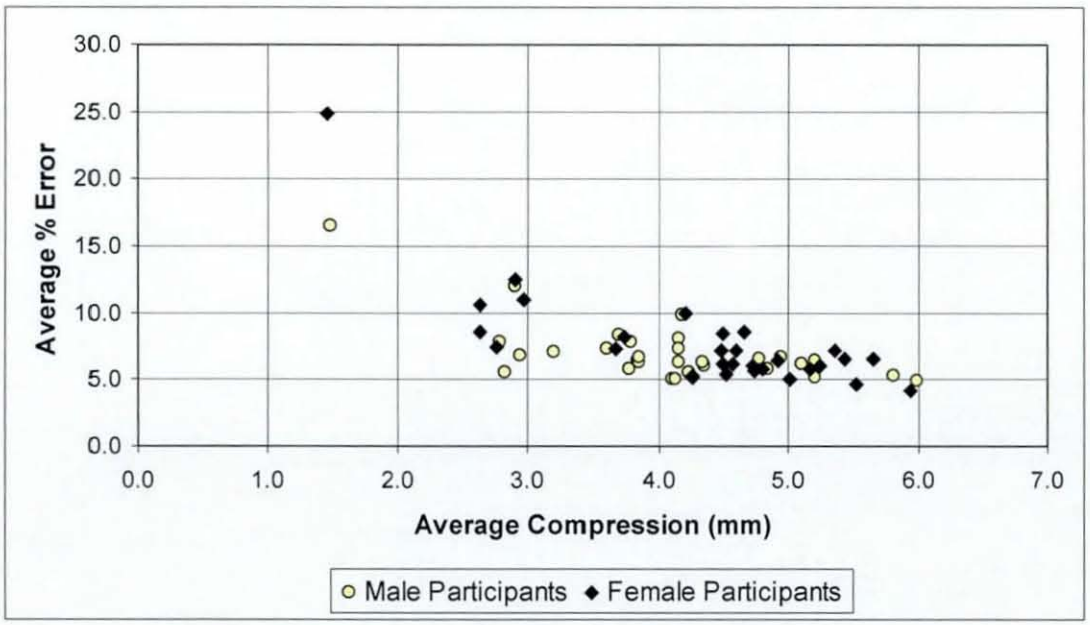

Figure 4.22 Average Compression Point Data Versus Average % Error

Figure 4.22 clearly shows the average compression data versus the average percentage error for each point. The absolute test-retest compression measurement error was less than 0.5mm for every point, which was comparable to that of the pilot study. The average compression distance for the female population was 4.3mm compared to 4.1mm for the men, with the percentage errors for the female and male population being 7.7% and 7.0% respectively. This was actually better than the pilot study, and was most probably due to the familiarity and increased expertise in operating probe movement.

The overall average percentage inaccuracy was still occurring mainly due to this relatively small human error. As mentioned in the pilot study, the speed of the probe movement is presently controlled by the degree of rotation of the joystick. Consistencies in probe speed are thus determined by the skill of the investigator, and so could be substantially improved by replacing the rotation method with a single 'low speed' button. Another potential source of human error occurs where the investigator has to judge when the probe is touching the surface of the skin without causing deformation. Replacing this method by using alternative sensors would result in more repeatable conditions, but to eliminate all human error would necessitate the entire procedure to be automated.

5.0 SWIMMING GOGGLE FIT USING FACIAL ANTHROPOMETRICS

5.1 Introduction

The public perception of how to find out whether a new pair of swimming goggles will fit correctly, is to adhere to the following steps.

- Hold the goggles to your eyes
- Press the eye cups into your eye sockets
- Let go – they should stay in place
- If they don't, they are a poor fit and so try another style

This simple technique is highlighting the fact that the strap of a pair of swimming goggles should not have to be that tight, if the shape and size of the goggle is correct for the users face in the first place. It therefore follows that, the most significant issue when given the task of manufacturing a pair of comfortable and leak free swimming goggles, is the shape of the face that the goggles will be designed around.

5.2 Chapter Aims

The aims of the chapter are simply to generate three dimensional facial surfaces, that are morphed averages of a given target population. These average surfaces can then be used as moulds for new goggles to be designed around.

5.3 Chapter Objectives

If a designer was given the task to produce a pair of goggles to fit the 95^{th} percentile of the entire male and female population, then the facial surface that the goggle shape would be designed around, would have to be a morphed 'average' of a selected sample of the entire population. Although this would be possible, the end result would most likely be a pair of swimming goggles, with extremely large and flexible seals to

accommodate the immense variations of facial shape and size. Consequently, the practicality and hydrodynamics of the goggles would be far from ideal.

To enable the swimming goggle to be closer fitting (and have better hydrodynamics), then there would need to be numerous different shapes and sizes for each specific target population. Depending on the number of variations, this could be commercially unfeasible for the manufacturer, and so a compromise would need to be made. Speedo International (the sponsor company) requested a small, medium and large 'average' face for both the male and female population. This face was to be represented in both three dimensional data point clouds as well as a sheet surface.

The objectives of the chapter are as follows;

- To evaluate all current methods of capturing three dimensional data.
- To capture accurate three dimensional data for a target population.
- To develop a technique that can accurately average the three dimensional data into categories of large, medium and small for both the male and female population.

5.4 Obtaining New Anthropometric Data

To obtain three dimensional point data of an object, a variety of techniques can be employed, one of the simplest making use of a standard 3D co-ordinate measurement machine. This is generally an accepted method when capturing the information of an uncomplicated, straight-edged object. However, when faced with a complex curved surface, it is necessary to increase the resolution of these points significantly. This can be extremely time consuming, as scanning a facial area such as in Figure 4.1, would approximately require about a 1000 points, and each point often has to be recorded manually.

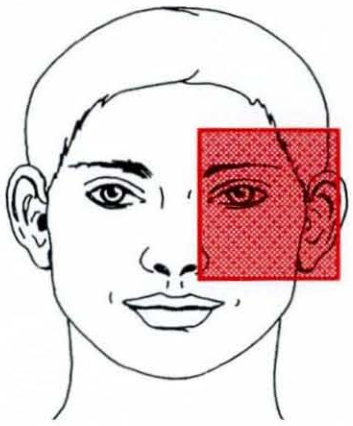

Figure 5.1, Approximately 1000 data points required to scan the highlighted area.

As capturing data for such a curved surface is considered to take an excessively long period of time, automated scanning devices are more commonly used.

5.4.1 Current 3D Scanning devices

Three dimensional scanning devices for the human form have advanced significantly in recent times. The requirements of such areas as medicine (assessment, audit, diagnosis and planning), e-commerce (clothing), anthropometry (vehicle design), video post-production (virtual actors and industrial design (workspace design) have been the driving force to get the technologies where they are today.

Although with the use of a relatively simple Co-ordinate measuring device, a 3D surface can be recorded and then re-created using a CAD based package, the process is extremely time consuming and only rigid objects can be accurately measured. High resolution 3D data can now be acquired without the need for physical contact of the object being measured. This is ideal when trying to measure the complex surface form of the human body with its pliant flesh without resulting in deformation.

A variety of non-contact optically based 3D acquisition techniques can now be utilised to scan the human form. The more prominent of these being:

- Stereo Photogrammetry
- Laser Scanning Triangulation
- Moiré Fringe Contouring

Deciding on which method to use is a compromise between practicality, cost, availability, time consumption and resolution of end product. As the time period over which this study takes is substantial, it is important that a certain depth of understanding of each technique is acquired, before selecting the preferred option.

5.4.1.1 Stereo Photogrammetry

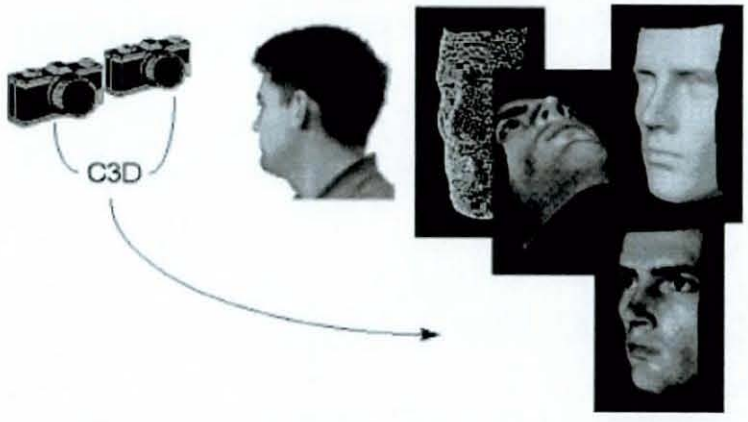

Figure 4.2, Images scanned using Stereo Photogrammetry

"Photogrammetry is the science, and art, of determining the size and shape of objects as a consequence of analysing images recorded on film of electronic media." (Konecny, 1985)

5.4.1.1.1 The History of Photogrammetry

The very first advancements of photogrammetry consisted of primitive investigations into perspective and central projections and date back as early as Leonardo da Vinci in the 16th century. He wrote that "Perspective is nothing else than the seeing of an object behind a sheet of glass, smooth and quite transparent, on the surface of which all the things may be marked that are behind this glass. All things transmit their images to the eye by pyramidal lines, and these pyramids are cut by the said glass. The nearer to the eye these are intersected, the smaller the image of their cause will appear" (Doyle, 1964).The next real revolution however, wasn't until 1979, when Johann Heinrich Lambert used resection to develop the mathematical principals of a perspective image to find where it was positioned in 3D space. Following this key breakthrough, there were four key development stages; Plane table, Analog, Analytical and Digital Photogrammetry, each lasting the duration of approximately fifty years (Konecny, 1985).

From the middle to the end of the 19th Century, Aimé Laussedat developed plane table photogrammetry. He was the first person to use terrestrial photographs for topographic mapping and used hot air balloon flight to experiment with aerial photography. When the stereo plotter and the aeroplane were beginning to be in use towards the end of this development stage, Edouard Deville inventented the first stereo-planigraph, but due to its complexity was of little use.

The combination of the inventions of the first stereoautograph (by Ritter von Orel, 1907), and the computer made it possible for significant advances to be made in multi-station analytical photogrammetry by Dr. Hellmut Schmid in 1953. Uuno (Uki) Vilho Helava then developed the first servo controlled analytical plotter in 1957 and went on to work for the Defence Mapping Agency (now NIMA).

Due to familiarity with the format and the relatively inexpensive equipment, Analytical and film based photogrammetry are still commonly used in Aerial Photogrammetry. However, for close range mapping, such as that of a persons face, digital photogrammetry is the only practical method, as there is no loss of data occurring when transferring the film data to digital format.

5.4.1.1.2 Science behind Photogrammetry

Stereo-photogrammetry utilizes the same principals that the human brain uses to enable us to have three dimensional vision. The simplest way to understand this method is to analyse a stereo or 3D photograph (which you would usually view through special 3D glasses).

Figure 5.3, 3D Photograph

Without the glasses, it can be seen that the photograph is actually made from two separate images (Figure 5.3), with one overlaid on the other and shifted fractionally to the left or right. When the glasses are worn, the left eye views one of the images, while the right views the other and the brain then unconsciously interprets how far you are away from the object depicted, thereby recreating the impression of depth.

A computer can be used to replace the function of the brain, and so when presented with two photographs of an object taken from cameras set slightly apart, it can accurately calculate all three dimensional data of the object. The calculations involved are relatively simple, and the mathematics is described by the following equation,

$$\Delta h = (\Delta x \cdot v) / (CB + x^1)$$

where,

$$\Delta x = x^1 - x$$

Here Δh is the height difference between two points, CB is the difference between the two camera positions, and v is the distance from the focal plane (pin-hole) in the camera lens to the image plane. Δx is the difference between distances of the two

points measured in the images. All the quantities involved are illustrated and described in Figure 5.4.

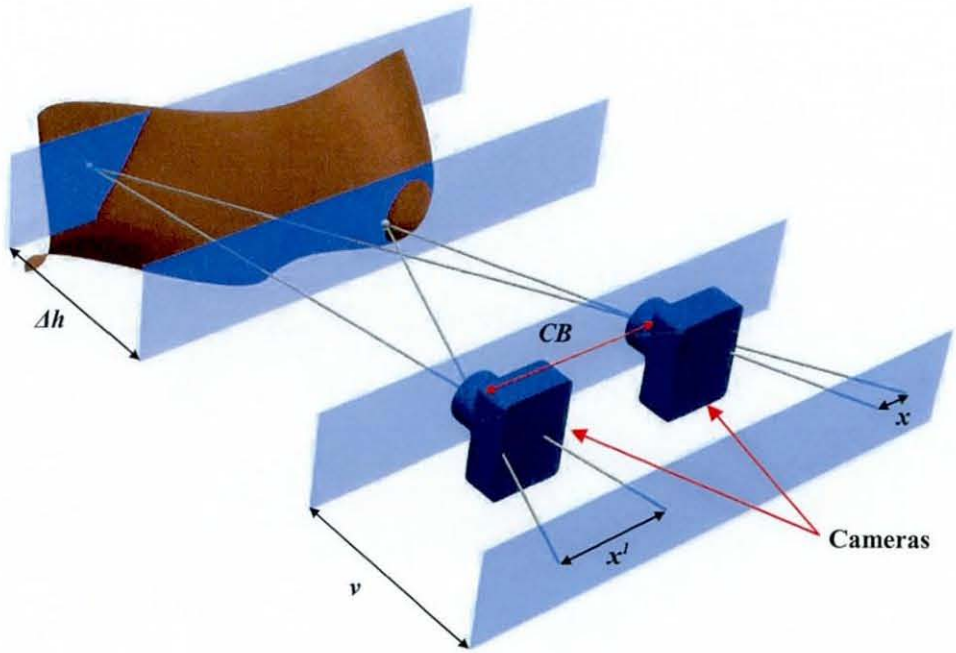

Figure 5.4, Set-up of stereo photogrammetry

Using complicated software technologies, it is possible to not only get high resolution 3D data of the measured object, but also possible to achieve photo realistic 3D models. In Figure 5.5 a 3D model of the shown cliff has been created using Stereo Photogrammetry.

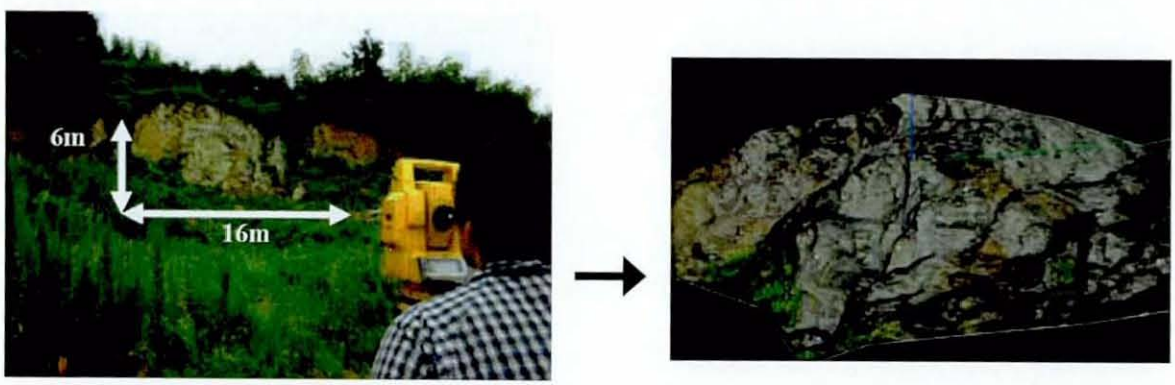

Figure 5.5, Model of cliff created using Stereo Photogrammetry

5.4.1.1.3 Limitations

Although at first glance, this technology would seem ideal, there are certain limitations that prevent this from being the chosen method of facial data capture.

Once the 3D model of a face has been created, the model then needs to be manipulated and sectioned so that it can be morphed with other faces to create a "mean" face. This would be extremely difficult with the current software available, and so although some striking 3D models would be generated, no useful data could be found.

There may also be certain problems with generating a model that could include all of the required facial area, and sewing two generated models together would cause more problems still.

5.4.1.2 Laser Scanning Triangulation

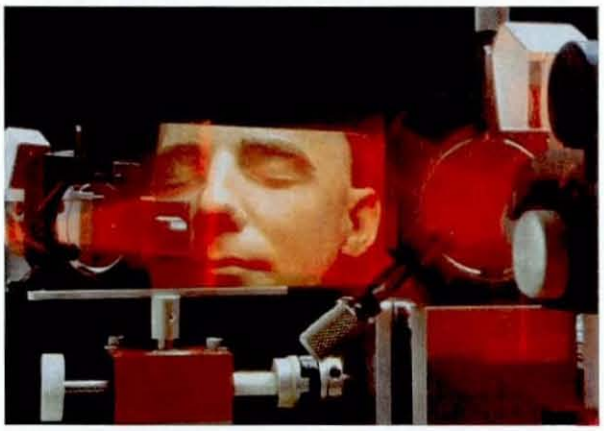

Figure 5.6, Laser Scanning Triangulation being used to scan a person's face

Laser Scanning Triangulation is conceivably the most commonly used form of data capture for the human form. Involving projecting a stripe of laser light onto the surface of the object to be measured and recording it through an offset camera, deformations in the image of the light stripe correspond to the topography of the surface.

5.4.1.2.1 History of Laser Scanning Triangulation

The development in Laser Scanning Triangulation is relatively new in comparison to other 3D scanning methods. The use of auxiliary data in Aerial triangulation, using an Airborne Profile Recorder (APR) was first successfully attempted in 1972 (Zarzycki, 1985). However, it wasn't until 1989, where the first Laser Profiling was completed at the University of Stuttgart by Prof. Ackermann, and was in relation to the development of High Precision Navigation. The technique became commercially viable in 1993 where the TopScan ALTM 1020 was developed in Germany. By 1999, thirty Laser scanners were available.

5.4.1.2.2 Science Of Laser Scanning Triangulation

The foundation on which Laser Scanning Triangulation has been developed is the more straightforward and vastly used Laser Triangulation (utilised in such areas as cartography and the Global Positioning System (GPS)). Laser triangulation is an Active Structured Light (ASL) technique, in which a laser dot is observed (through a lens) by a sensor. The system is active as the geometry of the laser beam is used in measurement and so needs to be known (Harding K, 1983).

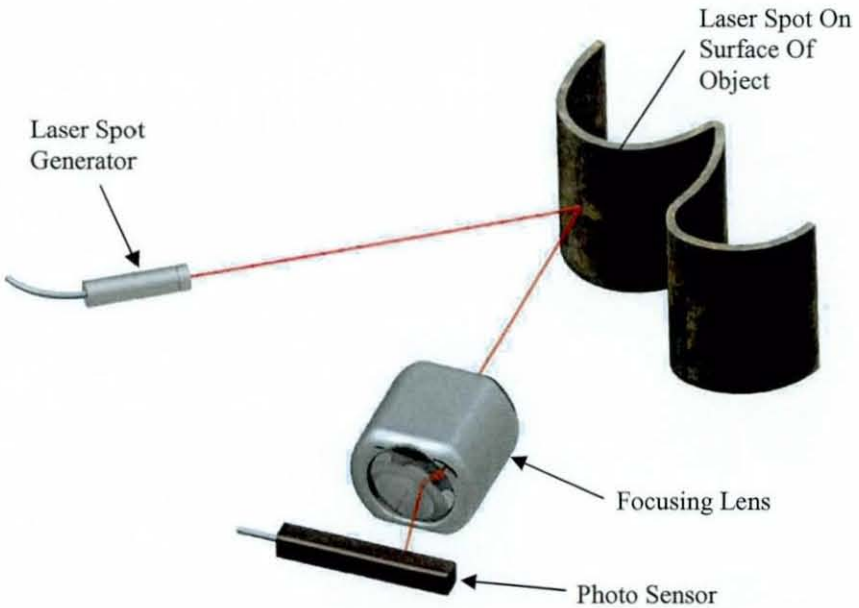

Figure 5.7 Simple set-up of laser triangulation

To achieve the required balance of range and accuracy, the triangulation angle can be manipulated (Harding K, 1989). In order to control the base line for the triangulation, it is essential that precisely controlled mirrors are used. As the laser is positioned at a non-zero angle, relative to the sensor, it is possible for part of the surface to obscure the camera's view of the line (generated by the laser). To over come this problem, a smaller angle (between laser spot generator and sensor) can be used, however this will eventually reduce accuracy. Triangulation is capable of providing high (sub-micron) accuracy over short ranges (Harding K, 1989) and as an analogue photo sensor can be implemented into the system, extremely high data rates are possible.

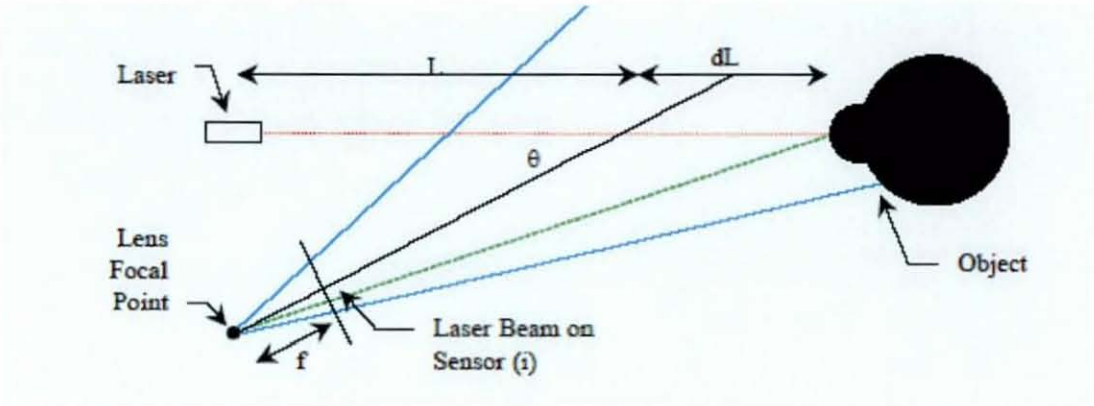

Figure 5.8, Single point laser triangulation

Taking Laser triangulation to the next stage, it is possible to use multiple laser points and an equal number of sensors to acquire 3 dimensional data of several positions at any one time. To simplify this and also achieve higher resolution, the laser point generators can be replaced with a laser line generator (Harding K, 1997), and the sensors can be replaced by a CCD camera. The CCD array has the added advantage of acting as a pixelised sensor, which allows multiple bright spots to be detected and the erroneous data to be discarded. Using off-the-shelf components, it is possible to achieve greater than 0.15mm accuracy.

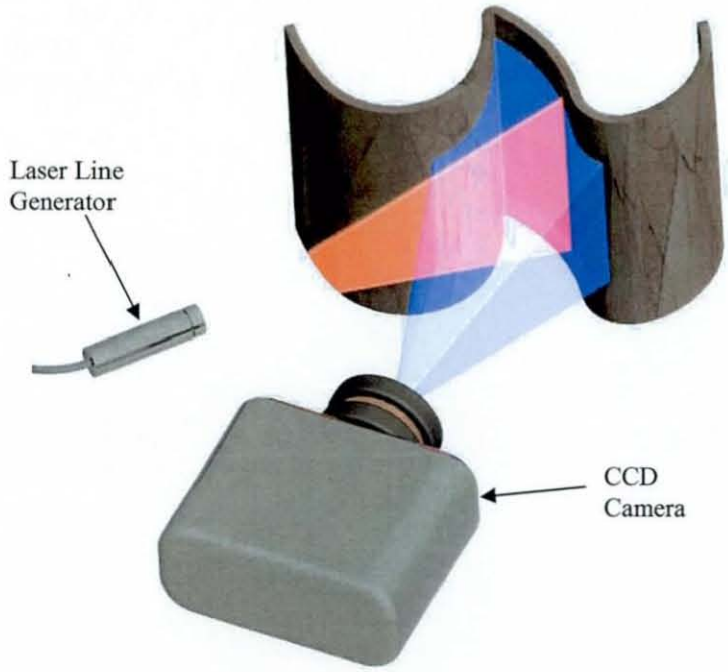

Figure 5.9, 3D surface laser triangulation

5.4.1.2.3 Limitations

Depending on the situation used, there can be several limitations when using the Laser Scanning Triangulation technique. The most notable of these being:

- Occlusion
- Edge Curl
- Illumination
- Surface Variance
- Motion

5.4.1.2.3.1 Occlusion

As with the point-based laser triangulation version, this system can also suffer from occlusion by the surface of the object. A number of techniques can be implemented to minimise this from happening,

- Reduce the angle (as described previously), or move the laser source to the opposite side.
- Use a pair of light sources that are both visible in the image.
- Use multiple cameras and have noisy readings removed

However, as the triangulation angle is never zero, it is always possible for occlusion to occur.

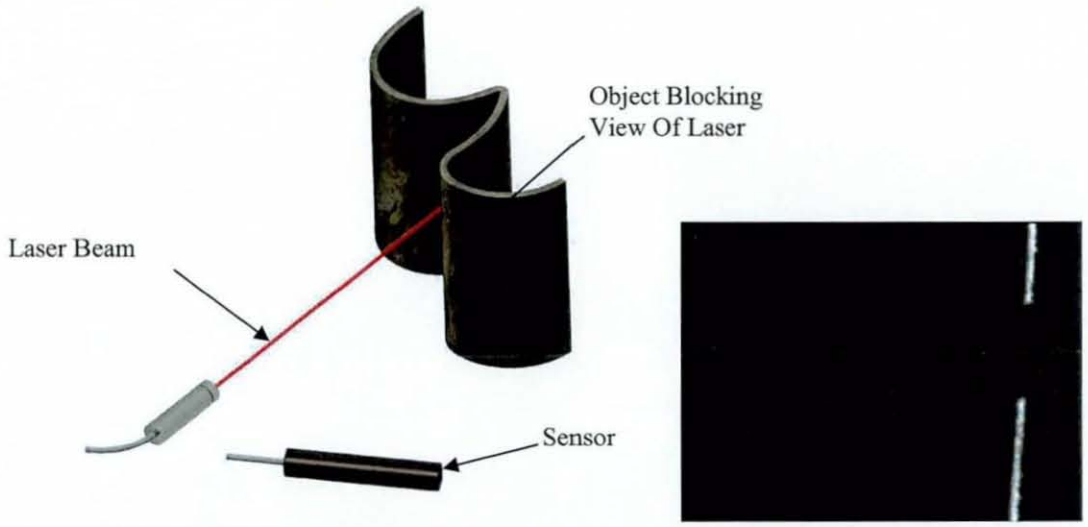

Figure 5.10, Occlusion of the laser generating incomplete image

5.4.1.2.3.2 Edge Curl

Depending on the resolution required, edge curl may or may not be an issue. Edge curl is where only part of the laser is seen striking the surface at the corner of objects (as seen in Figure 5.11).

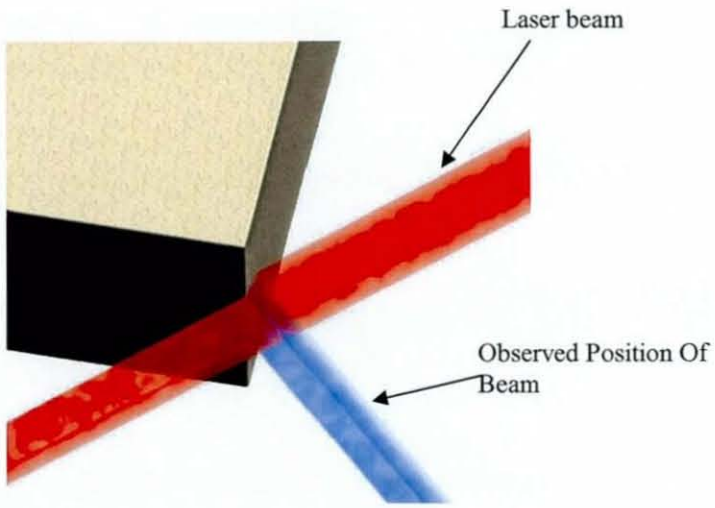

Figure 5.11, Representation of edge curl

The result of edge curl, is that the corner of the object will be lifted away from its position, by a distance proportional to the width of the beam. This is because the triangulation works by intersecting a vector through the observed beam, with the

vector/plane of the laser, the intersection point is computed incorrectly (Mertz L, 1983) (Bieman L et al., 1991) (Harding K, 1983).

5.4.1.2.3.3 Illumination

Another major problem with Laser Scanning Triangulation technique is adverse illumination. If the contrast of the image is greatly reduce due to it being illuminated too brightly, the laser light can not be separated from the background surface and hence unable to be detected. Figure 5.12 illustrates the difference between a laser line shining on a dark surface and an illuminated light coloured one. The laser line has become scattered due to the light coloured surface and hard to distinguish due to the lighting.

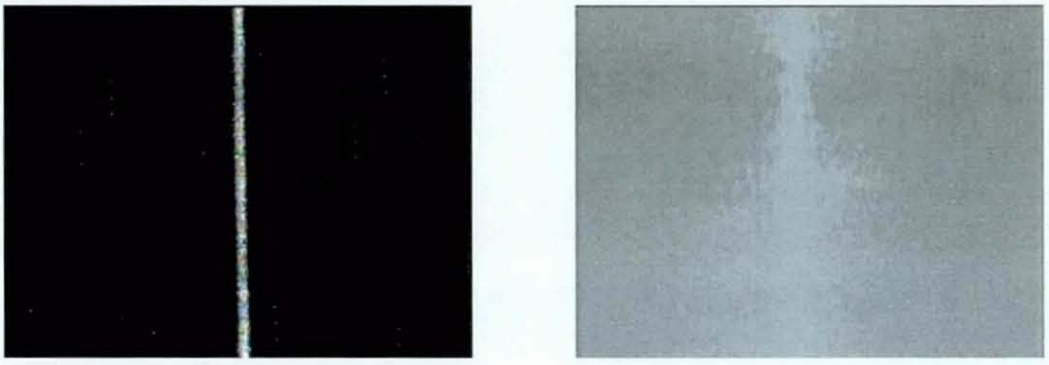

Figure 5.12, Laser line shining on a dark surface (left) and an illuminated light coloured surface (right)

To remedy the situation of a light coloured surface, narrowing of the aperture lens should reduce the scatter, and scanning objects in a dark room will obviously resolve the problems of too much light. When scanning can not be completed in a light-controlled environment, filters can be used to eliminate unwanted wavelengths (and keep only those produced by the laser). Unfortunately, many forms of light, sunlight for instance, contains a full range of wavelengths and would therefore reduce the effectiveness of the filter and possibly render the filter useless.

5.4.1.2.3.4 Surface Variance

When the scanner is set-up for a single type of surface, scanning a surface such as a human face can cause additional problems. The variations in people's skin tone, reflectivity (through make-up and sweat) as well as facial features such as eyebrows require numerous settings and therefore can be a lengthy procedure. Reflection is the greatest of these issues, as the laser light can be reflected on to other surfaces of the object. In most instances the object can be coated in a matt paint, but this might prove difficult on a persons face.

Sharply contrasting textures on the face could also have a similar effect to that of edge curl. At the boundary between light and dark areas, the laser is reflected at different intensities, allowing different quantities of the incident light to be reflected onto the sensor, at different positions. The result is loss in symmetry in the laser with occasionally part of the beam being completely lost.

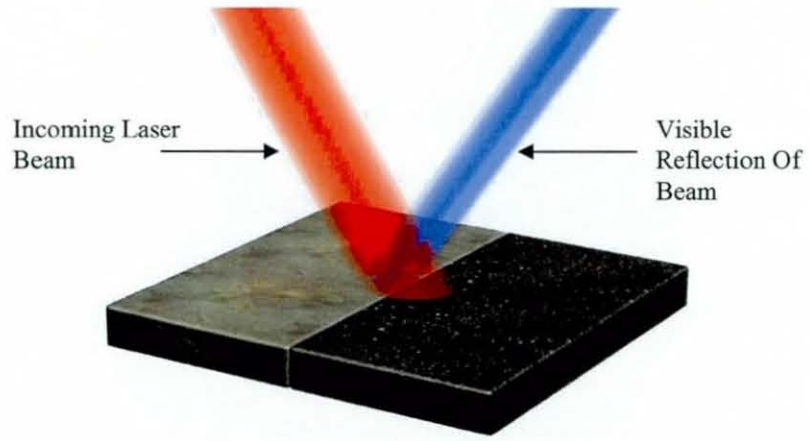

Figure 5.13, Representation of the impact of surface variance on a laser

The area on the face where these factors are most likely to cause the most significant problems, are the scalp, eyebrows and eye lashes. In this case, it is not the colour that causes the problem, but the irregular reflectance properties of hairy surface which diffuses incident light, so that the light reflected back to the sensor is negligible and featureless, resulting in no captured data.

5.4.1.2.3.5 Motion

Due to the nature of CCD cameras, the images it produces are sampled over a finite period of time. If the camera's motion is such that the beam moves through a number of positions during the frame integration period, then the image will be blurred. Faster shutter speeds can be used to alleviate this problem, although only to a certain extent.

Although not such a problem when scanning static inanimate objects, the slightest motion of a persons face will cause severe errors. The scanner will need to be passed over the face several times in order to obtain necessary coverage, with a slight overlap of laser-line each time. If the face has slightly moved during or between these passes, then the represented scanned surface will either have numerous layers, or large gaps at different levels. Maintaining a persons face stationary for a period of approximately 3 minutes (the time period in which it takes to scan a complete face), can be quite difficult.

5.4.1.3 Moiré Fringe Contouring

Figure 5.14, Moiré fringe contours being projected on a surface

Moiré Fringe Contouring is the method of capturing 3D data by projecting Fringe lines onto the surface of an object and recording the resulting patterns and deformations of the lines. Although there are numerous versions of this technique ,

including Fringe Projection, Shadow Moiré and Moiré Projection, they all use the same fundamental concept. Moiré Projection will be the specific technique described.

5.4.1.3.1 History of Moiré Fringe Contouring

Compared to a number of the other methods described, the use of moiré fringes to acquire 3 dimensional data of a surface, is a somewhat new technique. The word Moiré was originally used as it was decided that the patterns produced from overlapping grids were described as appearing similar to that of water silk (the French for watered silk being Moiré). In 1874, Lord Rayleigh discovered that these patterns (created by diffraction gratings) could be used to make accurate measurements.

Until 1970, advances in moiré techniques were primarily in stress analysis. Takasaki was the first to use this technique for capturing data of the human form, and in 1973 he successfully applied moiré topography to the measurement of the human body for medical purposes. There was however a major difference to that of the technique used today, as it was entirely manual, with the use of photographs produced by the shadow moiré method to evaluate the contours.

Unsurprisingly, this method was extremely slow and also required prior knowledge of the object being measured, in order to resolve ambiguities present when the patterns produced were too complex. This encouraged further research in the technique, and led to a semi-automatic process which was capable of producing cross-sections of an object (the face for example). Due to the necessity of operator intervention, this was still time consuming, with each cross-section taking around 2 minutes to measure. Advances in the early 1980's of video and computing technology, have finally meant that a fully automated moiré based imaging system is a viable method for scanning 3D objects.

5.4.1.3.2 Science of Moiré Fringe Contouring

Moiré fringes are an interference pattern that is formed when two similar grid-like patterns are superimposed. They create a separate pattern that does not exist in either of the originals. The result is a series of fringe patterns that change shape as the grids

are moved relative to each other. A dark fringe is produced where the dark lines are out of step by one-half period, and a bright fringe is produced where the dark lines for one grating, fall on top of the corresponding dark lines for the second grating. If the angle between the two gratings is increased, the separation between the bright and dark fringes decreases. These fringes can be seen in Figure 5.15 and are enhanced by the dotted red lines.

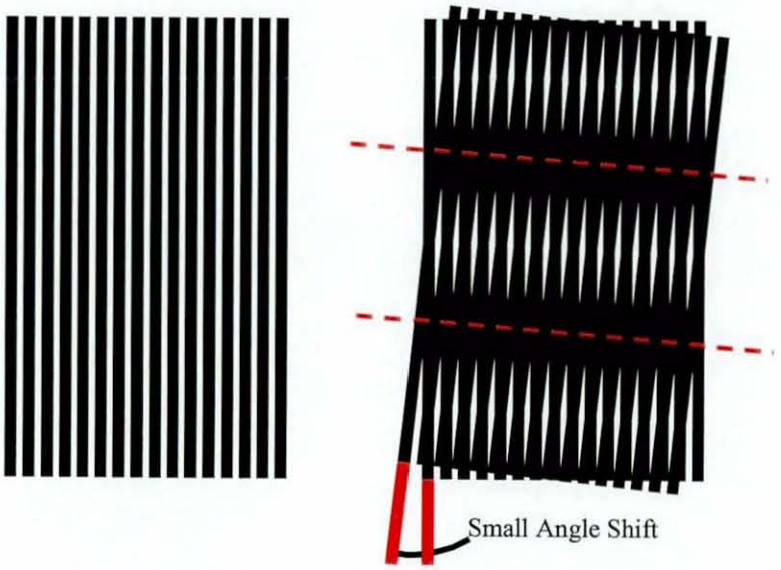

Figure 5.15, Fringe interference

In order to map 3 dimensional objects using this concept, parallel equispaced planes (or fringes) are projected onto a surface and then viewed through a second grating at an angle different from that at which the fringes are projected. The image is detected by a CCD array camera, linked via a video frame digitiser to a desktop computer. The interaction of the superimposed projecting grating lines with the reference grating causes moiré fringes to be produced which appear superimposed on the surface of the object being measured. As the projected grating is distorted by irregularities in the shape of the object's surface, the resulting fringe pattern describes surface contours. The contour interval depends upon the spacing of the fringes projected onto the surface and the projection angle and viewing angle.

Figure 5.16 represents the simplified set-up of this technique. It excludes the computer necessary to control the camera, pizzo-electric translator and frame store for the camera.

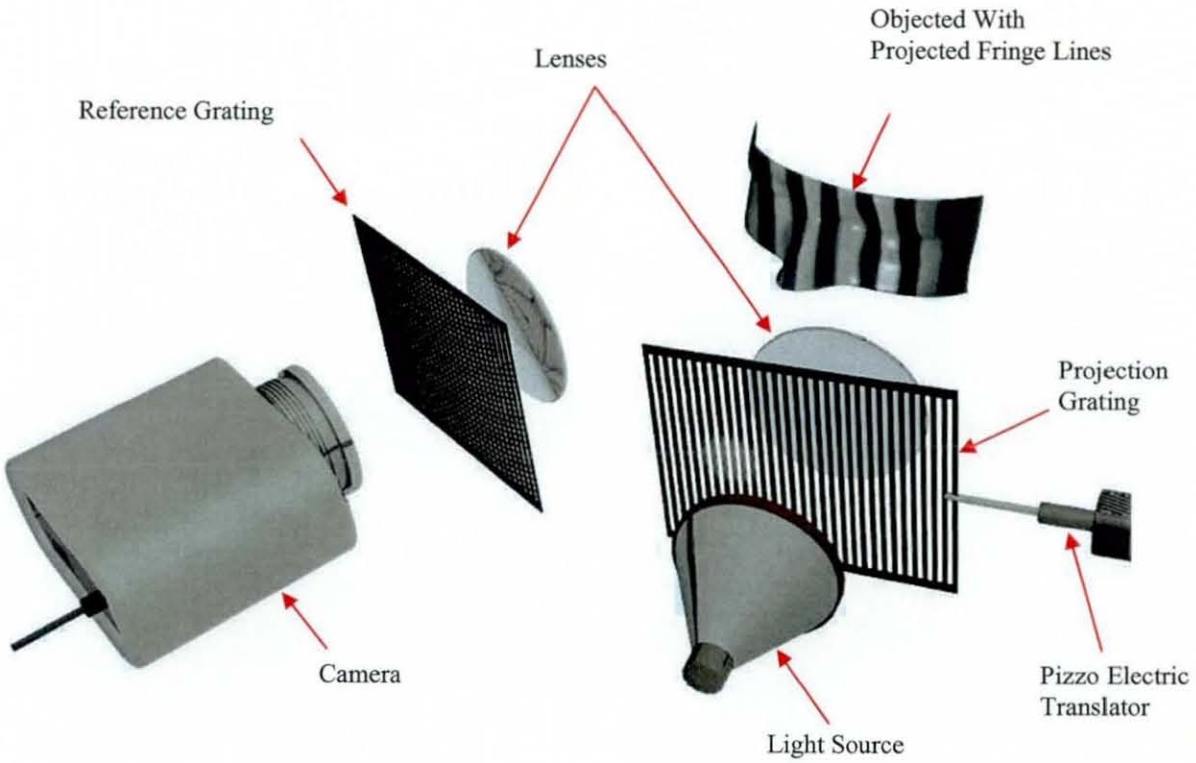

Figure 5.16 Simplified set-up of a Moiré Contouring System

In a conventional modern day moiré contouring system, computer software detects and analyses the fringe pattern and in turn calculates 3D co-ordinates for a set number of points on the surface of the object. However, more advanced systems are now using a process known as phase-stepping, to resolve ambiguities in the image and to achieve depth resolutions of higher than 10 microns. This technique requires several images to be processed, each image possessing a fringe pattern which has been changed by translating the projection grating (in its own plane) through a proportion of its own pitch (Figure 5.17).

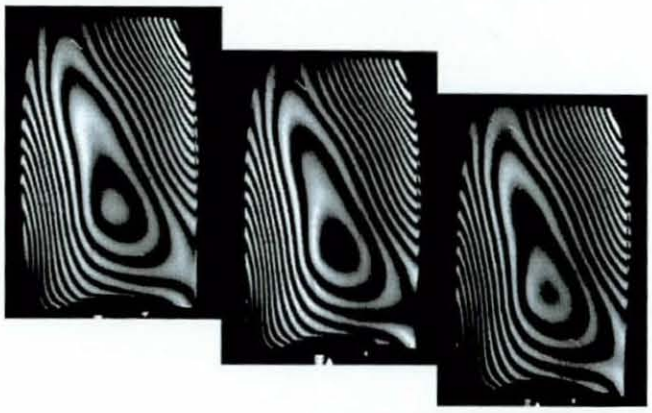

Figure 5.17, Phase stepped fringe pattern

A sine wave can then be applied to each set of intensity levels, and then the phase of the sine wave is calculated. This means that the fringe pattern can be transformed into a phase distribution, which unambiguously describes the shape of the surface and is therefore insensitive to spurious intensity changes in the image. Even with the numerous images required, it still only takes approximately 5 seconds to take the images and another 20 seconds to complete the calculations, resulting in a 3 dimensional computer image.

5.4.1.3.3 Limitations of Moiré Fringe Contouring

5.4.1.3.3.1 Light Conditions

Moiré Fringe Contouring relies on a fringe pattern being projected onto a given surface, and in order for the resultant patterns to be sufficiently visible by the receiving camera, there has to be almost no ambient light. This restricts any scanning to be performed in a room which can be completely darkened and is therefore not particularly mobile. A portable dark room tent can be incorporated around the scanner and subject being measured, but this only increases the already ample amount of equipment required.

5.4.1.3.3.2 Occlusion

As mentioned with the laser scanning, occlusion can also be a problem. The receiving camera may not be able to view the projected fringe patterns and will therefore not be able to compute the necessary calculations for that specific area.

However, there is also the added problem that with the Moiré Fringe Contouring technique, the apparatus as well as the subject being scanned are both maintained in a fix position throughout. This is not a problem when the object being scanned is quite small and has a somewhat flat profile, but when the projected surface is excessively steep, the Fringe Pattern becomes ineffective for contouring. This is shown in Figure 5.18, where the object being scanned is a human face.

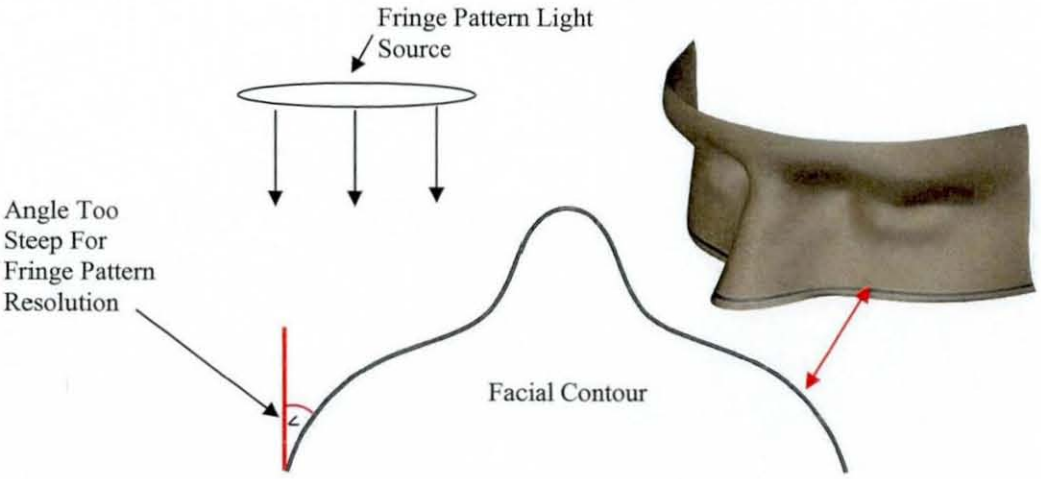

Figure 5.18, Ineffective contouring on a steep surface

Fortunately, there are solutions to these problems, but either requires more equipment or more expensive software. The addition of another camera or cameras, will mean more of the surface can be viewed at any one scan, and so a greater proportion of the surface can be calculated. The slightly slower, but certainly cheaper option, is to use software that allows two separate scans of the same object to be meshed together. Although it is possible to mesh two halves of the same object together in certain CAD programs, it is often difficult, time consuming and inaccurate, and therefore far better to do this with the source file.

5.4.2 Choosing the Scanning Method

As mentioned previously, a compromise between practicality, cost, availability, time-consumption and resolution of end product, needed to be made before the choice of scanning method could be decided. A small performance table was produced, scoring each of the techniques on each of the five criteria.

Cost	Although there was a budget available for spending on hiring a scanning system, the budget was finite, and so the lower the cost could be kept down, the better. If the scanner was available for free, then the highest score was awarded.
Time	The time it takes to get from the initial scan to the final 3D image.
Practicality	Ease of use of the equipment and processing techniques
Availability	How quickly the equipment would be available and for how long.
Final Product	How useable the final product would be, when considering morphing the faces together and retrieving dimensional information

The scoring rating was from 0 to 4 with 4 being the best. If in any of the categories, a technique scored 0, then that technique would definitely not be used.

	Cost	Time	Practicality	Availability	Final product	TOTAL
CMM	4	?	?	4	?	8
Laser Scanning triangulation	4	2	3	4	3	16
Stereo Photogrammetry	2	3	3	2	0	10
Moiré Fringe Contouring	2	4	3	2	4	15

Figure 5.19, Grading the different scanning methods, ? relates to unknown quantity.

From Figure 5.19, it can be seen that little is known about the time, practicality and final product for using CMM as a technique for capturing 3D data of a complex

surface. Although presumed unlikely as a viable method, further research needed to be done to competently assess it. The Laser Scanning Triangulation and the Moiré Fringe Contouring techniques were the only other viable methods.

5.5 Acquiring 3D Data Of A Single Face Using A Standard Co-ordinate Measurement Machine

5.5.1 Objectives

It was expected that the time taken to generate a 3D image of a face using CMM as the method of data retrieval would be too extensive, and therefore the objective of this trial was to simply get a better indication of this time-duration. The resolution of the final image was also of interest, but this would realistically depend on the number of points taken.

5.5.2 Methodology

A CMM was used to measure 1000 points on half of the face on one male participant. The co-ordinate data was then input into a CAD package where a 3D image was generated.

5.5.3 Apparatus

The specific co-ordinate measurement machine used was a Browne & Sharpe CMM. The head was held securely in position by a simple clamping system with ample padding, and small safety goggles were used to protect the eyes from the probe. The data was automatically recorded onto the accompanying software on a standard PC, where it was then input into Excel and organised for inputting into the CAD package. Unigraphics was the chosen CAD software to manipulate the point data and generate a solid surface.

5.5.4 Experimental design and Procedure

The CMM had already been used in the two previous studies measuring Facial Skin Sensitivity and Tissue Compression, and therefore additional Ethical and Health and Safety approval was not required.

Only half of the face was measured (in the vertical plane), and the area was from the middle of the forehead to the top of the mouth. Points were taken every 3mm in both the vertical and horizontal axis (to total 1000 points). Before the data points could be input into Unigraphics, they had to be rearranged into the correct formatting using an Excel spreadsheet.

Once the 3 dimensional point data was input into Unigraphics, the data had to be thinned. This meant that points which were not required, due to the surface in that specific area being very smooth, would be removed. This prevented ripple effects occurring, but unfortunately meant that the level of detail was also reduced. The points then used to create spline curves are shown in Figure 5.20.

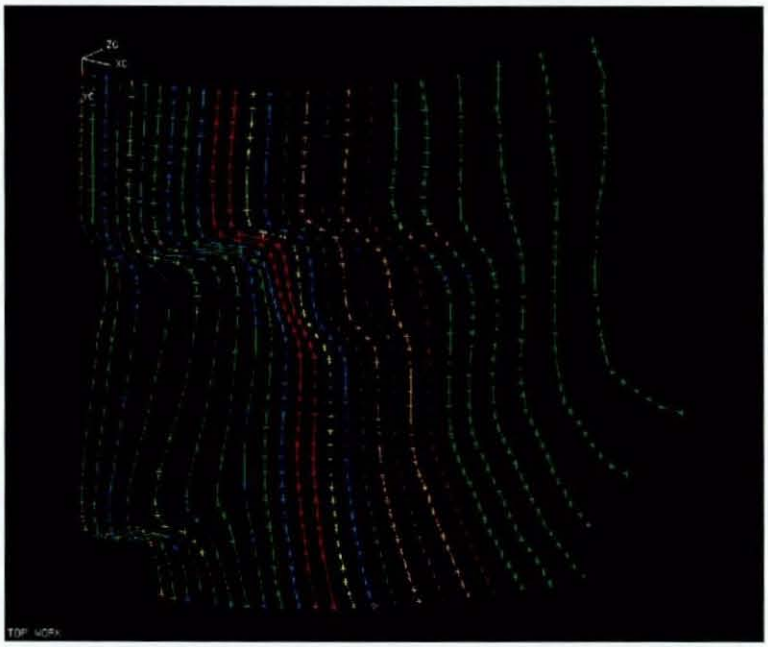

Figure 5.20, Point data with resulting splines.

From the spline curves generated, it was then possible to produce a sheet surface as shown in the results.

5.5.5 Results

The solid facial surface generated is shown in Figure 5.21. Although a reasonable representation of the initial participants face, there are certain highly noticeable problems. The eyes appear extremely large and bulbous due to the protective safety goggles (**A**), and prevent essential surface contours from being seen. There is also a significant crease on the side of the nose (**B**), caused from the resolution being too low.

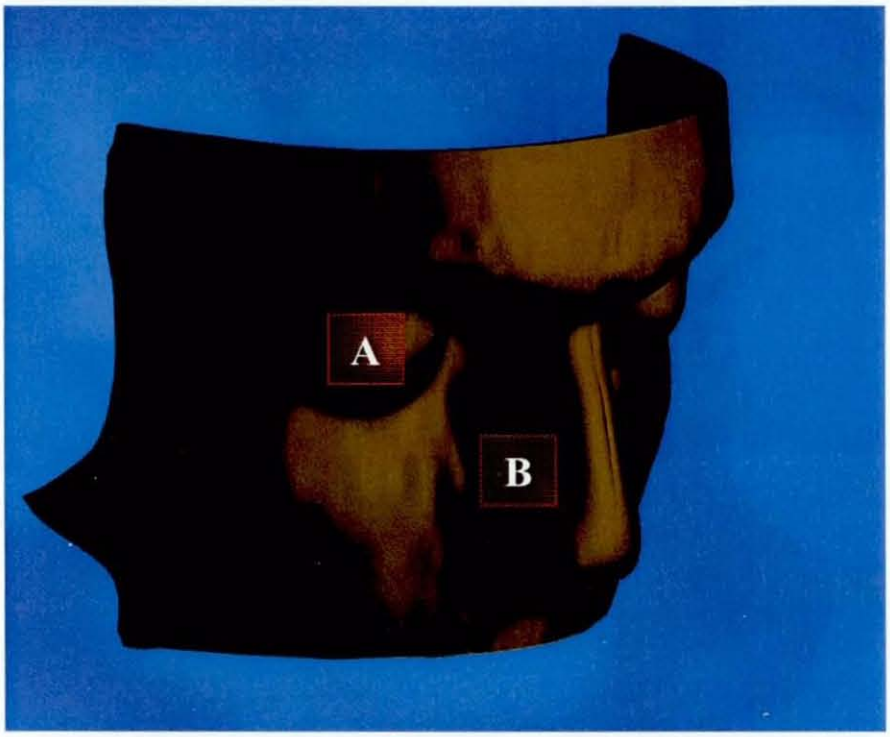

Figure 5.21, Generated 3D image of the participants face

5.5.6 Conclusion

Figure 4.21 took approximately 10 hours to get to the stage where it is shown and the surface is still far from perfect. Most importantly however, is that a great deal of the detail and actual shape around the eyes has been lost. Due to both the time and the loss of detail, this process is completely inadequate for the task. In order for any useful three dimensional point data to be used, more modern scanning techniques are required. The next best method to trial is the Laser Scanning Triangulation method.

5.6 Facial Scanning Using The Laser Scanning Triangulation Technique – Pilot Study

5.6.1 Objectives

The pilot study was completed in order to assess the viability of using Laser scanning Triangulation as a method of high resolution data capture for the use of creating 'average' faces. The key areas to be looked at were;

• Movement of the participant. Using head, support, could the participant be held still enough for the duration of the scan, so little or no processing (cleaning of data) would required?
• Time scale. How long would it take to get a useable 3D image for each participant? Would this time period be practical when scanning over a hundred faces?
• Final product. Although the technical data shows that the laser scanner has a resolution of more than 10 microns, would the final image represent this, and would there be any parts of the face the scanner could not pick up?

5.6.2 Methodology

A Laser Scanner was used to scan a small group of healthy adult men and women. The data has to be cleaned and transferred into a CAD package where an 'average' face for both the male and female population could be produced. The following sections describe the participant population, apparatus, methodology for optimisation of the system, experimental design and procedure and then conclusions.

5.6.3 Subjects

Following Ethical Advisory Committee approval and informed written consent, 10 participants (5 male) were to complete the scanning procedure. For the male population, the average age was 21.2years (S.D.= ± 2.7years), height was 1.82m (S.D.= ± 0.11m) and weight was 78.3kg (S.D.= ± 7.1kg). For the female population,

the average age was 21.5years (S.D.= ± 2.9years), height was 1.70m (S.D.= ± 0.12m) and weight was 66.4kg (S.D.= ± 5.6kg).

As can be seen from the standard deviations, the ages, heights and weights varied quite considerably. This was intentionally done, so as to test the entire procedure to its limits. There would be little point in scanning very similar faces, as there would be no real assessment of the morphing technique. The reason for 10 participants being scanned was to give a realistic idea of how long the complete study would take, as well as giving a large enough sample to test the morphing technique.

5.6.4 Apparatus

The specific laser scanner used was a Model Maker X70, with the associated processing software. The participants head was held in position using a simple clamping support system, attached to a standard office chair (an example of this type of set-up can be seen in Figure 5.22). The cleaned image was then put into Unigraphics for analysis and morphing.

Figure 5.22, Example of chair used to support participants head during scan

Due to the manner in which the scanner shines a laser line onto the surface of the object being measured, it was thought that protection for the eyes was needed. Even though the low power laser would not penetrate the eyelids and cause any harm, eye protection was used in case the participants opened their eyes for any reason.

The surface area required to be scanned, was surrounding the eyes and so the eye protection had to be custom made to take up as little space as possible (Figure 5.23). The pads were completely opaque (and still only 1mm thick) and were held in place by a harmless, semi- tacky glue.

Figure 5.23, Protective eye pads

5.6.5 Optimisation of the system

It was found through a few trial runs, that the scanner was having difficulty picking up several areas of the face, due to the varying texture and reflectivity. In order to rectify this problem, a matt, white face paint was used to cover all of the required facial area. This was especially significant on the eyebrows and inner corners of the eyes.

Lighting also seemed to effect the performance of the scanning ability. The standard room lighting was turned off and replaced with three low power halogen lamps, to give a constant ambient lighting effect on the facial area, with no shadows being produced.

5.6.6 Experimental design and Procedure

5.6.6.1 Scanning

Before commencing scanning, the participant was given a quick demonstration of how the system worked. They were then asked to sit in the chair and secure their head

in the padded clamping device. The eye protection was then secured into the correct position and scanning could start.

The more passes the scanner made over the facial surface, the more cleaning the image would need in processing. Therefore the scanner was passed vertically over the facial area approximately five times, and then any areas needing extra scanning could be done with smaller passes focused specifically over the problem area. If the number of passes got too high, then the procedure was started again. Once the image was complete, the participant was thanked and then left.

5.6.6.2 Image Processing

Before the 3D image could be imported into Unigraphics for analysis, there were a number of problems that had to be resolved. The most important of these being overlapping surfaces, or corrupt jagged surfaces. Both of these being caused by the slightest movement of the participants face (even with the use of the clamping device). This was an extremely slow but simple process, with the user having little input as to how the surface would be cleaned. This meant that the surface was sometimes made worse, or the corrupt area would be deleted leaving a gap in the necessary facial area.

The gaps in the face were then filled using either one of two methods. If the gap was relatively small and uncomplicated, the software could predict what the surface should actually be like, by analysing the curved surfaces leading up to the edge of the gap. If the gap was too large or complex for this method, then a simple patch could be used which would basically join one edge to the other with a straight line. This was far from ideal, and therefore it was crucial that the original scan was as satisfactory as possible.

Due to the fact that processing took between 30mins and 3 hours, it was decided that after the first 5 participants had been scanned, the pilot study was cancelled.

5.6.7 Conclusions

Spending between 30mins and 3 hours to complete a scanned 3D image was completely impractical, as another 2 hours was required to analyse each face, before morphing could even be started. This would mean that if 140 faces were to be scanned using this method, the whole process could take as long as 700 hours (a minimum of approximately 18 weeks work).

Even if this amount of time was spent completing the scans and processing, the end result would be less than ideal, with improvised surfaces and eye protection blocking important information. It was therefore decided that the pilot study would have to be repeated (with the same objectives), except using the Moiré Fringe Contouring technique instead.

5.7 Facial Scanning Using The Moiré Fringe Contouring Technique – Pilot Study

5.7.1 Methodology

A Moiré Fringe Scanner was used to scan the same small group of healthy adult men and women, (the original Laser Scanning pilot study participants). The data was cleaned and then transferred into a CAD package where an 'average' face for both the male and female population was produced. The following sections describe the participant population, apparatus, methodology for optimisation of the system, experimental design and procedure and then results and conclusions.

5.7.2 Apparatus

A Moiré Fringe Contouring scanner used was in conjuction with its associated processing software. A Framed dark room tent was used to block out any ambient light, so the equipment could be transported anywhere. A standard free rotating swivel chair was used for the participant to sit on.

5.7.3 Experimental design and Procedure

5.7.3.1 Scanning

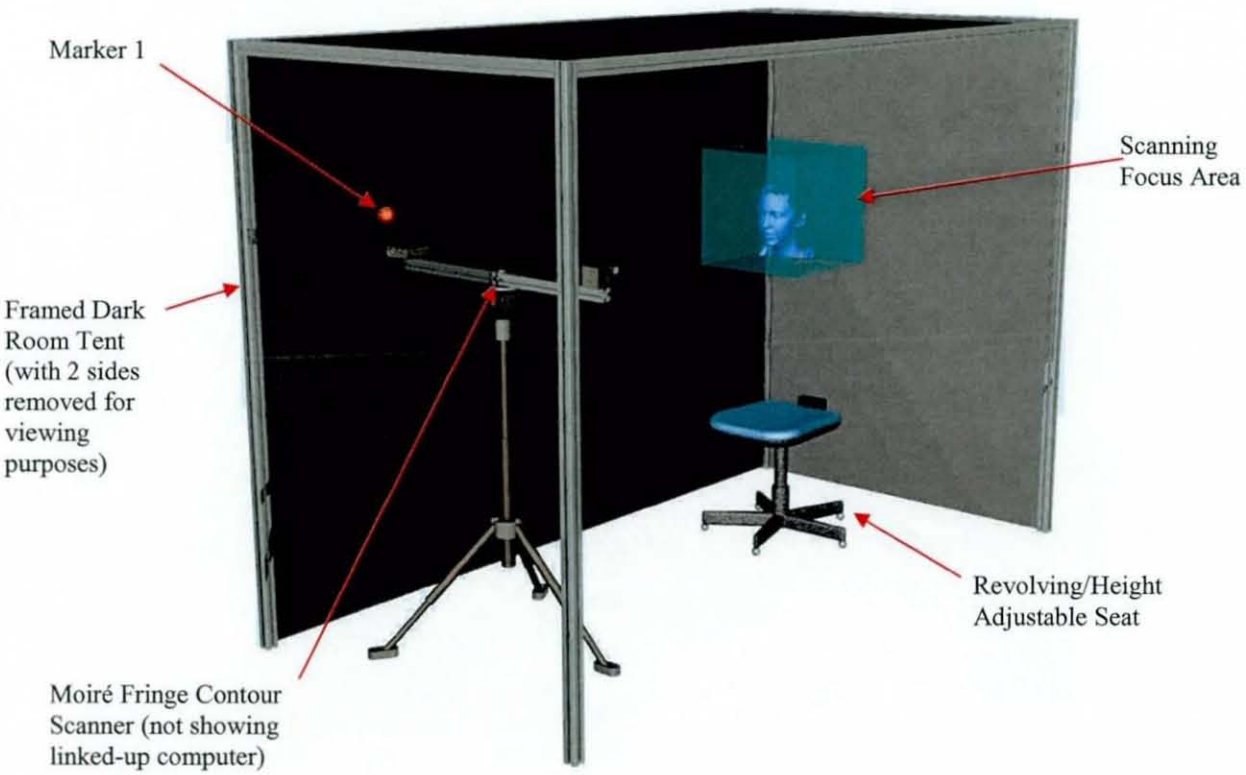

Figure 5.24, Set-up of Moiré Fringe Contouring experiment

Before commencing scanning, the participant was given a quick demonstration of how the system operated (set-up shown in Figure 5.24). They were then asked to sit in the chair and rotate their entire body and face Marker 1 in the corner of the tent.

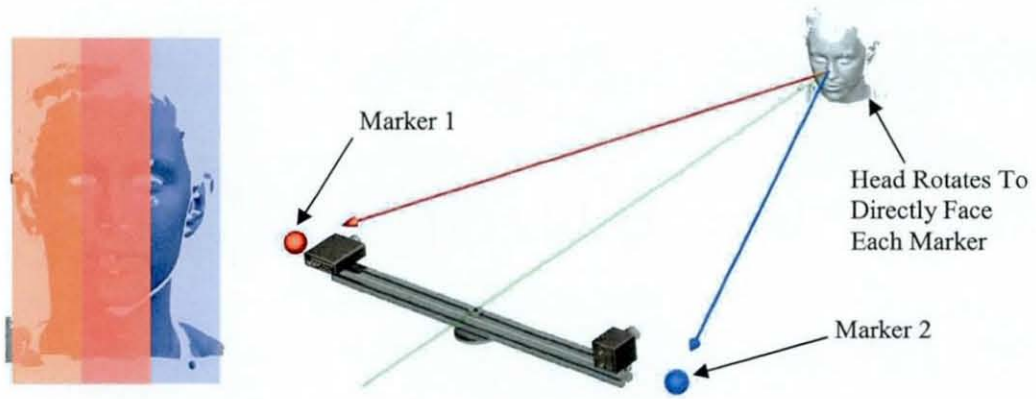

Figure 5.25, Diagram representing rotation of head to achieve overlapping of scans

The reason for two markers, was due to the fact that the scanner could not scan the required area of face at one time, and so a scan of each side of the face was necessary (Figure 5.25). As long as there was a significant overlap of the two scans, they could be sewn together to create a complete image.

The seat height was then adjusted to prevent the participants head from being outside of the focus area for the scanner. If outside this 3 dimensional area of space, the scan would either be incomplete or not work at all. They were then asked to maintain a relaxed facial composure with no expression, and to close their eyes during scanning. It was decided to keep the eyes closed for all participants, as the lights from the projector might be quite uncomfortable. It was also assumed that skin would scan better than the eyeball. Once the first scan was complete (which took approximately 5 seconds), the participant was asked to face marker 2, and the process was repeated. Once the both scans were complete, the participant was thanked and then left.

5.7.3.2 Image Processing

Using the provided software package, the only processing required was to sew the two separate halves of the face together. This took a matter of seconds, and simply required selecting 3 separate pairs of points, with a point from each pair being in the same relative position on each face (hence the required overlap).

The software would then compute numerous calculations to find the best fit. The only times where there seemed to be a problem, was when erroneous scan data (surfaces such as clothing, picked up during scanning which were not on the face), had been included in the calculations, and therefore disrupted the averages for best fit. Once an image was successfully completed, it would be saved as an stl file (stereolithography) and imported into Unigraphics.

5.7.3.3 Image Analysis & Morphing

The method chosen for morphing the various scanned faces together was quite simple in theory, but unfortunately laborious in its application. Each face first needed to be

oriented into a relative absolute axis and then separated into the specified number of 3D surface data points. The faces then had to be categorised into small and large for both the male and female population, via key anatomical measurements. Each equivalent data point was then averaged for each category, allowing surfaces for the respective facial categories to be generated.

5.7.3.3.1 Facial orientation

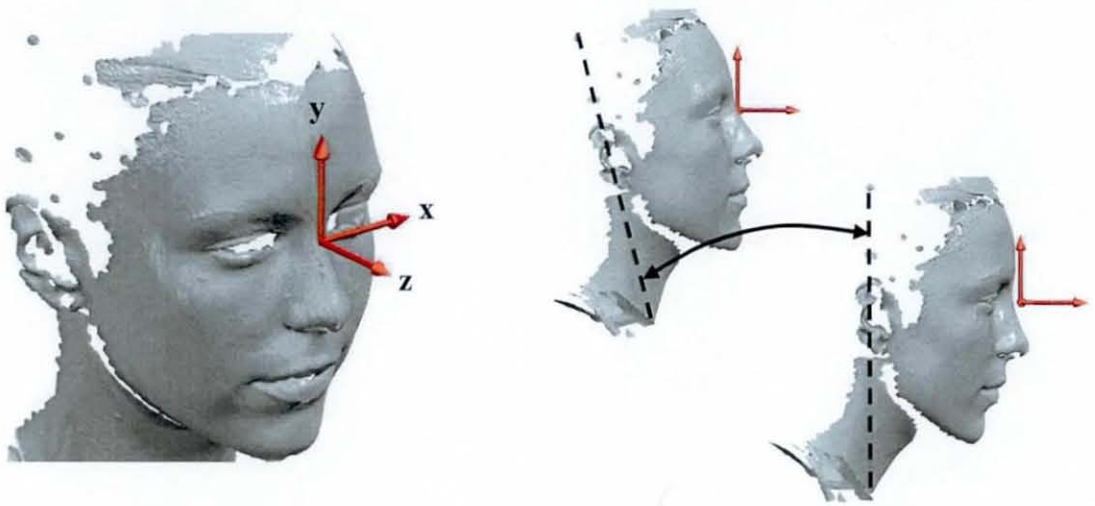

Figure 5.26, Illustration demonstrating exaggerated variations in a rotation about the x-axis, while still appearing as if looking straight forward.

Before any 3D data co-ordinates could be recorded, each face had to be oriented onto the same relative absolute axis. This is made quite difficult due the large variations between shapes of people's faces. Even with any given person, it is impossible to say when the face is directly facing forwards, as high-lighted in Figure 5.26, and therefore a method for positioning using key anatomical features had to be used.

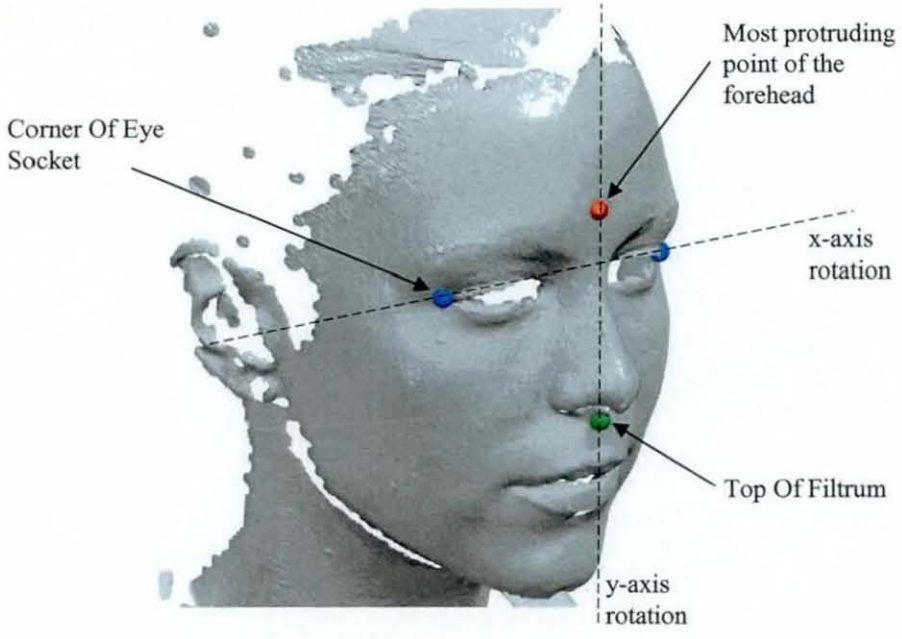

Figure 5.27, Points used to orientate each face

The anatomical points used for aligning each face had to be in areas where there was little or no fatty tissue. The most protruding area of the forehead (approximately 2cm above the eyeline, and central in the horizontal plane) and the top of the filtrum was used to fix the rotation about the y-axis, while the outer corners of the eye sockets were used to fix the rotation about the x-axis. Although not an exact science, this method gave more than satisfactory relative orientations between faces.

5.7.3.3.2 Surface area boundaries for analysis

Although having average surfaces for the entire face might be ideal, it would be unnecessary and extremely time consuming. In order to significantly reduce the information required, half of the face was analysed so the resultant data could then be mirrored through the vertical plane. This is making the assumption that peoples faces are symmetrical, which is known to be incorrect. This is fortunately not an issue, as there is no evidence showing that either side of the face is always larger (in any particular anatomical measurement), and swimming goggles would never be designed or manufactured with one seal being different to the other.

Even with halving the data, there is still an excessive amount of information to be evaluated, and certain surfaces such as the chin, mouth, ears and top of the forehead are not required when designing swimming goggles. A specific target facial surface area needed to be determined in order for any viable shape and size of standard swimming goggle to be designed.

The approximate spatial area that the largest of the available high-street swimming goggles cover the face for both the male and female population is shown in Figure 5.28.

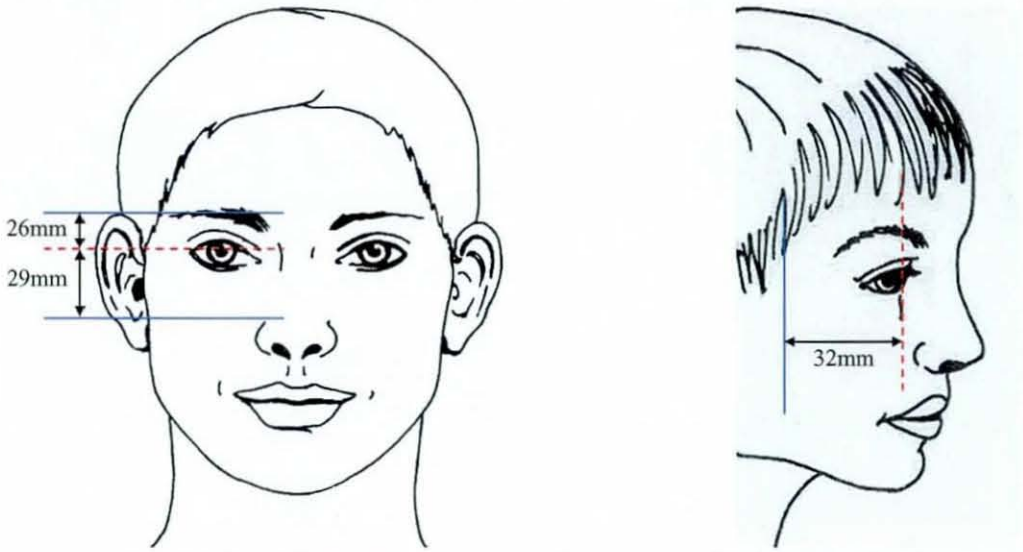

Figure 5.28, Maximum limits of facial area used by a variety of high street swimming goggles

This restricted surface area would be satisfactory if a 'standard' swimming goggle was being developed, but as earlier conceptual work illustrated, these boundaries are likely to be pushed, and therefore the surface area needs to be increased. The area can be increased in three directions (Figure 5.29), ***Vu***, ***Vd*** and ***h***.

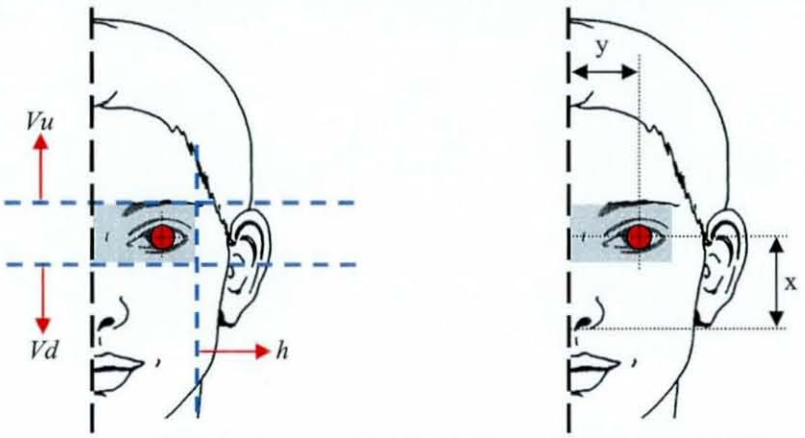

Figure 5.29, Vectors for increasing spatial envelope

Vector ***h*** can only be increased by a nominal amount, as the scanned images are incomplete where there were sideburns or hair of any type. This is not an issue, as a swimming goggle manufacturer would not want interference between seal and hair, as leaks are more likely to occur. Subsequent to a brief analysis of all the facial scans, it was found that 160% of distance **y** would be a sufficient extension, without including corrupt scan data.

Vector ***Vd*** is limited by distortions of the face from movement of the mouth. In order for the seal to remain leak free, it has to be positioned on a surface that changes relatively very little while the mouth opens and closes for breathing. Although no specific measurements have been taken, an approximate limit to where this movement starts to become satisfactory is above the horizontal section going through the top of the filtrum. Although no swimming goggle seals are likely to come down this far, it is a recognisable facial feature, and suitable for the purposes of defining an analysis region.

If the seal were to be positioned so that part of it would be above the eyebrow, there would most likely be very little gap between them, and so vector ***Vu*** has been set at 169% of distance **X**. This ensures that there would be a minimum of 10mm above the eyebrow included within the analysis area (using the scanned images generated).

5.7.3.3.3 Number of points to be measured

The resolution of the final 'average' faces depend entirely on the number of 3D data points recorded on each face. A compromise has to be made however, as the higher the number of data points, the longer the total data set takes to be analysed. One of the most important objectives (besides testing the scanning technique itself) of this pilot study was to ascertain where, and how many 3D data points were required to deliver a suitable resolution of the resultant average facial surfaces.

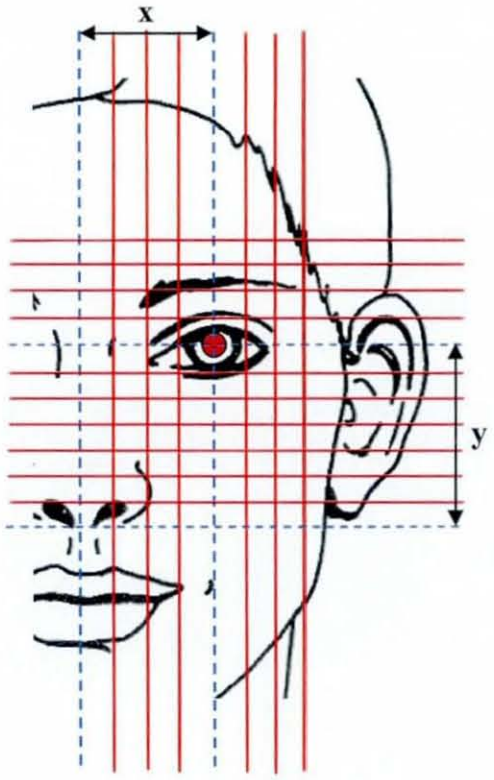

Figure 5.30, Image showing positioning of section lines.

The reference lines used to position the section lines can be seen in Figure 5.30 and represented by the dashed lines. The vertical reference lines are positioned at the central point of the face and through the centre of the eye, while the horizontal reference lines go through the top of the filtrum and the centre of the eye. The vertical section lines are spaced equally at a distance of (1.6 **x**)/7, while the horizontal section lines are spaced equally at a distance of (1.6 **y**)/11. The 3D data points were then recorded at each section, totalling a number of 96 sets of co-ordinates.

5.7.3.3.4 Categorisation of faces

Before the process of morphing could begin, each face had to be classified into a specific category. It was decided for the pilot study, that small and large groups for both the male and female population would be sufficient for assessing the technique Using the data points alone to do this would be possible, but a simpler method would be to take entirely new measurements.

The facial form is extremely variable and complex and therefore the task of classifying a particular face into small or large is not straight forward. One possible solution to try and deal with this issue, would be to measure the volume of each persons head. Even if this data was available (without undertaking a separate study), it might be that one person has a relatively large lower half of the head, therefore increasing the volume. This person's total head volume might then be classified as large, whereas the facial surface area concerned might be quite small. Therefore, only data within the surface area being analysed should be used.

There are a number of key anatomical measurements that can be used in order to help when designing and fitting swimming goggles. However, for classification purposes, it was simplest to use the three most important. Ideally, it would be best if the three dimensions represented both the height, width and depth of the target facial area (the eye socket for e.g.). Unfortunately, the height is particularly difficult to specify, as there are no clear features on the face which are constant through all people and easily identifiable by the scanned images (Figure 5.31).

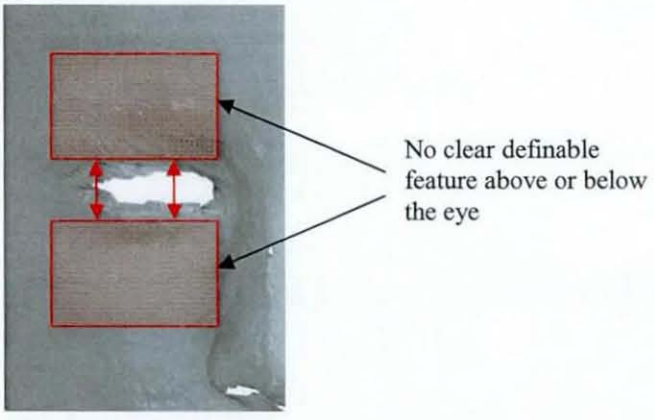

Figure 5.31, Illustration showing lack of features for measuring in the vertical axis

It might be debateable that measurements could be taken from the crease below the eye, to the crease directly above the eye. This would not be practical, as the measurement would not include important information, but most importantly, the crease is variable in position (relative to the shape and size of the eye socket) and on several people would not be visible at all.

Figure 5.32 shows the only suitable anatomical features which are clearly identifiable in all of the scanned images. However, even the location of these points is practically impossible to determine to any level of high resolution in certain faces.

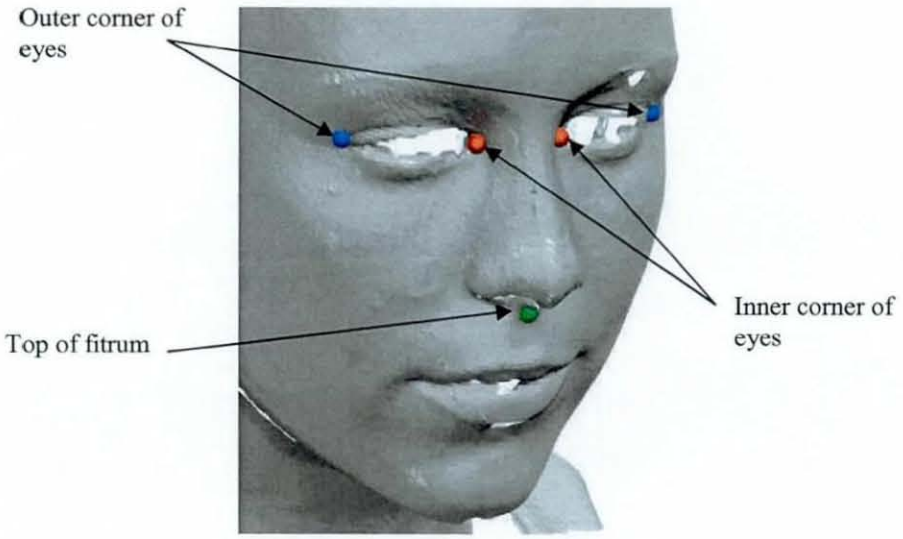

Figure 5.32, Points suitable for taking measurements from

As these are the only suitable points, they had to be utilised in obtaining measurements incorporating height, width and depth. Figure 5.33 shows how these points were used, and the resulting measurements are of the overall width of the eye, the gap between the eyes and a combination measurement of depth and height of the target area.

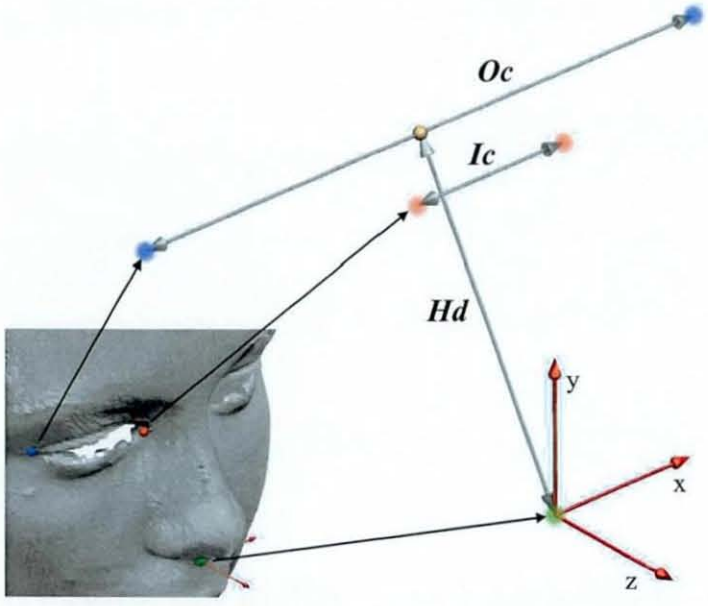

Figure 5.33, Measurements taken for categorisation

The means for each of the measurements ***Oc***, ***Ic*** and ***Hd*** were found for all the faces in both the male and female population. Each face would then be classified into large if two of its measurements were above their corresponding mean measurements, otherwise the face would be classified as small.

5.7.3.3.5 Morphing

In order to morph all of the faces together to produce an 'average' surface for each category, each set of matching data co-ordinates needed to be averaged. This was completed using an excel spreadsheet, and then inputting the resulting averages back into Unigraphics as point data. Splines were then put through these points to create sectioned curve profiles. Using free form modelling, a sheet surface was then extruded through these curves, in order for a solid surface to be generated.

5.7.4 Results

It was clear from the early stages of the morphing, that the final 'average' surfaces would not be detailed enough, and would therefore not be particularly useful when designing swimming goggles. It was therefore decided to only produce the 'average' large male surface (Figure 5.34), to highlight problem areas and help provide information on how to improve the technique.

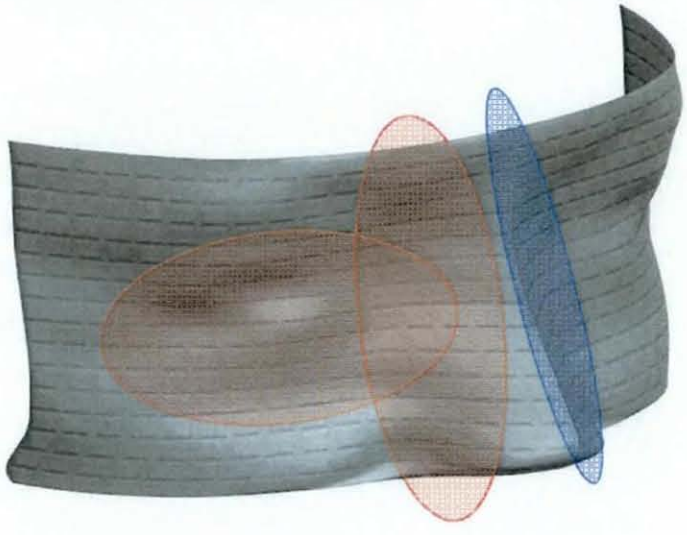

Figure 5.34, Large male 'average' surface with highlighted problem areas

Although the overall form of the 'average' facial surface seems to be reasonable, there are certain creases where there should be none, and areas of the face seem to be filled in.

5.7.5 Conclusions

5.7.5.1 Scanning

The greatest concern when using the Laser Scanning technique was the overall time it took to produce a final scanned image that could be imported into Unigraphics. Most of this time was spent processing (cleaning) the image, and as this current technique described does not require any cleaning, just a very quick and simple sewing operation (automatic joining of the two halves), then time has vastly improved. It took approximately 2mins to complete each facial scan (including sewing and saving), once the equipment had been all set-up.

The resolution and accuracy of the scans were greater than required, as the scanner had been scanning on one of the higher resolutions. This resulted in large image files (of approximately 12mb), which although not being a problem when dealing with only a few faces, data transfer and storage of 150 faces would be an issue. Even with this high resolution, there were however certain areas of the faces that had gaps in the images (Figure 5.35), and were due to the problems described previously.

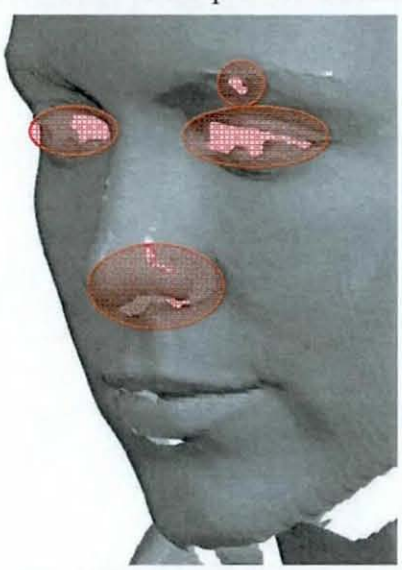

Figure 5.35, Gaps in the scanned images

Unfortunately, as there was no cleaning software, the gaps remained, and if a data point was positioned over the gap, its exact position would simply have to be manually predicted.

5.7.5.2 Image Analysis & Morphing

From the 'average' male facial surface, it can be clearly seen that the detail has been lost in areas where there should be steep contouring This may be partially due to the fact that there were not enough data points measured in these areas, although this is not the only significant reason.

The data points were positioned via only two horizontal and two vertical reference lines (which had been positioned using key anatomical features). Unfortunately, this method is only suitable when analysing faces of different scales but equal proportions. This resulted in supposedly 'relative' points (between faces) existing in different 'relative' positions on the face. Figure 5.36 exaggerates and highlights this problem and shows a point five section lines across in the horizontal and seven down in the vertical on two different peoples faces. On both faces, the point should be in the same 'relative' position, whereas the point is on the inner corner of the eye for face 1 and nearer the centre of the eye for face 2.

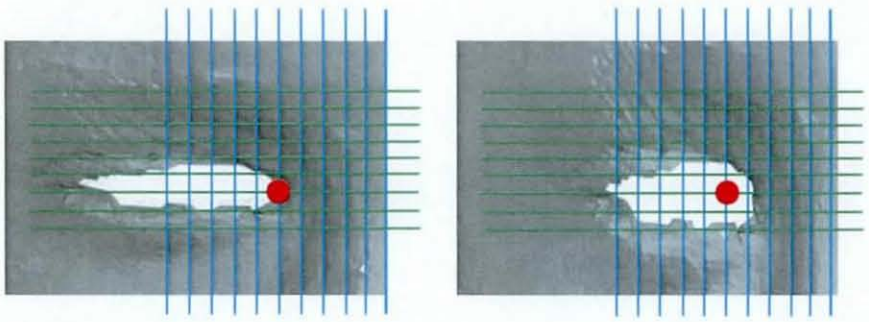

Figure 5.36, Locations of equivalent data points in two separate faces using inadequate reference lines

When these two points are combined and averaged, the result is a 3 dimensional co-ordinate with no true position allocation, and therefore practically worthless. This is

represented in the male 'average' facial surface by its loss of features. In order for this problem to be significantly reduced, more anatomical references had to be utilised.

Although time spent scanning was quite insignificant, sectioning of the images and translating 3D co-ordinates into an excel database was certainly not. Reducing the duration of this process, was of key importance. Automation of data capture and manipulation would have been ideal, but unfortunately not practical, and so the only real solution was to decrease the number of points to be analysed. The points to be removed had to be selected carefully, as the resolution of the final 'averaged' surface was already too low. It was therefore important to significantly reduce the number of points only in areas where they were not required, such as the lower cheek (areas of low contour profiling). Where there were areas of higher contour profiling (around the eye and nose), more points needed to be added.

5.8 Development of technique

5.8.1 Improving Resolution

There are two methods that significantly improve the resolution of the final 'average' facial surfaces in areas of high contour profiling, without developing an entirely new technique. The simplest of these is to increase the number of points surrounding those areas. However, this would not be of any use, unless they were located in the correct 'relative' position, and this can only be done with the use of more reference lines.

The pilot study only made use of two anatomical reference points to generate the four reference lines (centre of eye and top of filtrum). The more anatomical reference points that can be clearly identified on the scanned facial images, the more reference lines can be utilised, and therefore points are more likely to be positioned in the correct 'relative' position. There are two other anatomical features that can be seen in all the scanned images, but unfortunately they are both on the same horizontal plane as the centre of the eye (Figure 5.37). These extra points provide two more vertical reference lines for better positioning.

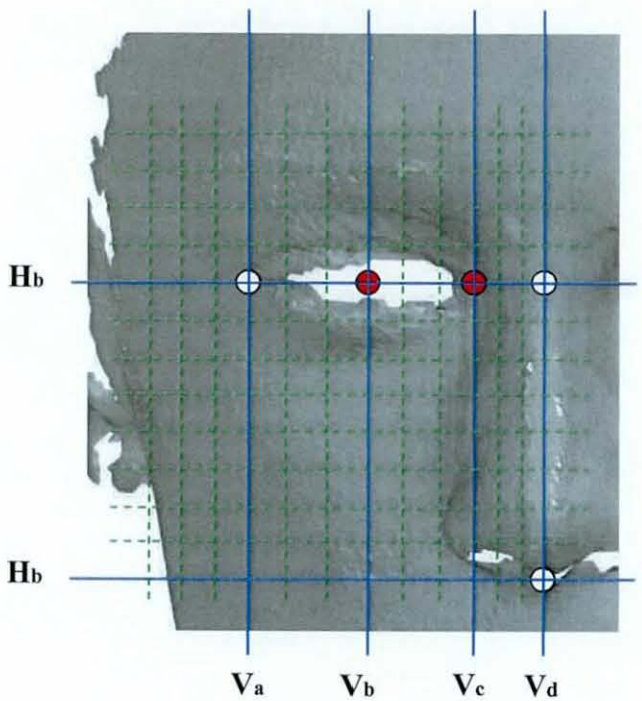

Figure 5.37, New reference points for improved resolution

In Figure 5.37 it can be seen that in between each of the vertical reference lines, two other equally spaced section lines have been introduced. This means that where there is higher contour profiling, and where the vertical reference lines are closer together (**V_c & V_d**), the resulting resolution is therefore higher. The additional section lines to the left of **V_a** in Figure 5.37, have no suitable outer reference line and therefore are simply spaced 5mm apart.

Although not ideal, the resolution in the vertical axis using horizontal reference lines can not be variable, and therefore remain as previously stated in the pilot study. The only area where this causes slight problems is the area between the eyebrow and top of the eye.

5.8.2 Reducing Point Quantity

The results of improving resolution in the horizontal axis, has led to the total measured number of points increasing from 104 to 169. This dramatically increases processing time, and therefore needed to be significantly reduced. Points had to be removed where they were not required. This was done by both reducing the area where points were recorded, and by removing points where the profile was less contoured.

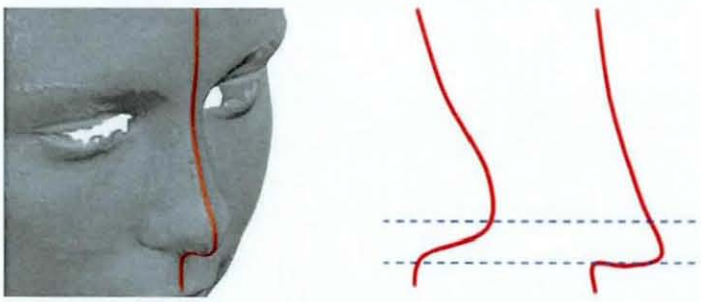

Figure 5.38, Exaggerated variations in profiling of nose tip shape

In order to reduce the target area where points are recorded, the lower section was the only suitable area for omission. The variations of shape of the tip of the nose are too acute for any meaningful averages to be calculated (Figure 5.38). The points along the

same horizontal section lines are also unlikely to be required when designing even the most radical pair of swimming goggles. For both of these reasons, it was decided that the two bottom rows of points could be removed, therefore resulting in a total of 143 to be recorded.

To reduce this number further still, points that had surfaces on either side with very low contour variances could also be removed. In Figure 5.39, surface **A** shows the six points (dark centres) that are either at the end or have high contour variances on two either side. To reduce the number of points and to maintain an almost identical profile if a curve were to be drawn back through, the highlighted points in either options **B** or **C** could be removed.

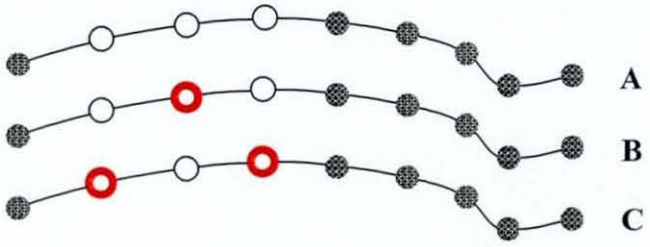

Figure 5.39, Points that can be removed without effecting profile shape

If more than the suggested points in Figure 5.39 are removed, then when it comes to extruding a sheet surface through the final averaged point data, an inaccurate or rippled surface would most likely be produced (Figure 5.40).

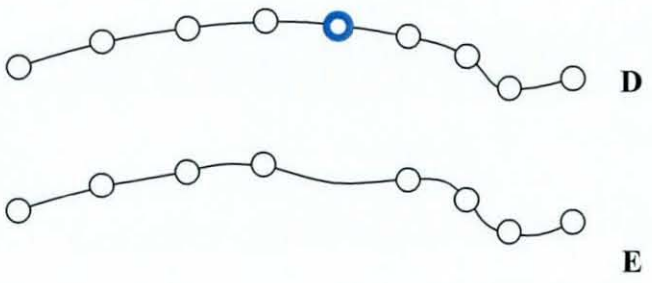

Figure 5.40, Exaggerated errors occurring (shown in surface **E**) when highlighted point in surface **D** is removed

Although it would be possible to remove specific points, processing time would only be reduced if a complete line of points was removed. There was only one line of points that this was possible with, and Figure 5.41 shows the final layout with a total of 130 recorded data points (at each intersection).

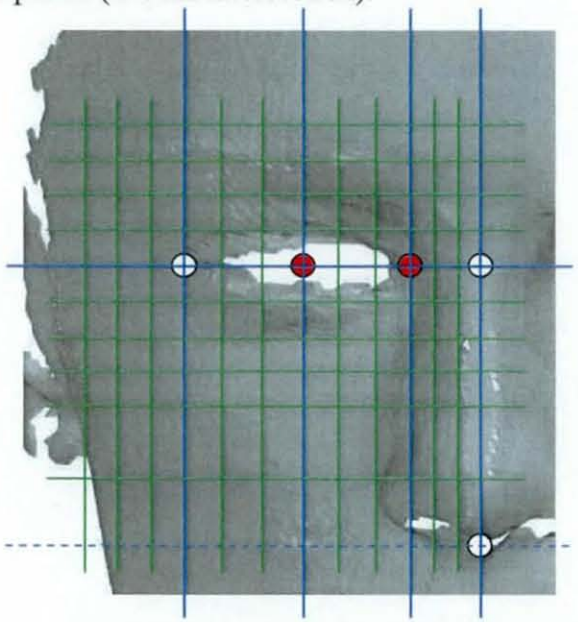

Figure 5.41, Final layout of point data to be recorded (points at intersections of solid lines only).

5.8.3 Reducing Holes In Image

The final scanned images from the Pilot Study often had gaps where the eye detail should have been. Unfortunately this problem could not be completely resolved unless major changes were made to the scanner or software. However, it was found, that if the participants opened their eyes, slightly more detail in the image was restored. There was also the additional benefit of the participants expressing a more relaxed facial composure (and more realistic to when swimmers have their eyes open while wearing goggles).

5.8.4 Reducing File Size

Although not essential, reducing the file size from approximately 15mb per scanned image would reduce handling problems. On lower spec CAD machines, files of this size would also severely affect its performance and therefore increase processing time. During the pilot study, the resolution of the scanner was set too high. This

amount of resolution is wasted, and the medium setting was more than sufficient and resulted in file sizes of less than 4mb.

5.9 Facial Scanning Using The Moiré Fringe Contouring Technique

5.9.1 Methodology

The Moiré Fringe Scanner was used to scan a large cohort of healthy adult men and women. The resulting two halves of each face were sewn together and transferred into a Unigraphics operated CAD system. Small, medium and large 'average' facial surfaces were then generated for both the male and female populations. The following sections describe the participant population, apparatus, experimental design and procedure, results and then conclusions.

5.9.2 Subjects

Following Ethical Advisory Committee approval and informed written consent, 150 participants (80 male) were to complete the scanning procedure. For the male population, the average age was 22.4years (S.D.= ± 2.9years), height was 1.84m (S.D.= ± 0.13m) and weight was 77.8kg (S.D.= ± 7.4kg). For the female population, the average age was 22.2years (S.D.= ± 3.0years), height was 1.73m (S.D.= ± 0.12m) and weight was 70.2kg (S.D.= ± 4.9kg).

5.9.3 Apparatus

A Moiré Fringe Contouring scanner was used and operated via a standard PC with the scanners associated processing software. A Framed dark room tent was used to block out any ambient light, so the equipment could be transported anywhere. A standard free rotating swivel chair was used for the participant to sit on. The 3D images were analysed using a standard PC with Unigraphics as the chosen CAD software, and the point co-ordinate information averaged in an Excel database.

5.9.4 Experimental design and Procedure

The procedures that took place in the Pilot study were copied exactly apart from those areas mentioned in Developing Of Technique.

5.9.5 Results

The co-ordinate data for the entire scanned population can be found in the Appendix – Anthropometric Data, along with the small, medium and large (for both male and female) average facial surface co-ordinate data. Although not particularly useful to a design engineer, an isometric representation of the rendered scanned surfaces can be seen in Figure 5.42.

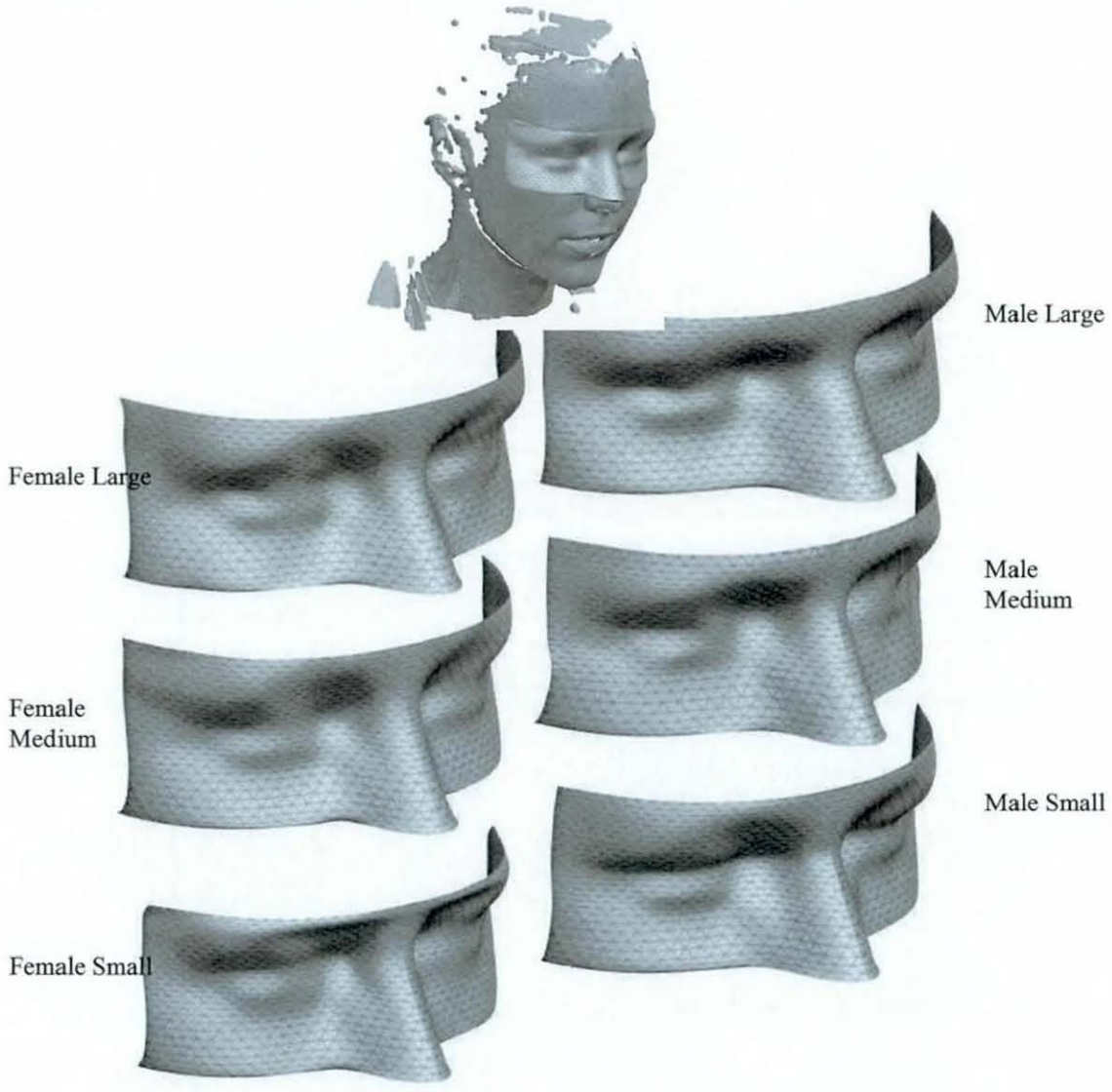

Figure 5.42, Representation of 3D facial 'average' surfaces

The variations in both size and contouring of the 'average' facial surfaces is quite significant, although quite difficult to see using a standard texture rendering. For a

visually clearer method of contour comparison, Figure 5.43 displays the facial surfaces as an iso-map of the surface radii.

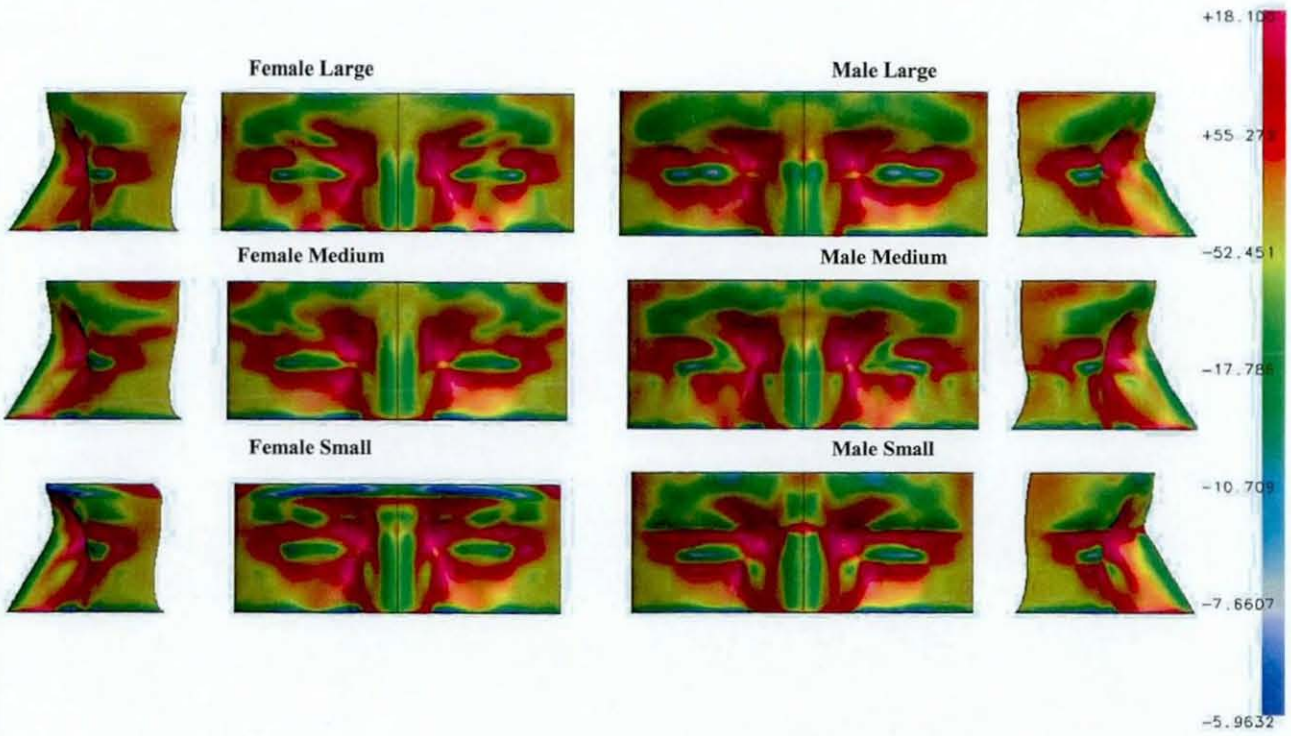

Figure 5.43, An iso-map of the facial radii (scale in mm radius)

For a simple comparison of the measurements between anatomical features in the 'average' facial surfaces, Figure 5.44 illustrates an example segmented surface, with the relative measurements for each face category.

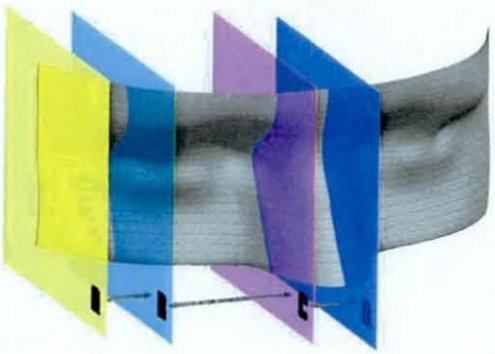

		A-B (mm)	B-C (mm)	C-D (mm)	A-D (mm)
Male	Large	15.0	36.7	16.2	67.9
	Medium	15.0	35.5	14.3	64.8
	Small	15.0	34.3	13.8	63.1
Female	Large	15.0	37.0	13.3	65.3
	Medium	15.0	34.7	13.3	63.0
	Small	15.0	34.2	11.3	60.5

Figure 5.44, Segmented facial surface and distances for each facial category

The measurements shown in Figure 5.44, are given to one decimal place. However in reality, they can not be this accurate, as there is no visually definable point at where

the section plates (**B** and **C**) should be precisely positioned. Figure 5.45 gives an exaggerated example of how section **C** could be positioned in a region of almost 5mm wide.

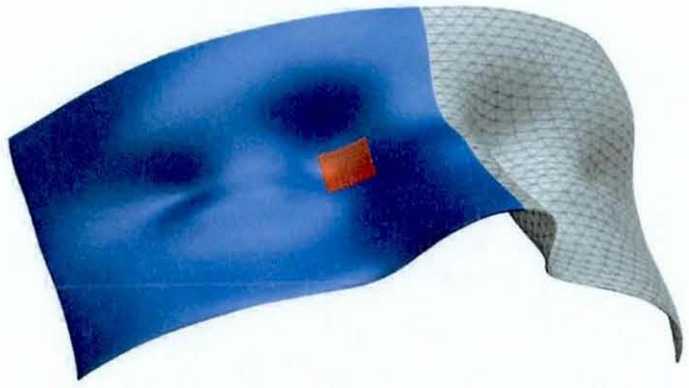

Figure 5.45, Exaggerated example of imprecise positioning of sectioning (shown by region in red square).

The table however, is not intended for swimming goggles to be based on, only intended as an indication of size differences.

Due to the complex nature of the surfaces, it would be impossible to write a descriptive comparison of every permutation for all the surfaces, and therefore a comparison between female and male for each 'average' size has been made.

In addition to the obvious differences of size between the 'average' large male and female surfaces, there are some notable variations in the shape and form (Figure 5.46). The most apparent of these being the position of the eyes. The eyes in the male surface are considerably wider apart and also seem to be more defined (**A**). The width of the nose in the male is proportionally wider (**B**) and in profile there appears to be more of a dent at the nose bridge (**C**). The only other significantly visible difference is the steeper slope below the brow on the male surface (**D**).

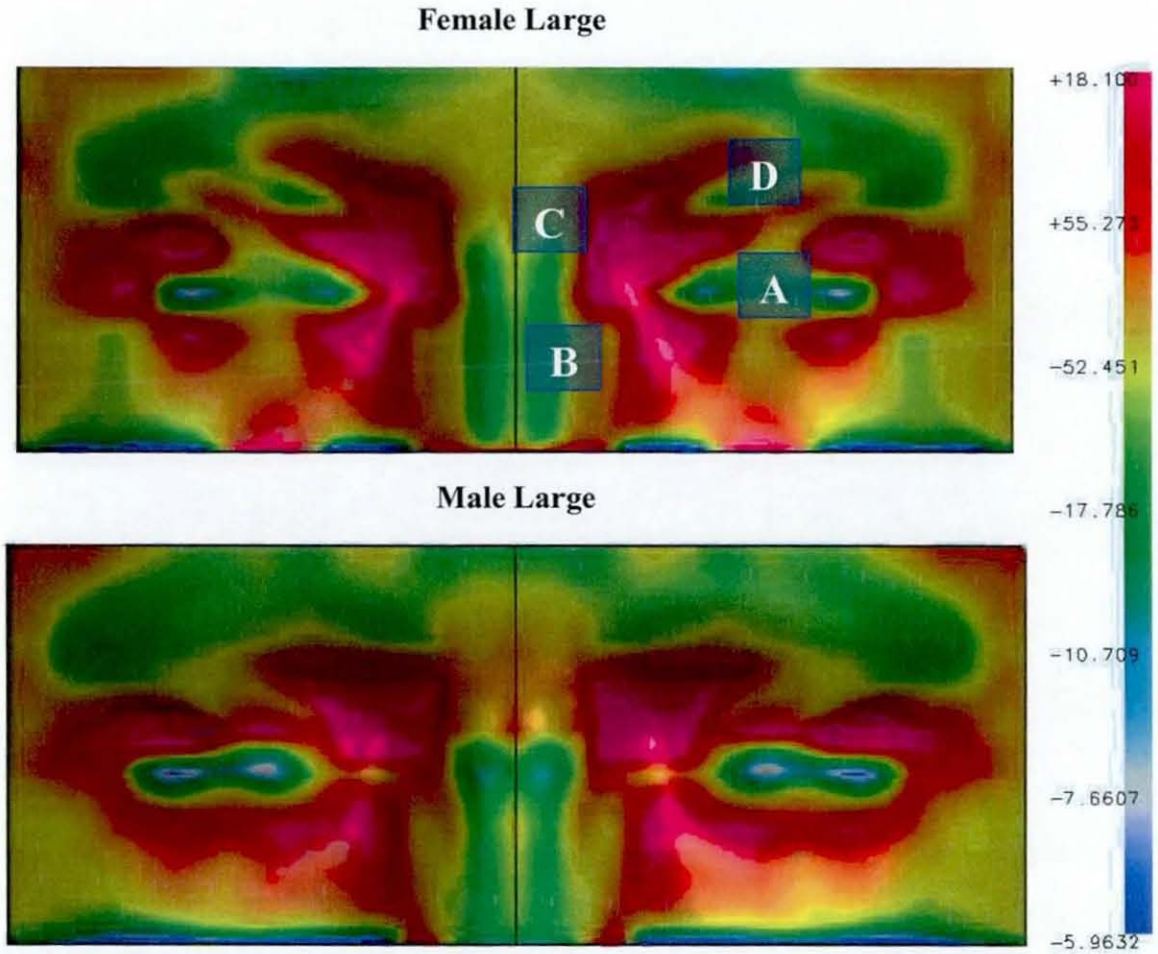

Figure 5.46, Comparison of shape between 'average' male and female for the large category.

The distance between the eyes for the medium 'average' facial category is proportionally negligible (Figure 5.46), although still larger for the male (**E**). The most evident dissimilarity is with the shape of the nose. The female nose is relatively constant in its width and cross-section for a much greater proportion of its length, with the male having a very similar dent at the nose bridge to that of the large male (**F**). The gradient of the bottom half of the nose in the male is far gentler (**G**), therefore increasing the overall width of the nose. The brow is again far more defined in the male surface (**H**), while the eyes are less so and therefore opposite to that of the large category in that respect.

Female Medium

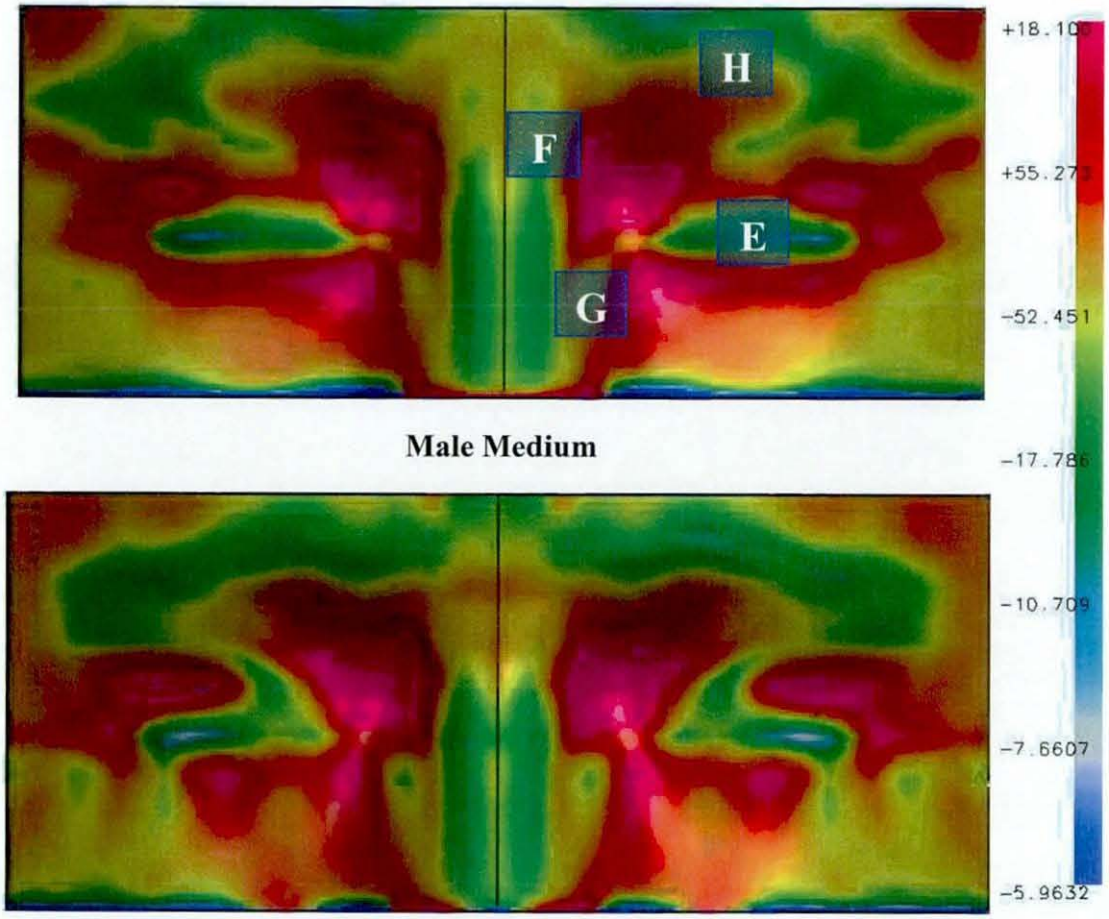

Male Medium

Figure 5.47 Comparison of shape between 'average' male and female for the medium category.

The variations between the male and female small 'average' facial surfaces are far greater than for any other category. Unlike the other two categories, the brow of the female is substantially more defined with a far steeper gradient relatively higher up on the face (**I**). The creases above the eyes on the male seem more concentrated and go far wider on the face (**J**). The same dent in the nose bridge found on both the large and medium categories can again be found here, but this time being even more prominent (**K**). The nose in the female is again relatively constant in cross-section for a greater proportion of its length (**L**).

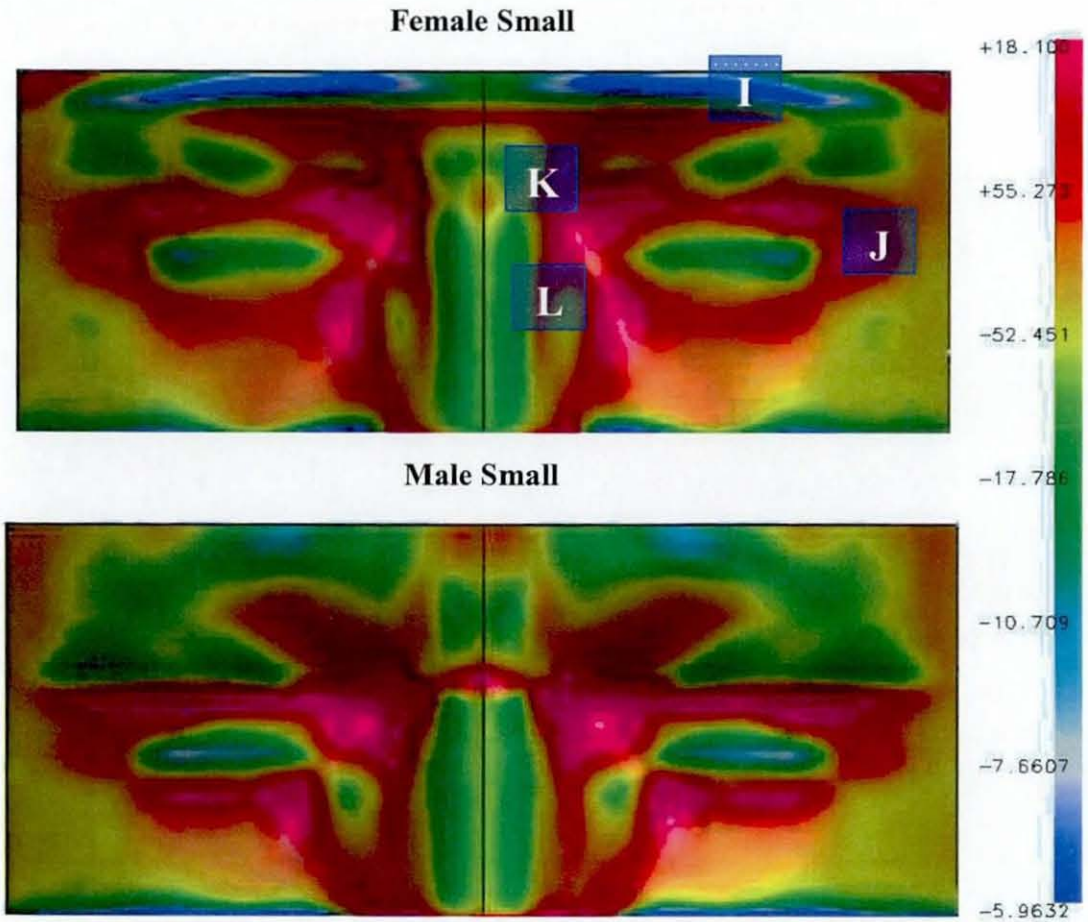

Figure 5.48 Comparison of shape between 'average' male and female for the small category.

5.10.6 Discussion

5.10.6.1 Duration of study

One of the main issues when creating 'average;' facial surfaces is compromising between achieving accurate and high resolution final images with the duration time for completing the study. The method chosen offered the ability to have as high a resolution as required, but unfortunately was especially time consuming. Even with the relatively low resolution chosen, the study still took approximately three months to complete. Although this time period was acceptable for the given circumstances, to follow the same procedure for all ages, nationalities and body statistics would probably be impractical.

Software to automate the process of morphing would be a more acceptable method for future studies. At the time of commencement, there were a limited number of morphing software packages, but all were aimed at creating visually attractive images, rather than producing accurate 'average' surfaces. The medical industry is the area which has necessitated recent significant developments of such morphing software packages. However, even with these programs, flexibility of the morphing parameters are limited. Further research in assessing all new packages would have to be completed before a decision could be made as to whether they are a viable technique.

5.10.6.2 Resolution of final images

The accuracy and resolution of the regions of the facial 'average' surfaces to the left, right and below the eye (Figure 5.49, A, B & C) are more than adequate for their intended use. However, details of the curvature of the brow (D) are somewhat questionable. This is more evident in the small category for both the male and female population, where the difference between the two is excessive. For the female/small surface, the brow is too high, while the male brow seems too low (Figure 5.50).

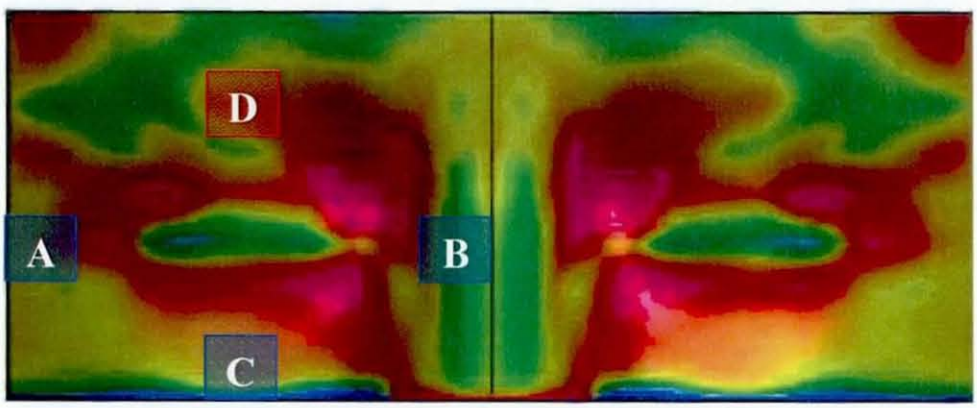

Figure 5.49, Areas of high and low accuracy (Blue square = High, Red square = low)

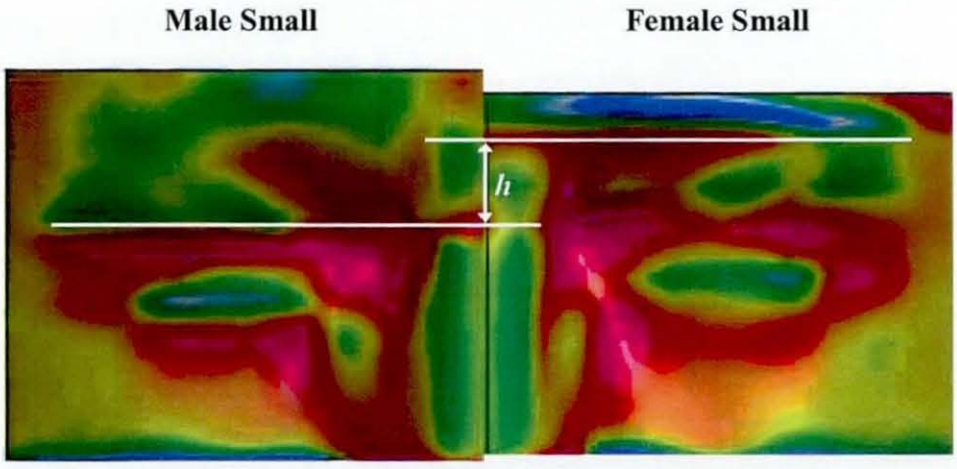

Figure 5.50, Variation in height of brow between sexes

As it is very unlikely that the brows of the final 'average' surfaces are a fair representation of the participant population for both the male and female small categories, there must have been certain errors introduced at some stage of the technique. Increasing the number of participants scanned, may have helped, but the error has more likely arisen from the lack of horizontal reference lines being used. As there are no other clear and definable anatomical reference points that can be selected, the technique is therefore inherently flawed, in this respect.

5.10.6.3 Effectiveness of final images

Given the flaw that is inherent within the technique, it is apparent that the 'average' surfaces can not solely be used to design and develop a new pair of novel swimming goggles. However, as Figure 5.51 shows, there is only a small percentage that can not be reliably accurate.

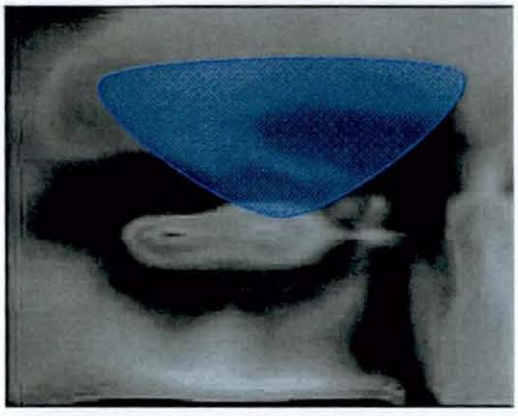

Figure 5.51, Approximate area of 'average' surfaces that is unreliable in its accuracy

The shaded area of the surface, should not simply be discarded, but be compared alongside the existing designs of goggle seals, so a blending of the two can be made.

Using the 'average' facial surfaces, together with the Facial Skin Sensitivity and Tissue Compression data, designers will then be able to make significant improvements to the fit and comfort of future swimming goggles.

6.0 CURVED LENS DESIGN & EVALUATION

6.1 Introduction

The use of curved lenses within swimming goggle design is relatively new, but not particularly ground breaking. Only a few goggles within the market use the technology, even with their potential for improved hydrodynamics and aesthetic appeal. Unfortunately, there are various inherent optical problems with all of the curved lens products currently on the market, and so rather than being targeted at the performance athlete, they are sold as 'fun' goggles.

A curved lens with excellent clarity, no distortion, no magnification and that does not mist is required, so it can be used in conjunction with a racing swimming goggle.

6.2 Chapter Aims

The purpose of this chapter is to effectively further the research in the area of lens design. More specifically, it is to develop a number of techniques that can be used to identify whether there is the potential for a curved lens that could be used in elite racing goggles.

6.3 Chapter Objectives

Time restraints and limited expertise in the field of lens design, result in it not being viable to prototype the "ideal" curved lens. The design of an optically correct curved lens for underwater use, is significantly complex and therefore beyond the remit of this particular PhD. It was therefore decided to source out the actual lens design itself to an expert in the field, Dr. Jeremy Coupland of Loughborough University.

The chapter therefore concentrates on proving the sourced prototype lens by a number of scientific studies. The objectives are listed below;

• To provide the specifications for a curved lens in order for it to be designed by a third party.
• To manufacture a goggle housing (that incorporates the prototype lens) that can be used by participants in a swimming pool environment.
• To design techniques that can be used to assess the performance of the curved lens (and any other lens) in the areas of visual acuity, stereoscopic vision, magnification and visual distortion.
• To implement the developed measuring techniques, and directly compare the prototype lens with other goggle lenses on the commercial market today.
• To state whether or not there is potential for the use of a curved lens in an elite racing swimming goggle.

6.4 Specification For The Prototype Curved Lens

6.4.1 Stipulating a Lens Type

Discussions with the lens designer (Dr. Jeremy Coupland) revealed that the task of designing a new curved lens that could be used underwater and in the air within very tight dimensional limits would in effect be a PhD all by itself. It was decided to therefore simplify the task as much as possible so that some useful knowledge could be gained in the first development phase.

By removing the element of the goggles being used in air, there would be no need for a bi-focal lens design, which not only severely reduces the time scale for the process, but also opens more avenues for the manufacturing techniques (as the lens would now be a cross-section revolved about a central point). This of course would be impractical in terms of an all-round useable swimming goggle lens, but it would give the chosen concept the necessary proofing required.

As earlier research has shown, there are really only two different avenues that could be taken with regards to the type of lens the prototype should be. It was agreed by

both parties that a lens system similar to the Ivanoff-Rebikoff correcting lens would be best suited to the task. Although a Fresnel lens in theory would be possible, it was an unknown quantity, and as there was only chance for one lens to be manufactured and tested, it would be a high risk strategy. The Fresnel lens would have also been extremely difficult and expensive to manufacture, and so the finite budget played a part in the decision process.

6.4.2 Dimensional Limitations

Without a complete understanding of the design process for a lens system such as this, it is easy to give the designer a very specific specification and tiny tolerances. In reality, this specification would practically be laughed at and ignored. Therefore, at this early stage of the process, it is best to give a few preferred guidelines and not be too stringent with the details.

However, there is one dimension that can not be ignored by the designer, as getting it wrong would make the lens all but useless. As the lens would be designed with a pre-specified distance from the centre of the eyeball, the lens would have to remain in that position when being worn. Therefore, enough space would need to be allowed for the movement of the eyelids and adjoining eyelashes.

In order to specify the minimum distance the lens needs to be from the eye (when the seal is compressed), three measurements need to be identified. These being the eyeball diameter, the eyelid thickness and the eyelash length.

6.4.2.1 Diameter of the human eyeball

The human eye is not completely spherical and is usually measured less in the transverse diameter. The variations in the recorded average measurements of the eyeball is quite minimal and Figure 6.1 identifies these different measurements from a range of bibliographic entries.

Bibliographic Entry	Result w/surrounding text	Standardised measurement
Glencoe Health 2nd Edition. Mission Hills: Glencoe Inc., 1989: 61.	"The eyeball is about 1 inch (2.5 cm) in diameter"	25 mm
Encyclopedia Britannica Macropedia: Sensory Reception . USA: Britannica Inc., 1997.	"The dimensions of the eye are reasonably constant, varying among individuals by only a millimetre or two; the sagittal (vertical) diameter is about 24 millimetres (about one inch) and is usually less than the transverse diameter."	24 mm
Magill's Medical Guide Revised Edition; Brain. Salem Press, 1998: 608.	"The adult human eye weighs approximately 7.5 grams and measures approximately 24.5 millimeters in its anterior-to-posterior diameter."	24.5 mm
Zinn, Walter and Solomon, Herbert. *Eye Care, Eye Glasses and Contact Lenses.* City: Lifetime Books, 1965: 10.	"The eyeball is roughly about an inch in diameter brimming with many specialized structures and tissues."	25 mm
World Book 2001. Chicago: World Book Inc., 2001: Page 460.	"The human eyeball measures only about 1 inch"	25 mm

Figure 6.1, Bibliographic entries regarding the diameter of the eyeball

6.4.2.2 Thickness of the eyelid

Regarding the thickness of the eyelid, the skin in this area is actually the thinnest within the entire human body, measuring at only 0.5mm (approx.). The edge of the eyelid (where the eyelashes grow from), is the thickest point of the eyelid ad measures at approximately 2mm.

6.4.2.3 Length of the eyelash

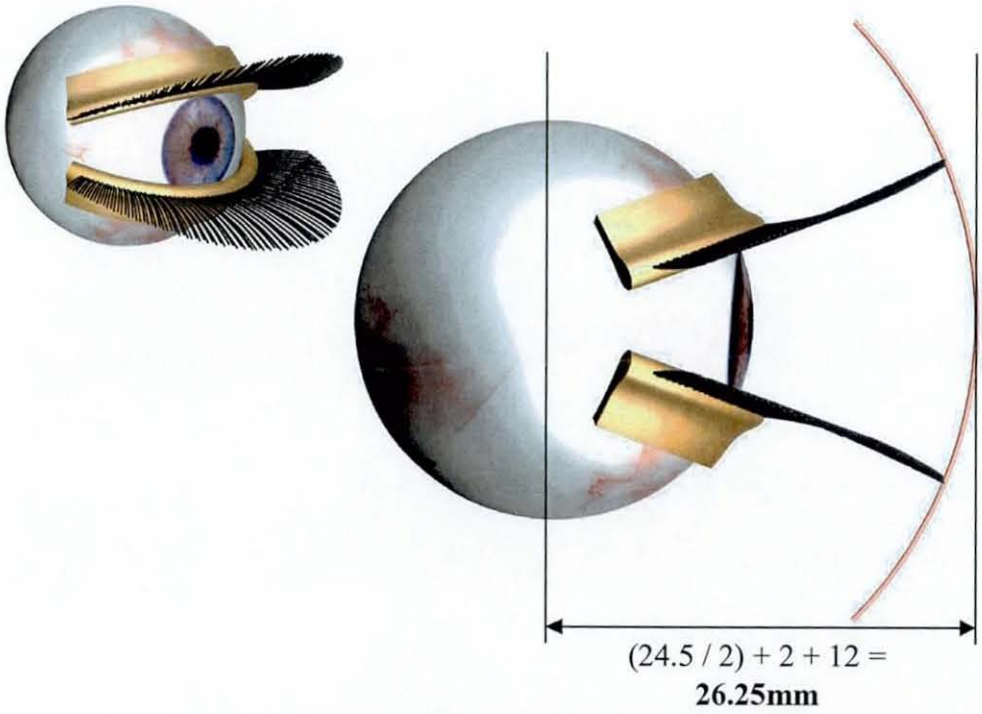

Figure 6.2, Minimum distance between lens and centre of eyeball

Finding the average length of the upper eyelash (being the longer of the two) is difficult due to the extreme variations. Within the female population, it is often desirable for excessively long lashes, and is achieved with use of either make-up or false extensions. Illness, such as Vernal keratoconjunctivitis (VKC) is a chronic conjunctivitis that results in the increased lash length so as to protect the eyes from sunshine, wind and foreign bodies (Neri Pucci, MD et al, 2005) can also be a cause. The longest of the false eyelash products measures approximately 12mm, and although the swimming goggles should not be designed based on this length and that no natural lash would be this size either, it would make sense for the minimum gap between the eyelid and the lens to be approximately 12mm. This would then take into account the variations in the proximity of the lens depending on facial shape and tightness of the swimming goggle strap. Figure 6.2 represents the minimum distance the lens needs to be from the centre of the eyeball.

6.4.2.4 Curvature of the outer lens surface

As mentioned previously it is pointless specifying an absolute radius of curvature, as it may prove almost impossible to implement. Therefore, it was decided best to simply build an understanding with the designer, and talk through why a curved lens was needed in the first place. This allowed him to appreciate the requirements involved, namely the 'gimmick' factor. The radius of curvature of the outer surface had to therefore visibly be curved from a distance, but not so much as to interrupt the natural flow of the face, i.e. the 'fish eye' effect.

6.4.3 Prototype Lens Design

The detailed design plans and specification of the new curved lens system can be found in the Appendix – Lens Specification. However, Figure 6.3 gives a simplified overview of their layout and some of the key dimensions involved.

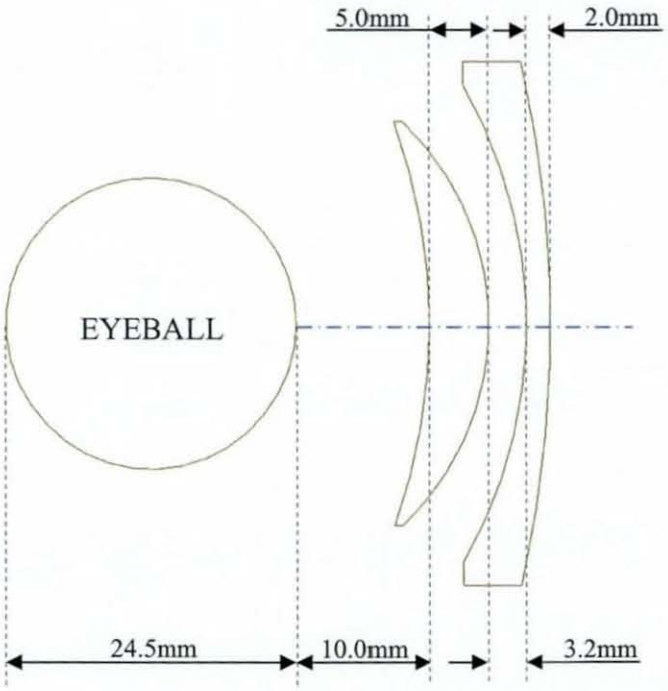

Figure 6.3, Key dimensions in prototype lens system

An example of a set of rays traced through the lens system is shown in Figure 6.4.

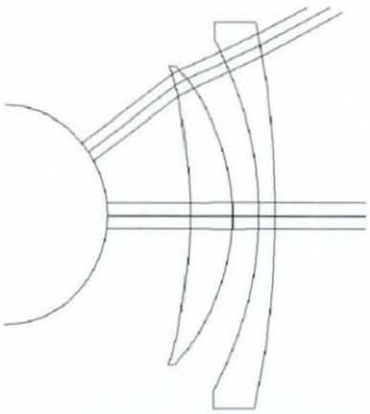

Figure 6.4, Raytraces through prototype lens system

A pair of lenses were manufactured using a precision grinding technique to a very high optical industry standard. At £2500 the lenses were expensive, but it was necessary that they should have no flaws which might affect the optical properties in any possible way.

6.5 Foundations for the Development of Underwater Lens Testing Technologies

6.5.1 Introduction

There are many aspects of vision that can be evaluated, however, this chapter is solely concerned with measuring the optical capabilities of the new prototype lens. The lens would eventually be intended for use in goggles worn by not only the elite competition swimmer, but right through to the 'splash around' leisure swimmer. Therefore, the lenses should ideally be tested in both air and water. However, as the prototype lens has only been designed for use in water at this current development phase, the performance of the optical properties in air would be relatively poor. Although having said this, testing in air gave an idea to the extent of how vision would be impaired, and whether it really is an issue.

Only those optical functions of the lens that are required to be superior by the swimmer needed testing. It was therefore decided that areas such as the colour change caused by the lens were not important, and did not require measurement.

The four areas that were deemed important by the swimmer were all tested,

- Visual Acuity / Optical Distortion
- Perception of depth
- Degree of magnification
- Field of vision

Through the research completed in Optometry, it was found that there are many parallels with the criteria stated above. The already established measurement techniques in that area were therefore used as a basis to develop new methodology's that could be used to test the underwater lens.

Testing the new prototype lens on its own provides no means of assessing how well or by how much the underwater vision has been improved, if indeed it has at all.

Therefore, it was necessary to evaluate the results as a comparison with current designs and common technology. By improvement, it is necessary to define an ideal situation or compare against other benchmarks. The generic outline of the majority of the tests were completed on a comparative basis, and as no reference data has been published, a control was established. It was therefore considered that an underwater lens achieving vision on par with the human eye in air was taken as optimum.

The main assessment of the prototype lens was mainly carried out in its intended environment. Testing other than this would have not been as useful or as relevant in finding the direct function of the goggle as a whole system. The environment was therefore underwater in either the swimming pool, or a similar structure where the test piece was able to be fully submerged.

It is common knowledge that quality of vision in humans varies substantially. This automatically implies that results could not be evaluated together as the interference of human error would severely affect the outcome. Indeed, the end use product was mostly assessed by the subjective criteria of the user. Human vision was a major influencing factor in the majority of the tests, as there are many forms of eye problems. Therefore, the 'ideal' perfect vision was never a reality, and in certain cases may have unknowingly disguised the effects of the lens's function.

The extent of each participant's impairments could have been taken into consideration when evaluating the data, as this might help to re-adjust the results for inter-participant evaluation. Also, their vision could have been corrected with the use of contact lenses. However, ascertaining participant's visual impairments would have been both extremely time consuming and costly. The most reasonable approach was to therefore conduct comparative tests of the lenses for each individual based on the perception in air and water.

Along with the subjective testing which was considered fundamental to mimic the end user point of view, a small section of qualitative measurements were also conducted.

6.5.2 Ethical Community Approval for all Test Procedures

As the testing procedures required the participants to use un-proven prototype goggles in an environment which can be inherently dangerous, it was deemed necessary to seek Ethical and Health & Safety approval from the University. On the understanding that a lifeguard was present at all times and that no testing technique or method was used that contradicted with pool safety guidelines, the studies were allowed to proceed. Although there was more than one testing procedure, the environments and conditions under which they were carried out was always the same, and therefore approval was only required once.

6.5.3 Participant Recruitment

For all of the test procedures, candidates were called upon from two main underwater disciplines. Both competition / club swimmers and Scuba divers within the Scuba club at Loughborough University were used. These are two groups of people who have a vested interest in the improvement of vision underwater and are therefore more familiar with the environment and the aspects of the goggle. Their feelings, advice and feedback was noted as each individual had their own opinion and concerns about how they felt. Essentially, the two activities are very similar in their visual requirements, except the divers are even more particular when it comes to optical clarity and performance.

With regards to the participants own vision, only people who had no known eye defects and did not require any glasses or contact lenses were used. Obviously, certain participants may have had small eye defects without actually realising it, but as already mentioned, there was no inter-participant comparison. Therefore these guide lines were solely intended to reduce masses of erroneous data being produced.

6.5.4 Development of Housing for Prototype Lens

Before the prototype lens could be properly tested, a housing for it needed to be manufactured similar to that of a normal swimming goggle. Due to the time constraints, it would not be possible to develop a housing with all of the conventional luxuries (such as separate flexible seal) that a modern swimming goggle might have. Therefore the housing had to be a one-piece design, with enough rigidity to support both the inner and outer lens, but enough flexibility that it would fit a reasonable percentage of the population.

Unfortunately, at this point in time, the anthropometric work of the face had not been completed, and so there was no 'average' surface that could be utilised to mould the housing around. The only facial surface that was available was the very primitive CAD representation of my own face. As mentioned in chapter 4, it was acquired from using a co-ordinate measurement machine to map three dimensional points of a facial casting. The resulting facial surface can be seen in Figure 6.5. Although there were numerous errors within the surface, it offered a sufficient template for the housing to be based upon.

Figure 6.5, CAD representation of a human face

The housing itself was relatively simple to design, although it was always known that it would not fit a large percentage of the population particularly well. This was mainly

due to the temporary lack of knowledge surrounding facial anthropometrics. The prototype housing design is shown in Figure 6.6.

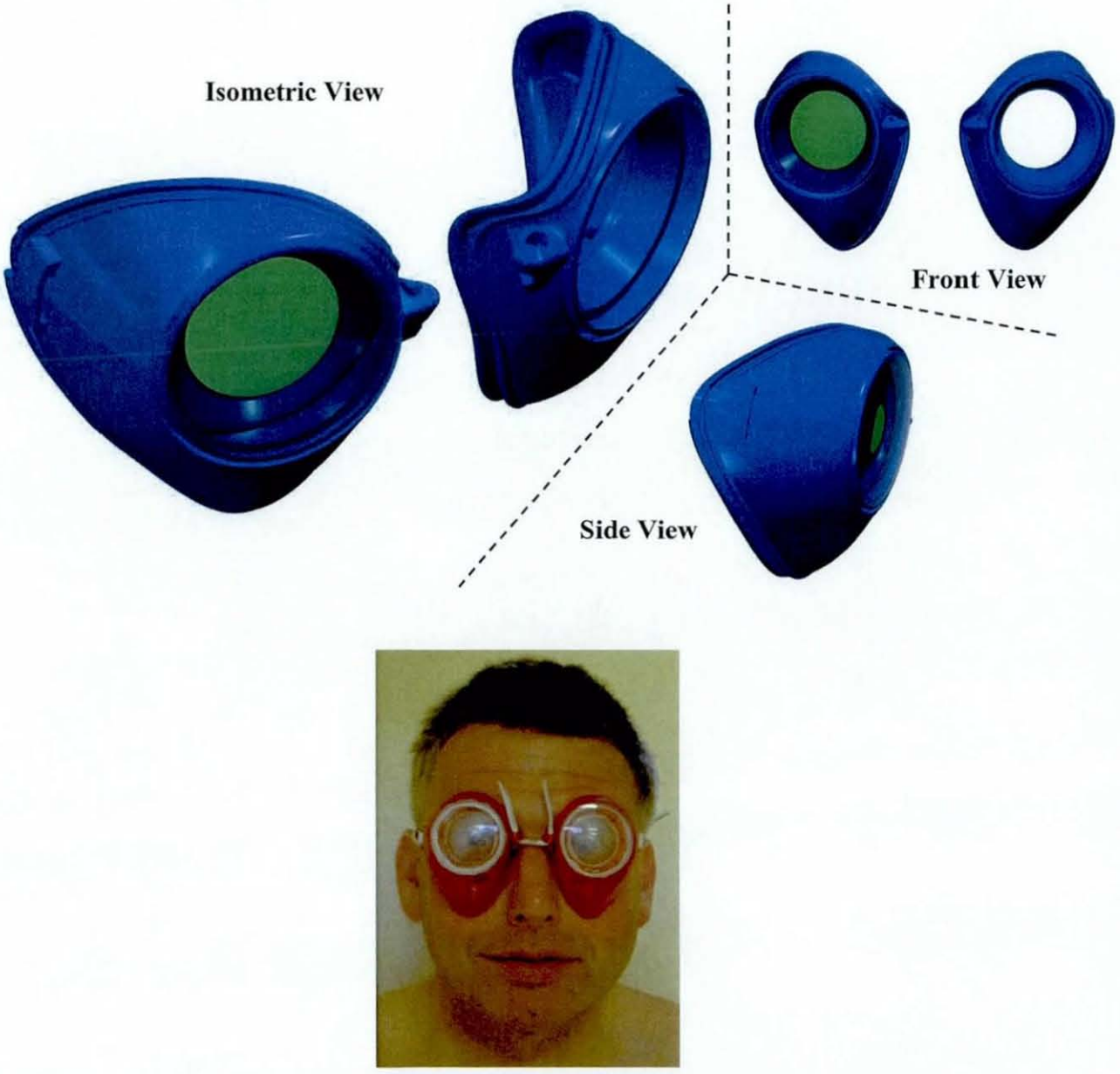

Figure 6.6, CAD renderings of the prototype lens housing, and final product.

The design was initially rapid prototyped using stereolithography, but the resin which was used was completely rigid and would therefore only fit myself and maybe a handful of others. The original resin also degrades quite rapidly when in constant contact with the sun or water. The housing needed to therefore be re-moulded into a far more flexible material, and so silicone moulds were produced which the new softer rubber resin could be poured into.

6.5.5 Lens's chosen for comparison

The Prototype curved lens was only compared to lenses found in existing swimming goggle products. Ideally there would have been one of each of the four types:

- Flat (Plano) lens
- Arc shaped lens (2D curve)
- Spherical shaped lens (3D curve)
- Prototype curved lens

Unfortunately, there was no existing spherical lens goggle on the market that was not tinted. The tinted lens would have affected the results as the light levels and the image contrast would be altered as the light passed through the lens.

For the flat (plano) lens, a Swedish style goggle was used, while for the arc shaped lens a new Speedo goggle (soon to be launched) was tested. The prototype lens was encased in the one-off prototype lens housing.

6.6 Development of the Visual Acuity Test Procedure

6.6.1 Introduction

This test is used by practising opticians as a method of diagnosing a person's state of vision. It assesses the ability of the eye to resolve detail by reading letters of a known size from a chart.

6.6.2 Aim

The aim of this test was to compare the ability to resolve detail while viewing through the three different lens types. The assessment was intended to indicate as to how the prototype lens would perform both in the air and in the water in relation to other goggle lenses in terms of overall performance and lens clarity.

6.6.3 Methodology Selection and Development

Opticians use a number of different test charts to measure visual acuity, some of which are listed below:

- Snellen Test
- Logmar Test
- Illiterate E Test
- Landholt C Test

All of the above tests could have been implemented to produce a viable test for the goggles affect on visual acuity. However, the Landholt C test (Figure 6.7) was chosen because of its simplicity. From a practical point of view, a swimmer completing the test under water, would be able demonstrate the direction of the 'C' being seen, easier than demonstrating a specific letter or symbol (through use of hand signals etc.).

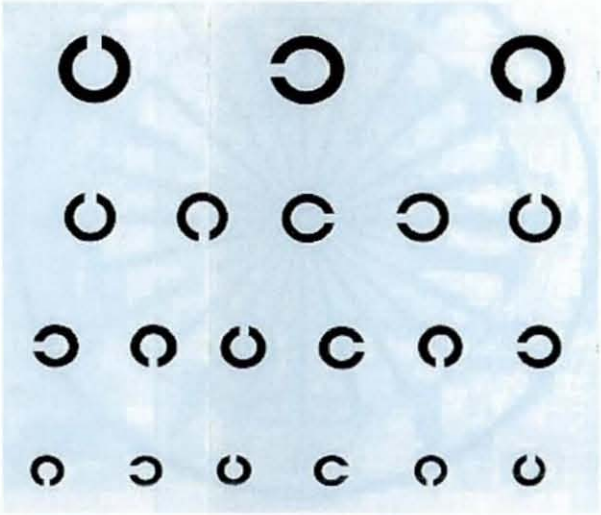

Figure 6.7, Landholt 'C' Visual Acuity Test chart

6.6.4 Subjects

Following Ethical Advisory Committee approval and informed written consent, 15 participants (9 male) were to complete the study. For the male population, the average age was 20.8years (S.D.= ± 2.2years), height was 1.87m (S.D.= ± 0.13m) and weight was 78.8kg (S.D.= ± 8.2kg). For the female population, the average age was 21.2years (S.D.= ± 1.4years), height was 1.69m (S.D.= ± 0.15m) and weight was 65.8kg (S.D.= ± 4.9kg).

All participants were free of any known eye defects, and all claimed to have excellent vision.

6.6.5 Apparatus

The key piece of equipment for this study, was the Landholt 'C' test chart itself, and therefore it was important that the chart was as accurate as possible. The chosen chart had been manufactured by 'Precision Vision of America' and was a 4m version. The chart obviously had to be waterproofed to ensure longevity and prevent bleeding of the ink, and therefore was laminated.

To ensure the test results were as reliable as possible, the same swimming pool at approximately the same time of the day (in the morning) was used for all the different investigations. A swimming pool has many influences that can have an effect on the quality of water. Some examples are the type and amount of chemicals used in the pool, the time of day, the amount of prior use of the pool, the rate of water flow through the filters and the recycling method of extracting dirty water and clean water intakes.

The chosen pool's cleaning system is very effective, as clean water from the filter tanks and plant room is pumped directly into the pool via a grid located along the centre, from deep to shallow end on the pool floor. This positive flow of water into the swimming pool spreads from the floor in the centre to the surface and out towards the sides. The exact path is dependent upon the temperature profiles of the current water and the new water entering the pool. In general terms, the water volume is increased by pumping in new water so in order to maintain a level within the pool, the surrounding sides have a continuous overflow channel of which is the non-return design. The important aspect is that the surface water (which contains the scum from dirt, sweat and other foreign objects) is skimmed off and not allowed to wash back in the pool

The other items of the study included:

- The three swimming goggles being tested
- Snorkel
- Suckers
- Tape measure
- Antiseptic wipes
- Test results table

6.6.6 Test Procedure

The quality of the test results is largely dependent upon the correct setup of the equipment and following the test procedure in a systematic and methodical approach.

Figure 6.8 shows the layout of the equipment used in the water phase of the test, and the same layout was used for the in-air test.

Figure 6.8, Layout of Visual acuity Test

The test chart was positioned at a distance of 4m from the participant and the centre of chart aligned at the approximate eye level (as much as possible). The 4m distance was ideal in both the air and the water as the participants were able to clearly see the top line and progression to each line of letters below was increasingly difficult.

The test was also conducted in a well lit environment and in the case of the underwater section, away from any water turbulence or strong current flows (such as a filter inlet).

The exact procedure that was undertaken is highlighted below:

1. Explain the nature of the test, so that the participant is clear as to what the experiment entails.
2. Ensure the equipment is correctly setup and accurately laid out.
3. Ask the participant to become familiar with the goggle lens and adjust correctly to ensure a comfortable and as best fit possible.
4. Ask the participant to position themselves at the required distance in front of the chart. Adjust if necessary so the chart is at eye level.
5. Ensure the participant understands the test.
6. Ask the participant to cover one eye with their hand.
7. Begin the test and record the participants response at each symbol.
8. When complete, repeat the test with the other eye.

The first sequence of testing was completed in the air with the naked eye (on both sides). This was to establish a control that was specific to each participant. The prototype goggles were then worn and the subject was asked to repeat the above procedure. It was decided that there would be little point in measuring the visual acuity using the flat and standard curved lens while in the air, as initial tests demonstrated negligible distortion.

The second phase of testing was in the water, where the participant repeated the above procedure with the flat, curved and new prototype lens. Each test was completed with both eyes.

Performing the test in water meant that conventional communication was impractical. This problem was explained to each participant after the first phase of testing, but before they entered the pool, so that maximum concentration was achieved on one element of the test at a time.

To communicate efficiently, a sample card with the letter 'C' was given to each participant, so that they could orient it to the perceived view of the specific 'C' on the chart they were looking at. To ensure that the signal was interpreted correctly and not reversed, the readings were taken from behind the participant, therefore, signals for the left were read as being left. To ensure that there was a certain level of continuity, the participant used a snorkel to reduce the need to surface. Unfortunately, due to problems with housing fit, and the lens sealing, the test was interrupted repeatedly because of leakage and misting.

6.6.6.1 Prototype housing malfunctions

The majority of test participants struggled to obtain a good fit between the goggle and face. The design of the goggle was effectively produced to only fit one particular facial profile, and the seal gasket area did not have sufficient flexibility (Figure 6.9). Many subjects had to resort to excess pressure (from tightening the strap) to force the facial tissue to compress enough so that complete contact could be achieved.

Figure 6.9, Limited seal gasket flexibility

Although in ideal circumstances, the housing would have been re-designed, the time restrictions and the fact that the housing still worked (in sorts), meant it was not a viable option. The only temporary solution that could have been implemented to attempt to reduce the leakage and the misting effects, was to use a layer of sealant. Unfortunately, the additional material between the face and the goggle inherently increased the distance between the lens and the pupil. As mentioned previously, this deviation of distance from lens to pupil can severely affect optical performance, and so the housing had to be left as it was. This simply meant that testing took considerably longer than planned.

6.6.7 Results

The raw data can be seen in Appendix – Visual Accuity Test Raw Data, along with the results compiled in tabular form. The appropriate LogMAR values have been converted (with the use of Figure 6.10) into actual acuity values relating to the distance at which a person can read the letter size corresponding to 'normal' vision (more commonly termed 20/20, 6/6 or this case 4/4). Hence, this would be the limit of a normal persons vision at 4m, as the test is calibrated to 4m. The values in Figure 6.32 show the relevant size of the letter read. A value of 5 would represent the size of letter a normal person could read at 5m, therefore a participant with a value of 5 on a 4m test chart would have poorer visual acuity than a 'normal' person. The values for the prototype lens in air have not been included but will be discussed in Section 6.38.

LINE NUMBER	LOGMAR VALUE	LETTER SIZE (MM)
1	1.0	40
2	0.9	32
3	0.8	25
4	0.7	20
5	0.6	16
6	0.5	12.5
7	0.4	10
8	0.3	8
9	0.2	6.3
10	0.1	5
11	0.0	4
12	-0.1	3
13	-0.2	2.5
14	-0.3	2

Figure 6.10, Conversions for the LogMAR test chart

PARTICIPANT	LEFT EYE				RIGHT EYE			
	AIR	WATER			AIR	WATER		
	Control	Flat lens	Curved lens	Prototype lens	Control	Flat lens	Curved lens	Prototype lens
1	5.0	3.0	4.0	5.0	5.0	4.0	4.0	5.0
2	4.0	3.0	3.0	4.0	3.0	2.5	2.5	4.0
3	4.0	3.0	3.0	5.0	10.0	8.0	8.0	10.0
4	4.0	2.5	3.0	4.0	4.0	3.0	3.0	4.0
5	4.0	3.0	2.5	4.0	4.0	3.0	2.0	4.0
6	4.0	3.0	2.5	5.0	3.0	3.0	2.5	5.0
7	6.3	5.0	5.0	6.3	6.3	5.0	5.0	8.0
8	5.0	4.0	3.0	5.0	4.0	3.0	3.0	4.0
9	3.0	2.5	2.5	4.0	4.0	3.0	3.0	5.0
10	6.3	5.0	4.0	6.3	6.3	4.0	5.0	6.3
11	5.0	4.0	4.0	5.0	5.0	4.0	3.0	6.3
12	4.0	3.0	2.5	4.0	4.0	3.0	3.0	4.0
13	6.3	5.0	5.0	8.0	4.0	4.0	4.0	5.0

Figure 6.11, Results from compiled data

6.6.8 Discussions and Conclusions

To the present the data in an easier format to interpret, it is best if the variation in optical performance between each lens compared to the control is shown (Figure 6.12). A value of 0 shows no change to the image viewed, whereas a positive value shows an increase in visual acuity and a negative score indicates a reduction in visual acuity.

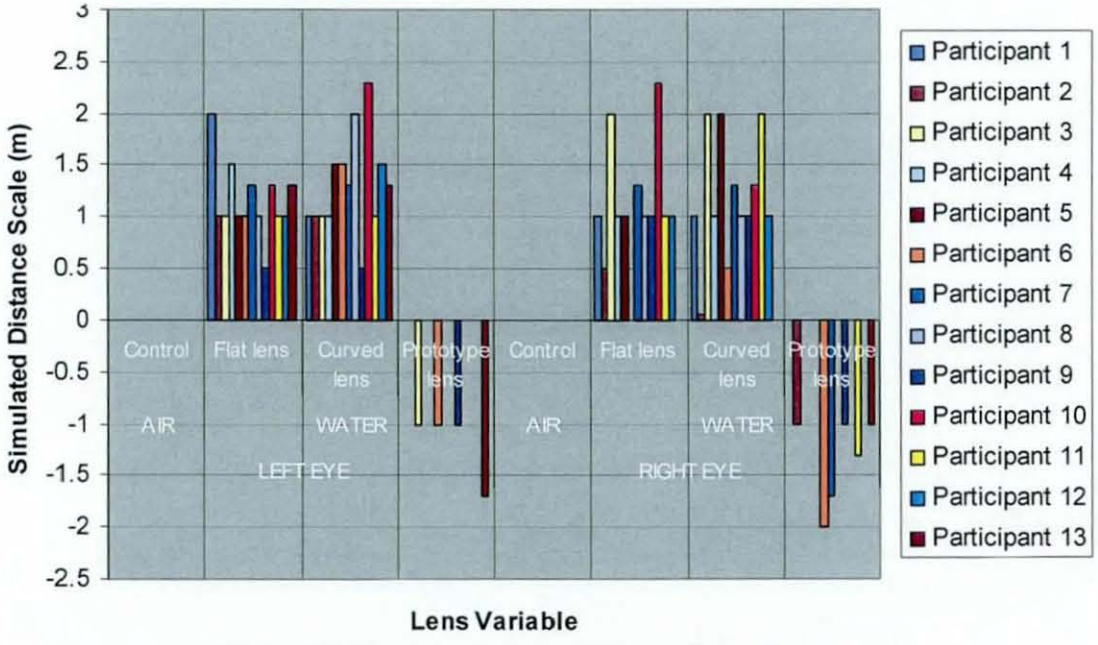

Figure 6.12 Visual Acuity Lens Difference Comparison

The immediate trend in figures 6.11 and 6.12 show lower simulated distance values for the flat and curved lens in water than the control, while the prototype lens approximately matches (or closer to) the control. These results indicate that the flat and curved lens actually improve the visual acuity compared to normal vision in air, whereas the prototype is very similar if slightly worse. In retrospect, the radius of curvature of the normal curved lens was larger than that of the prototype outer lens, and so if they had been equal, the prototype would have most likely performed relatively better.

Although there is a possibility that the results are not reproducible and that more participants are need to give a clear evaluation, there is more likely to be scientific answer for the seen improvement. As mentioned earlier, magnification underwater is a side effect of wearing either flat or curved standard goggle lenses. This

magnification effect is most likely the cause of the improvement, and as the prototype lens has been designed to eliminate any magnification, it did not have the same advantage.

The times where the prototype lens reduced the visual acuity, could have been caused by either a number of reasons, but was most likely a product of them all.

- The original lens design was very slightly flawed.
- The misting effect impaired the ability to see through the lens.
- The lens was positioned at the wrong distance from the eye, due to the ill-fitting goggle housing.

With regards to the prototype lens in air, the results clearly show that the goggle lens severely reduces visual acuity. The scores could not be displayed as the majority of candidates failed to read the top line of the chart. The participants commented on what they assumed to be the lens misting up and blurring their vision. On inspection of the lens, there was no misting, and therefore it was simply a direct response of the lens system design.

It was known from the beginning that using the prototype lens in air would have a detrimental effect on visual acuity, however, it was not clear as to the severity of the problem. After completion of this study, it is apparent that a bi-focal design would be necessary for the next lens development phase.

In conclusion, the prototype lens is more representative of vision in air than other swimming goggle lens on the current market, but does fractionally reduce the visual acuity. In reality, this difference was hardly noticed during general swimming, and would probably not considered to be a problem. However, the fact that visual acuity is actually reduced (however slight), might outweigh the need to reduce magnification effects.

6.7 Development of the Measurement of Stereoscopic Vision

6.7.1 Introduction

The evaluation of the effects of wearing different types of lens on Stereoscopic vision can be performed with a variety of tests. When a pair of goggles is worn, the lenses must compliment each other providing similar optical performance to create the best possible 3D image.

6.7.2 Aim

The aim of this test was to establish how much a person's stereoscopic vision was affected by wearing the different lens types compared to a 'control' situation.

6.7.3 Methodology Selection and Development

Although there are a variety of tests that can be used to evaluate Stereoscopic vision, the Howell Phoria test is considered to be the simplest to employ while still achieving repeatable quantitative results (Wong *et al.,* 2002).

The test distance used is 3m and requires the participant to view the chart with both eyes. A prism is then placed in front of the right eye which causes a vertical shift of the viewed image. The perceived view is of two scales, one above the other. The arrow from the top scale will then be pointing to a number on the bottom scale, and this is the number the participant reads. This number refers to the instantaneous phoria value. In the optical profession, this test is used to assess the brain and eye's function at recreating a 3D image. However, this test will be used as a comparison between the goggles and the participants normal in air vision. Figure 6.13 shows the actual test card used.

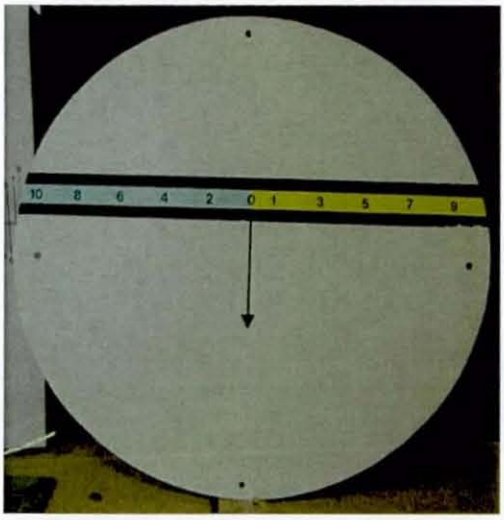

Figure 6.13, Howell Phoria test card used

6.7.4 Apparatus

A list of the apparatus used in conducting the stereopsis test:

- Laminated Howell Phoria Test Chart
- 6 Dioptre Prism
- Suckers
- Tape measure
- Three goggle types
- Antiseptic wipes
- Test results table

The prism had a lanyard attached and was also captivated in a rubber housing so there would be no sharp edges. This was not only completed from a Health & Safety point of view, but also prevented the prototype lens from being scratched.

6.7.5 Test Procedure

The quality of the test results were largely dependent upon the correct set up of the equipment and accurately following test procedure in a systematic and methodical approach. Figure 6.14 shows the general layout of the equipment used.

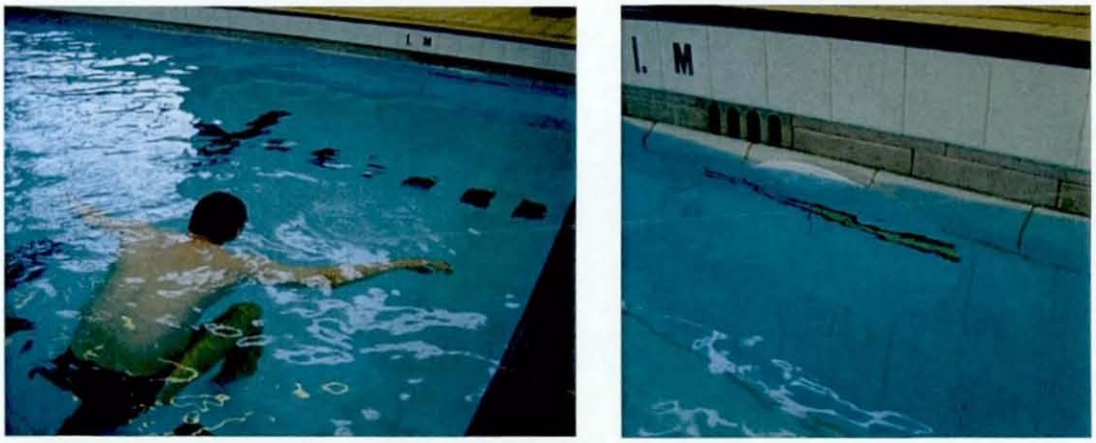

Figure 6.14, Layout of Howell Phoria test

The test chart was positioned at a distance of 3m from the participant, and the centre of the chart was approximately aligned at the eye level. The test was conducted in a well lit environment and in the case of the underwater testing, away from any water turbulence and strong current flows.

The step-by-step procedure that was completed is shown below:

1. Explain the nature of the test so the participant is clear as to what the experiment entails.
2. Ensure the equipment is correctly setup and accurately laid out.
3. Ask the participant to become familiar with the goggle lens and adjust correctly to ensure a comfortable and as best fit as possible.
4. Ask the participant to position themselves at the required distance in front of the chart. Adjust if necessary so that the centre of the chart is at eye level.
5. Ensure the participant understands the test.
6. Ask the participant to cover one eye with the prism.
7. Begin the test and record the participant's response.
8. When complete, repeat the above sequence wearing the various goggle lenses.

The first sequence of testing was completed in the air with the naked eye. This was to establish a control that was specific to each participant. The test was completed on each eye, and then repeated with all three lens types. The whole procedure was then repeated in the water.

Unfortunately, the testing was again severely hampered by functional problems with the goggle housing, resulting in misting and leaking. This could not be helped and so the testing procedure simply took longer than expected.

6.7.6 Results

PARTICIPANT	AIR				WATER			
	Control	Flat lens	Curved lens	Prototype lens	Control	Flat lens	Curved lens	Prototype lens
1	0	0	0	X	X	0.5	0.5	0
2	0	0	0	X	X	0.5	0	0
3	1.5	2	1.5	X	X	2	2	2
4	1	1	1	X	X	0.5	1	1
5	0	0	0	X	X	0	0	0
6	2	2	2	X	X	3	2.5	2
7	1	1	1	X	X	0	0.5	1
8	1	1	1	X	X	1.5	1	1
9	1	1	0.5	X	X	0.5	1	1
10	0.5	0.5	0.5	X	X	1	0.5	0.5
11	0	0	0	X	X	0	0.5	0
12	0.5	0.5	1	X	X	0.5	0.5	1
13	2	2	2	X	X	2.5	2	1.5

Figure 6.15, Howell Phoria Test results

The Phoria scale ranges from 0 to 10 and results marked with an x could not be taken due to the participant not being able to read the chart.

6.7.7 Discussions and Conclusion

Solely for the ease of viewing, the results from Figure 6.15 have been displayed in graphical form (Figure 6.16). Only the important information needed to be included and therefore, the results using the lenses in air were disregarded at this stage.

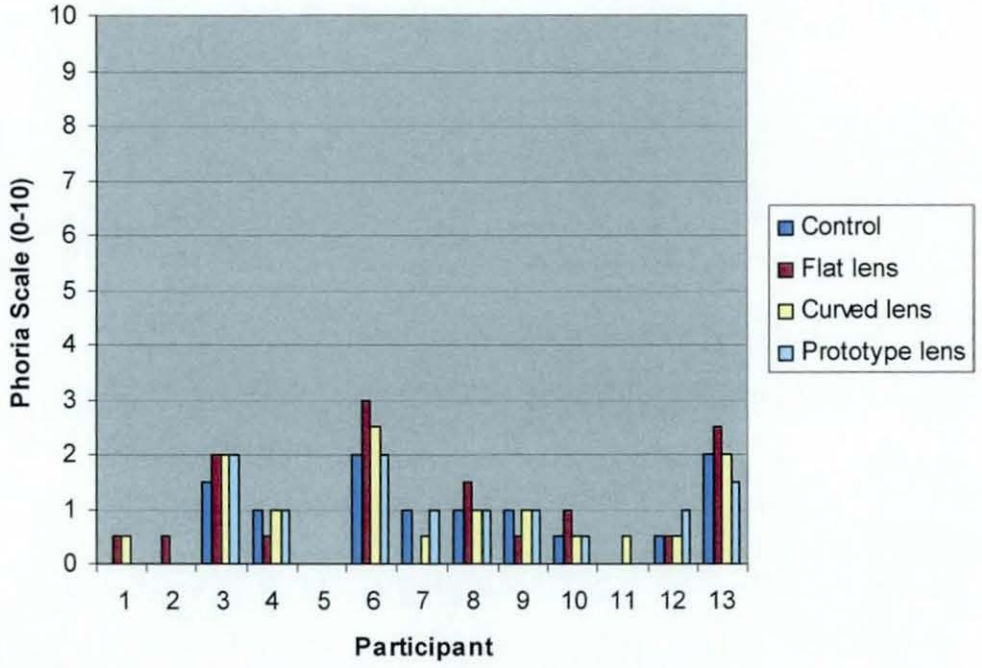

Figure 6.16, Howell Phoria Test results shown in graphical format (excluding lenses in air)

Initial inspection of the data shows minimal deviation from the control situation. This was supported by comments from the participants, stating that the goggles did not produce any ghosting or overlapping images once the goggles were adjusted correctly to the face. However, problems did occur when one of the goggle's lens was misaligned in relation to the opposite goggle lens. This produced an overlap image (as expected) due to the refraction of the misaligned lens.

In Figure 6.16, it can be seen that the flat and the curved lens is less frequently a match for the control compared to the prototype lens. The Phoria scale is from 0 to 10, with 0 being excellent stereoscopic vision with no deviation from the true image. The results obtained therefore show little change from the control in each specific case, when any of the lenses were being worn. This small amount of deviation may also be a product of the compensation of the participant's eyes that independently adjust and accommodate to combine the image in the brain.

The geometry of the prototype lens has a curved outer surface, which allows for more compensation when ensuring the lenses are aligned to the test chart. In all the goggle cases, there were no detrimental effects to stereoscopic vision providing the goggles were aligned correctly. The arrangement of the test only accounted for vision through the goggles at one point. This point would not be the same for each individual, but would depend on their facial dimensions and in particular the inter-pupillary distance. The lens location and relative angle when placed on the face would have a diverging normal to the lens face. This alignment for a flat lens goggle would cause the stereoscopic vision to be impaired as each eye would receive two separate images of different objects due to the refracted rays of light from the misaligned goggle interface. However, with the new prototype goggle lenses, the profile lends itself to allowing the pupil to look through the majority of the lens and maintain a path of vision normal to the lens surfaces.

In conclusion, the new swimming goggle lenses performed equally well in comparison to current swimming goggles lens designs. More importantly, the results were comparable to the control test in air with the naked eye, showing that none of the tested lens types noticeably impaired the stereoscopic vision while viewing underwater.

6.8 Measuring the Magnification Effect Underwater

6.8.1 Introduction

Due to the effects of refraction, upon wearing current modern day swimming goggles underwater, objects are perceived to be closer than is actually the case. Although the brain makes an attempt to correct this magnification effect (to prevent a person swimming into a wall), the situation is less than ideal. The prototype lenses were therefore designed to have no magnification effect.

6.8.2 Aim

The aim of this test was developed specifically for this study to establish how the new prototype lens affected the perception of distance underwater.

6.8.3 Methodology Selection

To be able to measure the magnification effect underwater, it was necessary to devise a new test specifically tailored to evaluating the perceived distance as viewed through the goggle lens. The test involves simultaneously viewing a graduated chart both in air and water. To fully evaluate the difference between in air and in water vision, the test must be carried out simultaneously. The principle of this test reflects the nature of use of the swimming goggle, and so the testing procedure was a comparative study based on the trials of participants.

The test chart (Figure 6.17) consists of two graduated scales and a sized rectangle of known dimensions. The rectangle is defined as two contrasting halves with a scale on each side of the rectangle for each half. The chart is immersed in water so that the horizontal centre line of the chart matches the surface level of the water. The graduated scale acts as a reference by which the lower half of the rectangle can be compared to the upper scale for the numerical result, or visa-versa.

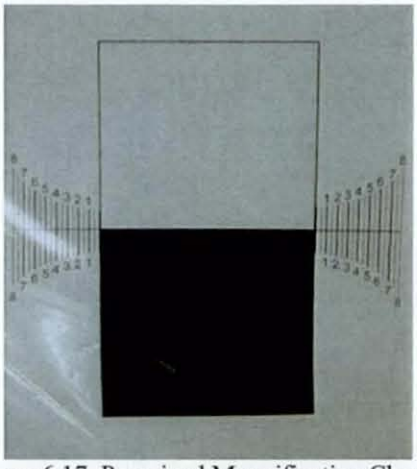

Figure 6.17, Perceived Magnification Chart

The evaluation is based on a simultaneous comparison with the same object in air, and due to the fact that the test parameters are unchanged, the resulting comparison is a result of the optical effects of the lenses. To ensure a good result, the participant must align the face of the goggle lens perpendicular to the normal of the test chart. Once this is achieved, the bottom rectangle can then be read against the upper scale ensuring both are centrally aligned along the vertical axis, so that the same numerical reading on each side is obtained.

6.8.4 Apparatus

The apparatus used in the study is listed below:

- Laminated magnification chart
- Three lens types
- Suckers
- Tape measure
- Antiseptic wipes
- Test results table

6.8.5 Test Procedure

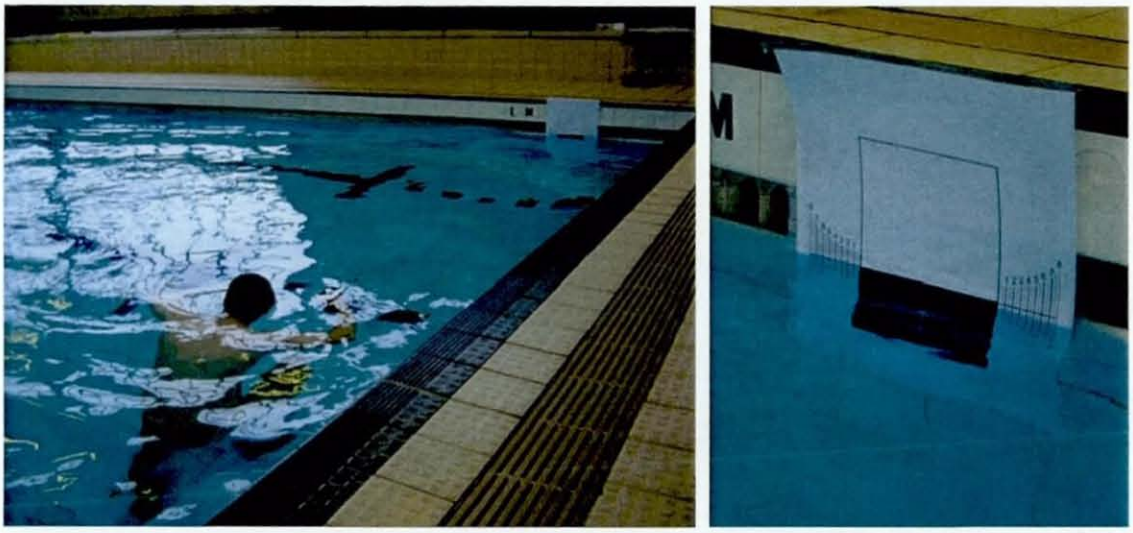

Figure 6.18, Perceived Magnification Measurement Setup

The general setup of the study can be seen in Figure 6.18. The test chart was positioned at a distance of 2m from the participant and the centre of the chart aligned at the exact eye level. The test was conducted in a well lit environment and in the case of the underwater testing was away from any water turbulence or strong current flows.

The step-by-step procedure used to complete the tests is stated below:

1. Explain the nature of the test so the participant understands the experiment details.
2. Ensure the equipment is correctly setup and accurately laid out.
3. Ask the participant to become familiar with the goggle lens and adjust correctly to ensure a comfortable and as best fit as possible
4. Ask the participant to position themselves at the required distance in front of the chart. Adjust if necessary so that the centre of the chart is at eye level.
5. Ensure the participant understands the test.
6. Ask the participant to cover one eye with their hand
7. Begin the test and record the participants response.
8. When complete, repeat the test with the other eye.

6.8.6 Results

Figure 6.19 shows the key results with the correct magnification factor.

PARTICIPANT	FLAT LENS	CURVED LENS	PROTOTYPE LENS
1	35	30	15
2	35	25	10
3	40	35	15
4	35	30	15
5	35	25	15
6	35	30	15
7	35	25	10
8	35	30	15
9	35	30	15
10	40	30	15
11	35	30	15
12	40	30	15
13	35	25	10
14	35	25	15
15	40	25	10
Average	**36**	**28**	**14**

Figure 6.19, Magnification effects of different lenses

It can be clearly seen that viewing through the Flat lens gives the largest magnification of 36%, with the curved lens closely following with a magnification of 28% and the Prototype lens giving a relatively small magnification average of 14%.

6.8.7 Discussions and Conclusion

The results obtained in this test show a distinct difference between the lens types. The data shows how the geometry of the interface between the goggle lens and the water alters the magnification power and therefore affects the scale of what is viewed through the goggle.

The flat lens goggle represents a 36% increase in image size based on the mean results of this test. This closely follows that of other documented research where suggestions of approximately an increase in 1/3 of the viewed object is seen. The curved lens by comparison has less of a magnification effect, but is only marginal due to the very slight curve of the lens. A lens with a smaller radius of curvature (with constant lens thickness) would have a smaller magnification effect, as the lens when placed in water would become closer to that of a negative lens. However, in doing so,

this lens would also suffer from severe distortion, hence the nature of this chapter, to evaluate a lens with zero magnification of an image and zero distortion.

The ideal magnification would be 0% indicating that the goggle had restored the underwater vision to the same as air. The prototype lens achieves an average result of 14%. Therefore improved performance is achieved in comparison to current swimming goggle lenses, but is still not an ideal solution.

In conclusion, the prototypes performance underwater is more close to the ideal of the naked eye viewing in air. Therefore, the lens is a marked improvement allowing the swimmer to better judge distances underwater. Further work would however be suggested in redesigning the lens to achieve zero percent magnification.

6.9 Visual Distortion

6.9.1 Introduction

An optical system is prone to distortion and unwanted visual effects that result from the system being a compromise between its various design parameters. Earlier work that measured the visual acuity when looking through the various lens designs, was based upon what the eye was seeing. To evaluate distortion of simply the lens, the eye has to be removed from the equation.

6.9.2 Aim

The aim of this test was to establish whether, if any, the various goggle lenses contributed to visual distortion. This test was inspired by the literature of underwater photography and the associated visual problems that result from the lens being used underwater.

6.9.3 Methodology Selection

Using a camera to photograph an object through each of the lens types allows the resulting images to be directly compared. The object itself that was being photographed had to be uniform throughout its entirety, symmetrical, simple and have a contrasting black on white format. It was important that the image was black on white, as this allowed the extent to which each lens generated chromatic aberration, as well as pincushion or barrel distortion.

The object used was a grid (as seen in Figure 6.20) that consisted of a uniform array of known geometry. Each black square is 6mm x 6mm with a spacing of 3mm separating them.

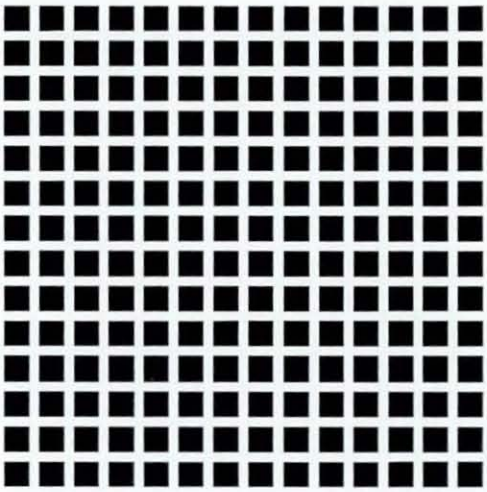

Figure 6.20, Grid used for visual distortion test

6.9.4 Apparatus

A digital photographic camera was used that had a macro mode and an aperture lens diameter similar to that of the pupil. The camera lens housing was small enough to fit inside of each goggle housing. A collet around the end of the camera was used to maintain a specified distance of 10mm from the grid. A glass tank filled with pure water was used to house the entire setup.

6.9.5 Test procedure

Each goggle was placed in front of the lens and the image of the grid was recorded. The goggles were tested both in air and water. This was achieved by taking the images vertically and positioning the lens just below the water surface.

6.9.6 Results

The results of this test are based on the captured images through each of the lenses. The images have been compared to the control image taken with no lens and in the air. However, due to the size of the camera lens used, there is a degree of barrel distortion, which has to be allowed for when assessing the images. Assessment is based on grid size, shape distortion and the presence of chromatic aberration. The

high quality images are found in the Appendix – Visual Distortion Images and should be referred to with the documented results below.

6.9.6.1 Results in air

By comparing the flat lens and curved lens to the control, there is very little difference to the extent of distortion and no change in grid size. This was to be expected as the lenses have no magnification power in air. Chromatic aberration does occur at the points of the image where barrel distortion is greatest, but this is similar in all three cases. The prototype lens shows the familiar problems with focus in air, but the image has less barrel distortion than the other indicating an element of pincushion distortion. The grid size has also increased indicating a magnification effect.

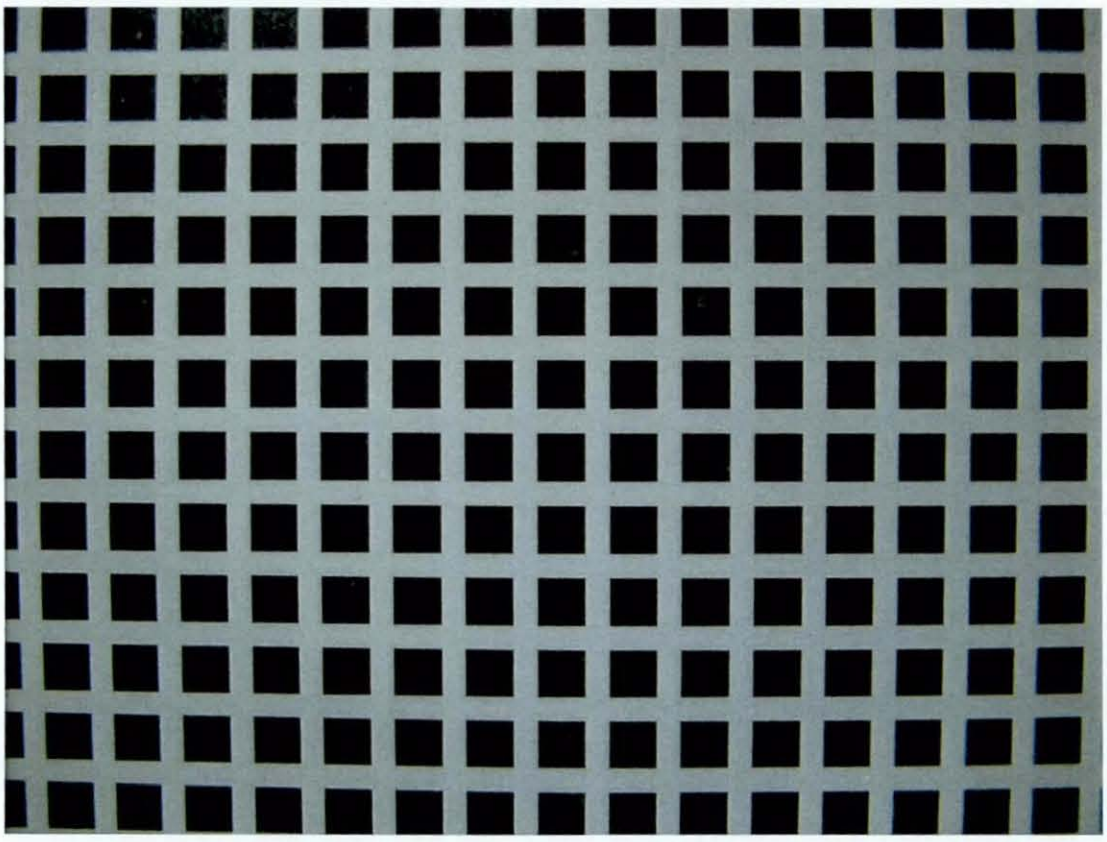

Figure 6.21, Control photograph taken in air

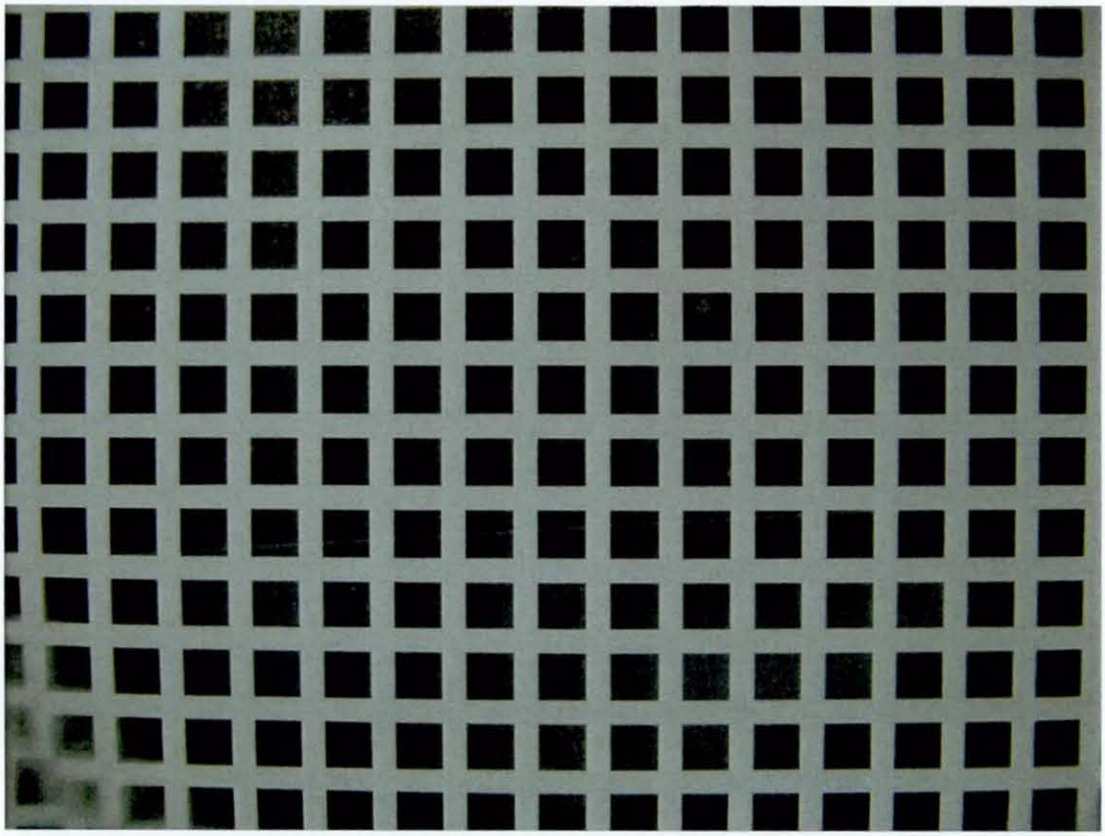

Figure 6.22, Photograph taken through flat lens in air

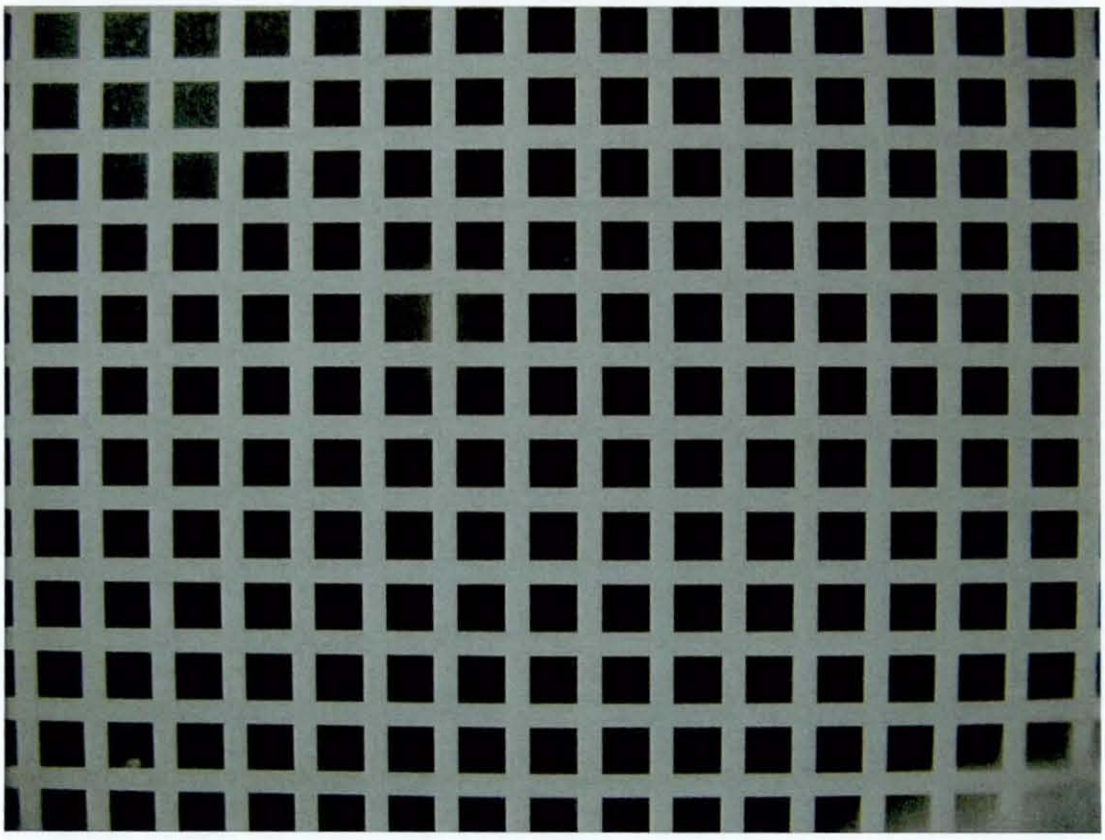

Figure 6.23, Photograph taken through curved lens in air

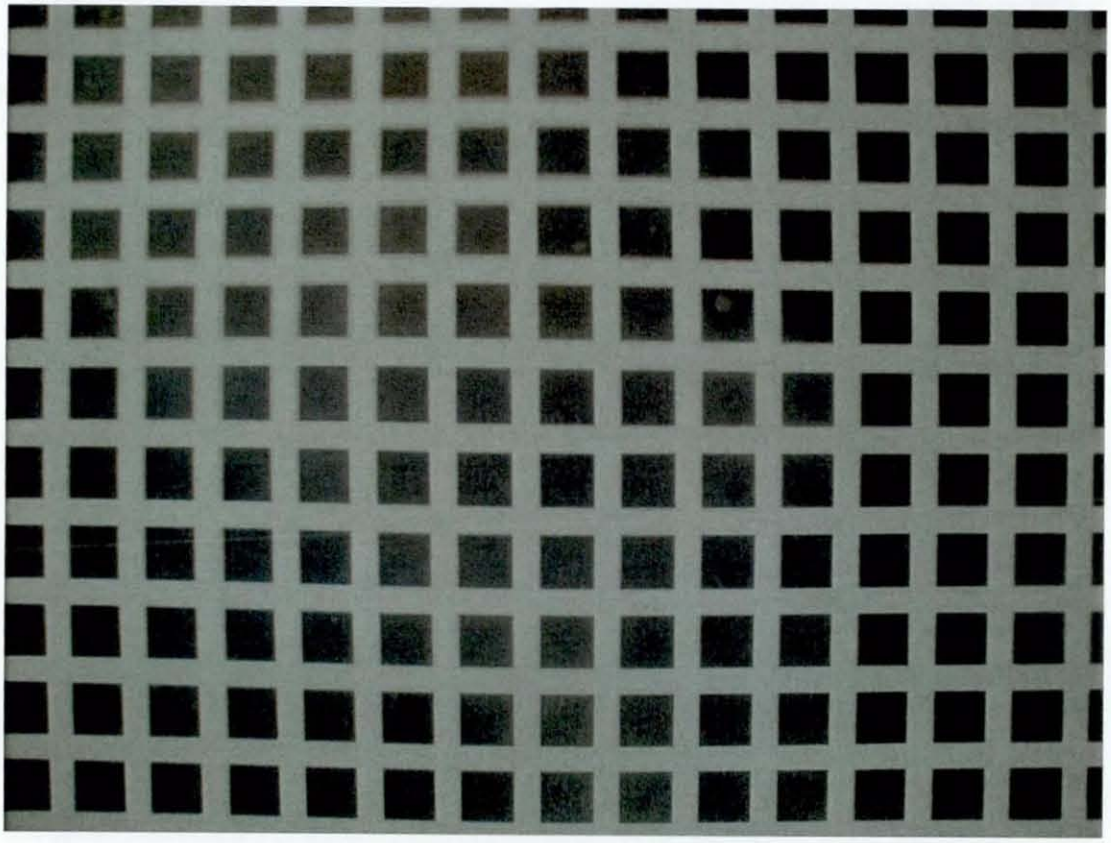

Figure 6.24, Photograph taken through prototype curved lens in air

6.9.6.2 Results in water

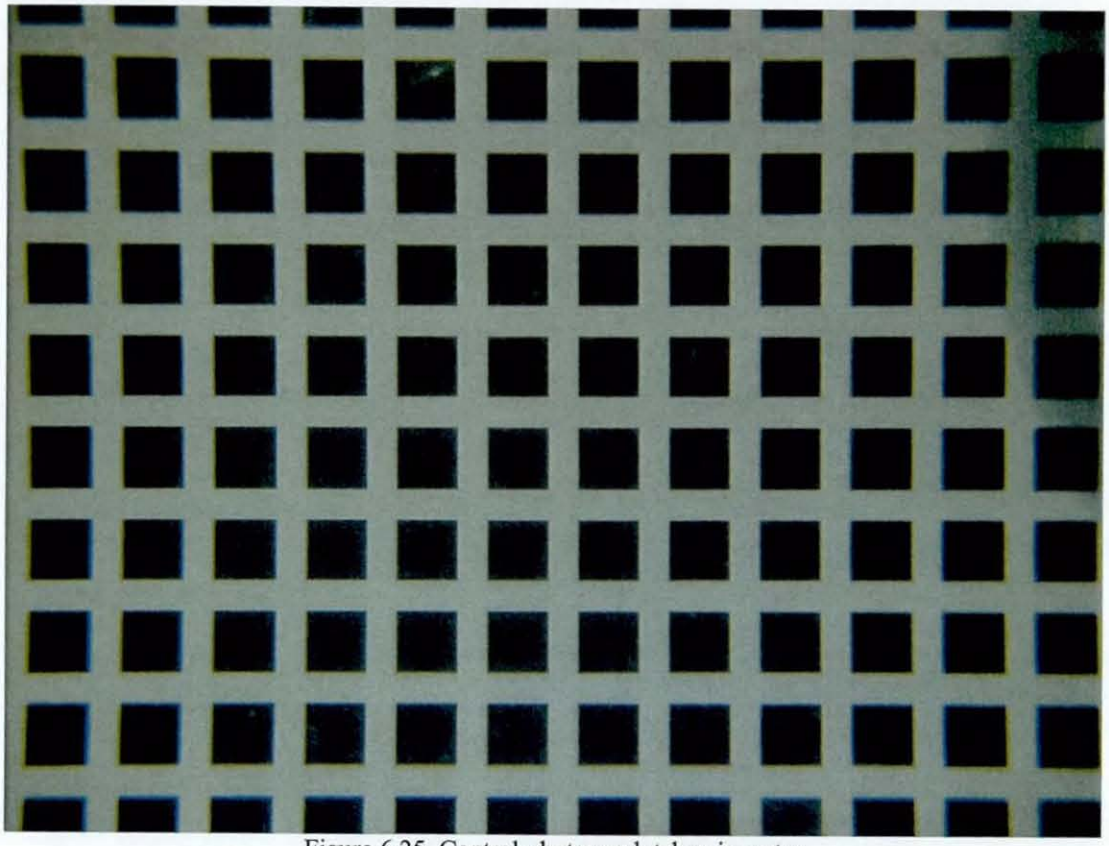

Figure 6.25, Control photograph taken in water

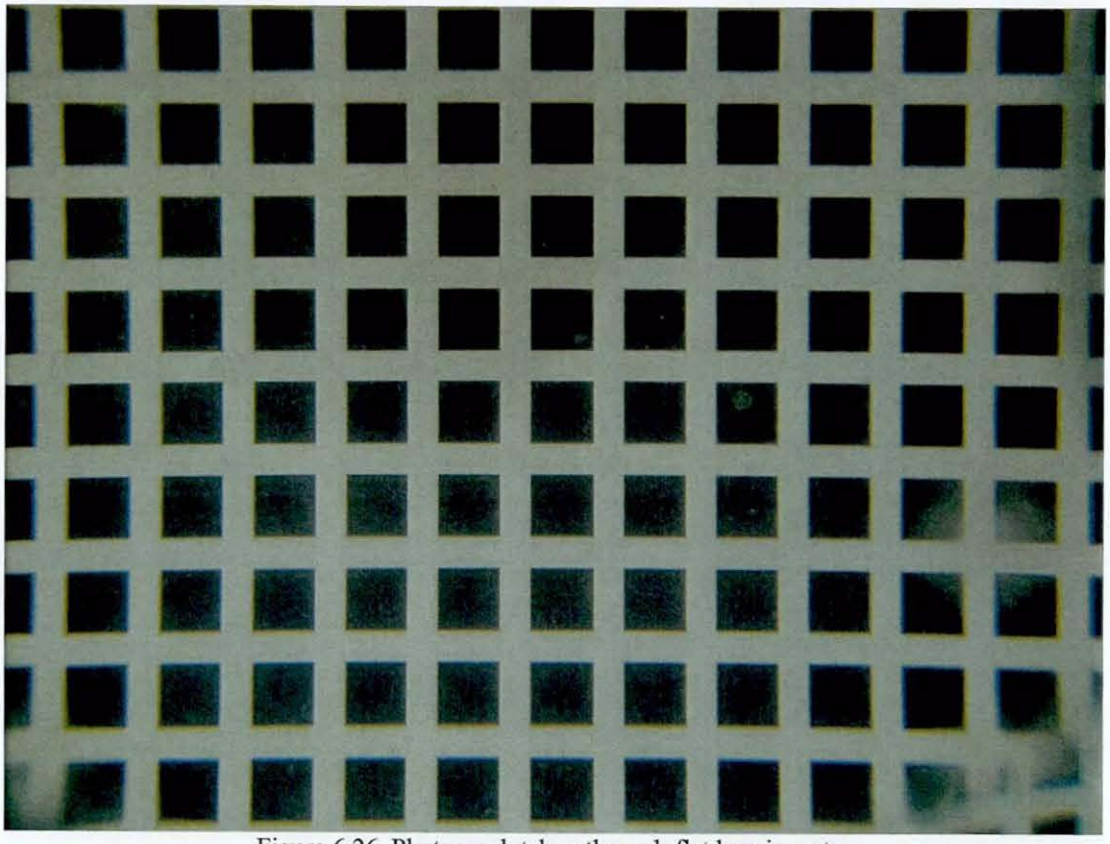

Figure 6.26, Photograph taken through flat lens in water

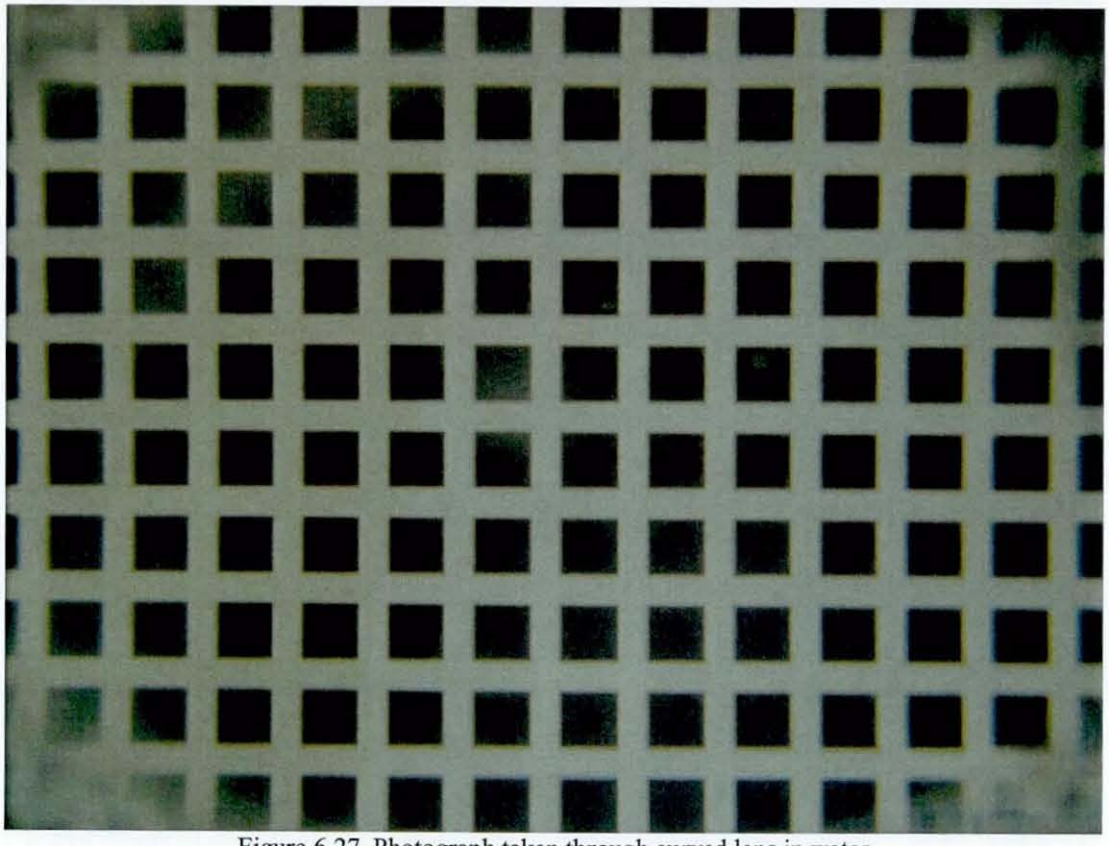

Figure 6.27, Photograph taken through curved lens in water

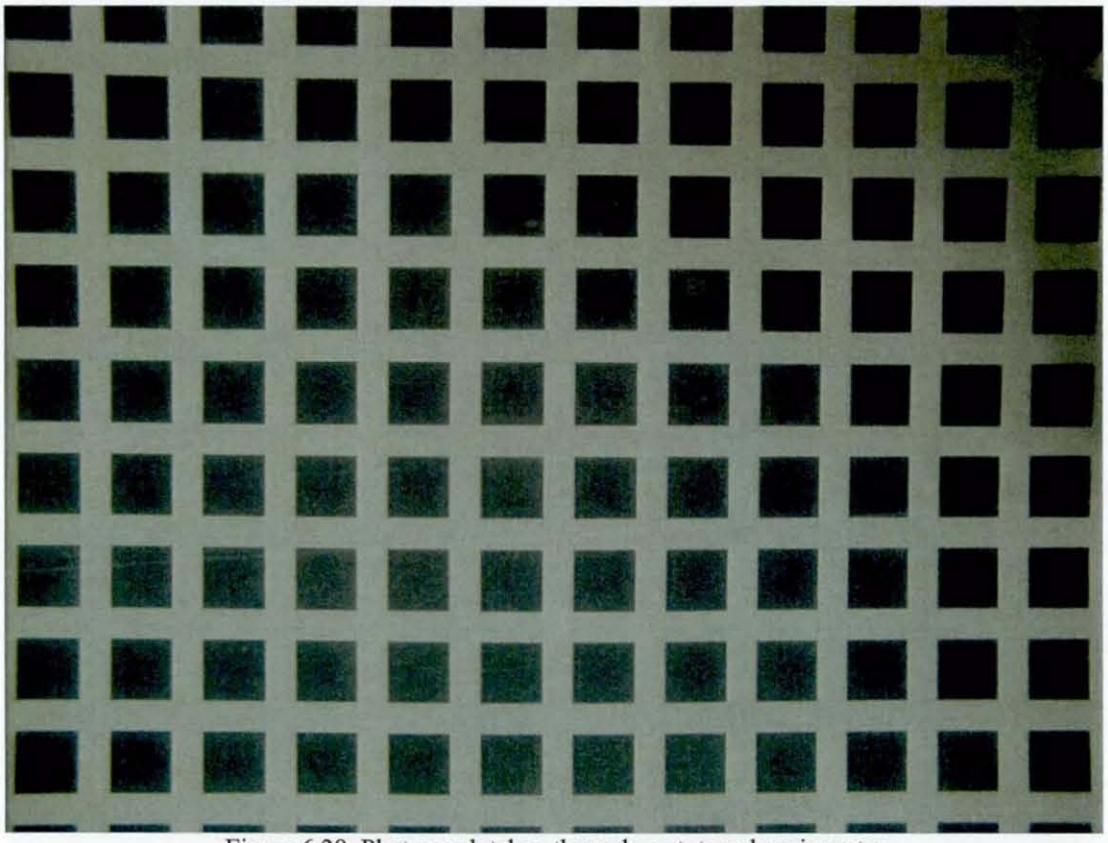

Figure 6.28, Photograph taken through prototype lens in water

The results from the in-water test highlight the differences between the lenses. Firstly, the flat lens goggle magnifies the grid size from 12mm to 16mm (thus a magnification effect of 1/3). The grid is uniform in the centre of the image, but exhibits pincushion distortion at the edges. The pincushion is displayed less than the 'true' amount, due to the barrelling effect of the camera lens. Additionally, a larger degree of chromatic aberration occurs at the edges of the image, as seen in Figure 6.29.

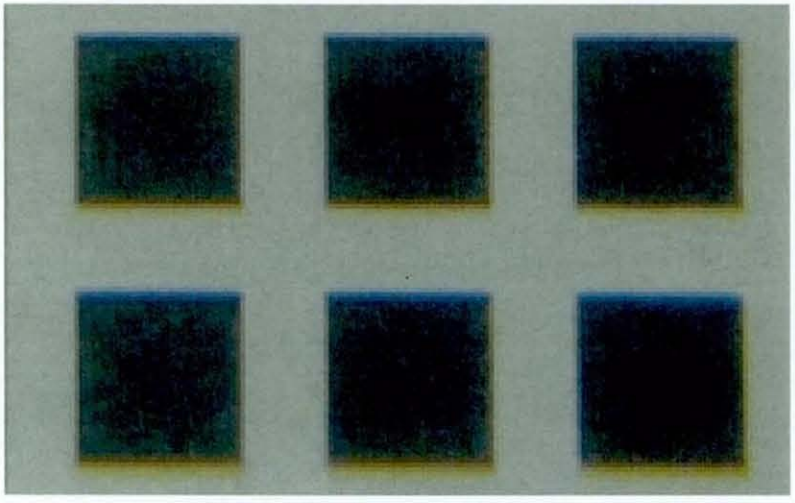

Figure 6.29, Chromatic Aberration

The curved lens exhibits the same problems as the flat lens when underwater, with the difference between them being negligible.

Comparatively, viewing through the prototype lens gives good definition throughout, with very little chromatic aberration, even at the edges. The edges of the image show slight effects of pincushion distortion, even though the camera lens reduces the appearance.

6.9.7 Discussions and Conclusion

Although this is a fairly simplistic test, with no quantitative results to back it up, it is an excellent method of visually displaying the key effects of using lenses underwater. The test shows the contrast between the flat / curved lens goggles and the benefits of the new prototype.

The lens has minimal distortion and very little chromatic aberration which allow a more detailed and defined image to be seen by the eye. Its performance is better than a single lens goggle but not as good as 'normal' vision in air.

6.10 Effects of Prototype Lens Being Located at Different Positions Relative to the Eye

6.10.1 Introduction

As shown by some of the earlier studies (and the design phase), it is quite apparent that the prototype lens needs to be maintained at a very specific distance from the eye, to be at its maximum optical performance. Unless a custom pair of rigid goggles were to be made for every swimmer wanting to use the goggles, this 'specific' distance is unlikely to be adhered to. It is therefore necessary to find the extent to how much the vision is impaired, when the lens is positioned at different locations compared to the eye.

6.10.2 Aim

The purpose of this study is to get an idea of the levels of degradation in vision, when the lens is not located in its optimal location. Comparisons of photographs through the lens is sufficient, rather than results that produce quantitative results.

6.10.3 Methodology Selection

A similar technique to the Visual Distortion section was used except for a few key points. Obviously the camera would be positioned at different distances from the lens, but in relation to the overall experiment setup, certain changes were beneficially made.

Previously, the distance between the camera lens and the prototype goggle lens was quite small. This caused certain problems that were formerly unknown, and therefore had to be increased substantially. Within the old setup, this would mean that the object grid would need to be placed quite deep in the pool due to the vertical camera mounting. Unfortunately, the visibility within water radically reduces as you get deeper, as the light from the surface interacts with the water particles (refraction, diffraction and reflection). Therefore, the object and camera needed to be mounted

horizontally at a set distance below the surface. As the camera was now to be positioned below the water, a waterproof camera housing was required that would use the prototype lens.

6.10.4 Underwater Camera Housing Design

The key functions that the new underwater camera casing had to feature were,

- Completely waterproof (up to at least 1m)
- Easy access to remove the camera from casing
- The ability to turn the camera on/off, take a photo and be able to zoom in / out
- The ability to be able to view the digital LCD display while underwater

Reducing the areas where possible leakage might occur was paramount to the design, and therefore it was decided to remove the option of a zoom out button. With the specific camera being utilised, if the camera was turned off, the zoom would automatically return to is preset position. This meant that if, once zoomed in, the camera would simply need to be turned off and then turned back on again.

The end result was a relatively basic housing designed specifically for 5.0 Mega Pixel Casio Exilim (Figure 6.30).

Camera Specification

- 5.0-megapixel CCD captures high-resolution images up to 2560 x 1920 pixels for photo-quality prints
- 3x optical/4x digital/12x total zoom; smc Pentax lens
- 2" digital interface colour TFT-LCD monitor with acrylic scratch-resistant panel; histogram and grid display modes; optical viewfinder

Figure 6.30, Camera Specification

The waterproof housing can be seen in its various states of being open and shut in Figure 6.31. The housing was initially rapid prototyped using Selective Laser Sintering, but unfortunately the specific end product is quite porous (which is hardly ideal for a waterproofing product). The housing had to be therefore soaked in superglue, which seeped into the pours and ensured it remained watertight.

Figure 6.31, CAD renderings of the waterproof camera casing.

6.10.5 Test Procedure

The experiment was setup in a 2m tank filled with pure water (no chlorine etc.) The camera was simply placed 1m away from a similar grid to that of the previous experiment, except the squares were 10 x 10mm with 5mm gaps. Photos were then

taken with the camera lens being 8, 10, 12, 14 and 16mm away from the prototype lens. Distances of any greater would be pointless, as the lens would never be that far away from the human eye. Unfortunately, due to the camera design, the distance could also not be any less than 8mm, as the camera casing itself was already in contact with the prototype lens.

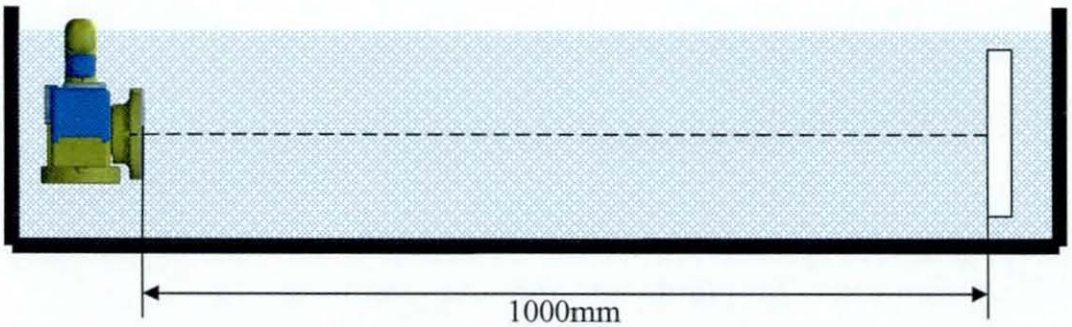

Figure 6.32, Experiment Setup

6.10.6 Results

As can be clearly seen from the photographic images found in the Appendix – Varying Lens Distance to Eye, the quality of the image was gradually worsened as the distance increased. The image was actually noticeably inferior after only being 2mm either side of the optimum location.

6.10.7 Discussions and Conclusions

Although there has been no measurement of the loss of optical performance, it is quite clear that the lens does need to be correctly aligned to achieve its intended function. To a certain extent this had already been made aware before this particular study was even begun. However, the severity of the matter has now been made even more apparent. This will directly relate to future lens housing designs, where the seal gasket should only have a specified level of compression. This has now been made achievable with the previous work relating to facial anthropometric data, and the requirement of more than one housing size.

6.11 Discussion

The key elements of this chapter focused on the performance of the various lenses. It identified the important visual functions and described techniques used for testing. The various goggle lens types were tested and evaluated by comparing the results between the lenses and also the ideal situation of naked eye vision in air. The primary intention was not to prove that the prototype lens was the 'best', but was to develop a number of testing techniques that could be used to evaluate underwater lens design. The secondary intention was to demonstrate that the prototype lens has the potential, through future development, to eventually be used in mass production swimming goggles.

Comparing the prototype lens to the single lens goggles showed that the prototype lens gave a better representation of the control image, suggesting it reduced the effect of image magnification when underwater. The test showed that the prototype only magnified the image by 10%, while in comparison the flat and curved lens magnified the image by approximately 30 to 35%. For a swimmer, this in theory would allow better judgement of distances to the wall and other swimmers. However, due to the fact that the brain is used to the larger magnification and makes its own relative compensation, a short accommodation period would most likely be required to get used to the reduced magnification effect. From magnification alone, it can be stated that the prototype shows a radical improvement.

The prototype lens also performed better at reducing the distortion effects around the perimeter of vision. This is believed to be due to the curved outer lens surface being more uniform in direction in terms of the way light is refracted. The prototype also reduced chromatic aberration, as the lens system specification ensures the different coloured light rays are not separated.

Although there was a reduction in visual acuity compared to the other lens types, the difference was only negligible, and wasn't noticed by the swimmers in general use. This was again the case with the slight reduction in Stereoscopic vision, and so although not ideal, would be perfectly acceptable for a mass production goggle

With use of the prototype lens underwater, all of the aspects of underwater vision were either comparable to that of the standard flat lens or a marked improvement. It can therefore be recommended that the new lens technology should be taken to the next stage of development.

7.0 Data Driven Goggle Design

7.1 Introduction

The purpose of generating new data to help design innovative swimming goggles, is primarily to improve their comfort and fit. The current design method of simply taking existing goggle designs and then using a trial and error process to attempt improvements is inefficient and often unsuccessful. A good example of this is the Speedlite Racing goggle, where production was rapidly stopped due to a high percentage of the goggles not fitting the intended target population. This is not to say however that past examples can not influence future design, but more that they should not lead the design process.

7.2 Chapter Aims

The aim of this chapter is to provide simple methodology on how the data generated in the previous chapters can be used to design a 'better' pair of swimming goggles. Therefore it will be data driven design and giving the user what they require, rather than providing an aesthetic pair of goggles based on existing 'inferior' technology.

7.3 Chapter Objectives

As comfort and fit are the primary issues, function of the goggles should take priority over their form and styling. The goggles should therefore be initially designed for ideal comfort, with almost complete disregard for their aesthetics. After this stage, compromises can then be made to ensure the goggles are appealing to the swimmer, so as to ensure that they would actually be bought, and not remain an 'ideal' laboratory goggle. There is little requirement for further development of design detailing, manufacturing, materials or assembly, as this is not the objective of the thesis.

The objectives are therefore;

- To create a step-by-step guide on how to generate a data led designed pair of swimming goggles.
- To adhere to a simple specification and generate an example data led conceptual design of a pair of swimming goggles.
- To generate novel design features that have been generated as a result of data led design.

7.4 Utilising the Scientific Data

7.4.1 Seal Location

Using the detailed research on the measurement of skin sensitivity in chapter 2, it was found that the ideal location for the seal can be seen in Figure 7.1.

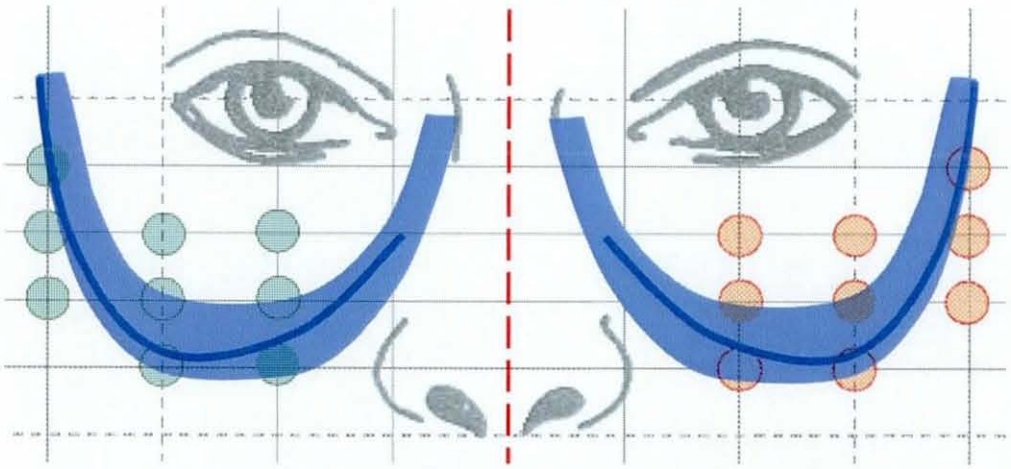

Figure 7.1, Preferred seal footprint location with regards to skin sensitivity.

It is quite apparent that only half the seal location is shown, and therefore the remainder should be decided taking into account current goggle designs, preferred hydrodynamics, seal contact and facial movement. If the seal were to be positioned above the eyebrow, not only would the hydrodynamic performance be decreased, but the resulting increased drag on the seal lip would increase the probability of the goggles being ripped away during the swimmers dive (Figure 7.2).

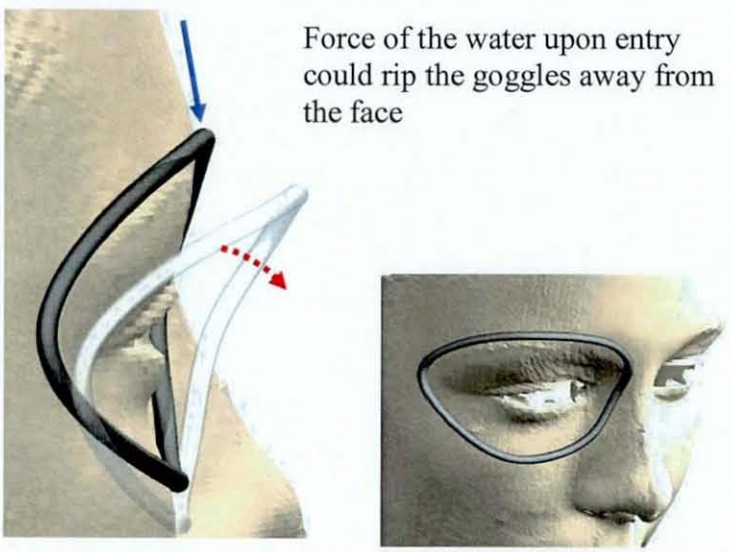

Figure 7.2, Problems with seal be positioned above eyebrow.

If the seal were to be positioned directly on the eyebrow (or even partially on the eyebrow), the seal contact would be dramatically reduced in performance, and would also be susceptible to the same problems as mentioned for a seal positioned above the eyebrow. Therefore, the only logical position for the upper seal would be where all current swimming goggle upper seals are positioned. Figure 7.3 illustrates a band of surface where the seal location should fall within.

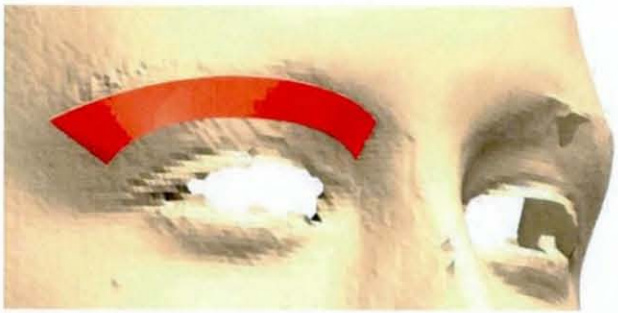

Figure 7.3, Problems with seal be positioned above eyebrow.

For the complete 'ideal' seal location, the surface areas in both figures 7.1 and 7.3 need to be joined together. Although, not an exact definitive curve, the curve shown in Figure 7.4 is a very close approximation to the amalgamation and where an 'ideal' seal should be located.

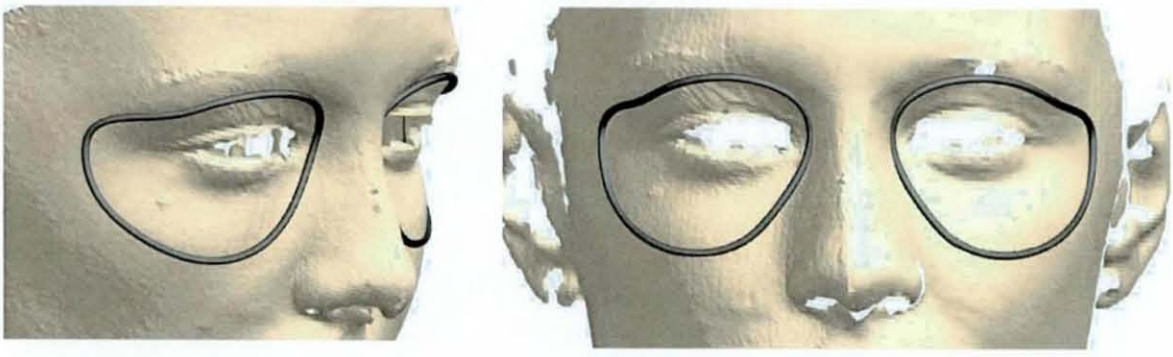

Figure 7.4, Ideal seal position

7.4.2 Seal Compression

Using the detailed research on the measurement of facial tissue compression in chapter 3, it was found that the tissue compresses as shown in Figure 7.5.

Point position	Female average compression (mm)	Male average compression (mm)
A1	-4.26	-4.15
A2	-4.21	-3.84
A3	-4.57	-3.84
A4	-4.50	-3.85
A5	-4.74	-4.16
B0	-2.90	-2.94
B4	-4.59	-4.19
B5	-5.01	-4.36
B6	-5.52	-4.95
C4	-4.92	-4.78
C5	-5.44	-5.21
C6	-5.94	-5.99
D0	-2.64	-2.79
D4	-3.67	-3.69
E1	-2.77	-3.21
E2	-1.46	-1.49
F0	-2.63	-2.83
F4	-3.73	-4.16
G4	-5.24	-5.11
G5	-5.35	-5.20
G6	-5.66	-5.82
H0	-2.97	-2.90
H4	-4.67	-4.10
H5	-4.73	-4.14
H6	-5.16	-4.84
I1	-4.48	-4.24
I2	-4.27	-3.77
I3	-4.53	-3.79
I4	-4.49	-3.61
I5	-4.81	-4.34

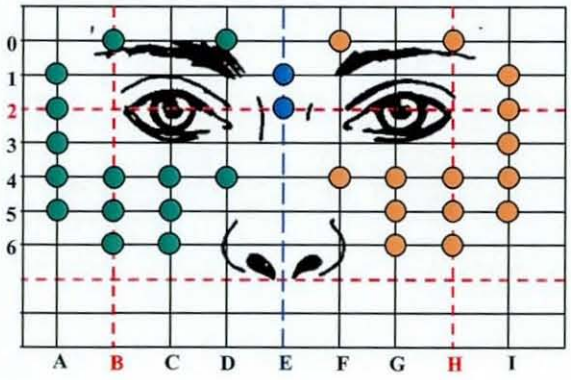

Figure 7.5, Average tissue compression for each point for both the male and female population

The compression data can be used to calculate how much the seal needs to compress at each point along the seal. When the desired seal location is overlapped on top of the compression data, it is unlikely that the seal path will pass directly over the measured intersection grid points. It will therefore be necessary to make approximations based on the nearest measured points.

7.4.2.1 Gaps in measurements

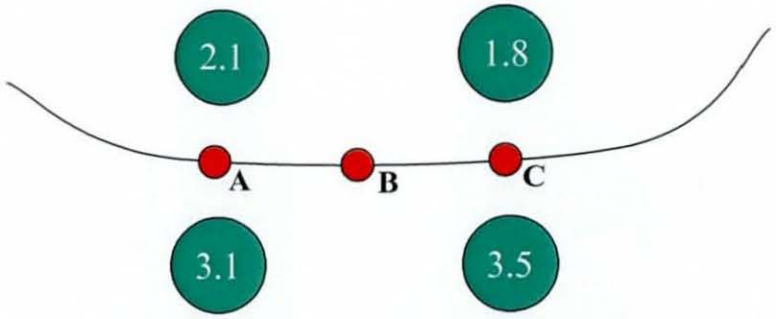

Figure 7.6, Example tissue compression points

If a seal were to be positioned along the path shown in Figure 7.6, there would be no compression measurements located directly over the path. Therefore (depending on the resolution required), points **A**, **B** and **C** would need to be calculated as show n below.

$$\mathbf{A} = (2.1 + 3.1) / 2 = \mathbf{2.60}$$

$$\mathbf{B} = (2.1 + 3.1 + 1.8 + 3.5) / 4 = \mathbf{2.63}$$

$$\mathbf{C} = (1.8 + 3.5) = \mathbf{2.65}$$

The above calculations are only applicable however, if the point unknown is directly half way between the two measured points. In the situation where the seal is positioned between two points as shown in Figure 7.7, then more detailed calculations are required.

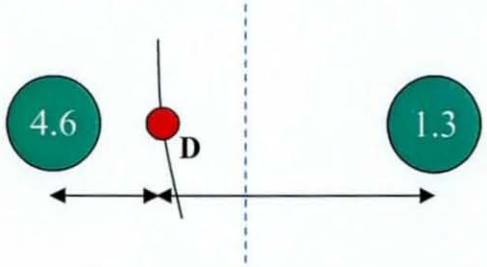

Figure 7.7, Example tissue compression points

In Figure 7.7, it can be seen that the unknown point is approximately ¼ of the distance across between the two measured points with a resulting ratio of 3:1. This

ratio represents the weighting relating to the nearer point. Point **D** could therefore be calculated as shown below.

$$\mathbf{D} = ((4.6*3) + 1.3) / 4 = \mathbf{3.78}$$

7.4.2.1 Transferring the compression measurements to the seal design

The manner in which the compression data can be used to define the flexibility of the seal, is completely variable depending on the resolution required and the seal design in question. The requirement for points along the seal to have exact compression characteristics is completely unnecessary, however there should be a relative approximate correlation between facial tissue compression and its own compression.

The simplest method can be applied when using a solid circular seal (Figure 7.8), where the goggle frame is rigid and the seal is a soft rubber compound.

Figure 7.8, Circular rubber seal example

Depending on the flexibility of the rubber, the diameter could be simply increased where the compression measurement of the facial tissue is reduced. This would improve the likelihood of a better fit by providing more flexibility, without increasing the overall profile of the goggle by an unnecessary amount. An example of this can be seen in Figure 7.9, where the compression values for the facial tissue are given on the left and the diameter of the relative seal points are given on the right.

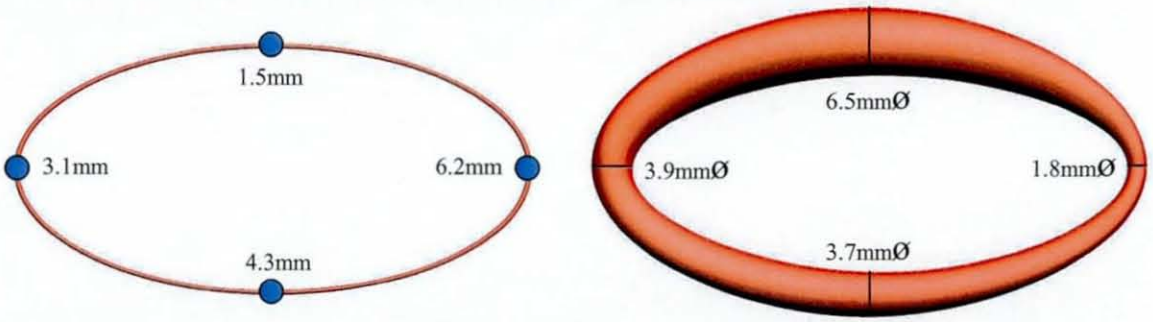

Figure 7.9, Example tissue compression readings with corresponding example seal diameters

The example diameter measurements have been calculated by simply subtracting the tissue compression measurements from a given value. In this particular circumstance, the value was 8 and was chosen as it resulted with diameters within a chosen diameter range of 1.5mm to 6.5mm. The unknown diameters between the calculated diameters are simply blended.

The above example is very simplistic, and might not result in a direct relationship between the compression of the facial tissue and the compression of the seal. This is due to the lack of consideration of the behaviour of the rubber at different thicknesses under constant load. In order for this to be remedied, studies would first have to be completed on the specific material compound that was to be used. This would be relatively simple when using the seal type as shown in Figure 7.8, but if more complex seal shapes were to be integrated, significant difficulties would arise. Fortunately, considering its application, there is little need for the resolution of accuracy to be this high. The variations in facial anthropometrics from person to person (even within a specific sizing category) would swamp any slight discrepancy due to not having exact compression characteristics of the seal material.

However, it is not to say that the exact compression values could not be calculated if required for a specific goggle design. For this particular chapter, this level of detail when simply designing an example concept would be impractical, as precise material specifications are not stated.

7.4.3 Facial Surface Anthropometrics

The research completed in chapter 5 resulted in the six categorised average facial surfaces found in Figure 7.10. For the duration of the initial conceptual design phase, the large male facial surface is used as a template foundation for the goggles to be based on. This particular surface was chosen as it represented the largest that the swimming goggle might possibly be, and therefore more likely represent possible problems with the goggle profile.

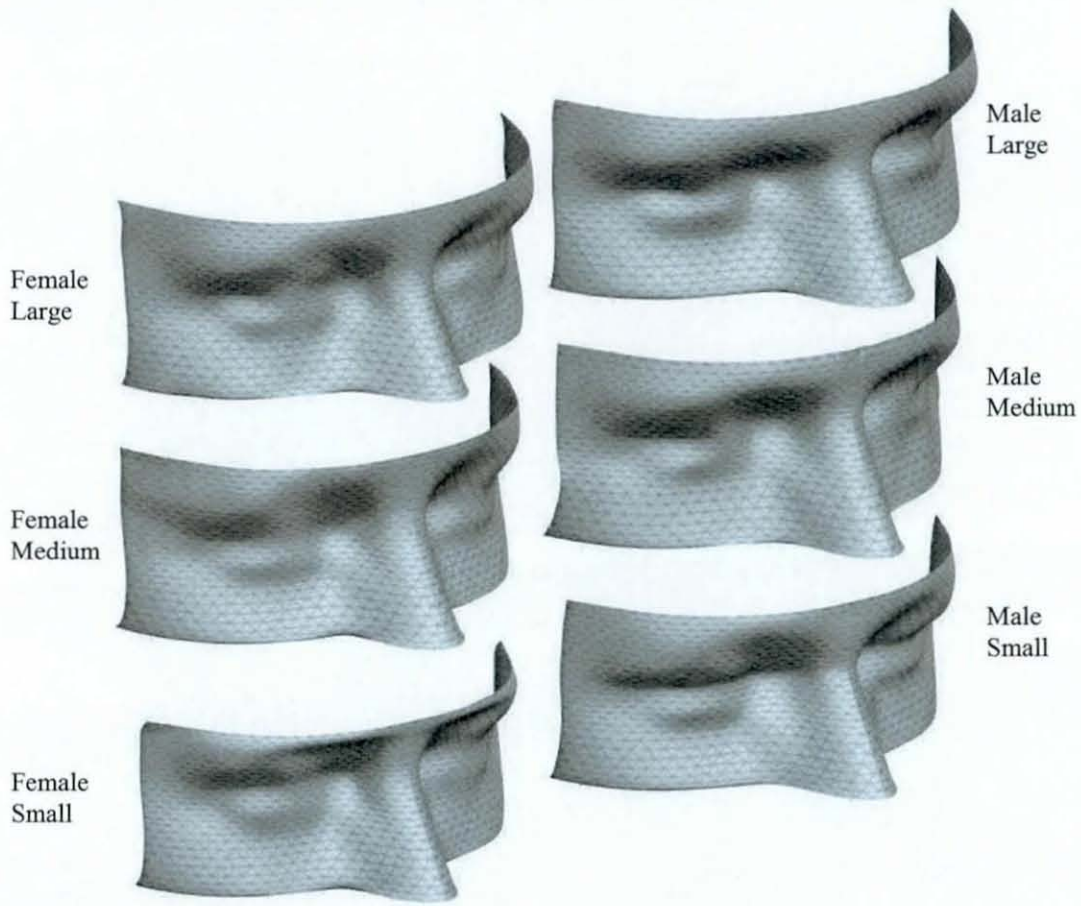

Figure 7.10, Categorised average facial surfaces

7.5 Design Specification

The purpose of this chapter is to develop a swimming goggle concept that incorporates all of the information learned in the previous research. However, this is not to say that other areas such as hydrodynamics and aesthetics should be disregarded, as if either of these were inferior to current goggles on the market, then the entire exercise would be pointless.

It is widely considered that the new Speedo Speedlite racing goggle (Figure 7.11) is very stylish and sporty in its appearance, and it was therefore decided to use similar aesthetic design cues for the final concept.

Figure 7.11, Speedlite Racing goggle manufactured by Speedo

Regarding the aspect of hydrodynamics, it was considered that reducing the overall profile of the goggles and attempting to 'fill-in' anatomical 'bumps' in the facial form were central to a new design. Figure 7.22 represents a pair of goggles that achieves this by extending the profile of the forehead down to the cheek.

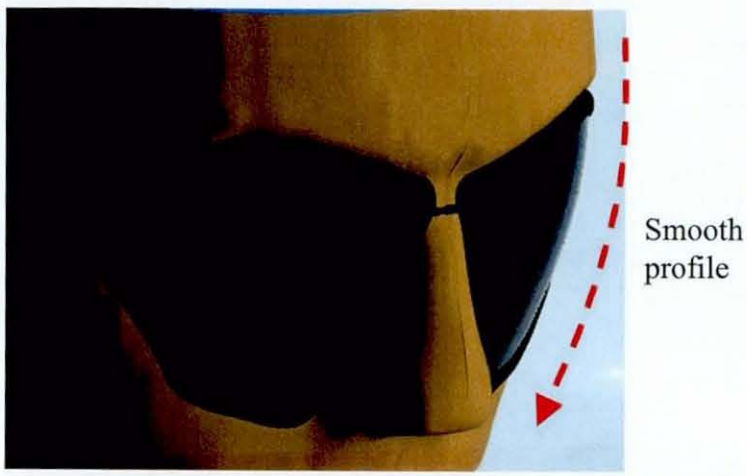

Figure 7.12, Example of an 'ideal' goggle profile

7.6 Initial Design Feature Concepts

There are various methods of design process when generating new product concepts. As this particular product is being designed with function primarily in mind, it is more sensible to separate the swimming goggle into specific design features. To improve design productivity, these features can be developed on their own, and then amalgamated to produce a complete conceptual goggle. At this stage, the complete goggle can be developed further to iron out possible problems and improve the overall aesthetics and detailing.

7.6.1 Fundamental Seal Designs

There are currently numerous variations of fundamental seal design, and yet there is still not one particular type that is considered optimally ideal. Figure 7.13 illustrates these different types in their simplest form.

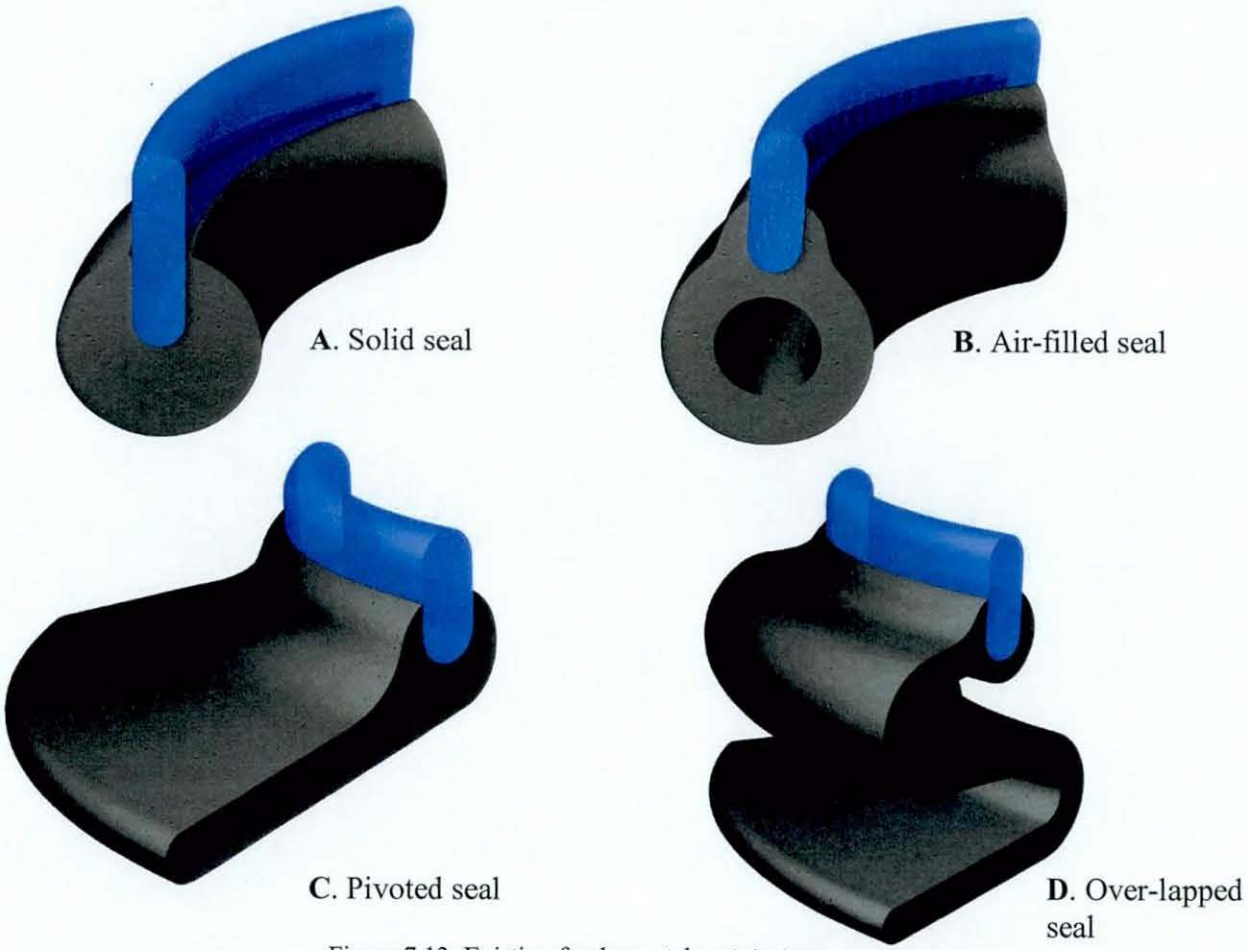

Figure 7.13, Existing fundamental seal designs

The problems associated with the existing technologies is that if the seal is comfortable for an entire target population, then it is most likely large and bulky creating unnecessary drag. The increased profile as shown in seal type **D** (Figure 7.12), also increases the likelihood of the goggle being ripped away from the face upon entry to the water (As mentioned previously).

A seal that is required is one that is extremely flexible so as to easily make complete contact with the skin, while being supportive enough to ensure contact is maintained throughout the swimming session. The most obvious answer is to therefore have more than one seal, with one providing the watertight contact, while the other provides the support and rigidity.

Figure 7.14, Double seal

Figure 7.13 illustrates and example of a double seal method, with the inner seal protruding slightly lower and being substantially more flexible than the outer seal. It is important when designing a seal of this type, that when under compression, the inner seal does not force the outer seal to break contact with the skin. There has to be sufficient space for the inner seal to bend more than the outer seal with minimal or no contact between the two under compression. This situation can be seen in Figure 7.15, where there are no obvious problems with the seal under compression.

Figure 7.15, Compression of seal

Minimising the overall size of seal while still maintaining similar performance characteristics, can be achieved with slight modifications to the above design. Figure 7.16 gives a clear representation of the developed concept seal design. At this stage the seal has not been designed for manufacture or assembly.

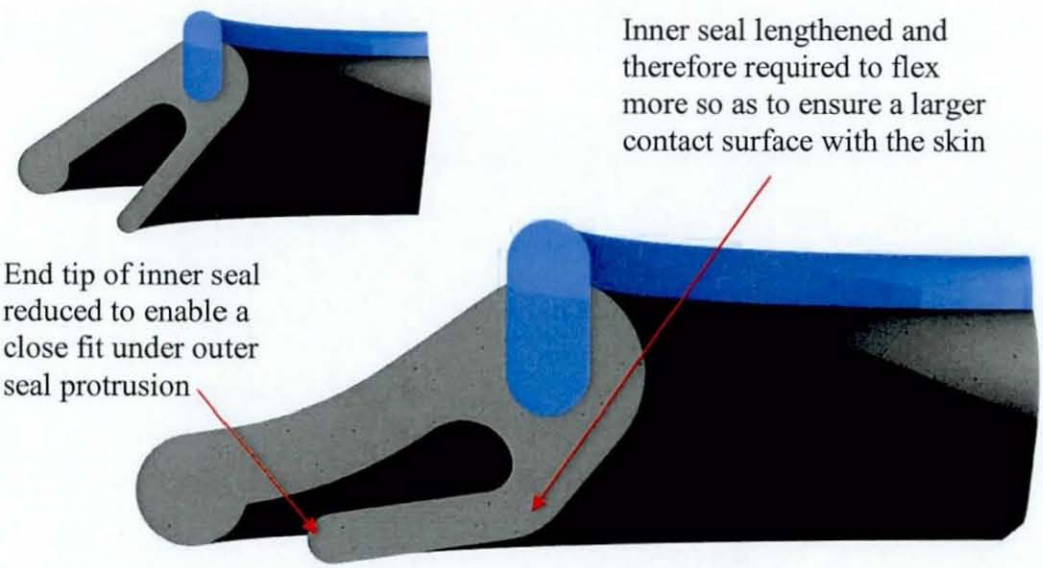

Figure 7.16, Double seal concept development

7.6.2 Fundamental Lens Shape Designs

As earlier work has shown, a curved lens design would be preferable, as it can significantly reduce the overall profile of the swimming goggle. Unfortunately, curved lens technology is only in its early stages of development and is therefore not included as a possible method.

A compromise has to be made between maximising the flat lens viewable area and reducing the overall swimming goggle profile. Figures 7.17 to 7.19 illustrate a number of lens variation layouts that might be used. Each of the lenses are shown attached to a standard solid seal of the same size for all.

7.6.2.1 Circular flat lens

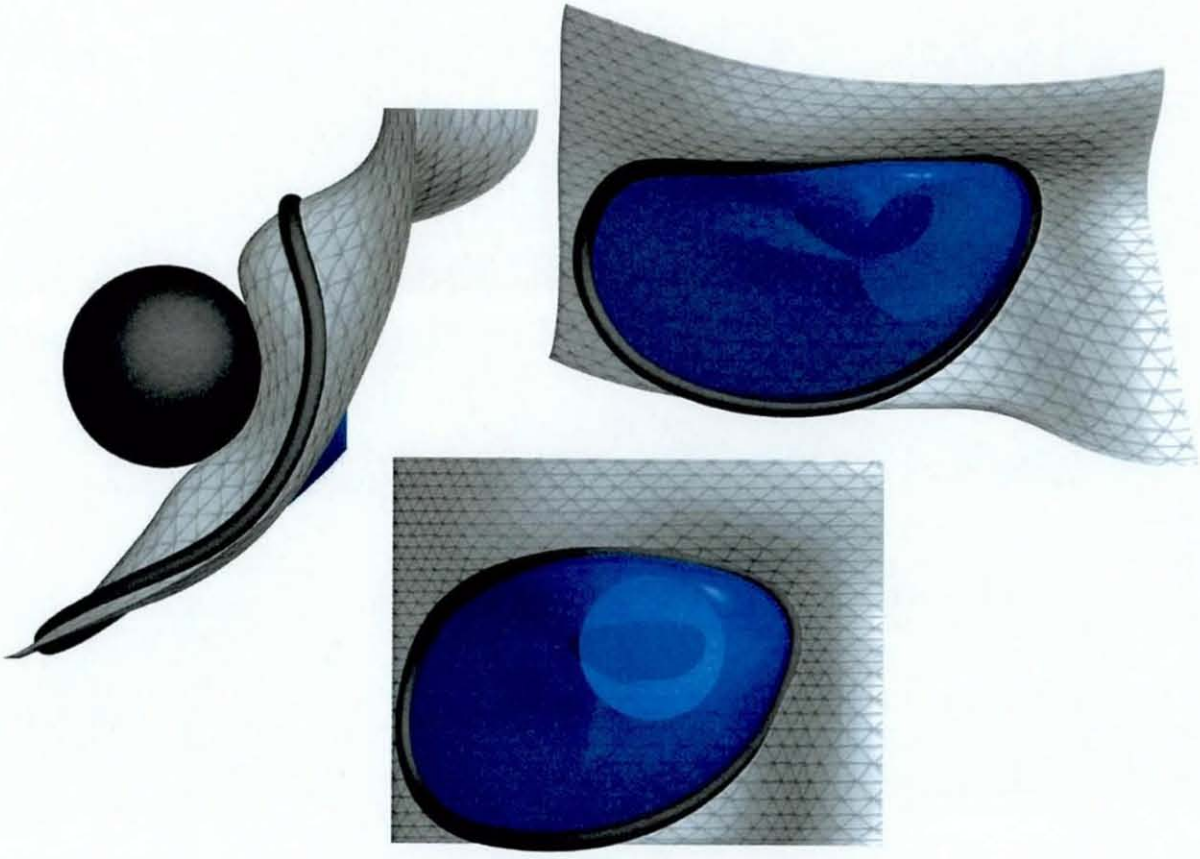

Figure 7.17, Circular flat lens example

Circular flat lens styles are generally only used in children's 'fun' swimming goggles, where there is little concern for hydrodynamics. In the example shown (Figure 7.17), the only reason the profile is quite slim with very little protrusion is due to a very small proportion of the lens being flat. Although the user would be able to see through the remaining curved lens section, vision would be severely compromised with significant distortion. Increasing the flat section to a diameter of 30mm, which would give the approximate amount of required periphery vision, would cause several problems. The overall profile of the goggle would be increased reducing the hydrodynamic performance of the goggle, but most importantly, the top of the lens would overlap the seal (as shown in Figure 7.18).

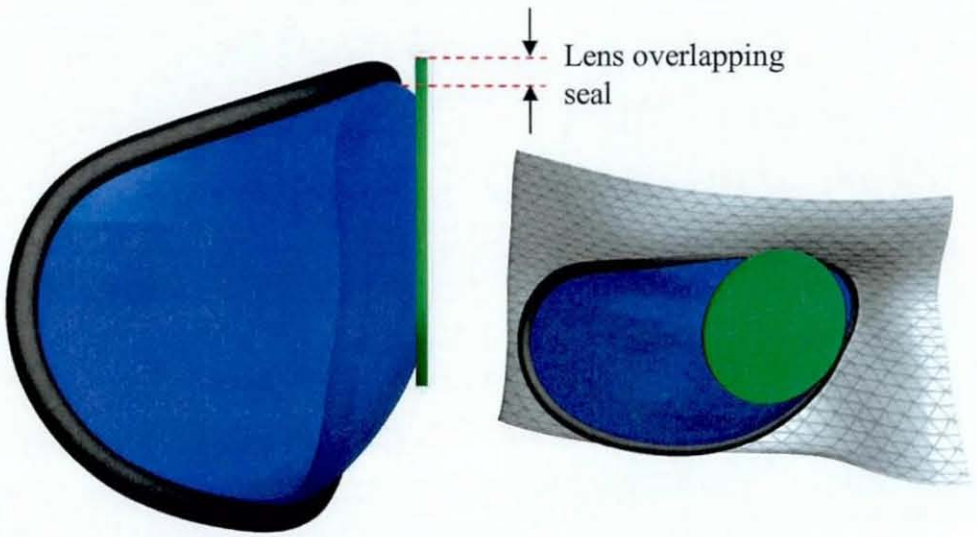

Figure 7.18, Increased flat lens size

The resulting lip shown in Figure 7.18, would significantly increase the likelihood of the goggles being ripped away upon diving into the water.

7.6.2.2 Ellipsoidal flat lens

The most common of lens shapes used in competitive swimming goggles in today's market, is the ellipsoidal flat lens. Figure 7.19 shows an example of this type of lens in its purest form. It can be clearly seen that the profile is increased over that of the circular lens, but the all important problem with side periphery vision has been resolved, without generating an overhang lip that would increase drag.

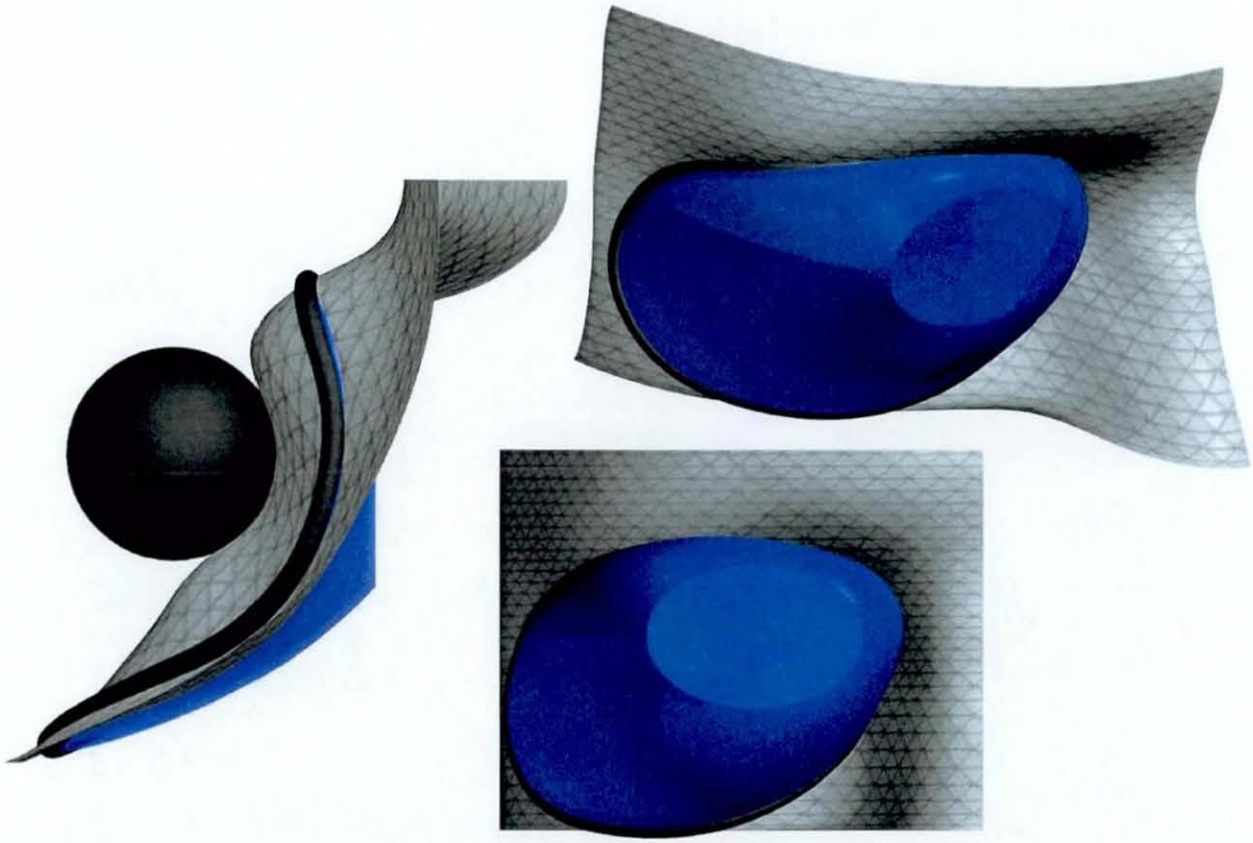

Figure 7.19, Ellipsoidal flat lens design

7.6.2.3 Split flat section lens

Reducing the profile of the swimming goggle while still retaining the use of a flat lens for the majority of vision can only be done by one of two methods. The first is to simply bring the lens closer to the eye. This can only be done to a certain extent, as there always needs to be sufficient space between the lens and the eyelash so as to ensure no contact is made. The second method is splitting the lens into two or more flat sections.

7.6.2.3.1 Lens distance from the eye

In order to specify the minimum distance the lens needs to be from the eye (when the seal is compressed), three measurements need to be identified. The eyeball diameter, the eyelid thickness and the eyelash length were all established in the previous chapter and can be seen in Figure 7.20.

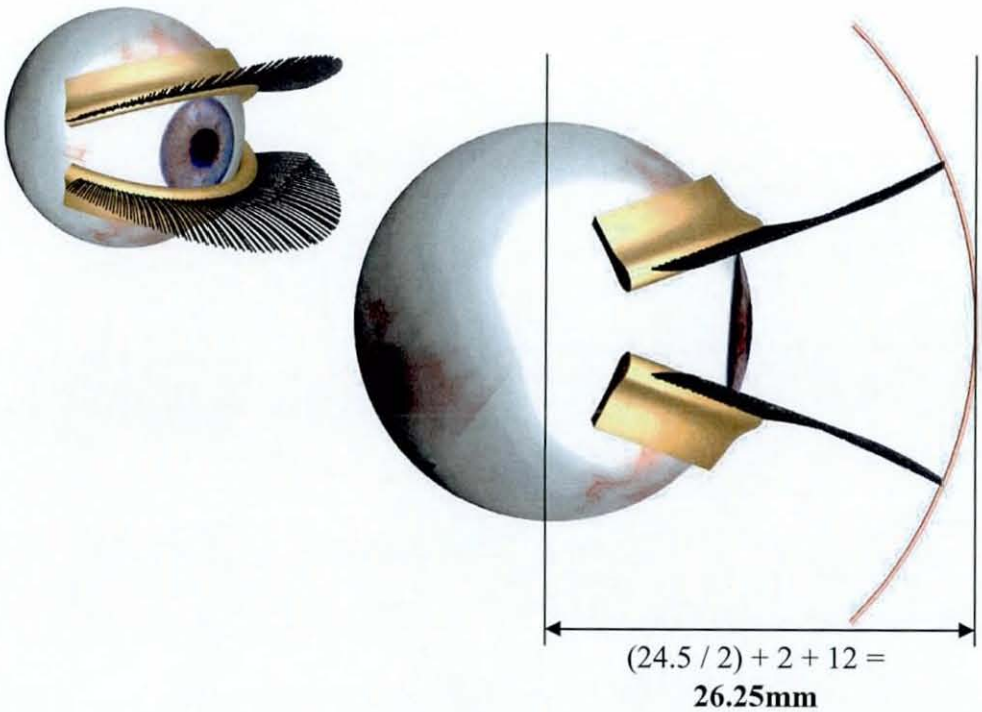

Figure 7.20, Minimum distance between lens and centre of eyeball

7.6.2.3.2 Sectioning the flat lens

The illustration in Figure 7.21 shows that when using a large flat lens, there will always be a significant level of protrusion from the facial profile.

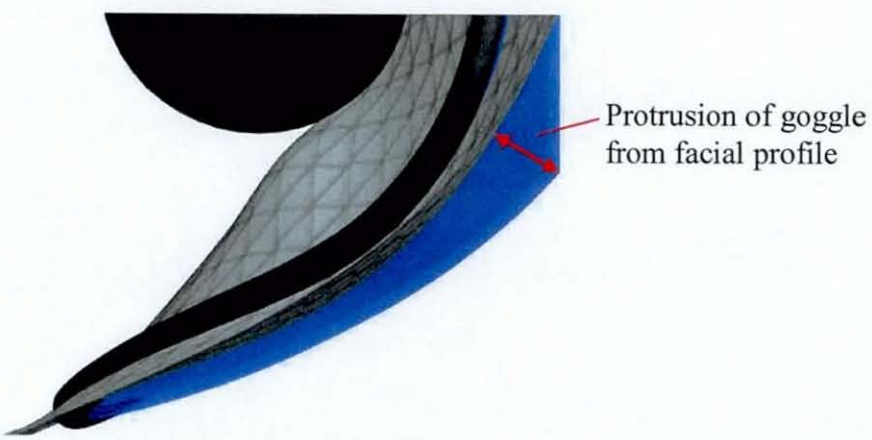

Figure 7.21, Protrusion of goggle

Sectioning the lens into more than one flat edge, can help to reduce this protrusion quite significantly. Figures 7.22, 7.23 and 7.24 illustrate the levels to which this sectioning can be completed.

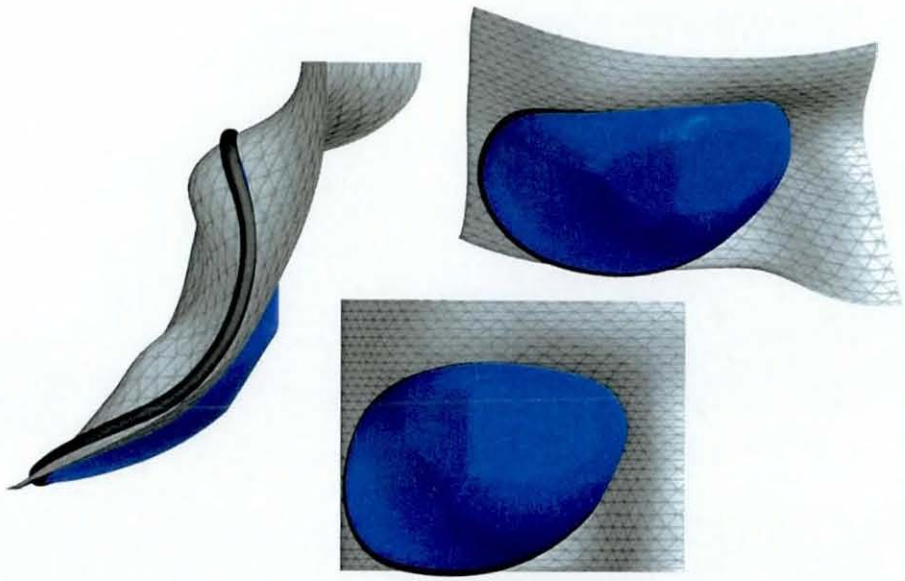

Figure 7.22, Lens made from 2 flat edges

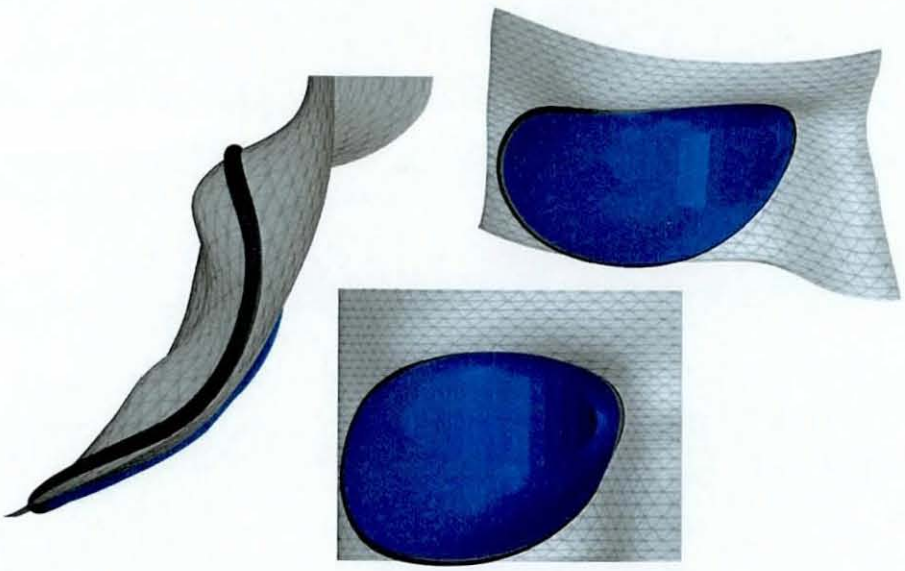

Figure 7.23, Lens made from 12 flat edges

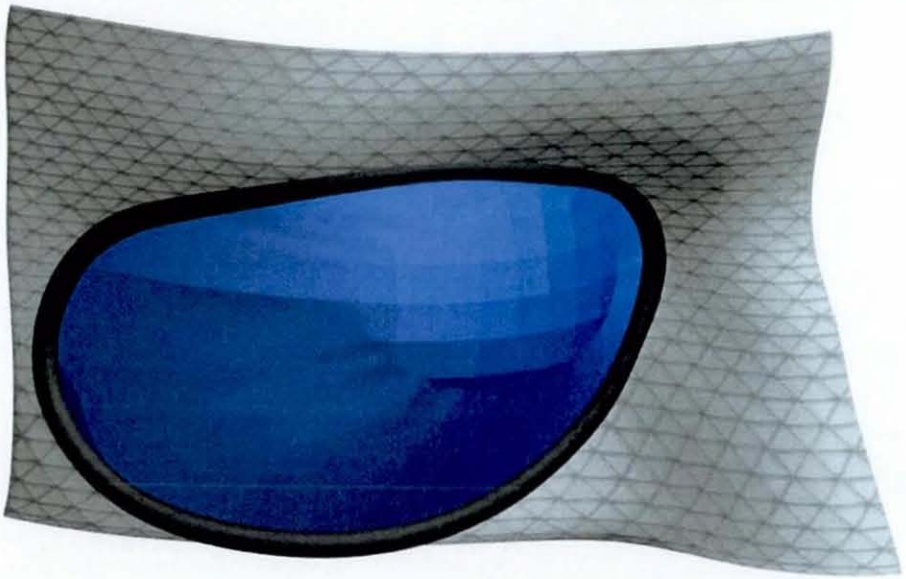

Figure 7.24, Lens made from 41 flat edges

Although significantly reducing the profile of the goggle, separating the flat area of the lens into sections causes visual side effects. Ensuring the centre of each flat panel is the same distance away from the eyeball, results in the magnification not being altered panel-to-panel. However, the joins of each panel will create blurred patches in the vision, which would therefore possibly render the lens impractical. Further research into these types of lens would have to be completed to assess practicality and user comfort.

A modified version of the ellipsoidal lens would therefore be most suitable for these initial concept designs.

7.7 Initial Swimming Goggle Concept 1

7.7.1 Design Process

The first concept has been designed with simplicity in mind, and has been created without use of the complex double seal. This has been done so as to gain an overall impression of the goggle (to aid future concepts) without wasting time in generating complex Unigraphics models There are also no design detailing such as the nose-bridge or strap attachments as these will be added during the detail design stage.

7.7.1.1 Stage 1, Seal generation

The exact path of the ideal seal location is mapped onto the large male facial surface and then points are positioned along this path. The distance between these points is decreased where the contours of the face are steeper (around the inner corner of the eye).

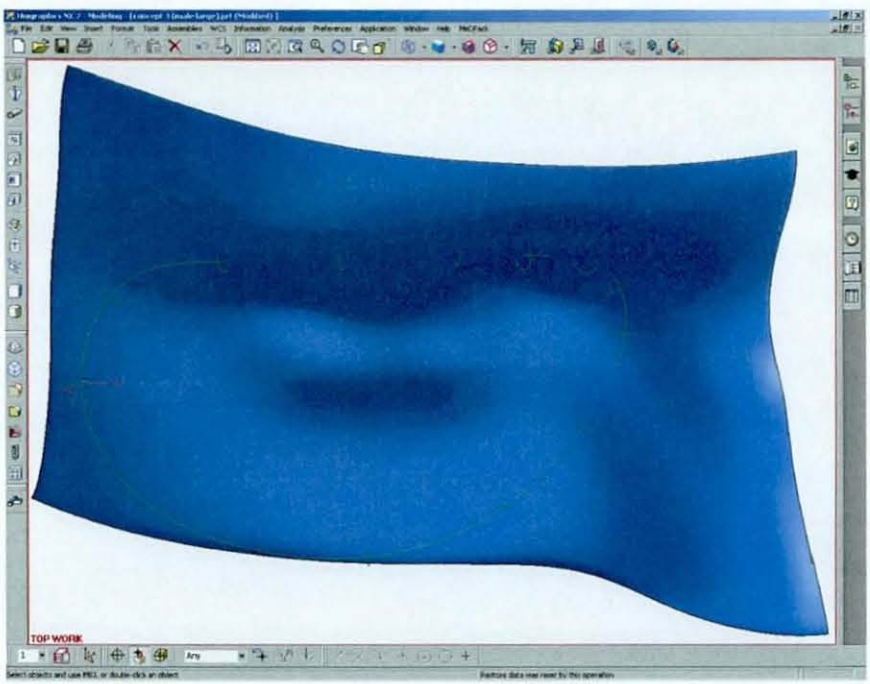

Figure 7.25, Stage one of design process

Circular curves are then created at each point and oriented so that the CSYS of the curve is standardised so that the X-axis is tangential to the face, the Y-axis is perpendicular to the face and the Z-axis is tangential to the seal path (Figure 7.26).

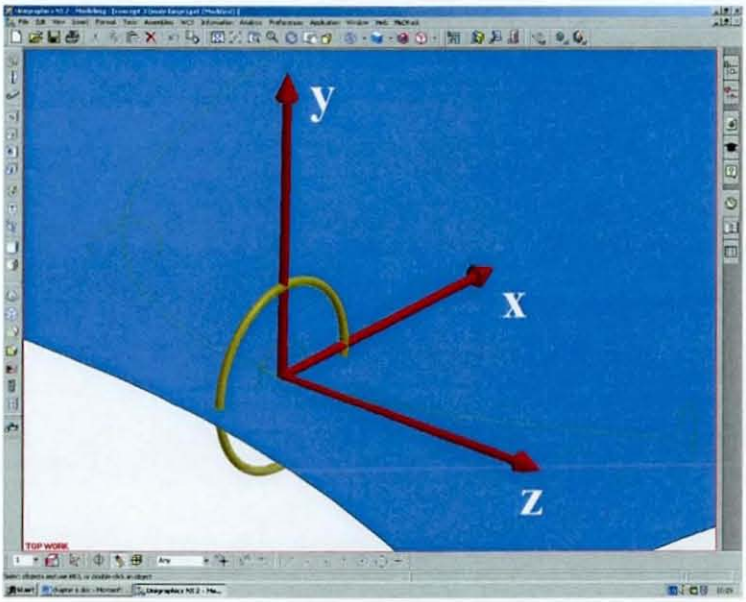

Figure 7.26, Orientation of circular curves for seal path

As this design is simply using the solid circular seal type, the orientation of the x and y axis is of little importance. However, these same circular curves are later used to generate more complex double seals, where the orientation can be used to ensure each seal makes contact with the facial surface in the correct manner.

The curve diameters are calculated using the information in section 7.2.2.1, and the variable seal is then generated through these curves. Although this seal could be created by simply using the 'through curves' function, is important that the seal closely follows that of its intended path and therefore the freeform 'swept' function is used, with the seal path acting as a guide.

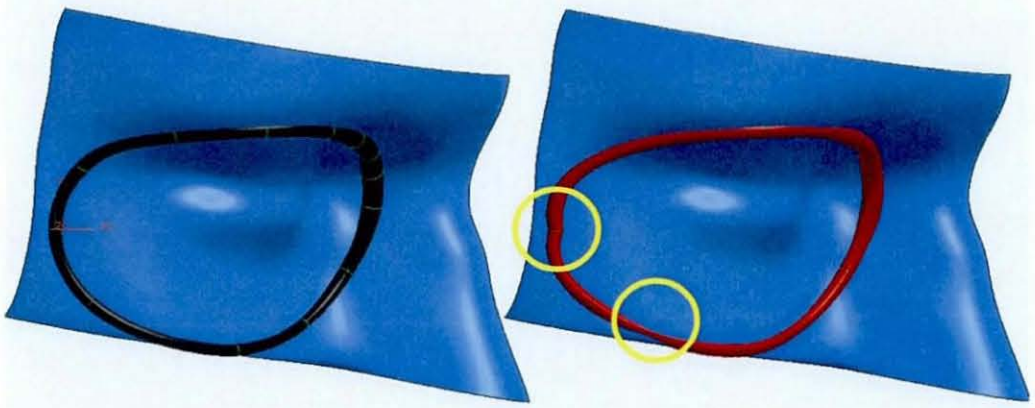

Figure 7.27, Variation between methods of seal generation, left uses 'through curves', while right uses 'swept' function.

As can clearly be seen in Figure 7.27, the example on the right using the 'through curves' function has two critical errors highlighted by the circles. The first issue is that the seal wanders away from its intended path between the selected curves, and results in the seal almost completely disappearing. The second issue is with the kink at the point where the first curve has been selected. This would happen whichever curve was selected first, and therefore only the 'swept' function can be used (represented on the left).

7.7.1.2 Stage 2, Flat lens generation and positioning

Due to the nature of the average facial surfaces, it is difficult to clearly identify where the centre of the eye is. This is required in order for positioning and sizing of the flat lens.

A virtual eyeball is positioned using the curvature of the facial surface around the eye area, taking into account that the eyelids were open during the 3D scanning phase. A sphere is then drawn positioned at the centre of the virtual eyeball, with a radius of 26.25mm (Figure 7.28). This sphere is the exclusion envelope in which the goggle can not be designed within, to prevent interference with the eyelashes.

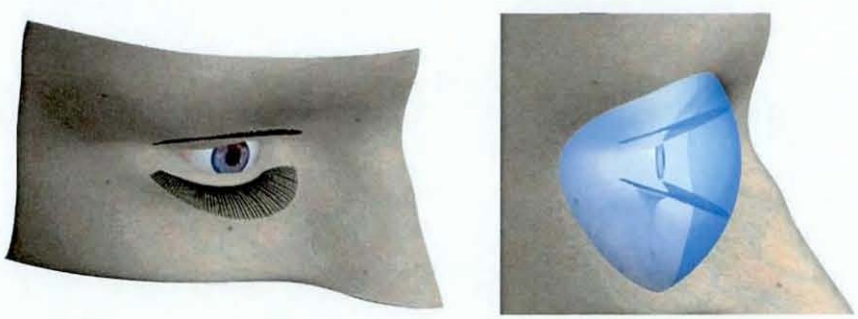

Figure 7.28, Goggle exclusion envelope

Using the exclusion envelope, a lens outline can be created with its centre directly in front of the eye. The size of the lens is only approximate as there is no specification for the required angle of periphery vision. However, the flat lens area is not the only area of the goggle which can be seen through, the remaining surface will also be

transparent (but somewhat distorted). Figure 7.29 illustrates a simple ellipsoidal lens with the resulting area of peripheral vision.

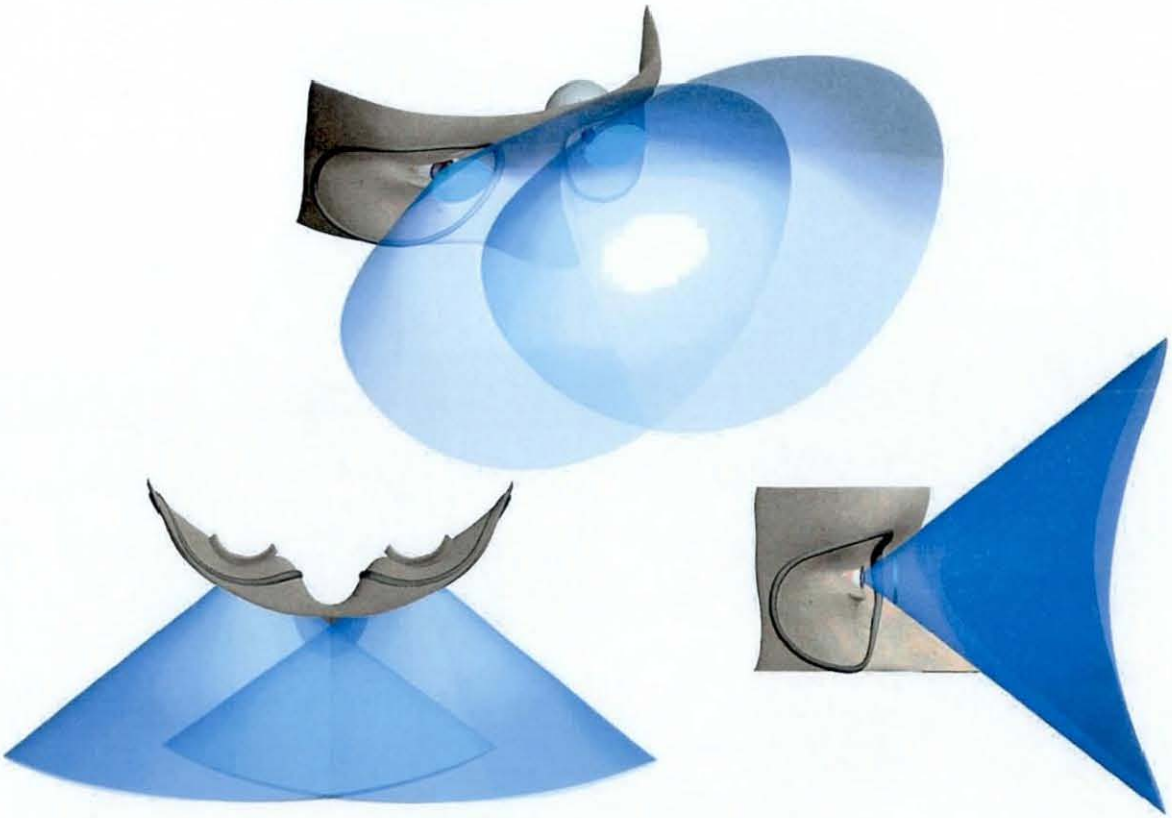

Figure 7.29, Peripheral vision through flat ellipsoidal lens

7.7.1.2 Stage 3, Remaining curved lens goggle structure generation

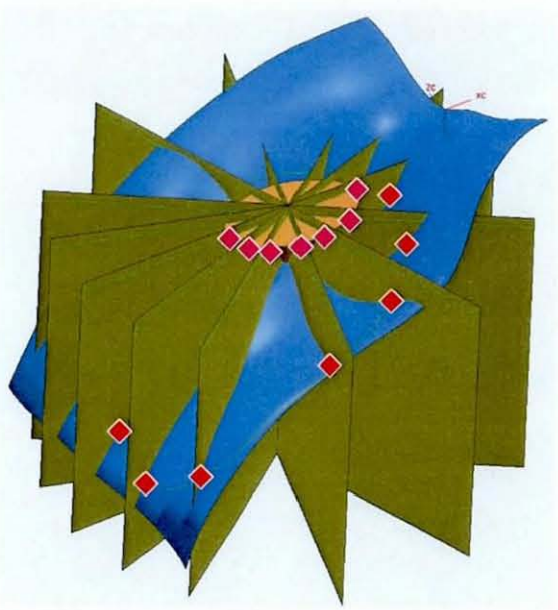

Figure 7.30, Construction data for curved lens area

Prior to the remaining area of the lens being generated, a certain amount of structural drawing needs to be completed. Figure 7.30 shows 13 sheet surfaces that have been drawn from the centre of the flat lens and intersect with both the edge of the flat lens as well as the guide spline for the seal. Once the points have then been drawn at these intersections to provide markers for the lens structural curves, the sheet surfaces are no longer required. The curves can then be drawn between the points (as shown in Figure 7.31) and a sheet surface can be generated using the 'swept' function (using both the flat lens curves and the seal spline as guides.

Figure 7.31, Partial curved lens sheet body

Sewing both the flat lens and curved lens surfaces together, allows for a platform for thickening the completed sheet into a solid structure. At this stage, the initial building foundation concept is finalized, with some minor aesthetic modelling to give a better representation of its potential (Figure 7.32).

Figure 7.32, Concept 1

7.7.2 Problems with Concept

The purpose of generating concept 1 was to create a simple building foundation to highlight potential future problems, as well as developing a straight forward system for modelling the remaining concepts in CAD.

Due to the complex surfaces that are involved in drawing swimming goggles of this type in CAD, the technique used seems to be relatively straightforward and is useful for developing a number of variations along a similar theme. The only issue that arose when using the technique, was in determining the number of structural curves to use. The more curves used, means that greater control of the final surface can be achieved, but this can also possibly cause creases in the surface as well as taking considerably more time.

Relating to potential problems in the design itself, there were a few areas that would require further development.

7.7.2.1 Surface clearance

Figure 7.33, Highlighted surface interference

Using the simplistic solid circular seal type, there is a very acute angle between the curved lens portion and the facial surface in certain areas (as highlighted in Figure 7.33), resulting in unwanted interference. Using the double lens seal would most likely lift the lens away from the face, but in doing so would increase the goggle profile in that area. It is important that a compromise is found in order to find an optimum shape and fit.

7.7.2.2 Peripheral vision

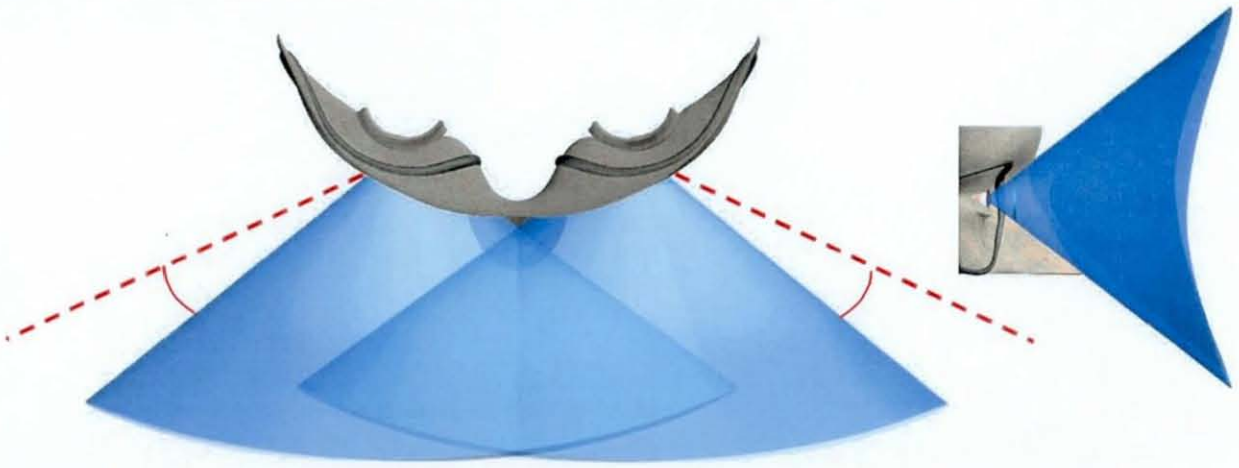

Figure 7.34, Limited peripheral vision

Using the current design parameters of concept 1, the outer peripheral vision through the flat lens portion of the goggle is somewhat limited in the horizontal axis. This is partially due to the blend (highlighted Figure 7.35), which significantly reduces the flat section for no particular reason apart from minimally reducing the corner goggle profile. Removing the corner blend would help, but an elongated ellipsoidal lens would also be necessary to achieve the required amount of peripheral vision.

Figure 7.35, Blended corner radius of flat lens section

7.7.2.4 Aesthetics

Although aesthetics is not a key issue at this stage of the design process, the overall size of the goggle is something that would be difficult to reduce in appearance if it is not dealt with in the early stages. Figure 7.36 illustrates how concept 1 gives the appearance of being quite bulky and almost sagging under the eyes. Unfortunately, due to how low the goggle seals are positioned under the eyes, this will always be an

issue. However, with minor reshaping and clever use of material choice and colour, this problem could be significantly reduced.

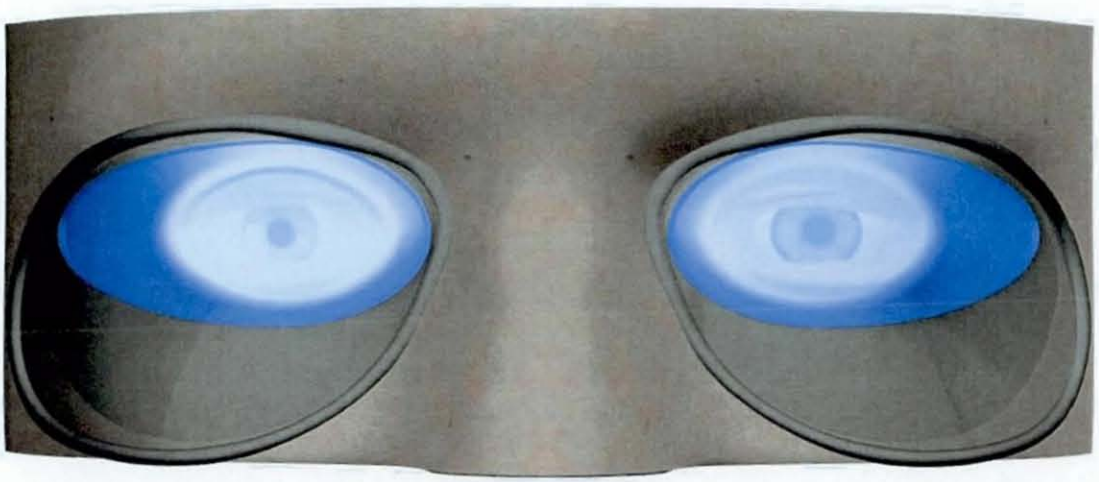

Figure 7.36, Front view of Concept 1

7.8 Initial Swimming Goggle Concept 2

7.8.1 Design Process

The 2nd concept was also designed at a very basic level, except with the application of a double seal and an extended flat lens surface. The method of attaching the seal to the lens structure has also been envisaged.

7.8.1.1 Stage 1, Seal generation

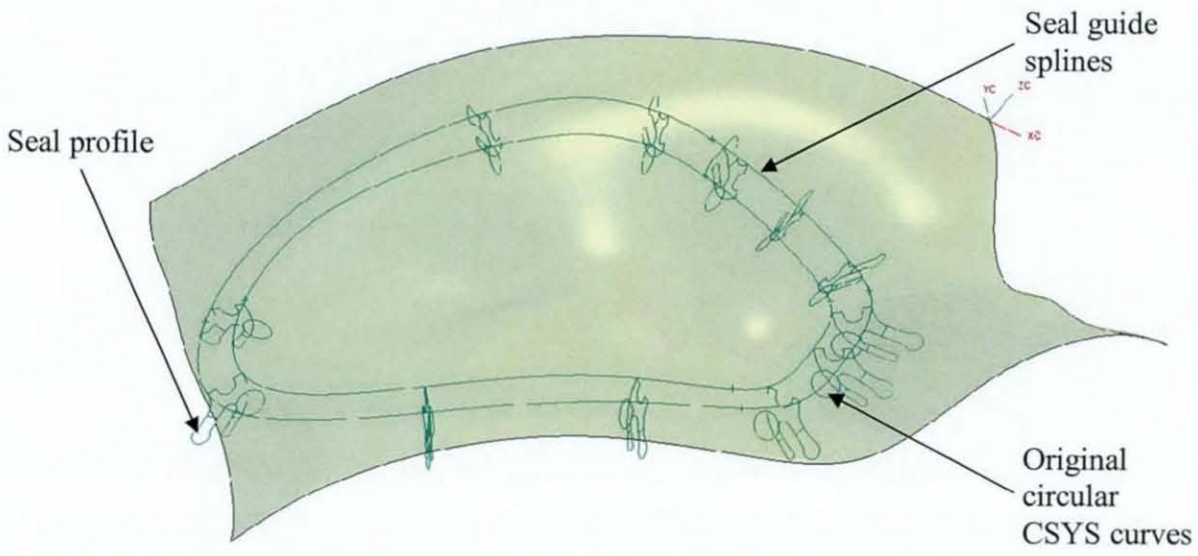

Figure 7.37, Structural lines for seal model

Using a very slightly modified seal path from that of concept 1, a profile of the seal was copied onto each of the CSYS of the circular curves used previously (Figure 7.37). The profile its self was similar to that of Figure 7.14, except lacking the precise detailing. The detailing was not required at this stage, and so would have been a waste of time. The lengths of the seal prongs at each profile spline were then adjusted so as to fit with the variable seal data.

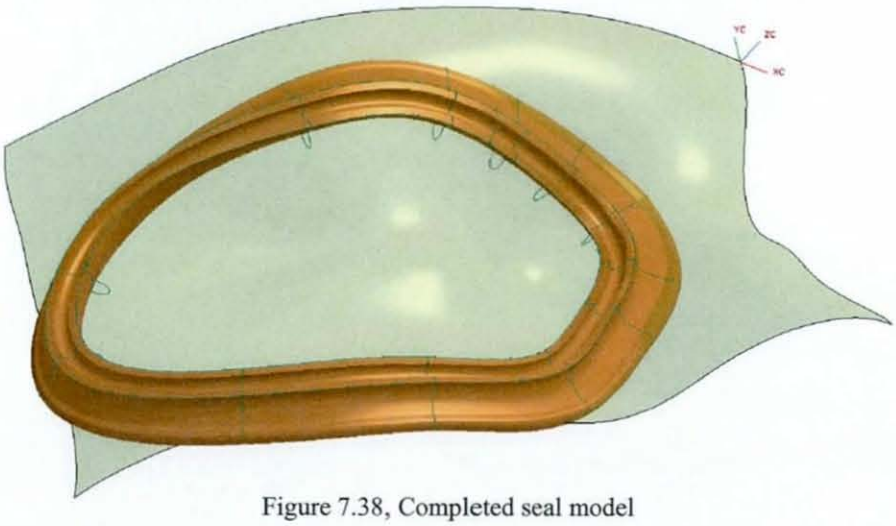

Figure 7.38, Completed seal model

Two extra guide splines were then created to prevent unwanted twisting of the seal between the drawn seal profiles. The seal model was then created using the 'swept' feature in freeform (Figure 7.38).

7.8.1.2 Stage 2, Flat lens generation and positioning

Using the same positioning method to that of concept 1, an ellipsoidal lens was generated with the modified, stretched outer side (Figure 7.39).

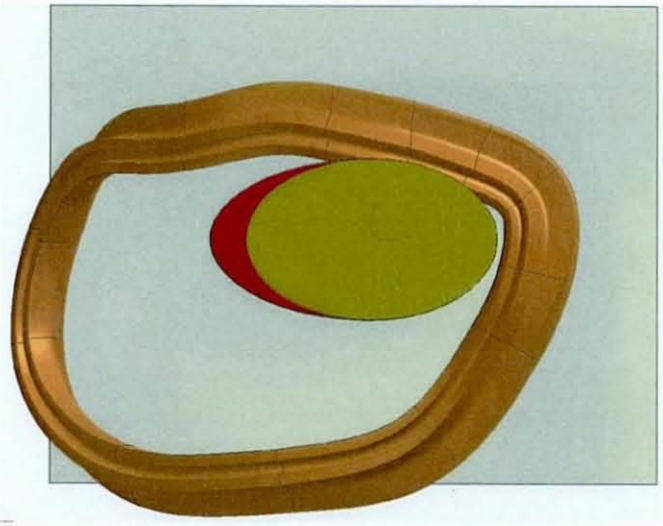

Figure 7.39, Extended ellipsoidal flat lens surface

7.8.1.3 Stage 3, Remaining curved lens goggle structure generation

Using the same techniques as those for designing Concept 1, the curve profiles for the remaining lens structure were generated. Using these curves, a sheet body could be created from which the solid model could be made (Figure 7.40).

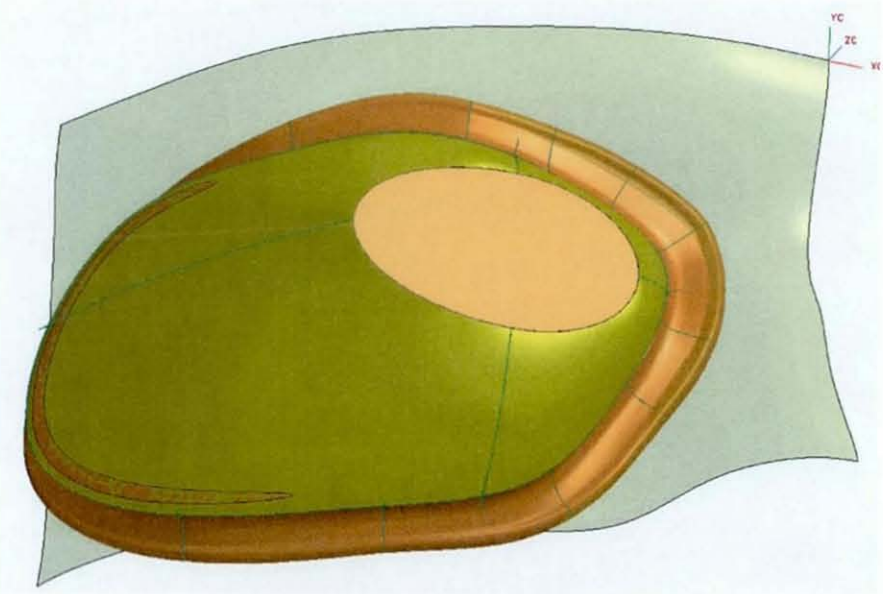

Figure 7.40, Curved lens solid model

To enable a better representation of what the concept 2 goggle would look like, the curved lens area has been separated as shown in Figure 7.41.

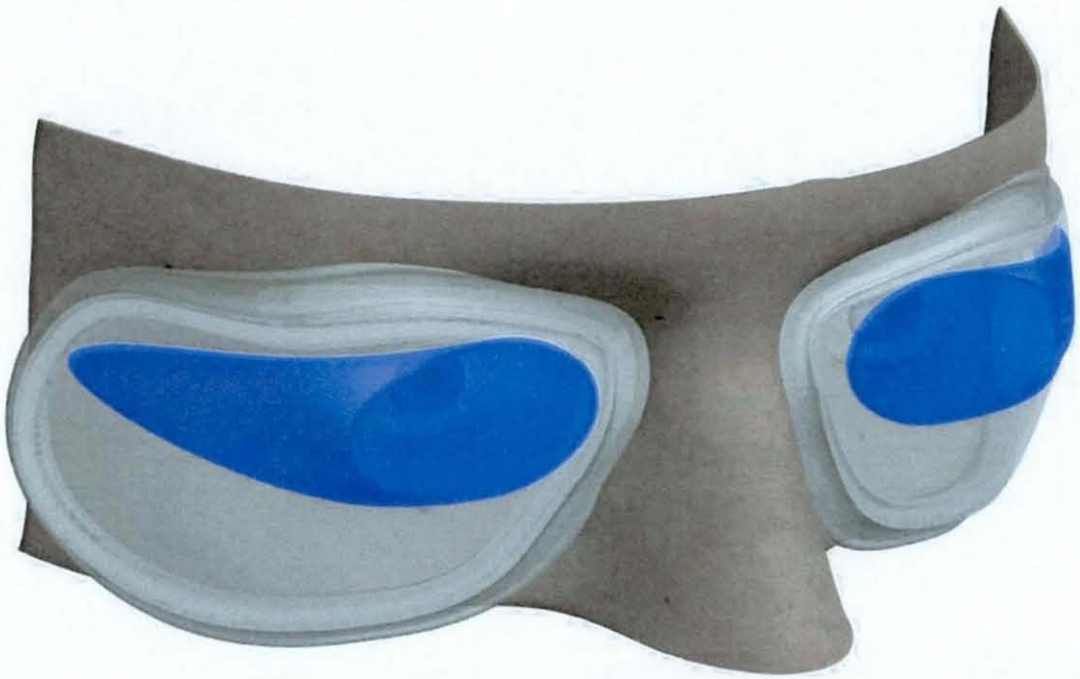

Figure 7.41, Concept 2

7.8.2 Problems with Concept 2

Without prototyping Concept 2, it would be impossible to conduct a complete analysis of its comfort and fit. However, assuming the data used to design the goggle was correct, then the only area remaining factor is to assess the goggles profile and aesthetics.

The aesthetics of the goggle is mostly affected by the sagging effect caused by having the lower seal positioned so far down on the face. Currently, the goggles look more like a bulky diving mask than an expensive pair of high-tech goggles. It would therefore be sensible to try and achieve a compromise of raising the seal slightly without dramatically effecting comfort. This would also help with the overall profile of the goggle to a certain extent.

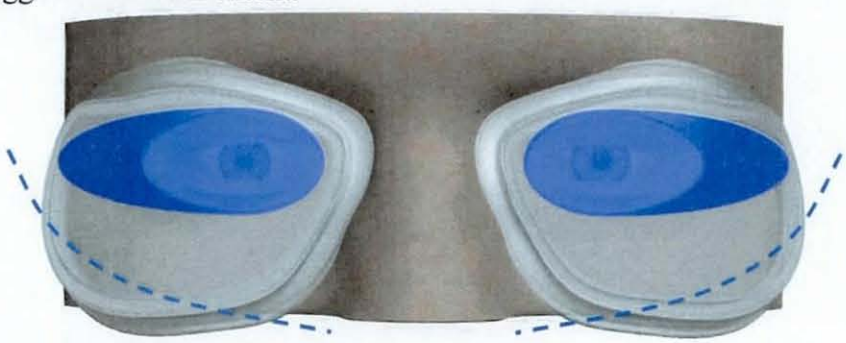

Figure 7.42, Visually too much goggle below the blue dotted line

Another area of possible concern is the wavy path that the seal profile follows. However, reducing this wavy effect to a path similar to that represented by the dotted line in Figure 7.43, might compromise the comfort and fit of the goggle. Keeping the effect might almost add to the organic image of the goggle, and therefore it should remain at this stage.

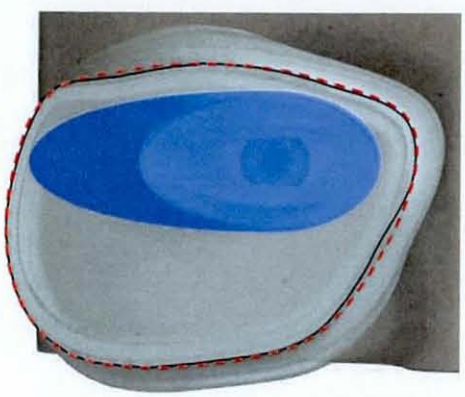

Figure 7.43, Reducing the wavy effect of the seal caused by the ideal path.

7.9 Design Development

7.9.1 Improving goggle proportions

The most significant of the previously mentioned problems for design concept 2 was its flawed proportions resulting from following an 'ideal' seal path. Analysing these proportions from either a hydrodynamic or an aesthetic point of view results in the same decision of a necessary change, even though the comfort and fit might be affected.

Removing the unwanted area of goggle as suggested in Figure 7.42, results in a goggle with far better proportions and can be seen in Figure 7.44.

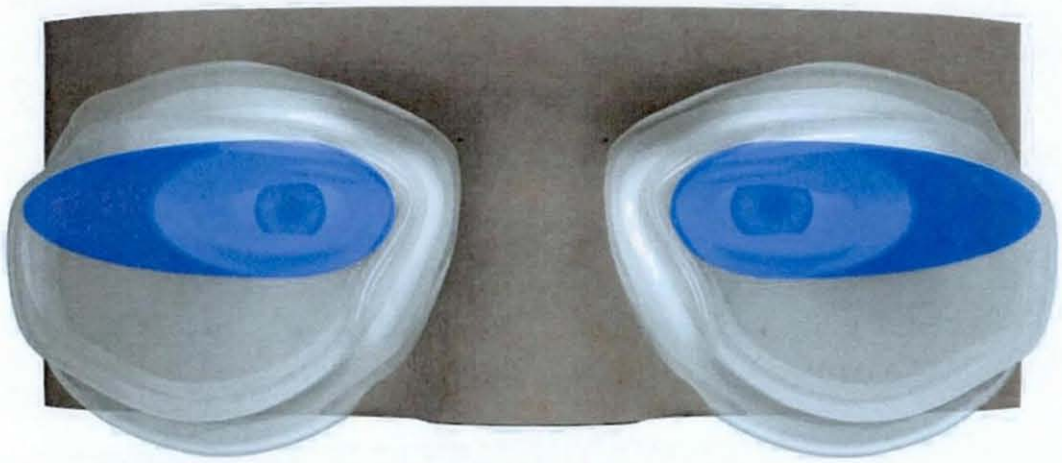

Figure 7.44, Improving goggle proportions

Even at the early stage of development, this simple change has transformed the feature-less bulky mask into something that is far closer to that of a pair of high-tech swimming goggles.

7.9.2 'Thinning' the goggles and improving their profile

Although the proportions of the concept goggles are now dramatically improved, the goggle is still more weighty (and therefore larger in profile) in certain areas than is actually necessary. The area where this is most apparent, is highlighted in Figure 7.45, where the goggles wrap around the side of the head. As there is no over-hang of the eyebrow in this area, the goggles profile has to be reduced significantly.

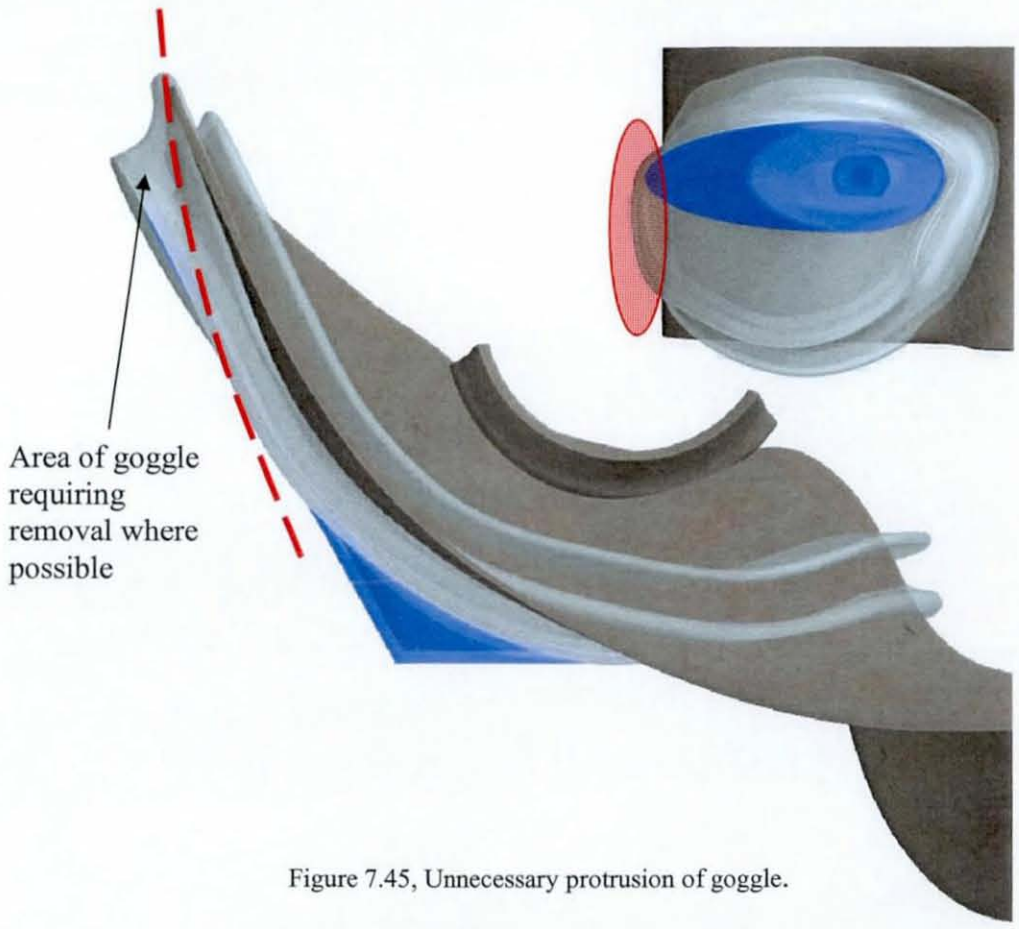

Figure 7.45, Unnecessary protrusion of goggle.

An area which needs slightly less modification, but still just as important is the lip created where the seal meets the curved lens (Figure 7.46). Upon diving into the water, a lip of this size would most likely prevent the goggles from staying sealed to the face as the localised drag would be relatively high. Blending the corner of the lip would probably be sufficient, although a smooth curvature throughout the entire profile would be preferable. This is not just important at the top of the goggle, but also at the bottom.

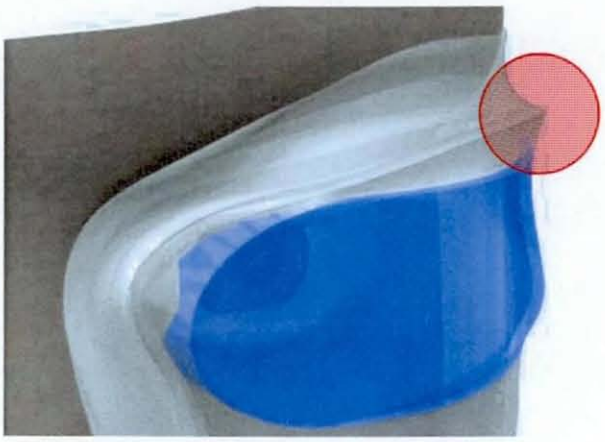

Figure 7.46, Smoothing goggle profile

7.10 Final Conceptual Design

Although the previously mentioned problems may seem slight, with little work being required to resolve them, a complete 're-think' on the seal generation had to be done. The principal issue was with creating a smoother profile without affecting the structural behaviour of the seal in any significant way. The nature of the facial surface results in the seal profile orientation being completely different for each one in relation to the flat lens section.

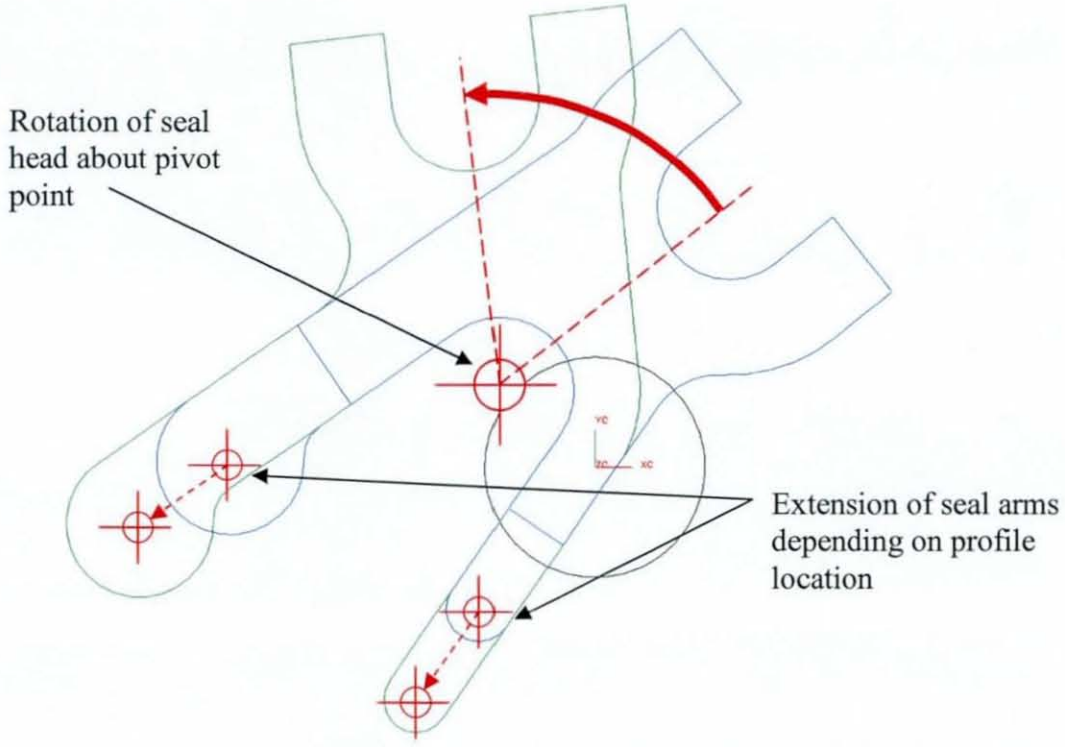

Figure 7.47, Seal profile manipulation

Figure 7.47 demonstrates how this issue can be solved via the use of a pivot point. The original profile can be positioned correctly in relation to the facial surface and the seal arms can be extended as required. The upper half of the profile can then be pivoted about the point shown so as to create the optimum goggle shape. The curves that attach the top half of the profile to the bottom half can then be extended/trimmed/blended as necessary.

This solution not only solves the problems highlighted in Figure 7.46, but also somewhat does the same for the problem highlighted in Figure 7.45.

Using this new seal profile, a final conceptual design has been generated and is represented in Figure 7.48.

Figure 7.48, Final Conceptual Design

7.10.1 Design features (a brief overview)

Although very little detailing has been shown, the goggle at this stage of development is made from 6 different components and can be seen in Figure 7.49.

Part	Description	No.
A	Seal Gasket	2
B	Curved lens section	2
C	Flat lens section	2
D	Nosebridge	1
E	Strap fixing	2
F	Strap	1

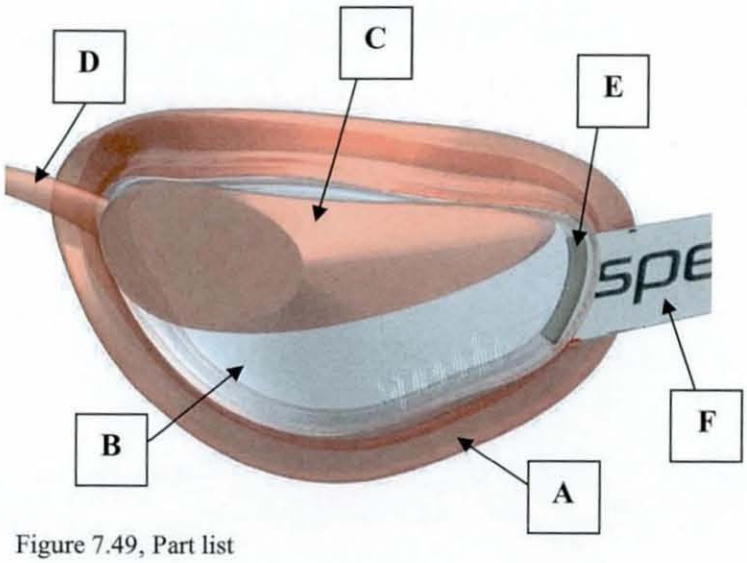

Figure 7.49, Part list

7.10.1.1 Seal

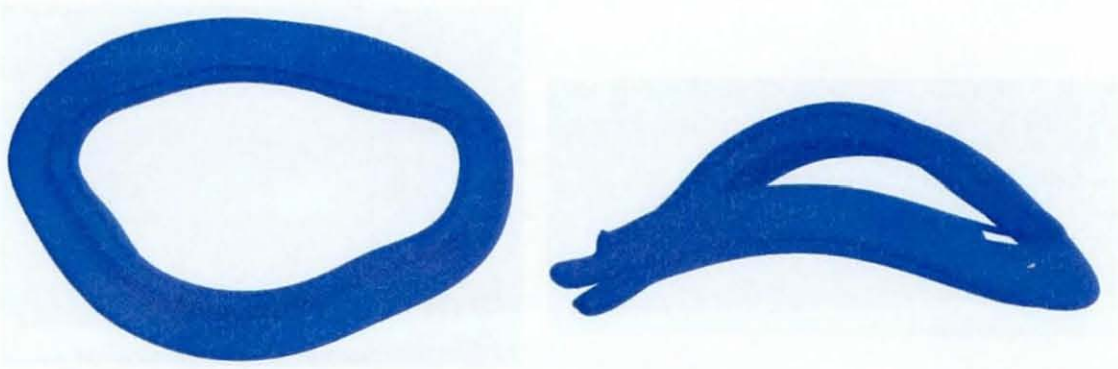

Figure 7.50, Seal Gasket

The seal, as mentioned before is using the double seal technology and in reality would have to be therefore be made from two separate components. This is due to the over-lapping areas of the design where it would be practically impossible to get tooling in (if injection moulding was the process to be used).

Assembling the two halves of the seal together would most likely be done via a push-fit or simply using an adhesive. Although this added component would add cost in the areas of tooling, material and assembly, the final goggle would be aimed at the 'high-end' market and would therefore be a negligible percentage overall cost increase.

7.10.1.2 Curved & Flat lens sections

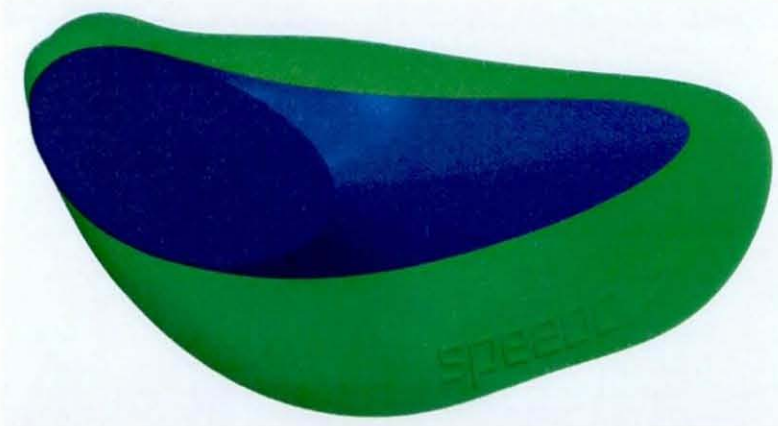

Figure 7.51, Two-piece Lens

The flat lens sections would be manufactured first, with the curved lens section being over-moulded onto it. This allows for two separate colours to be used (to aid with aesthetics) and prevent any leakage. The lens would then be slotted into the seal, and due to their interaction would require no adhesive for a watertight and secure fit.

7.10.1.3 Nosebridge

As no testing and little design research has been completed regarding optimum nose-bridges for swimming goggles, there is very little that can be stated about this area. The nose bridge would most likely be adjustable as they give the most flexibility to optimise comfort and fit.

7.10.1.4 Strap

Figure 7.52, Strap fixing

The design represented in Figure 7.52 would be a very suitable way of reducing the drag on a strap fixing, as it would all be housed within the goggle itself. The component should most likely be made from a rubber that has a 'tacky' texture. This texture would aid with sealing when snapped into position in the curved lens section of the goggle.

7.10.1.5 Strap

As with the nosebridge, no research has been conducted regarding which type would be the most suitable. However, as there are only really two distinct versions that are used in current goggles in todays market, it would be a very simple test at the prototyping stage to find the best for these particular goggles.

7.11 Discussion

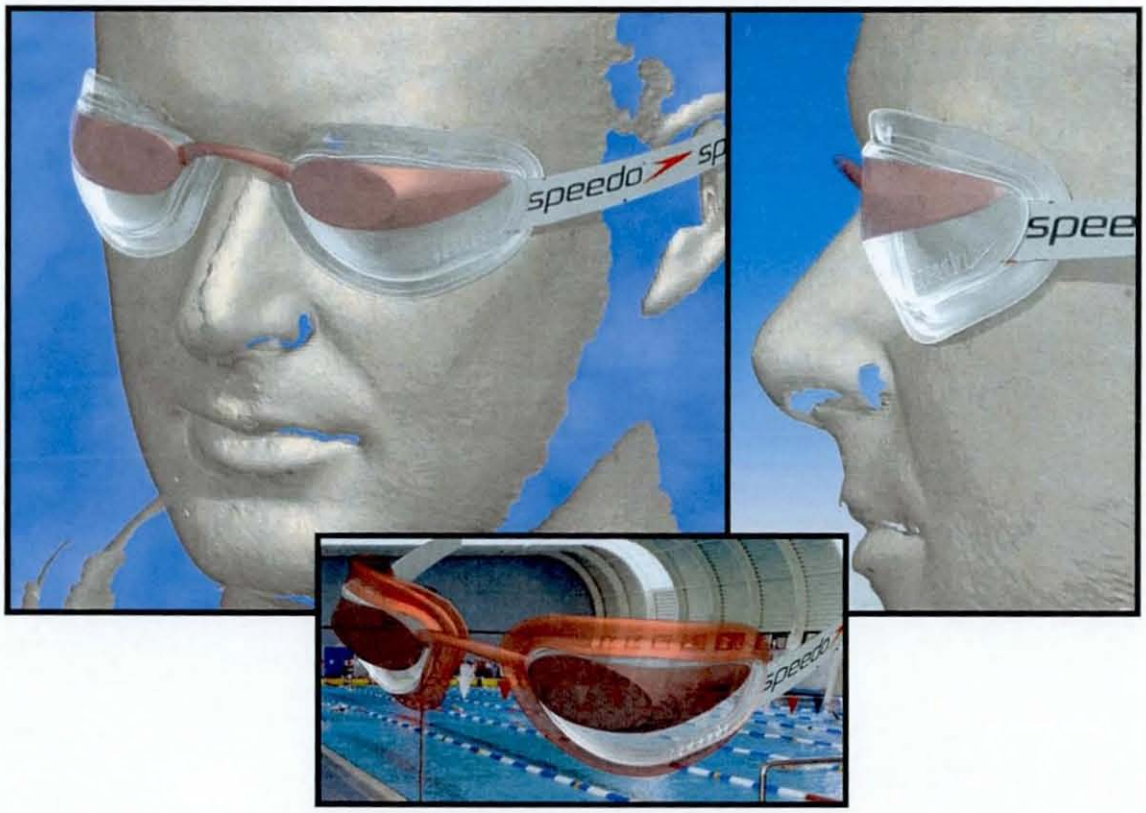

Figure 7.53, Conceptual design renderings

The purpose of this chapter was to demonstrate how the data found in the previous studies could be used to generate a data driven conceptual design with the potential for improved comfort and fit. The conceptual design itself is not particularly relevant, as it is by no means a finalised product ready for manufacture, neither has it been designed to a specific Speedo brief or specification. However, it is not to say that the swimming goggle illustrated in Figure 7.53 does not show signs of promise. Most importantly, it looks like a sporty, sleek racing goggle even though the goggle footprint is substantially larger than most others on the market today.

From a perspective of a product designer, the information within the previous chapters might prove quite daunting when given the task of using the data to design a better pair of goggles. However, when broken down into the aforementioned sections, the task becomes comparatively simple, and using this chapter as a 'designers guide', a better goggle is inevitable.

A substantial benefit of having data of this much detail, means that designers can pick and chose which areas they would like to use. It might be either impractical or difficult from a marketing point of view to include all of the features described, but at the very least, the anthropometrical work in generating facial surfaces is essential if swimming goggles are to progress forward.

8.0 CONCLUSIONS & FURTHER WORK

The conclusions for this thesis have been separated into a general overview, as well as evaluations relating directly to each chapter (and therefore each objective). These are then followed by recommended future work that could be completed to help further progress in each area of research.

8.1 Overview of Aims

This thesis can be split into two major aims, with one being concerned entirely with comfort and fit, and the other concerned with vision.

The primary aim of this thesis was to provide a comprehensive evaluation of the human face to be used to help improve the design of swimming goggles with regards to comfort and fit. The techniques and protocols which have been used to generate a substantial amount of data relating to the face, have not only been shown to help improve many aspects of swimming goggles through data driven design, but may also be useful within the medical industry, more specifically reconstructive surgery.

The secondary aim of this thesis was to identify whether a curved lens could be plausible for use in a performance racing goggle. Although no definitive answer to whether a curved lens could be used in a competitive goggle, significant progress has been made in this area of research, with the development of numerous techniques for lens evaluation. This will allow future work in this area to be comparatively assessed in relation to the prototype that has already be produced, and therefore help advance research at a much faster rate.

8.2 Overview of Objectives

There were 5 main objectives that were stated in the introductory chapter;

Objective 1) To generate data that could be used to identify the most comfortable path for the seal gasket.

• A technique (that was based on the Y-Grid Skin Sensitivity Measurement Technique) capable of accurately measuring skin sensitivity within the facial region, was developed in order to generate the required data. The data was used to identify that the seal gasket should be positioned lower down the face in order to improve perceived comfort to the user.

Objective 2) To generate data that could be used to help determine the compression values of the seal gasket throughout its circumference to also help improve comfort.

• A technique (using CMM) capable of accurately measuring facial tissue compression was developed in order to generate the required data. If used in the correct manner, the data can now be used to help determine the compression values of the seal gasket throughout its circumference. This will help improve perceived comfort to the user by achieving non-variable pressure throughout all points of contact between the seal and the facial tissue.

Objective 3) To generate an average facial surface, representative of a target population that could be used as a mould for designing a swimming goggle with improved fit.

• A technique capable of averaging facial surfaces to represent the specific target population (and any other measured target populations) was developed to provide moulds for designing swimming goggles with improved fit. Speedo International requested that the categories for the facial surfaces was to be split into small, medium and large for both the male and female populations, and so these were expressed in both three dimensional point data as well as 3D Surfaces that can be used in selection of CAD software (primarily Unigraphics).

Objective 4) To prototype an 'ideal' curved lens and evaluate its optical performance against a range of goggle lenses available on the commercial market today.

• Numerous techniques were developed to accurately evaluate the new prototype curved lens design, so as to assess the potential of using curved lenses in elite performance swimming goggles. Although the optical performance of the prototype was superior to all its competitors in the majority of aspects, there were problems with its size as well as it dual role of being used in both water and air. Therefore, although

a curved lens for use in an elite goggle is plausible, further work needs to be conducted for a complete evaluation.

Objective 5) To demonstrate how data generated from completion of the previous objectives can be used to help improve swimming goggle design.

• A technique for incorporating the aforementioned generated data in a data led designed pair of conceptual goggles was developed. This will help designers with the task of understanding how a large amount of data can be used to achieve a 'better goggle'. Features of the conceptual goggle were only achieved through this developed design process that was used.

8.3 Evaluation of the Secondary Objectives

Each primary objective was researched in its own chapter and broken down into a number of important secondary objectives, and these chapters are all evaluated over the following sections.

8.31 Measurement of Facial Skin Sensitivity – An aid to assess seal location

The secondary objectives of the chapter 3 were;

• To evaluate all current skin sensitivity measurement techniques.

• To either develop an existing measurement technique, or generate an entirely new method of measuring skin sensitivity with the required measurement resolution.

•To measure the facial skin sensitivity of a given number of participants and then calculate the averages for each measurement location.

In answer to whether the objectives of the chapter were completed, all current skin sensitivity measurement techniques were appraised on their relevance to wearing swimming goggles, and their measurement resolution (as well as less critical factors, such as ease of use etc.). However, there was insufficient time to be able to actually conduct a study where each would be directly compared in a laboratory environment.

This was not really a significant issue though, as there was only one technique that was viable for development.

The existing Y-Grid Measurement Technique was selected for its ease of development and was evolved to the stage where its repeatability and resolution was satisfactory for its intended purpose. The use of a co-ordinate measurement machine to guide the probe raised many issues with health and safety, but the numerous simple modifications to the machine and experiment set-up, means the technique could easily be copied by a third party.

The facial skin sensitivity of a relatively large sample target population was measured, and the averages of each point location was measured for both male and female. The resulting data will significantly aid designers in their decision on where the goggle seal path should be positioned. More measurements are however still required to generate 'average surfaces' for other target populations.

8.32 Seal Flexibility

The initial objectives of the chapter 4 were;

- To research all seal technologies, and assess whether there are any that might already partially prevent variable pressures throughout its contact with the skin.
- To evaluate possible methods of measuring compression of facial tissue under constant load.
- To develop a repeatable and accurate method of measuring facial tissue compression under constant load, and to then conduct a trial with a target population to calculate the average compressions for each point location.

In relation to the objectives that were set at the start of the chapter, there were no current seal gasket technologies that successfully generated an equal distribution of pressure. The Speedo Speedlite Racing goggle was the only goggle that attempted to do so, but the lack of scientific data caused severe design problems and therefore the product was withdrawn.

Although the device used for measuring the tissue compression was not designed for human application, the modifications and experiment set-up ensured a successful study. As the validity of experiment suggests (in the discussion section), the accuracy of measurement was more than sufficient for the intended purpose of the final data. However, the greater issue is whether or not the data would be useful for designing goggle seal variable flexibility. The level of benefits gained in having the generated data entirely depends on where the seal foot print would actually be positioned.

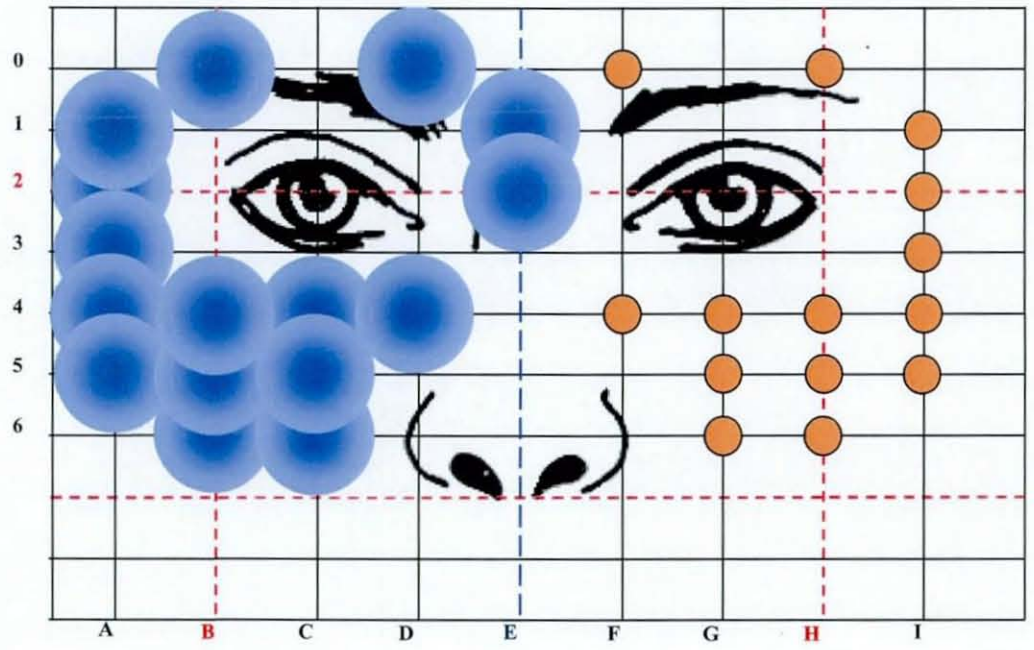

Figure 8.1, Usefulness of data regarding seal flexibility (darker blue=more useful)

Figure 8.1, gives an indication of how useful the data would be depending where the seal footprint would be positioned. The darker areas show the greater the use of the measured point, and either occur directly over the point or where two points are close together and the fields overlap.

As made apparent from the diagram, the regions very close to the eye, especially above the eye and on the inner corner, are severely lacking in data. Unfortunately, the current technique for measuring facial compression would be unsuitable for measuring in these areas. However, it is not to say that any other possible techniques would be an improvement on this, mainly due to safety implications and the irregularity in facial structure in these areas.

8.33 Swimming goggle fit using Facial Anthropometrics

The objectives of the chapter 5 were;

- To evaluate all current methods of capturing three dimensional data.
- To capture accurate three dimensional data for a target population.
- To develop a technique that can accurately average the three dimensional data into categories of large, medium and small for both the male and female population.

The evaluation of all the current methods of capturing three dimensional data was relatively limited, as in most cases there was not the time or money available to actually try each technique. However, the technique that was eventually used (the Moire Fringe Contouring Technique), was more than adequate, as the resolution was high enough, and the time to scan was relatively low. The only issue was with the scanning of the actual eye area itself, but this is a problem common to all techniques in this category.

Although the population size that was scanned was quite large, and appeared to give a reasonable representation for the average faces, it would still be better to scan even more participants. The variation between participants faces can be quite extreme, and so it is obvious that the more scans there are, the more representative the final average surfaces will be.

The technique that was used to average the scanned images gave sufficient user control to maintain accuracy for the majority of the face. However, due to inherent flaws within the process (lack of reference points due to incomplete images where the eyes were), the area of the inner corners of the eyes (on the average surfaces) were inadequate. This results in some prior knowledge of swimming goggle design to be known, and past successful goggle examples should be used to replace the seal profile where there is corrupt data.

The final data has been displayed in the form of small, medium and large for both the male and female population. However, the ability to be able to manipulate the data

with relative ease into any size category (such as small and large), makes the process incredibly versatile.

The overall aim of this section was to provide data that could be used by a designer to produce a better fitting pair of goggles, and the final data (if in capable hands) will definitely go some way to achieving this.

8.34 Curved Lens Design and Evaluation

The objectives of the chapter 6 were;

- To provide the specifications for a curved lens in order for it to be designed by a third party.
- To manufacture a goggle housing (that incorporates the prototype lens) that can be used by participants in a swimming pool environment.
- To design techniques that can be used to assess the performance of the curved lens (and any other lens) in the areas of visual acuity, stereoscopic vision, magnification and visual distortion.
- To implement the developed measuring techniques, and directly compare the prototype lens with other goggle lenses on the commercial market today.
- To state whether or not there is potential for the use of a curved lens in an elite racing swimming goggle.

Although the specification for the prototype lens was quite open ended, with many decisions left to the lens designer, this did not affect the purpose of the chapter. All that was required, was a curved lens that could be used in a swimming goggle housing, and the actual radius of curvature and lens thickness was not of key importance. The simplicity of the lens (in that it was only designed to be usable underwater), was probably more useful than starting with a complicated bi-focal lens. It meant that the participants could not look through the wrong section of the lens for any of the trials, and therefore lends itself to a solid appraisal of its optical performance.

The prototype lens housing provided the most problems throughout the trials, but due to the fact that it worked (and only increased testing time), meant that it was impractical to redesign and manufacture a superior version. The reason for its incorrect seal profile was that the facial anthropometric study had not been completed when it was designed, and so had to be simply designed around the features of a single participant. If more studies were to be completed, it would obviously make sense that the average facial surfaces (completed in the anthropometric chapter) should be used to design the lens housings.

Many of the lens trials were based on techniques used by opticians throughout the world, and so their value had already been established. The success in which they had been evolved to be used in water, is quite apparent through the results that were produced. The range of techniques was broad enough to cover every important aspect, although more work could be useful in the area of misalignment. Due to the nature of peoples faces, the goggle lens is always going to be positioned at slightly different angles in relation to the eye. If a test could be developed that could identify the limits at which the angle was too great for satisfactory lens performance, it would give tolerances for the lens housing designers.

As stated previously, the optical performance of the prototype lens underwater, was either comparable to that of the standard flat lens or a marked improvement. It can therefore be recommended that the new lens technology could be taken to the next stage of development. However, a professional lens designer would have to first do further research, to decide whether the same optical properties could be achieved in a much thinner 'lens package', and with an 'ideal' outer radius of curvature.

8.35 Data Driven Goggle Design

The objectives of the chapter 7 were;

- To create a step-by-step guide on how to generate a data led designed pair of swimming goggles.
- To adhere to a simple specification and generate an example data led conceptual design of a pair of swimming goggles.

• To generate novel design features that have been generated as a result of data led design.

The methodical guide that has been created uses all of the information previously learned in the comfort and fit research. The relatively simple step-by-step process would be easily followed by a competent design engineer, but the fact that the process is accurately followed is not a guarantee of an improved goggle design. It has always been stated that areas of knowledge outside the remit of this PhD is also required to complete the overall package. The design process itself is completely data driven, and at no point is there mention of the swimmers thoughts and preferences, and without this aspect, an 'ideal' goggle is less likely to be produced.

The aesthetics of the example conceptual design is comparable to that of a current manufactured swimming goggle, yet it has a substantially larger footprint and includes a double seal gasket. The idea of the double seal gasket may well have been missed through a conventional design process, yet it is something that could add true value to the progress of goggle technologies.

8.4 Conclusion Summary

In terms of improving comfort and fit of swimming goggles, this thesis has developed a number of key studies that can be used to generate data for 'better' design. However, the particular participants being measured, were only selected from a small target population, and so although the presented data can certainly aid goggle designers, further data still needs to be generated (using the developed techniques).

If Speedo (or any other company) wanted to produce more data for either of the comfort and fit related issues (for a larger or different sample target population), a major limitation of the studies would soon be highlighted. Unfortunately, the amount of time any of the studies (especially gathering anthropometric surface data) take to complete, is quite significant, and therefore it would require a fairly substantial financial commitment from the company. Due to the current methodology of goggle

design being comparatively simple, this major leap might not be practical or financially viable for such a company.

With respect to each of the different aspects of the thesis and whether each aim and objective was achieved, there were minor problems or inherent flaws in some of the techniques, although an overall success was realised with significant added value to the research areas.

8.4 Further Work

8.41 Achieving Improved Comfort

The next stage for the comfort investigations would most definitely be to automate as many of the processes as possible. This would drastically reduce the overall time of the studies if hundreds of participants required measurement. However, if less participants required measurement, the best use of time might be to simply use the techniques as they are.

The number of points being measured could be increased in both the Skin Sensitivity Measurement study as well as the Tissue Compression Measurement study. Although a higher resolution may not necessarily effect where either the seal should be positioned or the extent to its variable compression, the extra data might help eliminate particular uncertainties.

The largest task that needs to be undertaken, is to measure more participants in both the target population that has already been measured as well as any other population that the goggles would be intended for. However, even with the required further studies being completed, the data will only ever be a tool, and can not be the substitute of an innovative and experienced designer.

There are also other areas of research where the data could be of significance, once the recommended work had been completed. The most important being in the medical industry and more specifically reconstructive surgery. The knowledge of how human

tissue behaves under pressure, could be used when repairing large areas of damaged tissue after burns or other injuries.

In a slightly less critical area of research, the techniques could be used on other regions of the human body, so that products such as shin pads and other body armour can be designed to be more comfortable to the user.

8.42 Achieving Better Fit

The key problem with the facial morphing was the missing data in the original scanned images. If the scanning technique could be improved to ensure all the three dimensional information was recorded, especially in the areas of the central point of the eyes, the inner corners of the eyes and the eyebrow region, then significant advancements could be made. With the improved scanned images, it might also be possible to generate more reference points and again improve the final average surfaces even more.

Within the Data Driven Goggle Design chapter, a concept was generated using the 'Large Average Male' surface as a design mould. Further work needs to be conducted, so as to truly assess the percentage of large males the concept would actually fit, and how well they would fit. This could be linked with researching into how many different sizes of goggle would be required to satisfactorily fit a specified percentage of a given target population.

The largest task that needs to be undertaken, is to again scan even more participants in both the target population that has already been measured, as well as any other population that the goggles would be intended for. Automation is again the key for advancement in this area. If computer software could be written to replace the laborious task of facial orientation, reference point selection, grid separation and the averaging of the three dimensional points, then large population samples could be analysed, with relatively low human input.

The solution to achieving ideal fit for all users of swimming goggles, would be to ultimately go towards full customisation. If the public were able to go to a retail outlet and have their face scanned, with a one-off rapid prototype being made while they waited, there would never be the issue with bad fit. The main problem here, is that the software required to design the goggle around the subjects face would be extremely difficult (if not impossible) and expensive to produce.

8.43 Future Lens Developments

The prototype lens was generally considered to be a success in relation to its underwater optical properties. However, this is obviously not the only area where the lens has to perform, as a large percentage of the time, swimmers view through their goggles while out of the pool. This causes a dilemma as to which path the next development stage should take. Either the lens could be designed to incorporate a bi-focal element, or the whole lens could be designed compromising both air and water visual performance. In the latter case, this would certainly give an image that is inferior to the flat lens in every aspect (except maybe magnification) and would therefore render the product practically pointless. The only foreseeable way forward is to therefore use bi-focal technology. This would mean that further studies would have to be conducted in order to evaluate which sectors of the lens are viewed through, in relation to being in or out of the water. Unfortunately, it is quite obvious that some sectors would be used for both, and so a compromise would still have to be made.

The size of the prototype is also an issue, as at present the cross-sectional profile is far larger than that of any competitive pair of swimming goggles. If the outer surface of the lens had a smaller radius of curvature, a slightly larger profile would be less of an issue, as the hydrodynamic properties could be improved greatly. According to the lens designer, this would be feasible, and should be therefore looked at further.
However, it is not to say that this type of lens is the only future for curved lens design, as other avenues such as Fresnel technology should also be evaluated. Either way, the various optical performance measurement techniques that have been developed will be extremely useful for further evaluations, and the data that has been generated will provide an appropriate benchmark.

9.0 REFERENCES

AM J (1994). Random Dot E Test.
Optometry Association, September; 65 (9) pp. 637-641

ARENDT-NIELSON L (1997). Induction and assessment of experimental pain from human skin, muscle and viscera. In: Jenson TS, Turner JA, Wiesenfeld-Hallin Z. Proceedings of the 8th World Congress on Pain, Progress in pain research management, Seattle. pp. 393-425

ASZMANN OC, DELLON AL (1998). Relationship between cutaneous pressure threshold and two-point discrimination.
Journal of reconstructive microsurgery. 14: 6: 417-421

BERARDESCA E, GABBA P, FARINELLI N, BORRONI G, RABBIOSI G, (1989). Skin extensibility time in women. Changes in relation to sex hormones.
Acta Dermatologica Venerologica. 69: 431-433.

CAROLA R, HARLEY JP, NOBACK CR (2ND Edition) (1995). Human Anatomy & Physiology. The Senses. 463-468

DEACON A, ANTHONY A, BHATIA S, MULLER J (1991). Evaluation of a CCD-based facial measurement system
Medical Informatics. 16: 2: 213-228

DELLON AL et al (1995). The relationship between skin hardness, pressure perception and two-point discrimination in the fingertip.
Journal of hand surgery (British and European Volume). 20B: 1: 44-48

DOYLE SJ (1994): Acute corneal erosion from the use of anti-misting agent in swimming goggles.
Br J Ophthalmol;78(5):419

ESCOFFIER C, DE RIGAL J, ROCHEFORT A, VASSELET R, LEVEQUE J-L, AGACHE PG, (1989). Age related mechanical properties of human skin: an in vivo study.
Journal of Investigative Dermatology. 93: 353-357

FARKAS L, HAJNIS K, POSNICK J. Anthropometric and anthroposcopic findings in the nasal and facial region in cleft patients before and after primary lip and palate repair.
Cleft Palate Craniofac. Journal. 30: 1

FOX SI (7TH Edition). Human Physiology. 242-245

FRUHSTORFER H, Gross W, SELBMANN O (2001).
European Journal of Pain (London)
5, p341

GOULD WR, VIERCK CJ, LUCK MM (1979). Cues supporting recognition of the orientation or direction of movement of tactile stimuli. In: Sensory function of the skin of humans. Proceedings of the Second International Symposium on the Skin Senses. 63-73.

HARDING K (1997). Moire methods make shape recognition easier
Vision System Design, 32

HARDING K, BIEMAN L, BOEHNLEIN A (1991). Absolute measurement using field shifted moiré.
Illumination and Image Sensing for Machine Vision, 259

HARDING K (1983). Moiré Interferometry for industrial inspection
Lasers and Applications p73

HAMMER RW (1997). Swimming and diving, in Mellion MB, Walsh WM, Shelton GL (eds): The Team Physician's Handbook
Ed 3. Philadelphia, Hanley and Belfus, pp 718-728

HATCH SW, RICHMAN JE (1994). Stereopsis testing without polarized glasses: a comparison study on five new stereoacuity tests.
New England College of Optometry, Boston, MA 02115.

INOKUCHI S, SATO K, OZAKI Y (1984). Range-imaging system for 3-D range imaging.
7th ICPR 806

JOHANSSON RS (1978). Tactile sensibility in the human hand: receptive field characteristics of mechanoreceptive units in the gabrous skin area.
Journal of Physiology. 281: 101-123

JORDAN DR (2001). Eyelid masses associated with competitive swimming goggles.
Can J Ophthalmol.
October, 36(6): pp. 339-40.

JONES PA et al (1996). The Scarlet Light Concentrating Solar Array.
25th IEEE-PVSC 1996

KAWAI T, NATSUME N, SHIBATA H, YAMAMOTO T (1990). Three dimensional analysis of facial morphology using moiré stripes: Part 1.
International Journal of Oral Maxillofacial Surgery. 35: 484

KIRMAN JH (1983). Tactile apparent motion: the effects of shape and type of motion.
Perception Psychophysics. 34: 96-102

KNIZE DM (1995). Muscles that act on glabellar skin: A closer look.
Plastic Reconstruction Surgery
105: 350, 34: 264

LINDAHL OA, OMATA S, ANGUIST KA, (1998). A tactile sensor for detection of physical properties of human skin in vivo.
Journal of Medical Engineering and Technology. 22: 4: 147-153

MARTALO O, HENRY F, PIERARD GE (2001). Liminar perception threshold of cutaneous distension.
Ann Dermatol Vener 128: 2: 119-122

MERTZ L (1983). Real time fringe pattern analysis.
Appl Opt, Vol 22, No 10, 1535

MISHIMA K, SUGAHARA T, MORI Y, SAKUDA M (1996). Application of a new method for anthropometric analysis of the nose.
Plastic Reconstructive Surgery. 21:38

MOSS J, LINNEY A, GRINDROD S, KARRON D (1989). A laser scanning system for the measurement of facial surface morphology.
Optics Lasers England. 10: 179

MURPHY D (2000). The Scarlet Solar Array: Technology validation and flight results.
Deep Space 1 Technology Validation Symposium. Pasenda, 2000.

NERRI PUCCI, MD et al.(2005). Long Eyelashes in a Case Series of 93 Children with Vernal Keratoconjunctivitis
PEDIATRICS Vol. 115 No. 1 January 2005, pp. e86-e91

NOBACK CR, STROMINGER NL, DEMAREST RJ (5TH Edition) (1996).
Structure and Function.
The human nervous system. 106-107

O'NEIL M et al (2003). The Stretched Lens Array (SLA)
IEEE Aerospace and Electronic Systems Magazine
Vol 18, No.1, January edition 2003

PESTRONK A, PESTRONK S (1983). Goggle migraine.
N Engl J Med
308(4): PP. 226-227

RENFREW S (1960). Aesthesiometers.
Lancet 1: 1011

RENFREW S (1969). Fingertip depth sensation – A routine neurological test.
Lancet. 1: 396-397

SCHLERETH T, MAGERL W, TREEDE R-D (2000). Spatial discrimination thresholds for pain and touch in human hairy skin.
Pain 92: 187-194.

SMAJE JC, McLELLAN DL (1981). Depth sense aesthesiometry: an advance in the clinical assessment of sensation in the hands.
Journal of Neurology, Neurosurgery and Psychiatry. 44: 950-956

TORTURA GT (8TH Edition) (1996). Principles of human anatomy. Pp. 593-595

WATTS D, TASSLER PL and DELLON AL (1994). The effect of double gloving on cutaneous sensibility, skin hardness and suture identification. Contemporary Surgery. 44: pp. 289-292.

WEINSTEIN S (1968). Intensive and extensive aspects of tactile sensitivity as a function of body part, sex and laterality. In: Kenshalo DR, editor. The skin senses, Springfield, IL: Charles C. Thomas. pp. 195-222.

WHEAT HE, GOODWIN AW (2000). Tactile Discrimination of Gaps by Slowly Adapting Afferents: Effects of Population Parameters and Anisotropy in the Finger pad.
Journal of Neurophysiology. 84: 3: pp.1430-1444

WHITSEL BL, ROPPOLO JR, WERNER G (1972). Cortical information processing of stimulus motion on primate skin.
Journal of Neurophysiology. 35: pp. 691-717.

WIRTA DL (1998). Eyelid Neuroma Associated With Swim Goggle Use
Arch Ophthalmol.
116: pp. 1537-1538.

WOOD EJ, BLADON PT (1985). The human skin.
Studies in biology no. 164. 6-20.

WONG, EVA P. F. B Optom; FRICKE, TIMOTHY R. MScOptom; DINARDO, CARLA BOptom (2002). Interexaminer Repeatability of a New, Modified Prentice Card Compared with Established Phoria Tests.
Optometry & Vision Science. 79(6):370-375, June 2002.

YAMADA T, SUGAHARA T, MORI Y, SAKUDA M (1998). Rapid three-dimensional measuring system for facial surface structure.
Plastic and reconstructive surgery. 102: 6: 2108-2113

APPENDIX 1

A1.1 Speedo International – The Company

Figure A1.1, An example of the modern day Speedo logo (www.speedo.co.uk – 10/09/05)

In 1914, Speedo was originally founded in Australia by a 22 year old Scottish immigrant called Alexander MacRae. The company was actually an underwear hosiery manufacturer, when it was decided to begin producing swimwear. However, the Speedo name was only started to be used in 1928 after the introduction of the 'Racerback' costume, when Captain Parsonson coined the slogan 'Speed in your Speedos'.

Although the company went through various stages of evolution, the more significant events are when Speedo (Europe) Ltd subsidiary was established in London in 1964, and then in 1991, the Speedo Group was sold to the British company, Pentland Group PLC. Although Speedo Australia was formed as a separate company, Pentland purchased a controlling interest in Speedo USA and Speedo Europe. This effectively brought the brand under one management team for the first time since 1986.

Currently, Speedo produce a wide range of swim related products (including clothing and shoes) in over 170 countries around the world. They are continually trying to push the boundaries and stay ahead of their competitors by spending more and more time and money in development and research (which is mostly completed at the Speedo Aqualab). Speedo has also announced that they have extended their 20 year partnership with USA Swimming through until 2012, which is another part of their strategy to solidify its standing as the world's leading swimwear brand in anticipation of the Beijing Olympics in 2008.

The relatively small scale collaboration with Loughborough University, is intended to provide scientific expertise in areas of novel swimming goggle technology. The results will hopefully ensure that the market leader for this product area will also remain to be Speedo. The consequences of industrial sponsorship for a PhD does however result in the company being able to set their own requirements, and these need to be negotiated and then accomplished where possible.

APPENDIX 2

A2.1, Brief History of Swimming Goggles

Ever since as early as 4500BC, diving under water for food-gathering, commerce or warfare was found in many coastal cultures such as those found in Greece and China. The actual date of when the first swimming goggles were used is debated between experts and varies considerably, within a range of over 1500 years. A painting on a Peruvian vase (dating to 200AD) illustrating a diver wearing something over his eyes and holding a fish, is the first known possible evidence of people using watertight protection around the eyes to aid seeing under water. Unfortunately, this was the only artefact found dating between 200AD and 1300 that showed any signs of "goggles" being used. Therefore, the painting may well have been simply an artists impression, and not of what was actually used.

Figure A2.1, Detail from 'Coral Divers', an early 17th century print
(www.lakesidepress.com/pulmonary/books/scuba/sectiona.htm - (06/03/06)

In the 14th Century, there is further evidence to suggest that Persian divers used polished shells or tortoises as a method of underwater eye goggles. Again, this was quite possibly an artists imagination being put down on paper. A print dating from the 17th Century was also found (Figure A2.1) and is widely believed to be the first representation of a diver wearing glass eye protectors. The purpose of these glass goggles may or may not have had the intended optical properties to help the user see the reefs below the surface. It has yet again been suggested that the artist had never seen goggles before attempting to draw them.

There is even less recorded information from this time onward suggesting little or no development for hundreds of years. Concentration was instead focused on diving masks, with the earliest efforts taking the form of large blown glass bowls or buckets with small glass windows turned upside down over the head. This combined the functions of improved vision with a limited measure of breathing accommodation, but prevented the user from actually swimming.

Goggles, in approximately the form we know of today (and actually used for standard swimming), date back well into the 1800s. Mathew Webb (Figure A2.2) was the first person to swim the English Channel and did so wearing a pair of glass goggles. The lenses were delicate and posed serious danger to the eye and face if shattered, and so a safer alternative was required.

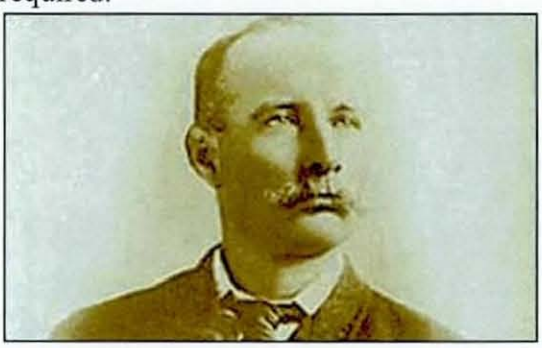

Figure A2.2, Mathew Webb, the first person to swim the channel.
(www.doverpages.co.uk/captain_matthew_webb.htm)

In the 1940s, a British swimming coach called Godfrey produced the first plastic goggles from moulds he cut by hand. Although crude in their form, they are in actual fact somewhat close in design to the modern day Swedish racing goggle. The reality of the modern day, inexpensive, compact, lightweight and 'comfortable' swimming goggle has evolved from this 1940s goggle with no particular significant leaps in design evolution.

The fact that swimming is considered as one of the highest for sports participation in the world, would suggest that something as simple as a pair of swimming goggles would be practically perfect in design. However, a significant proportion of the population still find it difficult to find a pair that meet all of their needs, no matter how much they are willing to spend. Bearing in mind that their needs are as simple as

that they need to be comfortable, watertight and have good vision, it is quite appalling.

APPENDIX 3

A3.1 Skin Sensitivity Pilot Study Data

Due to the substantial amount of data that was recorded, the data can be found in the accompanying compact disc at the back of the thesis, and is found in the folder 'Chapter 3'

A3.2 Skin Sensitivity Study Data

Due to the substantial amount of data that was recorded, the data can be found in the accompanying compact disc at the back of the thesis, and is found in the folder 'Chapter 3'.

APPENDIX 4

A4.1 Tissue Compression Pilot Study Data

Due to the substantial amount of data that was recorded, the data can be found in the accompanying compact disc at the back of the thesis, and is found in the folder 'Chapter 4'

A4.2 Tissue Compression Study Data

Due to the substantial amount of data that was recorded, the data can be found in the accompanying compact disc at the back of the thesis, and is found in the folder 'Chapter 4'.

APPENDIX 5

A5.1 Anthropometric Data

There are two different types of Anthropometric data that are referred to in the thesis;

The raw three dimensional point data of all the scanned participants was too substantial to be included as a paper version, and so had to be included in the accompanying compact disc at the back of the thesis, and is found in the folder 'Chapter 5'

The three dimensional average surfaces have been saved as *.prt files so that they can be opened in certain CAD packages such as Unigraphics. These files are also found in the accompanying compact disc and is found in the folder 'Chapter 5'

APPENDIX 6

A6.1 Visual Distortion Images

Although the images are already shown in the results of section 9, their quality is somewhat limited. Differences between each image can be quite small, and therefore high quality images have been included in the accompanying compact disc and is found in the folder named 'Chapter 6'.

A6.2 Varying Lens Distance Images

Differences between each image are quite small, and therefore high quality images have been included in the accompanying compact disc and is found in the folder named 'Chapter 6'.

APPENDIX 7

A7.1 Final Conceptual Design

The three dimensional data led designed conceptual swimming goggle has been saved as a *.prt file so that it can be opened in certain CAD packages such as Unigraphics. The file is found in the folder named 'Chapter 7' and is included in the accompanying compact disc found at the back of the thesis.